Université de Montréal

ROLE OF K^+ AND CL^- CHANNELS IN MODULATING ELECTROMECHANICAL ACTIVITY IN VASCULAR SMOOTH MUSCLE

par

Carmelle V. Remillard

Département de Physiologie

Faculté de Médecine

Thèse présentée à la Faculté des études supérieures

en vue d'obtention du grade de

Philosophiæ Doctor (Ph.D.)

en Physiologie

Avril, 2001

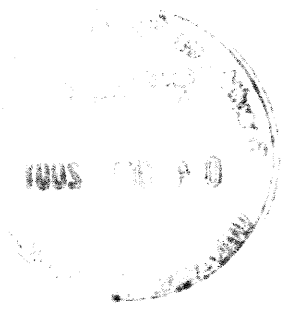

Université de Montréal

Faculté des études supérieures

Cette thèse intitulée:

ROLE OF K^+ AND Cl^- CHANNELS IN MODULATING ELECTROMECHANICAL ACTIVITY IN VASCULAR SMOOTH MUSCLE

présentée par:

Carmelle V. Remillard

a été évaluée par un jury composé des personnes suivantes:

Rémi Sauvé	Président-rapporteur
Normand Leblanc	Directeur de recherche
Jacques Billette	Membre du jury
Lucie Parent	Membre du jury
Ghassan Bkaily	Examinateur externe

Thèse acceptée le: _____

SOMMAIRE

Les canaux ioniques présents dans la membrane des cellules musculaires lisses vasculaires, et surtout des cellules retrouvées au niveau des artères de résistance, jouent des rôles prépondérants dans le contrôle du potentiel membranaire et de la contractilité vasculaire. Nos deux études ont porté sur 1) les propriétés biophysiques et pharmacologiques des canaux potassiques (K^+) et 2) les propriétés fonctionnelles des canaux perméables au chlore (Cl^-) dans la régulation de l'activité électromécanique des cellules artérielles.

Dans la première partie de cette thèse, nous décrivons le mécanisme de l'interaction entre la 4-aminopyridine et un courant K^+ sortant à rectification retardée (K_{dr}) dans des cellules d'artères coronaires de conductance de lapin. Parmi les multiples canaux K^+ identifiés au niveau des cellules musculaires lisses vasculaires, K_{dr} joue un rôle majeur dans le maintien du potentiel membranaire de repos entre –70 et –40 mV. La 4-aminopyridine (4-AP) est un inhibiteur relativement spécifique du canal K_{dr} et a été utilisée abondamment pour caractériser ses propriétés biophysiques et son rôle physiologique. Malgré son usage répandu, on ne connaît pas la nature de l'interaction entre la 4-AP et le canal K_{dr}.

Nous avons caractérisé le mode d'interaction de la 4-AP avec le canal K_{dr} dans des myocytes coronaires en utilisant la technique de "patch-clamp" en configuration "whole-cell". À partir de nos observations, nous concluons que la 4-AP lie préférentiellement le canal lorsque ce dernier est dans son état fermé, et que l'ouverture du canal par la dépolarisation membranaire libère la 4-AP et renverse l'inhibition de K_{dr}. En plus, la liaison de la 4-AP au canal diminue le niveau d'activation du courant à des potentiels membranaires négatifs en déplaçant la courbe d'activation vers le droite, i.e. vers des potentiels plus positifs. En comparant nos données avec les informations moléculaires disponibles

concernant les canaux K^+, nous estimons que le canal K_{dr} coronaire est possiblement un hétéro-multimère de plusieurs sous-unités fonctionnelles α et modulatrices β.

Le but de notre deuxième étude a été d'évaluer le rôle des canaux Cl^- dans la contraction vasculaire induite par la stimulation des récepteurs α_1-adrénergiques, et de mesurer l'influence de changements de la pression transmurale sur cette réponse. Malgré l'importance des canaux calciques de type L (Ca_L) dans la contraction vasculaire, des études récentes suggèrent que deux canaux perméables au Cl^- dépendants du Ca^{2+} intracellulaire (Cl_{Ca}) ou sensibles aux changements de volume (Cl_{vol}) sont impliqués, respectivement, dans la dépolarisation et contraction engendrées par certains agonistes vasoconstricteurs ou lors d'une élévation de la pression transmurale ("réponse myogénique"), propriété à laquelle on attribue un rôle important dans les mécanismes d'autorégulation dans plusieurs lits vasculaires.

En condition isobarique, nous avons évalué le rôle des canaux Cl^- dans les réponses α_1-adrénergique (stimulée par la phényléphrine – PE) et myogénique des artérioles (70 – 100 µm diamètre interne) mésentériques de lapin. Nos observations nous ont permis de tirer les conclusions suivantes. *i*) La PE cause une vasoconstriction liée à l'activation des canaux Cl_{Ca} et Ca_L. *ii*) L'acide niflumique (NfA) ou le 4,4'-diisothiocyanatostilbene-2,2'-disulfonic acid (DIDS) ne modifie pas la contraction induite par l'activation des canaux Ca_L. *iii*) La dilatation induite par l'inhibition de Cl_{Ca} par la NfA est dépendante de la pression pour des concentrations faibles et modérées (0.5 à 1 µM) de l'agoniste PE. *iv*) L'étirement de la paroi causée par une hausse de la pression transmurale active possiblement un courant sensible au DIDS qui "masque" en partie la vasoconstriction induite par la PE attribuée à l'activité des canaux Cl_{Ca}. *v*) La dépolarisation induite par la PE est renversée complètement par la NfA.

vi) Le courant sensible au DIDS contribue à la réponse myogénique. Ces travaux mettent donc en évidence l'importance physiologique des canaux Cl^- dans la dépolarisation et la contraction de la microcirculation mésentérique associées à la stimulation par le système nerveux autonome sympathique dans des conditions normales de pression transmurale.

RÉSUMÉ

Les petites artères, les artères de résistance jouent un rôle prépondérant dans le maintien du débit sanguin, de la pression artérielle, de la résistance périphérique totale, et de la perfusion tissulaire. Au repos, ces artères sont généralement dans un état partiellement contracté appelé le tonus basal. De cet état, les artères peuvent se contracter ou se dilater et ainsi modifier le diamètre vasculaire interne de façon à ajuster le débit sanguin face à divers stimuli. Cette capacité de modifier leur diamètre interne provient de la couche de cellules musculaires lisses (CMLs) que l'on retrouve au niveau de la *tunica media*. La stimulation des CMLs par des facteurs physiques ou par des hormones et neurotransmetteurs endogènes entraîne des changements sélectifs de la perméabilité membranaire à différents ions qui ont pour conséquence de moduler le potentiel de repos des CMLs, le taux d'entrée des ions Ca^{2+} en régime établi, et leur état de contractilité. Dans cette thèse, nous avons réalisé deux études distinctes ayant un objectif général commun de mieux comprendre les propriétés biophysiques et pharmacologiques ainsi que le rôle fonctionnel de canaux ioniques participant à la genèse du potentiel de membrane des CMLs des artères coronaire et mésentérique de lapin.

Dans une CML au repos, le potentiel de repos membranaire (PRM) se situe entre –40 et –70 mV. Bien que cette gamme de potentiels membranaires s'avère plus dépolarisée que la valeur théorique du potentiel d'équilibre (E_K) des ions potassiques (K^+) dans les CMLs vasculaire ($\cong$ –85 mV), il est reconnu que les canaux K^+ sont majoritairement responsables de la genèse du PRM de ces cellules. Ces canaux déterminent en grande partie, mais de façon indirecte par leur influence sur le PRM, la probabilité d'ouverture des canaux calciques

(Ca^{2+}) voltage-dépendants de type L (Ca_L) qui représentent la principale voie responsable de l'entrée des ions Ca^{2+} et donc du maintien du tonus vasculaire.

Au moins cinq classes de courants potassiques ont été identifiés jusqu'à maintenant au niveau des cellules musculaires lisses vasculaires: 1) le courant Ca^{2+}- et voltage-dépendant, 2) le courant voltage-dépendant à rectification retardée (K_{dr}), 3) le courant sensible aux nucléotides intracellulaires (e.g.: ATP et GDP), 4) le courant transitoire sortant, et 5) le courant à rectification entrante. On considère que le courant résultant de l'activité des canaux K_{dr} ($I_{K(V)}$) est responsable en grande partie du maintien du PRM dans les CMLs, en particulier lorsque la concentration interne en Ca^{2+} est faible ou modérée. $I_{K(V)}$ s'active rapidement lors d'une dépolarisation et s'inactive lentement. Ce courant est régulé par *i*) la phosphorylation, *ii*) l'activité métabolique, *iii*) les agents vasoconstricteurs, et *iv*) la dépolarisation membranaire. D'un point de vue plus clinique, on associe une baisse de l'activité des canaux K_{dr} à l'hypertension pulmonaire induite par l'hypoxie et à l'hypertension pulmonaire primaire. $I_{K(V)}$ se distingue des autres courants K^+ vasculaires par son inhibition sélective par la 4-aminopyridine (4-AP). Plusieurs études ont suggéré que le site de liaison de cette molécule sur le canal K_{dr} se situe du côté interne de la membrane. Cependant, le mécanisme d'action de la 4-AP sur ce courant demeure obscur. Dans une première étude, nous avons tenté d'élucider le mécanisme d'inhibition de K_{dr} par la 4-AP au niveau des myocytes coronaires de lapin en utilisant la technique de patch clamp.

Nous avons observé que la 4-AP se lie préférentiellement au canal K_{dr} lorsque ce dernier s'avère dans un état fermé, tel que démontré par l'inhibition complète du courant quand la cellule est incubée en présence de 4-AP à un potentiel de conditionnement de –60 mV, potentiel situé hors de la zone d'activation de K_{dr}. Les constantes de temps de

déactivation, d'inactivation et de réactivation demeurent inchangées en présence de 4-AP. Cependant, la 4-AP quadruple la constante de temps d'activation et déplace la courbe d'activation vers des potentiels plus positifs. L'inhibition n'est pas augmentée par des dépolarisations répétitives puisque l'amplitude et la cinétique de $I_{K(V)}$ en présence de 4-AP demeurent constantes durant un train de dépolarisations.

Nos résultats démontrent aussi que la 4-AP demeure emprisonnée dans le canal. Le lavage de la molécule pendant 10 minutes lorsque la cellule est maintenue à potentiel de conditionnement de –60 mV ne résulte qu'en une récupération partielle du courant induit par une première impulsion de 250 ms à +20 mV, alors que le courant retourne rapidement vers son niveau contrôle durant les impulsions subséquentes, suggérant que l'ouverture répétitive du canal permet de déloger la 4-AP de son site de liaison. Des simulations mathématiques utilisant les mesures d'amplitude et de constantes de temps des courants dérivées de nos données expérimentales ont été en mesure de reproduire de façon quantitative nos observations expérimentales faites *in vitro*. Ceci appuie notre hypothèse que la 4-AP se lie préférentiellement au canal à l'état fermé et cause ainsi une dépolarisation qui rend les canaux K_{dr} moins disponibles aux potentiels membranaires physiologiques.

L'inhibition de $I_{K(V)}$ et l'inhibition sélective de l'expression des sous-unités du canal K_{dr} pourraient jouer un rôle important dans plusieurs formes d'hypertension ainsi que dans la maladie coronarienne chronique et aigue. L'élucidation du mécanisme d'inhibition de K_{dr} par la 4-AP, en conjonction avec des techniques d'ADN recombinant, permettront d'identifier les sous-unités spécifiques responsables de la genèse du courant K_{dr} en conditions physiologiques normales et leur implication dans certaines maladies vasculaires.

Contrairement aux canaux K^+ qui maintiennent le potentiel de repos membranaire vers des valeurs relativement négatives, l'activation des canaux perméables aux ions chlorures (Cl^-) entraîne une dépolarisation membranaire et une contraction vasculaire. Ceci est dû au fait que le potentiel d'équilibre des ions Cl^- est plus positif que le PRM des CMLs, se situant aux environs de –25 mV. L'ouverture de tels canaux a pour conséquence de promouvoir une sortie nette de Cl^-, effet qui résulte en une dépolarisation membranaire et, par le fait même, en une vasoconstriction.

Les canaux Cl^- peuvent être activés par de nombreux agents vasoconstricteurs (e.g. endothéline, angiotensine II, norépinéphrine) et par des stimuli de nature physique (e.g. hausse de pression artérielle, étirement, forces de cisaillement). Nous nous sommes intéressés au rôle des canaux Cl^- dans les réponses vasculaires de la microcirculation mésentérique induites par stimulation α_1-adrénergique par la phényléphrine (PE) et comment une augmentation de la pression transmurale de vaisseaux intacts module cette réponse.

Les canaux Cl^-, en particulier ceux qui sont activés par une élévation du Ca^{2+} intracellulaire, jouent un rôle important dans la contraction et la dépolarisation induites par l'action de la norépinéphrine (NE) sur les récepteurs α_1-adrénergiques. La NE produit à la fois une dépolarisation et une contraction qui sont toutes deux biphasiques. Alors que la phase initiale de ces événements est attribuée à une mobilisation du Ca^{2+} intracellulaire par l'activation de canaux Ca^{2+} du reticulum sarcoplasmique sensibles à l'IP_3, la phase soutenue est généralement associée à une dépolarisation membranaire et à une entrée de Ca^{2+} au travers des canaux Ca_L ou des canaux cationiques non-spécifiques activés directement par le récepteur. Plusieurs études ont suggéré que les canaux Cl^- activés par le Ca^{2+} intracellulaire (Cl_{Ca}) contribuent à la dépolarisation soutenue induite par la NE dans plusieurs lits

vasculaires. La sérotonine, l'endothéline, la vasopressine et l'angiotensine II causent aussi une vasoconstriction et une dépolarisation (sérotonine) sensibles à l'inhibition des canaux Cl_{Ca}. Il a été proposé que l'activation des canaux Cl_{Ca} par la NE dépolarise les CMLs et active indirectement les canaux Ca_L menant ainsi à la contraction vasculaire. La majorité des travaux menant à cette proposition ont été effectués sur des cellules isolées puisqu'il s'avère plus facile de contrôler les conditions expérimentales. Dans ce modèle, les autres types de cellules présentes dans le vaisseau et pouvant libérer des facteurs vasoactifs (e.g.: endothélium, terminaisons nerveuses, etc.) sont absents et n'affectent donc pas la réponse cellulaire. L'hypothèse émise ci-haut quant à leur rôle physiologique demeure néanmoins à être vérifiée car très peu de travaux ont été effectués sur des préparations considérées comme "plus physiologiques" telles que des artères intactes, et surtout sur des artères de résistance.

En utilisant une technique permettant d'étudier la réactivité de petites artères dénudées de leur endothélium en condition isobarique, nous avons tenté d'évaluer par une approche pharmacologique la contribution des canaux Cl^- à la vasoconstriction et à la dépolarisation d'artérioles mésentériques (70 – 100 µm diamètre interne) de lapin induites par la PE. Nous avons effectué les observations suivantes. *1*) La contraction induite par la PE est entièrement inhibée par la nifédipine, un inhibiteur spécifique des canaux Ca_L. *2)* En présence de TEA (pour inhiber les canaux K_{Ca}), l'acide niflumique (NfA, un inhibiteur relativement sélectif des canaux Cl_{Ca}, n'inhibe que partiellement la vasoconstriction produite par la PE alors qu'elle n'a pas d'effet sur la contraction induite par le KCl en présence de TEA. *3)* En présence de concentrations intermédiaires de PE (0.1 à 1 µM) et de TEA, la dilatation induite par la NfA décroît lorsque la pression transmurale est érigée, un effet qui n'est pas apparent avec 10 µM PE dans le milieu. *4)* À toutes les pressions transmurales

étudiées (0 à 100 mm Hg), la dilatation causée par la NfA diminue en fonction de la concentration de PE. *5)* L'inhibition du courant Cl_{Ca} par la NfA renverse la dépolarisation induite par la PE à 40 mm Hg, suggérant un rôle important des canaux Cl_{Ca} dans la dépolarisation induite par la PE.

Comme il a été mentionné auparavant, les artères au repos développent en général un tonus basal que l'on peut évaluer en omettant les ions Ca^{2+} de la solution de perfusion (une courbe pression-diamètre obtenue dans ces conditions représente la réponse dite passive du vaisseau). Lorsque la pression artérielle augmente, les artères et plus particulièrement les artères de résistance, se contractent de façon à maintenir un débit sanguin constant; la réponse active myogénique est souvent associée à une dépolarisation membranaire résultant en : *1)* l'activation des canaux Ca_L, *2)* une augmentation relativement modeste des niveaux internes de Ca^{2+} (~ 150 - 200 nM), et *3)* une sensibilisation de l'appareil contractile au $[Ca^{2+}]_i$. Depuis quelques années, plusieurs études ont évalué la contribution des canaux ioniques responsables de la dépolarisation associée à cette réponse. Plusieurs hypothèses ont été émises: *1)* l'inhibition de canaux K^+ voltage- et Ca^{2+}- dépendants, et/ou *2)* l'activation des canaux Ca_L, cationiques mécano-sensibles, ou Cl^- sensibles aux changements de volume (Cl_{vol} ou Cl_{swell}). En utilisant la même approche qu'auparavant, nous avons évalué la contribution des canaux Cl^- à la réactivité myogénique des artérioles mésentériques, avec ou sans stimulation des récepteurs α_1-adrénergiques par la PE en présence de TEA. Nous avons trouvé que des canaux Cl^- autres que Cl_{Ca} pourraient contribuer indirectement à la réponse myogénique puisqu'en absence de PE, la contraction initiée par une hausse de la pression transmurale (réponse myogénique) n'était pas affectée par la NfA mais était fortement atténuée par l'acide 4,4'-diisothiocyanatostilbene-2,2'-disulfonique (DIDS), un inhibiteur

non-spécifique des canaux Cl^-. Cet effet du DIDS était indépendant de l'entrée de Ca^{2+} puisque la même concentration de DIDS n'a pas modifié la réponse au KCl. De plus, la relaxation induite par la NfA suite à une stimulation par la PE en présence de TEA était "augmentée" par le DIDS d'une manière dépendante de la pression transmurale, suggérant que l'activation d'un courant sensible au DIDS par l'étirement pourrait masquer partiellement la dépolarisation et la contraction induites par l'activation du courant Cl_{Ca} lors de la stimulation sympathique.

Une meilleure compréhension des mécanismes ioniques impliqués dans l'activité vasomotrice des vaisseaux sanguins est importante pour le développement de médicaments ciblant de façon spécifique les différents lits vasculaires. Nos données appuient l'hypothèse que les canaux Cl^- jouent un rôle fondamental dans la dépolarisation et la contraction induites par la stimulation sympathique et/ou par l'étirement de la paroi vasculaire au niveau de la microcirculation mésentérique. Ces travaux permettront de proposer de nouvelles thérapies pour les formes multiples d'hypertension qui affligent un pourcentage important de la population canadienne.

TABLE DES MATIÈRES

LISTE DES TABLEAUX

LISTE DES FIGURES

SIGLES ET ABBRÉVIATIONS

α_1-AR	Alpha$_1$-adrenoreceptor
4-AP	4-Aminopyridine
Ca_L	L-type Ca^{2+} channel
Cl_{Ca}	Ca^{2+}-activated Cl^- channel
Cl_{vol}	Volume-sensitive Cl^- channel
$I_{K(V)}$	Delayed rectifier current
IP_3	Inositol 1,4,5-trisphosphate
K_{Ca}	Ca^{2+}-activated K^+ channel
K_{dr}	Delayed rectifier potassium channel
NE	Norepinephrine
NfA	Niflumic acid
PE	Phenylephrine
PKC	Protein kinase C
RMP	Resting membrane potential
TEA	Tetraethylammonium chloride
VSM	Vascular smooth muscle

REMERCIEMENTS

Plusieurs personnes sont responsables pour l'évolution de ma carrière. Mon directeur, Dr. Normand Leblanc, m'a initié au monde de la recherche. Son enthousiasme m'a aidé à faire mon choix de carrière. Je le remercie pour ses idées, son encouragement, et, surtout, de son offre de travailler dans son laboratoire à Winnipeg.

Les techniques qui me sont maintenant indispensables ont été difficiles à acquérir. Je remercie Drs. Xiadong Wan, Ézequiel S. Morales, Antonio Guia, Rita Jabr, et Pak Ming Leung pour m'avoir enseigné tout ce que je connais à propos de l'isolation cellulaire et la technique du patch-clamp. Sans leur aide je n'aurais pas progressé rapidement pendant mes premiers mois au laboratoire. Marie-Andrée Lupien a consacré plusieurs semaines afin de m'aider à compléter les études des artères pressurisées, et je lui en suis énormément reconnaissante. Dr. Éric Thorin et Thang-Dung Nguyen ont offert beaucoup de support moral et des conseils dans ces expériences. Enfin, Jim Dewart, qui, au secondaire, m'a montré que la science était plus qu'un sujet obligatoire à l'école.

Ce projet n'aurait pas vu jour sans l'aide financière de la Fondation des Maladies du Coeur du Canada, le Conseil de Recherche Médicale du Canada, la Faculté des Études Supérieures et le Département de Physiologie à l'Université de Montréal, et le Fonds de Recherche de l'Institut de Cardiologie de Montréal.

Ma famille a accepté mon choix de quitter le Manitoba pour poursuivre mes études. Ils m'ont encouragé à poursuivre mon rêve même si celui-ci m'a mené loin d'eux. Je les remercie pour leur support.

Finally, to my husband and daughter, a big hug and kiss to say thank you. Thanks for the patience, and understanding you provided while I was working on this manuscript. For your love and support, I will always be grateful. *Obrigado.*

DÉDICACE

Cette thèse est offerte à mes parents, qui sont la source de mon ambition. Ils ont rêvé leurs rêves et ont atteint leurs buts dans la vie.

Plus important, ils m'ont encouragé à faire de même.

INTRODUCTION

The heart and blood vessels form the transportation system that delivers blood and its necessary nutrients to all cells of the body, and carries away the end products of their metabolic activity. The heart serves as the pulsatile working pump driving blood through the vascular system. The rate, rhythm and contractility of the cardiac pump are important points of regulation of the cardiovascular system. The blood vessels are the elements that ultimately regulate blood flow to the various organs of the body and control the cardiac output by providing feedback to the heart by changing the preload and the afterload. Fine adjustments of the lumen diameter of the various branches of the vascular system play a crucial role in the maintenance of overall and regional blood pressure and flow. The major goal of this thesis was to investigate, at the cellular and multicellular levels, some of the basic ionic mechanisms controlling the resting membrane potential of vascular smooth muscle cells that are the end effectors in the regulation of vasomotor activity of all blood vessel types.

I-1 Morphology and physiology of the arterial wall

The arterial wall can be dissected into three components [203] {Fig. *1*}. The *tunica intima* contains a monolayer of squamous endothelial cells in direct contact with the vessel lumen, and a thin basal *lamina propria* of dense, acellular connective tissue which delineates it from the *tunica media*. The outer wall, the *tunica adventitia*, contains mostly connective tissue elements such as elastin and collagen fibers, fibroblasts, and macrophages, but may also contain nerve bundles. The middle section, the *tunica media*, controls the mechanical activity of the vessel and is the major component of the vascular wall. It is comprised of two layers containing circularly (inner layer) and longitudinally (outer layer) arranged spindle-

shaped vascular smooth muscle (VSM) cells.

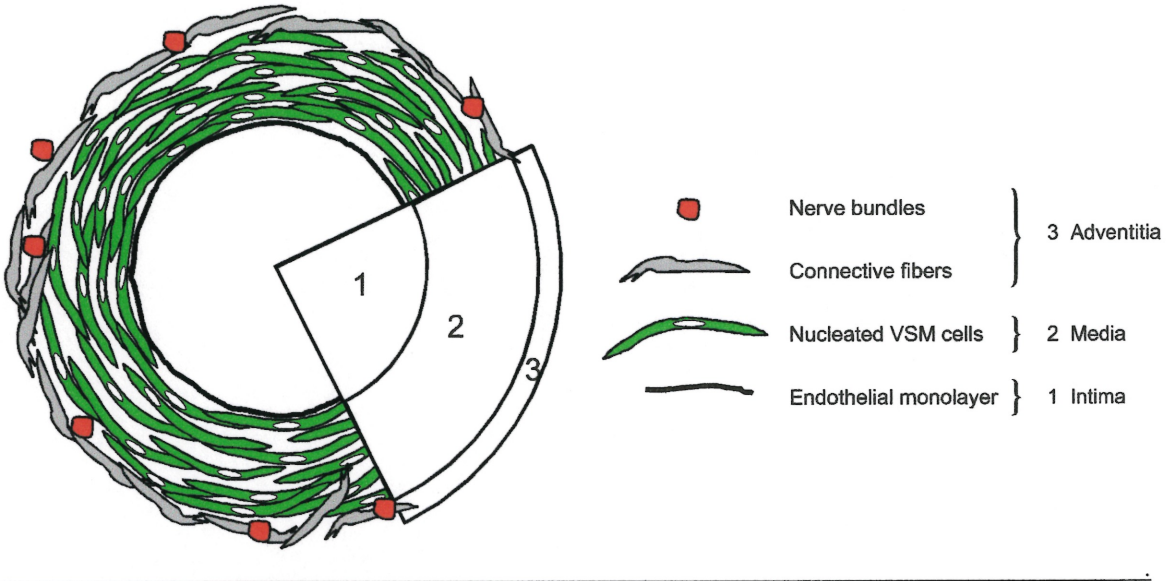

Fig. 1 Cross-section of the arteriole

Endothelial cells on the intimal cells surface of the vessels have many functions. They play a dynamic role in inflammatory responses, cell growth, differentiation and angiogenesis [187, 203]. They also modulate vascular tone by producing vasoactive agents such as *i*) endothelium-derived relaxing factor (EDRF), now believed to be nitric oxide (NO), *ii*) hyperpolarizing factor (EDHF), *iii*) constricting factor (EDCF), *iv*) prostaglandins (PGs), and *v*) epoxyeicosatrienoic acids (EETs), and *vi*) endothelin [290]. These compounds typically are produced in response to circulating hormones, platelet aggregation, endothelial receptor activation, mechanical deformation, and changes in laminar flow (shear stress) [132, 172, 174, 180, 233, 290, 308]. Factors released by endothelial cells modulate the contractile state of adjacent VSM cells through a paracrine interaction and may ultimately alter their membrane potential by influencing ion channels, intracellular Ca^{2+} levels, the Ca^{2+}-sensitivity of the contractile apparatus, and/or the contractile proteins themselves. Numerous studies over the last decade have indicated that many factors released by the endothelium exert their influence

predominantly on VSM tone by altering intracellular Ca^{2+} levels through changes in membrane potential which mediate the activity of voltage-gated L-type Ca^{2+} channels (Ca_L). Let us look at a few examples. The vasorelaxation induced by EDRF, EDHF and PGs has been associated with *i*) direct inhibition of Ca_L channels [240], *ii*) indirect inhibition of Ca_L by K^+ channel-induced hyperpolarization, and *iii*) activation of potassium conductances [209] sensitive to voltage [190, 326], intracellular Ca^{2+} [16, 28, 47, 77, 159, 189, 190, 241], and adenosine 5'-triphosphate (ATP) [205]. Activation of endothelin receptors on VSM cell membranes causes vasoconstriction, leading to *i*) sensitization of the myofilaments to Ca^{2+} [90], *ii)* activation of chloride channels [167, 250, 275, 287], voltage-dependent [111, 249, 322] and independent [143] calcium channels, or nonselective cation channels [46], and *iii*) inhibition of voltage-dependent potassium channels [258]. Activation of Ca^{2+}-dependent potassium channels [250] and the release of EDRF [305] can counterbalance the constricting effect of endothelin.

Vascular smooth muscle cells are responsible for the control of arterial and venous tone, and for distribution of blood flow throughout the body. Ultimately, they can determine cardiac output by dictating both cardiac afterload (total peripheral resistance) and cardiac preload (venous capacitance) [24]. This is accomplished by constantly readjusting the state of constriction or dilation of blood vessels in response to changes in perfusion pressure, metabolic factors, neural stimulation, or mechanical deformation of the cell membranes [24, 203]. Arterioles and small arteries together account for approximately 47% of the total peripheral resistance while accounting for only 8% of the total distribution of blood volume; hence, they have been termed "resistance vessels". In comparison, veins represent 64% of total blood volume capacity while only contributing to 7% of vascular resistance [74]. Thus

the change in arteriolar radii from the artery to arteriole will considerably affect the resistance to flow. This is stated clearly in the Hagen-Poiseuille law, $R = 8 \times l \times \eta \times \pi^{-1} \times r^{-4}$, where resistance ($R$) in a tube of defined length (l) depends on fluid viscosity (η), and is inversely proportional to the fourth power of the radius (r), meaning that an approximate 20% drop in radius will cause a two-fold increase in resistance [24, 74]. Furthermore, the Laplace relationship, $T = P_t \times r$, where T is wall tension, P_t is transmural pressure, and r is vessel radius, demonstrates that larger vessels must generate much more force (increased energy and tension) to contract by 20% as compared to smaller calibre vessels [24]. However, because of the high arterial pressure, it is energetically more economical to regulate the total peripheral resistance at the level of the small arteries and arterioles.

Notwithstanding vessel calibre as a critical determinant of resistance, various modulating factors can have a dominant effect on the reactivity of blood vessels. For example, some vascular beds are more sensitive to neural stimuli (*i.e.* cutaneous and splanchnic circulations), while others are more strongly regulated by the metabolic demand of the organ that is irrigated ("local factors") and/or transmural pressure variations (e.g. cerebral, renal, and coronary circulations) [24, 74]. Distinctive features between vascular beds can be explained by differences in the level and type of neural (e.g. sympathetic) innervation, the anatomical organization, the role of baroreceptors located within the vessel walls, or the unique function of the organ or tissue perfused by a given vascular bed.

I-2 Arterial tone

Vascular tone, the state of active tension of the vessel, is an intrinsic property of resistance arterioles. At rest, most blood vessels are in an intermediate state of tone, termed "basal tension" [24, 74]. Maintenance of vascular tone ensures 1) that there is minimum blood flow to all organs when the body is at rest or in action, 2) optimum regulation of blood pressure (homeostasis), and 3) redistribution of blood to an active organ at the expense of other resting organs to avoid overtaxing the heart during changes in the work load [74]. Modes of regulation of vascular tone can be divided into four or more physiological categories most notably: 1) local control, 2) nervous control, 3) neurohumoral and hormonal control, and 4) agonist-enhanced myogenic reactivity.

A. Local control: Autoregulation and role of metabolic factors

VSM cells contract or relax in response to physical stresses. For example, an arteriole initially will dilate in response to an increase in perfusion pressure, primarily due to the stress imposed on the vessel wall by the increase in transmural pressure, but also in part due to shear-stress-induced release of endothelial factors [132, 174, 180, 233]. This is followed by a constriction that will tend to return the rate of blood flow toward the previous basal level [18] {Fig. *2*}. This phenomenon,

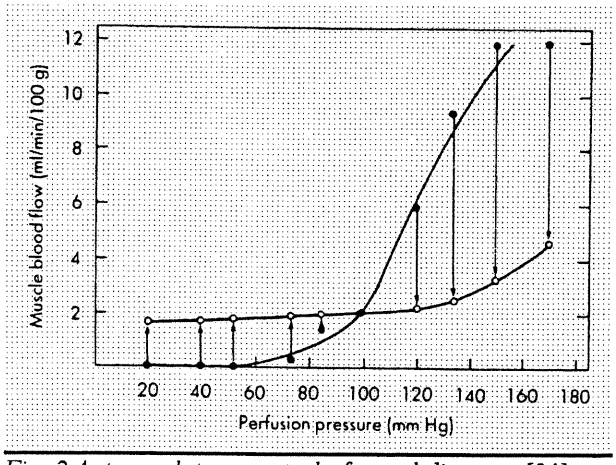

Fig. 2 Autoregulatory control of vessel diameter [24]

Data presented were obtained from canine skeleta muscle arterioles.
●: Flow obtained immediately after changes in perfusio pressure from the control level (intercept between th two lines)
○: Steady state flow attained at the new perfusio pressure.

termed *autoregulation*, is an important local mechanism for the control of blood flow within the physiological range of intravascular pressures. The main functions of autoregulation are to keep blood flow constant despite variations in blood pressure, and to adapt blood flow to meet the demand of local changes in metabolism within an organ [24, 74, 154]. The mechanisms producing autoregulation are complex and vary depending on the type of vasculature, but generally have been divided into three major categories: *i*) myogenic response, *ii*) metabolic control, and *iii*) hormonal control [74, 154].

i) In the example illustrated in Fig. *2*, autoregulation of blood flow occurs mainly as a consequence of **myogenic response**, a vasoconstriction elicited by an increase in perfusion pressure. This vasoconstriction originates in the tunica media and is thus mediated by the vascular smooth muscle cells. This phenomenon is independent of the endothelium although the latter is known to modulate this response [71, 97]. The VSM cells depolarize in response to the stretching of the membranes. Stretching produces graded Ca^{2+} entry into the cells, leading to modest elevations of intracellular Ca^{2+} concentration from a resting level of ~100 nM to ~250 nM, ultimately leading to contraction [126, 170, 196]. This mechanism will be discussed further later.

ii) During **hypoxia**, most blood vessels dilate to increase blood flow and supply oxygen to the tissues. This is likely the result of hypoxia-induced activation of potassium channels [31, 67, 101, 307] or inhibition of calcium channels [95]. An exception to this exists in the lungs, where decreased oxygen levels result in a potassium channel-inhibition-based vasoconstriction [222, 236, 264, 301, 307]. This is advantageous because it greatly improves oxygen uptake by diverting blood flow to better-oxygenated regions of the lungs [73]. Reduction of blood flow, or **ischemia**, lowers oxygen tension in the tissue because of the

decreased rate of oxygen delivery, and it results in the accumulation of metabolic by–products that are able to produce vasodilation (*vasodilator metabolites),* such as adenosine, lactic acid, CO_2, and hydrogen ions [74]. When these metabolic end products accumulate locally, vessels generally dilate and the resulting increase in flow washes away the metabolites. An example of this is the phenomenon called "reactive hyperemia"; after the partial or complete occlusion (in the order of tens of seconds) of an artery, a potent but transient (in the order of seconds to tens of seconds) vasodilation and enhanced compensatory blood flow is observed immediately following the return of flow (reperfusion). The latter process is ascribed to an ischemia-induced accumulation of metabolites including K^+, protons (mostly from lactic acid), inorganic phosphate, adenosine, prostaglandins, and perhaps changes in osmolarity [74]. Local accumulation of metabolites is a dominant vasodilator in tissues with high metabolic activity, such as the brain, the heart, and active skeletal muscles. The regulation by vasodilator metabolites ensures that non-working muscles do not take up a significant portion of the perfusion pressure, thereby diverting the cardiac effort to active muscle and to other tissues with high energetic demands. This is a form of conservation of energy.

iii) Various **tissue hormones**, such as bradykinin or angiotensin II, can be released locally in response to changes in perfusion pressure [74]. The release of these agents can occur from various cell types, including blood (mainly platelets), endothelial, VSM, and neuronal cells. For example, bradykinin from endothelial cells reacts with B_2 receptors on smooth muscle cells to cause vasodilation [41, 241], as will be discussed further in the following section. Norepinephrine stored in neuronal vesicles can be released upon stimulation to cause vasoconstriction of VSM cells.

B. Nervous control: Catecholamines

Blood vessel tone is determined, in part, by the extent of innervation from the autonomic nervous system. In the case of arteries, it is widely acknowledged that innervation occurs primarily via the sympathetic pathways, although the nature and extent of this innervation differ between *i)* vascular beds, and *ii*) vessel calibre. For example, it has been shown that sympathetic nerve stimulation of rat cremaster skeletal muscle arterioles (in the absence of central nervous control) can be attenuated by prazosin (α_1–antagonist; large arterioles) and rauwolscine (α_2–antagonist; small arterioles) [219].

A significant proportion of the nervous control of arteries is performed by catecholamines (norepinephrine and epinephrine) released from sympathetic nerve terminals. In vascular tissues, norepinephrine and epinephrine produce vasoconstriction or vasodilation depending on the type of adrenoceptor they stimulate.

Adrenoceptors are a family of G-protein linked receptors with seven membrane–spanning domains. They can be differentiated mainly by their effects on the cellular physiology, as well as by their sensitivity to various ergots or β–haloalkylamines [2]. Classically, "excitatory" and "inhibitory" effects occur via α– and β–adrenoceptors (or adrenergic receptors, "–ARs"), respectively [24, 74]. β–ARs have been further subdivided into three subtypes based on their pharmacological profiles and on their end-organ effects. The classification of α–adrenoceptors has also been further subdivided according to their localization in the microanatomy. Characteristics and pharmacological details about the different adrenoceptor families are described below and summarized in *Table 1*.

	"Excitatory"		"Inhibitory"		
Sub-classification	α_1	α_2	β_1	β_2	β_3
	postjunctional	prejunctional			
Tissue localization	VSM, heart, brain, kidney, vas deferens, spleen, liver, anococcygeus muscle	platelets, VSM, lung, kidney, brain, vas deferens, heart	Heart, adipose tissue, VSM, placenta	VSM, uterus, trachea, lung	adipose tissue, pancreatic islet, skeletal muscle, GI SM
Agonists:	Norepinephrine, epinephrine				
	phenylephrine, A61603	oxymetazoline	Donopamine, Ro 363, xamoterol	terbutaline, salbutamol, salmeterol, zinterol	BRL 37344, ICI 198,157, CL 316,243
Antagonists	CEC, prazosin, WB 4101, 5-MU, (+)-niguldipine, ARC 239	yohimbine, rauwolscine, BRL 44408,	metoprolol, practolol, atenolol, betaxolol, CGP 20712A	butoxamine, ICI 118,551,	ICI 118,551
Transduction pathway	$G_{q/11}$ – PLC - IP_3/DAG Activation of PLA_2 and PLD Activation of Ca_L	G_i - AC inhibition (not exclusive mech.) Activation of Ca_L	Gs – AC - cAMP	Gs – AC – cAMP	Gs – AC – cAMP
Vascular outcome / Physiological role	Increased Ca_i and subsequent contraction Control of blood pressure	Tissular contraction Control of blood pressure Negative control of cAMP production	Increased cardiac rate and contraction Stimulation renin secretion Relaxation of VSM and SM	SM relaxation (trachea, VSM, uterus)	Lipolysis in white adipose tissue Thermogenesis in brown adipose tissue Stimulation of insulin secretion Inhibition of glycogen synthesis Inhibition of contractile activity in GI smooth muscle and VSM
Molecular biology (cloned)	$\alpha_{1a/d}$, α_{1b}, α_{1c}	α_{2a}, α_{2b}, α_{2c}			
Subtypes (pharmacological)	A,B,C,D,L	A,B,C			

Table 1: α– and β–Adrenoceptor classification and characterization (previous page)

Abbreviations: AC, adenylate cyclase; CEC, chloroethylclonidine; GI SM, gastrointestinal smooth muscle; 5-MU, 5-methylurapidil; PLA_2, phospholipase A_2; PLD, phospholipase D.

Norepinephrine (NE, also known as noradrenaline) is the most common neurotransmitter released in blood vessels and generally produces vasoconstriction via effects on α–ARs of all the vascular beds. Its impact on contraction is more pronounced in mesenteric and epidermal blood vessels [24]. Circulating epinephrine (also known as adrenaline), released from the adrenal medullae, can generate vasoconstriction or vasodilation depending on its concentration and on blood vessel type [74]. In addition, epinephrine can increase NE release from postganglionic sympathetic fibers by binding to the β_2–adrenoceptors on axon varicosities, thereby increasing the contraction due to NE [73]. Parasympathetic neural stimulation, which releases predominantly the neurotransmitter acetylcholine, causes vasodilation in a small number of vessels in the meninges, salivary and sweat glands (indirectly via kinin production), genitalia, bladder, and large bowel [24, 74]. However, because only a small proportion of the body's resistance vessels receive parasympathetic innervation, the cholinergic contribution to the total peripheral resistance is negligible compared to the sympathetic influences. Since many adrenoceptors are targeted by these two neurotransmitters, it is worthwhile to look at each individually.

i) α_1–Adrenoceptors

'Post-junctional' α_1-adrenoceptors are quite prominent on vascular smooth muscle cell membranes, where they are primarily responsible for the control of blood pressure. They can also be found in the heart, brain, kidney, spleen, liver, vas deferens, prostate, skeletal muscle, and submaxillary gland [38, 76, 79, 181, 281]. The α_1–AR family can be further

subdivided into five major subtypes (A, B, C, D L) based on tissue localization, pharmacological profiles and physiological roles [38, 76, 118, 175, 188, 231, 254, 273]. The α_{1A} and α_{1D} (sensitive to BMY 7378 [231]) subtypes cause a tonic contraction dependent on influx of extracellular Ca^{2+}, whereas the α_{1B} subtype causes a phasic contraction dependent on intracellular Ca^{2+} mobilized by phosphatidylinositol hydrolysis [254, 273]. α_{1A} and α_{1B} subtypes co-exist in some arteries, such as the rabbit mesenteric and renal arteries [254], but all three subtypes (A, B, and D) are activated by NE stimulation [171, 175, 254]. The α_{1C} and α_{1L} subtypes have been identified pharmacologically, but their effects on Ca^{2+} mobilization are unknown. The α_{1C}–AR located in the liver and cerebral cortex is sensitive to 5-MU [38, 76]. The final subtype, α_{1L} is moderately sensitive to RS17053 and SB216469 while having very low affinity for prazosin [38, 76].

In addition to NE, α_1–AR stimulation is typically accomplished by the use of phenylephrine [73, 124, 281]. However, the list of known antagonists greatly outweighs the number of agonists. Chloroethylclonidine (CEC) produces irreversible inhibition of these receptors, while the inhibitory effects of prazosin, WB 4101, 5-methyurapidil (5-MU), (+)-niguldipine, and ARC 239 are reversible [38, 76, 181].

Three corresponding clones have been assigned to some of the known α_1–AR subtypes [38, 76]. The α_{1c} clone (corresponding subtype: α_{1A}-AR) is most sensitive to WB 4101, as well as to two novel compounds, SB216469 and RS17053, while being relatively insensitive to CEC. Clone α_{1b} (corresponding subtype: α_{1B}-AR) is more effectively blocked by CEC and prazosin. A final clone, $\alpha_{1a/d}$, is highly sensitive to WB 4101, 5-MU, and (+)-niguldipine, making it difficult to associate it with any specific α_1–AR.

The common effect of all α_1–adrenoceptors is to enhance the contraction associated with increased intracellular Ca^{2+} levels [48, 124, 153]. This occurs via the bound receptor associating with a $G_{q/11}$ protein and stimulating phospholipase C (PLC) [193, 194, 302]. Inositol 1,4,5-trisphosphate (IP_3) and diacylglycerol (DAG) produced by the activated PLC lead to activation of protein kinase C (PKC) and elevation of intracellular Ca^{2+} via release of Ca^{2+} from the sarcoplasmic reticulum or enhanced Ca^{2+} influx via the sarcolemma [36, 214]. There are indications that the transduction pathway may also involve activation of phospholipases A_2 or D, as well as direct activation of voltage-dependent Ca^{2+} channels [118, 210, 231].

ii) α_2–Adrenoceptors

α_2–Adrenoceptors have been named the 'pre-junctional' α-AR. This may be a misnomer since they have also been identified on post-junctional (i.e. post-synaptic) sites such as the uterus, kidneys, and pancreas [76]. Of the three pharmacological subtypes identified, the predominant pre-junctional adrenoceptor on noradrenergic nerve terminals is the α_{2A}, while α_{2C} may also be present. Postsynaptically, all three subtypes (α_{2A}, α_{2B}, and α_{2C}) are present on vascular smooth muscle [38, 76, 91, 181, 188, 219]. In addition to VSM, α_2–ARs can be found in platelets, vas deferens, lung, kidney, brain, and heart tissues [38, 76].

Oxymetazoline is a partial agonist for α_2–ARs but shows higher affinity for the α_{2A} subtype [76]. These α_2-adrenoreceptors are sensitive to inhibition by such compounds as yohimbine, and rauwolscine. ARC 239, spiroxatrine, imiloxan, and BRL 44408 are also antagonists with varying specificities for the different subtypes [38, 76]. The order of potency of all these compounds may be used to pharmacologically identify the different α_2–adrenoceptor subtypes.

The transduction pathway leading to α_2–AR-mediated contractions involves activation of G_i/G_o proteins and a subsequent decrease in cAMP production. Post-junctional α_2–AR stimulation may also cause a pressor response by indirectly activating voltage-dependent Ca^{2+} channels or by increasing the sensitivity of the contractile apparatus to Ca^{2+} [188, 230]. This type of contraction may occur in blood vessels, stomach muscle, trachea, and anococcygeus muscle [36, 38, 76]. Conversely, inhibition of pre-junctional α_2–ARs may cause membrane hyperpolarization and vasorelaxation of rat mesenteric and femoral arteries by inhibiting voltage-dependent channels or by opening K^+ channels [66, 93, 215].

iii) β–Adrenoceptors

Like their "excitatory" counterparts, β–adrenoceptors have also been extensively studied and characterized in numerous tissue types, including heart, adipose tissue, vascular and non-vascular smooth muscles, placenta, lung, pancreatic islet, and skeletal muscle [38, 85, 173, 260]. Pharmacologically and functionally, there are three subtypes of β–ARs. They are differentiated partially by their affinity for both NE and epinephrine [38]. Epinephrine is more potent for β_2– than for β_1–ARs, while NE is equipotent for both. With β_3–ARs, NE is more potent than epinephrine.

β_1–ARs are responsible for *i*) increasing heart rate and potentiating contraction, *ii*) stimulating renin secretion, and *iii*) causing relaxation of vascular and non-vascular smooth muscles [38]. Compounds such as donopamine and xamoterol activate this subtype, while metoprolol, atenolol and betaxolol inhibit its activity [38]. β_2–ARs are primarily responsible for the relaxation of vascular and non-vascular (trachea, uterus) smooth muscles [38]. Terbutaline, salbutamol, and zinterol are relatively specific agonists; butoxamine and ICI 118,551 are representative antagonists [38]. Finally, β_3–ARs have the most diverse functions

of all three subtypes [38]. They are involved in *i*) lipolysis and thermogenesis in white and brown adipose tissue, respectively, *ii*) stimulation of insulin secretion, *iii*) inhibition of glycogen secretion, *iv*) inhibition of contractile activity in gastrointestinal smooth muscle and VSM. The known agonists for the β_3–AR are still highly experimental (BRL 37344, ICI 198,157, and CL 316,243). There is one β_3-AR antagonist ICI 118,551 [38].

The common element between these three receptor subtypes is the signal pathway involved. In all cases, β–ARs are coupled with the stimulatory G_s protein, resulting in activation of adenylate cyclase and increased production of cAMP.

C. Neurohumoral and hormonal control

In addition to being released from nerve terminals, catecholamines are also produced by the adrenal gland and released into the circulation. Epinephrine has a varying effect depending on its concentration in the bloodstream and in/on the target tissue. At low concentrations, epinephrine has a vasodilatory effect that occurs via interaction with β_2–adrenoceptors, while contraction of blood vessels occurs via interactions with α–receptors at higher catecholamine concentrations [74]. Since its effect on α–adrenoceptors is predominant over that on β–adrenoceptors, circulating NE generally contracts blood vessels [38, 74]. Because of the proximity of nerve terminals to the effector muscles, the effect of NE released from the adrenal gland is less important than that of NE released at the neuromuscular junction [24, 74]. The effects of these catecholamines occur via mechanisms described in the previous section on the nervous control of vascular tone.

In addition to catecholamines, other vasoactive agents, e.g. endothelin, vasopressin or angiotensin II, produce powerful vasoconstrictions when they are produced and released into the body [19]. For each of these compounds, there is one or more sarcolemmal receptor. For

endothelin, these are the ET_A and ET_B receptors [90, 250, 322]. Vasopressin couples with V_{1A}, V_{1B}, and V_2 receptors on VSM cells [133]. Angiotensin interacts with AT_1 and AT_2 receptors to cause vasoconstriction, salt and water retention, aldosterone release, etc. [106, 284]. These are but a few examples of the neurotransmitters and other hormone messengers which control cardiovascular function.

In smooth muscles, neurohumoral and hormonal agents target ion channels. For example, vasoconstrictors such as angiotensin II, NE, endothelin, vasopressin, histamine, and serotonin activate Ca_L channels (directly or indirectly) [19, 61, 111, 121, 210, 276, 288, 322]. Well-known vasodilators such as acetylcholine and bradykinin inhibit Ca_L activity [19, 195]. Potassium channel activation is typically associated with vasorelaxation, as will be discussed in a subsequent section. Thus, their activation is targeted by adenosine, nitric oxide and calcitonin gene-related peptide, all powerful vasodilators [28, 41, 237, 267]. Conversely, their inhibition by endothelin and angiotensin II is also anticipated [30, 56, 258].

D. Agonist-enhanced myogenic reactivity

In the study of Cl^- channels, I have examined the contraction of vessels in response to increased transmural pressure in the absence of pharmacological agonists. The response under these conditions has been termed a "myogenic response" and conforms to the traditional definition of this physiological process. In my experiments, phenylephrine (PE), an α_1–adrenergic agonist, enhanced arterial responsiveness to increased transmural pressure. These contractions were similar in profile, but larger in amplitude, compared to the myogenic responses without agonist. This enhancement of the tissue's reactivity to pressure by NE has been reported previously in rat cremaster arterioles [191] {Fig. *3*}. The extent of the pressure-induced response is independent of the amount of contraction generated by NE, thus of NE

concentration, but is thought to rely heavily on increased activation of nifedipine-sensitive Ca_L channels, basal protein kinase C activity, and Ca^{2+} sensitivity of the contractile mechanism [91, 153, 164, 191]. Because of its characteristics, this enhanced response has also been described as a form of myogenic contraction [191]. In light of the classical definition of the myogenic response and its apparent enhancement by norepinephrine stimulation, the term "agonist-enhanced myogenic reactivity" was used subsequently to describe this phenomenon in our preparation.

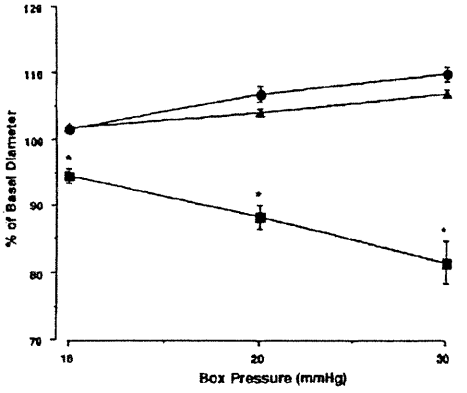

Fig. 3 Enhancement of arteriole myogenic behavior by NE [191]

Under basal conditions (●), after treatment with 30 mM KCl (▲), and after treatment with 0.2 – 2 μM NE (■). NE induced myogenic responsiveness.

Since vascular tone is a slave of cytosolic calcium content, which itself is largely determined by membrane potential, it is important to better understand the forces that control membrane potential. It is long known that hyperpolarizing membrane ionic currents (such as potassium currents that drive membrane potential in a negative direction) relax vascular tone, and depolarizing membrane ionic currents (such as sodium, calcium, and chloride currents that drive membrane potential in a positive direction, toward 0 mV) increase vascular tone. From this point, the focus of the discussion will center on ion channels and how they modulate arterial tone. The overview will be divided into two sections: *i)* the contribution and modulation of potassium channels to the maintenance of the resting membrane potential in vascular myocytes, and *ii)* the contribution of calcium and chloride channels in stimulated or active vascular myocytes.

I-3 Resting membrane potential and vascular tone

The membrane potential of VSM cells is an important regulator of arterial tone. In arterial smooth muscle, as in other excitable and non-excitable cells, membrane potential is generated by the interplay of various ion conductances. The major ions involved in establishing membrane potential are sodium (Na^+), potassium (K^+), calcium (Ca^{2+}), and chloride (Cl^-). Membrane potential depends on the relative permeability of the membrane to these ions (P_x/P_{total}) and their respective electrochemical gradients as determined by the Hodgkin-Huxley-Katz and Nernst equations {Fig. *4*}. The ion channels and pumps (secondary transporters, ATP-driven, uniporters) that maintain ion gradients across the cell membrane, are not fully active in all tissue types [217], nor do they always distribute themselves evenly on the sarcolemma of different cells within the same vascular bed [12]. This is due to metabolic or functional states, or, more importantly, due to cell diversity within the tissue [11, 32], *i.e.* phenotypically, and functionally different cells within a vascular bed.

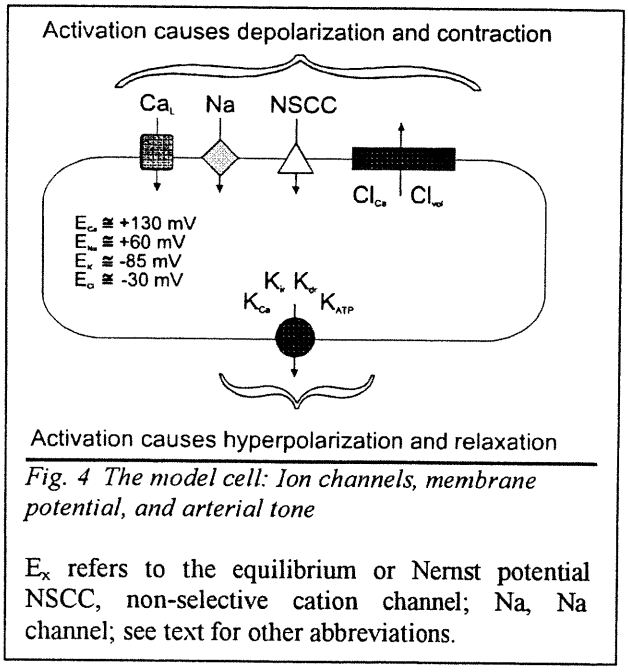

Fig. 4 The model cell: Ion channels, membrane potential, and arterial tone

E_x refers to the equilibrium or Nernst potential NSCC, non-selective cation channel; Na, Na channel; see text for other abbreviations.

A. Potassium channels

The electric potential difference recorded across the membrane of living cells at rest is called the resting membrane potential (RMP). In vascular smooth muscle, RMP ranges between -50 and -70 mV [149, 183]. At these potentials, the cells are said to be

"hyperpolarized" relative to the voltage range at which they will contract. For K^+ ions, the reversal potential is approximately –85 mV in smooth muscle cells. In many cell types, including VSM, K^+ channels are mainly responsible for maintaining RMP (or hyperpolarizing membrane potential), although there is a minor contribution from other ion channels in various cell types. Activity of K^+ channels also affects the activity of other ion channels. Membrane hyperpolarization, due to K^+ channel opening, closes Ca_L channels (which only open at membrane potentials > -50 mV) and leads to relaxation and vasodilation. On the other hand, closing of K^+ channels causes depolarization (shifting of membrane potential to more positive potentials), which then activates Ca_L and triggers Ca^{2+} influx and contraction {Fig. *4*}.

	Activators	***Inhibitors***
K_{Ca}	Ca^{2+}, EDHF, NO, NS1619 [28, 140, 209]	IbTx, ChTx, TEA, Mg^{2+}, Na^+ [35, 201, 209]
K_{dr}	ATP, NO, PKA [6, 89, 190, 326]	4-AP, Ca^{2+}, phencyclidine, TEA, tedisamil, quinidine [104, 142, 186, 209, 222, 232, 297]
K_{ATP}	ADP, levcromakalim, CGRP, cromakalim, lemakalim, NO, pinacidil, minoxidil sulfate, diazoxide [53, 68, 159, 205, 239, 267]	ATP, TEA, glibenclamide (sulfonylureas) [209, 239]
I_{to}		4-AP [22]
K_{ir}		Ba^{2+}, Mg^{2+} Cs^+ [22, 238, 245]

Table 2: Modulators of K^+ channels present in vascular smooth muscle

Agents are listed in their approximate order of potency. ADP, adenosine diphosphate; 4-AP, 4-aminopyridine; ATP, adenosine triphosphate; Ba^{2+}, barium; CGRP, calcitonin-gene related peptide; ChTx, charybdotoxin; Cs^+, cesium; EDHF, endothelium-derived hyperpolarizing factor; IbTx, iberiotoxin; Mg^{2+}. magnesium; NO, nitric oxide; TEA, tetraethylammonium

There are at least five different types of potassium channels currently identified in VSM. They are the Ca^{2+}-activated K^+ channel (K_{Ca}), the delayed rectifier K^+ channel (K_{dr} K_V), the ATP-sensitive K^+ channel (K_{ATP}), the transient outward channel (I_{to}), and the inward

rectifier K^+ channel (K_{ir}). They are listed in *Table 2*, along with some of their pharmacological properties.

Both K_{Ca} and K_{dr} channels are present in numerous vascular [35, 109, 156, 166, 170, 186, 198, 206, 309] and non-vascular [94, 148, 238, 298, 308] smooth muscle cells from multiple species. K_{ATP} channels have also been studied closely and, to date, have been identified in a few VSM types, including rabbit pulmonary and mesenteric arteries [53, 205, 239, 267]. I_{to} channels are present in VSM [22, 111, 221] and cardiac muscle [25, 81], and participate in the rapid early repolarizing phase of the action potential (phase 1). K_{ir} channels have been the least studied of the K^+ channels in VSM and have been identified in just a few tissues to date [238, 245, 308]. It has been found that K_{ir} channels are more abundant in resistance than conduit vessels [238].

The variety of potassium channels makes it possible for each to be active under different conditions. For example, K_{ATP} channels are involved in vasodilator responses to metabolic changes in the cell (e.g. hypoxia) and those due to naturally occurring vasodilators (e.g. CGRP, NO) [205, 239, 267]. K_{ir} is more active at very negative membrane potentials and is more abundant in small arteries and arterioles. It is likely to control RMP in unstimulated cells, but its precise role is unclear [209]. K_{Ca} has been implicated in the feedback mechanism regulating the myogenic response [35], as well as in the vasodilating actions of nitric oxide (NO) [26, 28] and estrogen [314]. K_{dr} channels, for their part, represent the major conductance regulating RMP in many VSM [170, 186, 206] and will be the focus of the upcoming subsection.

B. Delayed rectifier K^+ channels

The delayed rectifier K^+ channel (K_{dr}) is a member of a larger family of voltage-dependent K^+-conducting (K_V) channels activated by membrane depolarization. The family's nomenclature describes how K^+ efflux through the channel increases with membrane depolarization, due to increases in the open probability of the channel and in the driving force for K^+ efflux. K_{dr} channels have been identified in vascular [104, 110, 141, 170, 186, 262, 286, 324] and non-vascular [33, 43, 94, 144, 146] smooth muscles, as well as in neurons [15], lymphocytes [51], and cardiac myocytes [253, 292, 331]. Despite their rampant distribution, the channel proteins are unevenly and differentially distributed in VSM membranes [12].

This family of channels has been cloned from various sources [44, 128, 162, 248, 270, 319, 328]. The functional channels themselves consist of four pore-forming α subunits, associated with four regulatory cytoplasmic β subunits ($\alpha_4\beta_4$ complex). The K_V channel gene family can be further broken down into at least 11 subfamilies [328]: *Shaker* ($K_V1.1$-$K_V1.7$), *Shab* ($K_V2.1$-$K_V2.2$), *Shaw* ($K_V3.1$-$K_V3.4$), *Shal* ($K_V4.1$-$K_V4.3$), K_VLQT, EAG, K_V5 ($K_V5.1$), K_V6 ($K_V6.1$), K_V7, K_V8 ($K_V8.1$) and K_V9 ($K_V9.1$-$K_V9.3$). The K_V5, K_V6, K_V8, and K_V9 subfamilies are electrically silent K_V channel regulatory α subunits, i.e. they do not produce K^+ channel current when expressed alone. However, when they are co-expressed with other functional K_V α-subunits (e.g. $K_V1.5$), they can modulate the expression and the biophysical properties of K_V channels [328]. Non-inactivating K_{dr} channels are typically encoded by one of seven α subunits in vascular smooth muscle: $K_V1.1$, $K_V1.2$, $K_V1.5$, $K_V1.6$, $K_V2.1$, $K_V2.1$/ $K_V9.3$, and $K_V4.3$ [13, 44, 128, 162, 224, 247, 248, 270, 328]. The cloned K_{dr} channels are electrophysiologically (activation threshold, conductance) and pharmacologically (sensitivity to 4-aminopyridine) similar to their native counterparts in VSM. However, they do vary in

terms of their distribution, expression levels, sensitivity to various blockers (including 4-aminopyridine), inhibition mechanism, gating kinetics. In addition, from the known β subunits ($K_V\beta1.1$-$K_V\beta1.3$, $K_V\beta2.1$, and $K_V\beta3.1$) which regulate channel inactivation by associating with the α-subunits [243, 328], at least three are expressed in rat pulmonary artery ($K_V\beta1.1$, $K_V\beta2.1$, and $K_V\beta3.1$) [327].

i) Biophysical properties of K_{dr}

One important property of K_{dr} channels is their activation by membrane depolarization in a time- and voltage-dependent manner [21, 33, 94, 229, 296]. The current ($I_{K(V)}$) deactivates in a time-dependent fashion following repolarization [296], and displays slow inactivation during long (in the order of seconds) depolarizing steps [33, 94, 229, 258, 324], a process which is also voltage-dependent. Its conductance in VSM at physiological (~5 mM internal, ~140 mM external) K^+ concentrations ranges between 5 and 11 pS [21, 296], and ranges from 15 up to 70 pS in symmetrical (140 mM) potassium conditions [5, 103, 142].

ii) Modulation of channel activity by endogenous factors

K_{dr} activity is modulated not only by voltage, but also by phosphorylation. Protein kinase C (PKC) inhibits K_{dr} channels. More precisely, upon stimulation by either angiotensin II [56, 104, 106] or endothelin [250, 258], K_{dr} is inhibited due to subsequent PKC activation and ensuing channel phosphorylation. However, in cardiac myocytes, PKC activates K_{dr} channels [281, 291, 299]. Conversely, protein kinase A, activated by β–adrenergic stimulation of adenyl cyclase, activates K_{dr} channels in rabbit portal vein [6], frog atrium [84] and guinea pig ventricle [299].

Variations in the metabolic environment also modulate K_{dr}. There are indications that pH changes, either intra- or extra-cellular, influence K_{dr} activity [3, 23]. Intracellular ATP can

activate K_{dr} independently of K_{ATP} activity [89]. In addition, internal calcium and magnesium ions inhibit K_{dr} currents in frog atrium [84] and canine renal artery [103-105]. Finally, arachidonic acid, whose metabolites modulate K_{Ca} activity in VSM [188, 256], blocks K_{dr} currents in rat pulmonary arterial myocytes [263].

iii) Physiological roles of K_{dr}

The primary role of delayed rectifier K^+ currents in VSM is to maintain the resting membrane potential hyperpolarized relative to potentials that can activate Ca^{2+} entry [186, 198, 221, 236, 264, 325]. Since $I_{K(V)}$ is slow to activate, membrane potential in a stimulated or excited cell may transiently depolarize and produce a contraction, However, studies agree that, at low to normal intracellular Ca^{2+} levels, $I_{K(V)}$ represents the dominant repolarizing conductance within the physiological range of membrane potentials (-50 to 0 mV). Increasing transmural pressure [126, 127, 170] and agonist stimulation [111, 167, 258] can cause membrane depolarization well within the –50 to 0 mV range. Thus, it is not surprising that K_{dr} activation regulates myogenic reactivity (pressure-induced) [164, 170, 274].

Phasic smooth muscle [21], cardiac tissue [216, 259], and neurons [135] all share a common property: the ability to generate action potentials. In these tissues, K_{dr} activation is involved in the repolarizing phase {Fig. 5}.

Clinically, K_{dr} channels have been implicated as prime regulators of hypoxia-induced pulmonary vasoconstriction. Indeed,

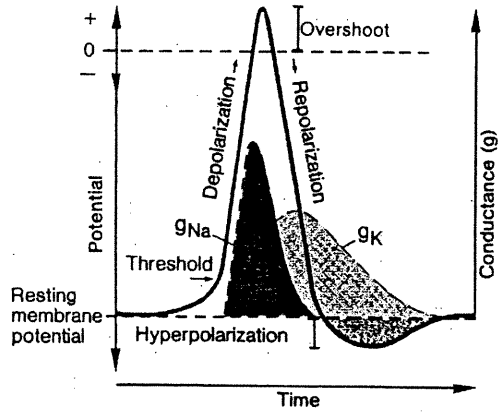

Fig. 5 The neural action potential: contribution of Na^+ and K^+ conductances [75]

Note that K^+ conductance increases during th repolarization phase of the action potential.

K_{dr} channels are inhibited under hypoxic conditions [229, 264, 325]. This may be due to different factors, including pH alteration [3], a rise in the intracellular Ca^{2+} concentration [102, 235], a change in the cellular redox potential [229], or selective gene expression of $K_V\alpha 1.5$ and 2.1 subunits [13, 301]. The latter is also observed in the case of primary pulmonary hypertension [328]. In addition, patients suffering from pulmonary hypertension exhibit pulmonary vasodilation when treated with inhaled NO. In this case, NO actually increases the open probability of K_{dr} channels, causing membrane hyperpolarization, lowered intracellular Ca^{2+}, and vasodilation [190, 326]. There is supporting evidence that the vasodilatory effect of NO occurs via the secondary activation of a 4-AP-sensitive mechanism, likely K_{dr} channels, in rat basilar [265] and pulmonary [329] arteries.

iv) Pharmacology

4-Aminopyridine (4-AP) has been used as a relatively selective inhibitor of both sustained and transient types of delayed rectifier K^+ channels that belong to the superfamily of voltage-gated K^+ channels. In VSM, half-maximal inhibition ($K_{½}$) of K_{dr} is achieved by 0.3 – 0.7 mM 4-AP at +10 mV [103, 221]. At these concentrations, 4-AP has no effect on K_{Ca} or K_{ir}, but may inhibit K_{ATP} [20]. 4-AP has also been shown to block an "I_A-type" of transient outward K^+ current in smooth muscle cells [22, 295].

Despite its common use in distinguishing between the different K^+ channels, few studies have elucidated the mechanisms involved in the inhibition of K_{dr} by 4-aminopyridine in VSM. A few have suggested the following mechanisms of action in different cell types. *i*) 4-AP decreases the open probability of the channel, with no effect on the amplitude of single channel unitary currents [33, 248]. *ii*) Either ionized or non-ionized, 4-AP permeates the membrane to bind the channel from the inside [221]. *iii*) 4-AP inhibition is less effective at

more positive potentials, suggesting that the binding of 4-AP may be less favorable when the channel is in the open state [103, 186, 221, 246, 296]. Despite these possibilities, the actual mechanism of action of 4-AP on native K_{dr} has not been determined in vascular smooth muscle cells.

Studies on the mechanism of action of 4-AP on various cloned K_{dr} channels have shown that 4-AP causes use-dependent, and open-state inhibition of $K_v1.1$, 1.2 and 2.1/3.1 clones [44, 162, 248, 270]. There has, however, been a report of closed-state block of $K_v1.1$ [270]. Nonetheless, it is commonly believed that 4-AP remains trapped within the closed channels and that block is relieved by channel activation. In all cases, the binding site for 4-AP appears to be intracellular [162, 270].

In addition to 4-aminopyridine, smooth muscle K_{dr} is also inhibited to varying degrees by tedisamil [232], phencyclidine [20, 21, 141], quinine [144], quinidine [20], the non-specific K^+ channel inhibitor tetraethylammonium (TEA) [21, 103, 142, 221], the K_{Ca} activator NS1619 [140], and by the tyrosine kinase inhibitors genistein and ST-638 [262].

v) Proposed research plan

K_{dr} activation is crucial to the maintenance of the resting membrane potential, and thus of basal tone in vascular smooth muscle. Understanding the interactions between pharmacological agents and their target channels at the molecular level helps to direct the engineering of better, more specific pharmacological tools that may be applied clinically in pathologies such as hypoxic pulmonary vasoconstriction and other hypertensive states. The identification of K_{dr} currents in smooth muscle has relied quite extensively on the use of 4-AP to distinguish it from other K^+ currents. In the last decade, however, the use of pharmacological tools has been overshadowed by the advent of molecular biology and

cloning techniques. It is now possible to positively identify K_{dr} channels by verifying for their expression in addition to showing the existence of the currents by more conventional electrophysiological and pharmacological isolation techniques.

4-Aminopyridine, being a highly specific inhibitor of K_{dr} channels, is a compound worthy of a more thorough investigation in native smooth muscle cells for two main reasons. *i*) Concrete knowledge on the mechanism of action of 4-aminopyridine on smooth muscle K_{dr} channels is lacking. *ii*) Information gained on the action of 4-AP may provide a better understanding of the molecular architecture and function of native vascular K_{dr} channels based on the interaction of 4-AP with different channel α subunits within the tetramers. Therefore, we propose to elucidate the biophysical interaction responsible for the inhibition of K_{dr} channels by 4-AP in freshly isolated rabbit coronary artery smooth muscle cells.

I-4 Electrical properties of VSM cells during stimulation

Stimulation of VSM often involves depolarization of the membrane from a resting state, enhancing Ca^{2+} entry into the cell and causing an elevation of intracellular Ca^{2+} levels and contraction by activation of myosin light chain kinase [71, 285]. The next few paragraphs will review some of the basic ionic mechanisms that have been postulated to participate in the depolarization initiated by various stimuli, with more emphasis on the role of voltage-gated Ca^{2+} currents and Cl^- conductances in determining membrane potential and tone.

A. Voltage-dependent Ca^{2+} channels

Ca^{2+} channels can be subdivided into a few families [272, 320]. In VSM, the most familiar are the voltage-dependent high-threshold L-type Ca^{2+} channels (Ca_L). These are the

slowly-inactivating dihydropyridine-sensitive channels activated at membrane potentials positive to –50 mV. The low-threshold T-type Ca^{2+} channels (Ca_T) have only been identified in a few VSM types, inactivate more quickly and are typically activated at more negative membrane potentials than Ca_L. The role of Ca_T channels in VSM remains to be determined. As such, our discussion limits itself to the role of Ca_L channels in agonist- and pressure-mediated phenomena.

Ca_L currents have been extensively studied in VSM. They are involved in the myogenic response [14, 196, 289, 310], and are directly activated by the vasoconstrictors endothelin [156, 249], vasopressin [288], norepinephrine [61, 191, 193, 194, 225, 228], serotonin [61], PACAP [50], and histamine [142]. Since influx of extracellular Ca^{2+} occurs mainly via Ca_L in VSM, Ca_L is a major determinant of vascular tone [208]. As a result, inhibition of Ca^{2+} channels decreases cytosolic Ca^{2+} available for contraction and causes relaxation. Alternatively, enhanced Ca^{2+} influx via Ca_L can also activate K_{Ca} channel and cause membrane hyperpolarization and cell relaxation. Ca^{2+} channel inhibition can result from a change in oxygen tension [95, 96], pH changes [166, 168, 311], or the production of vasoactive agents such as NO [240].

B. Cl^- Conductances

Chloride channels are distributed in various tissue types and have been implicated in volume regulation, transepithelial ion transport, and modulation of electrical excitability of the cell. These channels include the ligand-gated channels (γ-aminobutyric acid –GABA, and glycine receptors), voltage-gated Cl^- channels (ClC family), ATP-binding cassette transporters (cystic fibrosis transmembrane regulator –CFTR), and the recently characterized

Ca^{2+}-dependent Cl^- channel class. Many members of each superfamily have been cloned and studied extensively because of their clinical importance (CFTR, P-glycoprotein, GABA). In recent years, much interest has been focused on the voltage-gated Cl^- channels, especially since the first member, ClC-0, was cloned from the ray *Torpedo* electroplax in 1990 [152]. The superfamily has since expanded to include at least nine gene families from various mammalian tissues. {*Table 3*}

Clone	*Expression source*	*Physiological function*	*References*
ClC-0	Torpedo marmorata electroplax	Membrane potential stabilization	[152]
ClC-1	Rat skeletal muscle	Membrane potential stabilization Myotonia congenita	[268]
ClC-2	Epithelium, fibroblasts, neurons; heart; lung; pancreas	Cell volume regulation	[279]
ClC-3	Kidney, liver, brain; vascular smooth muscle	Cell volume regulation ??	[83, 156]
ClC-4	Liver, brain, kidney, heart, spleen, skeletal muscle	Prevention of kidney stones ??	[151]
ClC-5	Brain, kidney	Dent's disease Prevention of proteinuria, hypercalciuria and kidney stones	[269]
ClC-6	Kidney, brain, testes	SR function ??	[34, 37]
ClC-7	Kidney, brain, testes	??	[34, 37]
ClC-Ka/b	Kidney	Bartter's syndrome Kidney stone disease	[160, 278]

Table 3: Cloned voltage-gated Cl^- (ClC) channels

See Jentsch & Günther, 1997 [150] for a full review.

In smooth muscle [29, 83, 115, 178, 317], cardiac tissue [82, 318], neurons [184, 252], epithelia [266], neutrophils [271], and endothelial cells [212, 293], a volume-sensitive Cl^- channel (Cl_{vol}) has been identified which may correspond to either ClC-2 or ClC-3. Another Cl^- channel activated by calcium (Cl_{Ca}) does not yet figure among the family of voltage-gated Cl^- channels. However, a Ca^{2+}-activated Cl^- channel was cloned from bovine epithelial cells some years ago [63]. Since then, several members of this new family of Cl^- channels with some primary sequence homology to the ClC family have been cloned from the mammary

gland, and respiratory and digestive tracts of several species, including human [1, 100, 116, 117]. Evidence from the literature suggests that these channels are not ubiquitously expressed. Also, the cloned Cl_{Ca} channels expressed in heterologous cell systems do not display some of the properties (e.g. sensitivity to niflumic acid, voltage-dependence, single channel conductance) typical of the Cl_{Ca} channels identified in vascular myocytes. Whether the Cl_{Ca} channel expressed in VSM belongs to the cloned Cl_{Ca} family is presently unknown.

Cl^- currents are depolarizing currents (Cl^- equilibrium potential ranging between –35 and –25 mV in VSM [4]) which are postulated to cause vasoconstriction in various smooth muscle types. To counterbalance the depolarizing and vasoconstricting effects of Cl^- and Ca_L activation, the cell must activate a feedback mechanism to return the cell to a more relaxed and rested state. The depolarization by Ca_L activation activates voltage-dependent K_{dr} and K_{Ca} channels, leading to membrane hyperpolarization. The Ca^{2+} influx generated by Ca_L activation also can lead to relaxation in a few ways. First, the cell possesses ATP-dependent Ca^{2+} transporters which cause Ca^{2+} either to be extruded into the extracellular space or to be pumped into the sarcoplasmic reticulum where it will be stored. Secondly, intracellular Ca^{2+} can activate K_{Ca} channels, which will then drive the membrane potential down to more negative values and return the cell to a relaxed state. A recent observation that Ca^{2+} entry through Ca_L channels can indirectly activate K_{Ca} in VSM [120] provides evidence for a localized regulatory feedback mechanism that regulates membrane potential and vascular tone.

In the next two major sections, I will expand on the properties, roles, regulation, and pharmacology of the two Cl^- conductances currently identified in VSM cells: the Ca^{2+}-activated and the volume-sensitive (swelling-dependent) Cl^- channels. This will establish the

basic framework of this study on their roles in both the myogenic response and α_1–adrenoceptor stimulation.

a) Ca^{2+}-activated Cl^- channels

Ca^{2+}-dependent Cl^- (Cl_{Ca}) channels have been identified in many VSM types: portal vein [40], pulmonary artery [54, 228, 303, 323], aorta [136, 287], coronary artery [179, 185], cerebral artery [244], mesenteric artery [61, 131, 165], and afferent arteriole [276]. In addition, they have been recorded in non-vascular smooth muscle cells from the airway [7, 146, 147, 298], urethra [58], and neurons [64].

i) Sources of Ca^{2+} triggering Cl_{Ca} channels

Cl_{Ca} channels are activated by various stimuli, including Ca^{2+} entry through L-type Ca^{2+} channels [323], reverse-mode Na^+-Ca^{2+} exchange [185], and spontaneous cyclic Ca^{2+} release from the sarcoplasmic reticulum [138]. In addition, the vasoconstriction associated with hormones, catecholamines, and neurotransmitters has also been linked to Cl_{Ca} activation. More specifically, endothelin [156, 167, 250, 276, 287], vasopressin [287], norepinephrine [10, 39, 40, 60, 177, 194, 228, 286, 303], angiotensin II [121, 276, 312], serotonin (5-hydroxytryptamine) [61], and acetylcholine [14] all activate a small conductance (1.8 – 3.1 pS) [276, 287] Cl_{Ca} channel in smooth muscle myocytes. All of the aforementioned agents cause Ca^{2+} release from the sarcoplasmic reticulum, suggesting that intracellular Ca^{2+} plays a central role in regulating this channel. In addition to the agonist-stimulated current, it is possible for Cl_{Ca} to be activated upon spontaneous bursting Ca^{2+} activity from the sarcoplasmic reticulum, generating the "spontaneous transient inward currents" (STICs) that induce transient depolarizations in current clamped cells [199, 332].

It is now well known that NE induces vasoconstriction and membrane depolarization via activation of an α_1–AR / $G_{q/11}$ /PLC complex which results in IP_3 and DAG production and Ca^{2+} mobilization in the cell [36, 193, 194, 214, 302] {Fig. *6*}. The ionic mechanism underlying the NE-induced vasoconstriction is not completely understood. However, there is evidence that, in addition to Cl_{Ca} channels, NE can activate K_{Ca} channels [8, 138], non-specific cation channels (NSCC) [8, 134, 302], and Ca_L channels [188, 210] in VSM. The activation of Ca_L channels by α_1–AR stimulation has been disputed [73, 87]. Thus, the question remains unanswered: which, if any, of these proteins is responsible for the vasoconstriction produced by NE?

Intracellular calcium ions activate Cl_{Ca}. However, the threshold intracellular Ca^{2+} concentration ($[Ca^{2+}]_i$) necessary to activate Cl_{Ca} varies between cells [226, 227], so it is unclear precisely how much $[Ca^{2+}]_i$ is required to trigger activation. It is also unknown whether $[Ca^{2+}]_i$ must remain at this minimum concentration to prevent channel inactivation. Alternatively, is it possible that the purported voltage-dependence of Cl_{Ca} "takes over" soon after the threshold $[Ca^{2+}]_i$ has been surpassed [39, 167]?

ii) Possible regulation by phosphotransferase reactions

Emptying intracellular Ca^{2+} stores with caffeine, or preventing Ca^{2+} release from the sarcoplasmic reticulum with heparin, abolishes Cl_{Ca} activation by various agonists [10, 167, 225, 228]. Thus, it has been suggested that phosphorylation/dephosphorylation processes are not involved in the modulation of Cl_{Ca}. However, a Ca^{2+}/calmodulin-dependent protein kinase II (CaMKII) has been shown to have different effects on Cl_{Ca} channels in different cell types. For instance, CaMKII inhibits Cl_{Ca} in cultured human colonic HT-29 cells [202], cultured human biliary Mz-ChA-1 cells [255], and equine tracheal cells [304]. On the other

hand, the same CaMKII activates Cl_{Ca} in cultured human colonic T84 cells [315, 316]. Thus, the potential role of CaMKII activity is unresolved. A study by Loirand *et al.* [194] in rat portal vein myocytes has demonstrated that phorbol esters cannot activate Cl_{Ca} channels, hence negating an involvement of protein kinase C (PKC). In fact, that same study has suggested that NE-induced activation of Cl_{Ca} involves IP_3 production via PLC activation, but that PKC stimulation by diacylglycerol does not play a role. This observation has been verified in bovine tracheal cells [251]. However, other studies have shown that activation of PKC can have inhibitory [80, 82, 192], stimulatory [79, 155, 256], or null [52] effects on various Cl^- channels in different myocyte types.

iii) Physiological role

There are questions remaining as to the role of Cl_{Ca} channels in excitation-contraction

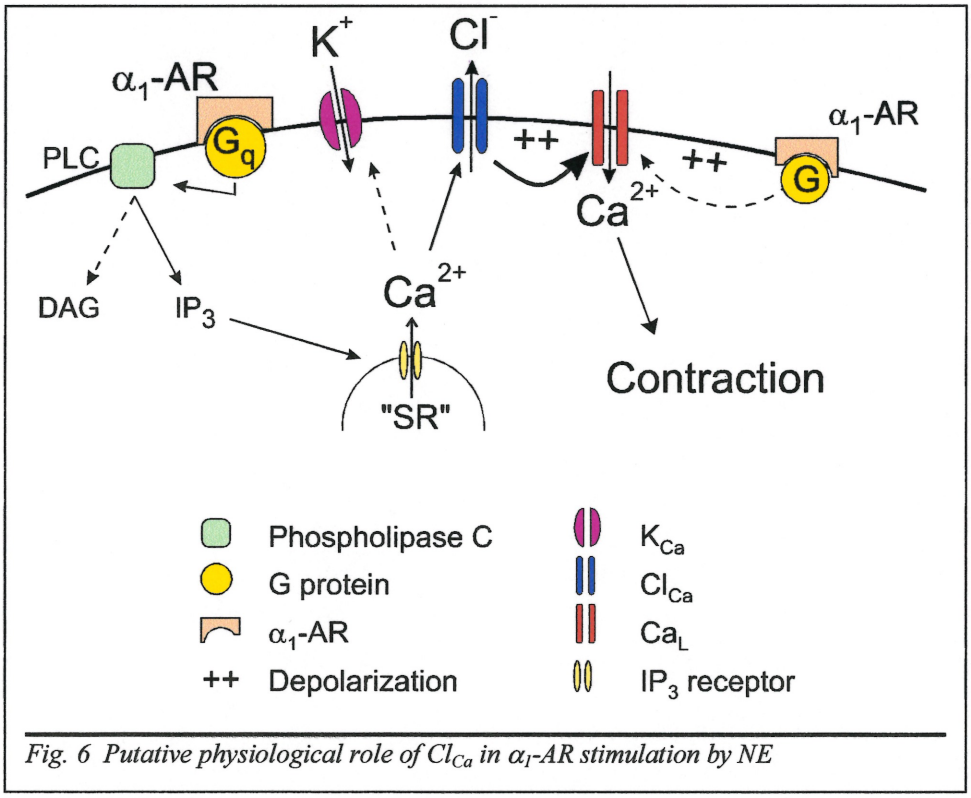

Fig. 6 Putative physiological role of Cl_{Ca} in α_1-AR stimulation by NE

coupling and the myogenic response. Few studies have been performed which have

systematically studied the role of Cl_{Ca} channels in both the vasoconstriction *and* the depolarization induced by NE. There are indications that Cl_{Ca} activation by cytosolic Ca^{2+} causes a depolarization, which then activates Ca_L, with the latter leading to further cytosolic Ca^{2+} release, and, ultimately, to contraction in isolated myocytes [40, 165] {Fig. *6*}. This scheme explains how the cell membrane potential can become depolarized by Cl_{Ca} activation, despite the hyperpolarization due to simultaneous K_{Ca} activation [35, 206] by the increased cytoplasmic Ca^{2+}. It also explains how the cell can maintain its Ca^{2+} homeostasis if a series of small releases were to activate sodium-calcium exchange which, by itself, could only extrude Ca^{2+}. However, there are conflicting studies which argue against a role for Cl_{Ca}, and the need for its activation, in the generation and, more importantly, in the maintenance of tone.

As indicated earlier, NE can directly stimulate Ca_L channels in rabbit mesenteric myocytes [210]. On the other hand, studies in rabbit portal vein and rat afferent arterioles suggest that NE- [225] and angiotensin- [276] induced vasoconstrictions are due to Cl_{Ca} channel activation via mobilization of internal Ca^{2+} stores, which subsequently activates Ca_L channels. This putative role of Cl_{Ca} has been proposed from observations in isolated myocytes. The few studies that have been performed in multicellular preparations have ascertained that Cl_{Ca} channel activation can account for approximately 30% of α_1–AR- and 5-HT-induced tone in intact (vessel or rings) rat aorta, mesenteric artery, and pulmonary artery [60, 61, 323].

The depolarization by α_1–adrenergic stimulation is well-documented [39, 122, 225, 228], and it is only logical to assume that Cl_{Ca} channels, which depolarize the membrane when activated, may underlie this effect. Unfortunately, no multicellular preparation studies

have focused on the potential modulation of NE-induced membrane depolarization by Cl_{Ca} channels.

The role of Cl_{Ca} in the myogenic response is also unclear. Takenaka *et al.* [276] have demonstrated that the cellular mechanisms mediating pressure-induced vasoconstriction of afferent arterioles involve activation of Ca_L independently of Cl_{Ca}. One recent study in intact rat cerebral arteries has, nonetheless, identified a Cl_{Ca} channel sensitive to both IAA-94 and niflumic acid which *does* modulate myogenic tone [244]. Nevertheless, the role of Cl_{Ca} in the myogenic response also remains obscure.

iv) Pharmacology

As with other ion channels, the study of Cl_{Ca} has been facilitated by the availability of inhibitors. Numerous antagonists have been tested in cardiac tissue [57, 333], vascular [7, 17, 113, 114, 138, 202] and non-vascular [130, 147] smooth muscle, endothelium [211], neurons [64], and *Xenopus laevis* oocytes [313].

Currently, the most commonly used agents are indanyloxyacetic acid (IAA-94), stilbene derivatives (DIDS, SITS), anthracene-9-carboxylic acid (9-AC), and niflumic acid (NfA), with a potency ranking of NfA > IAA-94 > DIDS > 9-AC > SITS in rabbit portal vein [183]. These compounds block Cl_{Ca} in different tissues to varying degrees, but they share one particular feature: a relatively low degree of selectivity, as indicated in *Table 4*. A large proportion of these agents share the property of also activating K_{Ca} channels in vascular smooth muscle [114, 138, 139, 223, 282]. Many have circumvented this problem by using K^+-free media, or by including K^+ channels inhibitors such as TEA in the medium to study the role of Cl_{Ca} channels.

Inhibitor	*Non-specific effect*	*Tissue*
Anthracene-9-carboxylic acid (9-AC)	+ K_{Ca}	rabbit portal vein [139, 282]
	- Ca_L	rat cerebral artery [78]
	+ Cl-cAMP	guinea-pig ventricle [330]
Indanyloxyacetic acid (IAA-94)	+ K_{Ca}	rabbit portal vein [282]
	- Ca_L	rat cerebral artery [78]
Ethacrynic acid	+ K_{Ca}	rabbit portal vein [282]
Fenamates (niflumic acid, mefenamic acid, flufenamic acid)	+ K_{Ca}	rabbit portal vein [114, 138] porcine coronary artery [223]
	+ K_{ATP}	rat portal vein [161]
	- NSCC	rat exocrine pancreas [107]
	- Ca_L	rat aorta [177]
Stilbene derivatives (DIDS, SITS)	+ Cl-cAMP	guinea-pig ventricle [129]
	+ K_{Ca}	rabbit portal vein [139]
	- K_{ATP}	guinea-pig ventricle [99]
	+ NSCC	rat exocrine pancreas [126]
NPPB	- Ca_L	rat cerebral artery [78]
Diphenylamine-2-carboxylate (DPC)	- Ca_L	guinea pig ventricle [300]
	- NSCC	murine mandible (ST_{885}) [234]

Table 4: Non-specificity of common Cl_{Ca} inhibitors

The "-" refers to inhibition; "+" refers to activation. K_{Ca} channels have been evoked by NE, caffeine, or 5-HT. Ethacrynic acid-induced inhibition of Cl_{Ca} can be attributed not to its action on the channel protein, but to its depleting intracellular Ca^{2+} stores [113].

Abbreviations: Ca_L, L-type Ca^{2+} channel; Cl-cAMP, c-AMP (PKA)-activated Cl^- channel; DIDS, 4,4'-diisothiocyanatostilbene-2,2'-disulfonic acid; K_{ATP}, ATP-sensitive K^+ channel; K_{Ca}, Ca^{2+}-activated K^+ channel; SITS, 4-acetamido-4'-isothiocyanato-stilbene-2,2'-disulfonic acid; NPPB, 5-nitro-2-(3-phenylpropylamino) benzoic acid; NSCC, non-specific cation channel.

Niflumic acid {NfA; [2-(3-trifluoromethyl-phenylamino)-3-pyridinecarboxylic acid]} appears to be the most potent and selective inhibitor of Cl_{Ca}. This non-steroidal anti-inflammatory agent has been used to characterize Cl_{Ca} channels in *Xenopus* oocytes [313] as well as an anion-exchanger in erythrocytes [59, 169]. Data indicate that NfA binds to the open Cl_{Ca} channel [138, 139] and that it can cause modest intracellular Ca^{2+} release [234]. Its effective concentration ranges between 2.3×10^{-6} M to 10^{-4} M for spontaneously activated and norepinephrine-induced Cl_{Ca} currents in rabbit portal vein [138, 227]. Activation of K_{Ca} channels by NfA in vascular smooth muscle is well documented [114, 138, 223]. There have

also been reports that NfA may block high-K^+-induced tension, thus Ca_L channels [78, 177]. Despite its inherent non-specificity, the use of NfA has proved helpful in elucidating the contribution of Cl_{Ca} channels to the vasoconstriction induced by α_1–adrenoceptor agonists (NE and phenylephrine), 5-HT, and endothelin [60, 61, 161, 177, 250, 303, 323]. In addition, the use of NfA has revealed that Cl_{Ca} is at least partially responsible for the depolarization induced by 5-HT [323], suggesting that it may also underlie the depolarization due to NE.

v) Rationale for the proposed study

Most of the available information about Cl_{Ca} channels has been garnered from work done with isolated myocytes. Despite the obvious clarity of the data obtained from these studies and the intriguing suggestions put forth from them, it is often difficult to transfer the knowledge obtained from a single cell to what is observed in an intact tissue. There are many factors that cannot be readily controlled in an artery yet which are taken for granted when studying the properties of a single cell. As a result, very little work has been done to delineate the functional properties of Cl_{Ca} channels in multicellular preparations, much less in microvascular tissues.

The activation of Cl_{Ca} by norepinephrine stimulation is well established. The nature of the current makes it such that it may be responsible for the membrane depolarization and/or vasoconstriction associated with NE stimulation in vascular smooth muscle. Its role in NE-induced vasoconstriction has been postulated. However, despite the inferences from observations in isolated myocytes, Cl_{Ca}-induced membrane depolarization and contraction by α_1–AR stimulation, as well as by other hormone and neurotransmitter systems, still remain to be firmly established in an intact small artery preparation.

b) Volume-sensitive Cl^- channels

Although not extensively studied, the seemingly mechano- and osmo-sensitive Cl^- (Cl_{vol}) channels have been identified in a few vascular smooth muscle types such as rabbit pulmonary artery [115], canine pulmonary and renal arteries [317], and human aorta and coronary artery [178].

i) Channel modulation

Cl_{vol} channels are most importantly modulated by volume changes within the cell. More specifically, decreasing external osmolarity (*i.e.* hypotonicity) has been used as a tool for activating Cl_{vol} channels, thereby permitting their study [115, 184, 271, 317]. Because of its sensitivity to physical changes induced by swelling, it is entirely plausible that the cytoskeleton might be involved in Cl_{vol} modulation [220]. Similar to many other channels, phosphorylation of the channel or associated regulatory proteins has been shown to modulate Cl_{vol}. Indeed, there are indications that G protein-linked phosphorylation by protein tyrosine kinase (PTK) [212, 294], but not by protein kinase A [252], activates Cl_{vol} in non-smooth muscle tissue. The role of PKC is still debatable as there are conflicting studies showing either inhibition [29, 115, 212, 317] of Cl_{vol} by PKC, or a lack of effect [184] on Cl_{vol} when phosphorylation is blocked.

ii) Pharmacology

Many common chloride channel inhibitors act upon Cl_{vol} channels. Like Cl_{Ca}, it is sensitive to IAA-94, NfA, NPPB, and stilbene derivatives (DIDS, SITS) [29, 115, 184, 212, 252, 317]. Tamoxifen, a potent anti-estrogen compound and reversible inhibitor of PKC, seems to be the most potent Cl_{vol} inhibitor currently available [29, 115, 212, 317]. Since we planned to study the modulation of Cl_{Ca} by PKC in this preparation in subsequent studies, and because it

might affect agonist-mediated tone independently of its inhibitory effect on Cl_{vol}, tamoxifen was not used in the current study. Phosphorylation by PTK seems important in the regulation of Cl_{vol}, hence various PTK inhibitors (tyrphostin B46, tyrphostin A25, genistein) are also used to control Cl_{vol} activity *in vitro* [212, 294]. Selective inhibition of cGMP phosphodiesterase by dipyridamole blocks Cl_{vol} in cultured rat cerebellar neurons [252]. Finally, mibefradil, a selective non-dihydropyridine T-type Ca^{2+} channel blocker [88] inhibits Cl_{vol} in the micromolar range in endothelial cells [212], further emphasizing the need for caution when choosing a channel inhibitor for a study.

iii) Physiological relevance

The physiological importance of volume-sensitive Cl^- currents is two-fold. First, they are relevant to the regulatory volume changes that occur when the cell is exposed to an altered osmotic environment. This is likely to be most important in polarized cells such as neurons [252] or intestinal cells [29], and is thought to play a role in cell volume adjustments that take place when membrane permeability is altered, such as during an ischemic episode.

Secondly, because of its mechano-sensitive nature, Cl_{vol} may play an important role in the myogenic response commonly observed in resistance arteries. As the cell membrane is stretched during passive vasodilation due to increased transmural pressure, Cl_{vol} may be activated to cause depolarization and, possibly, vasoconstriction. The changes in the cytoskeletal structure may also trigger Cl_{vol} activation. The myogenic response itself is modulated by Ca_L [196], K_{Ca} [35] and non-specific cation channels [70]. Mechano-sensitive cation channels also are purported to account for the depolarization and constriction associated with the myogenic response [70, 277].

Unfortunately, these conductances do not account fully for the initial membrane depolarization observed during the myogenic response. There are indications that activation of unidentified Cl^- channels may be responsible for this membrane depolarization and the subsequent contraction. In rat cerebral arteries, a NfA-insensitive, non-Cl_{Ca}, Cl^- conductance underlies the membrane depolarization and contraction associated with the myogenic response [207]. Recently, a channel belonging to the ClC-3 subfamily of voltage-gated Cl^- channels was cloned from mammalian heart [82] and expressed in canine vascular smooth muscle cells [318]. Since Cl_{vol} channels are sensitive to stretch and cytoskeletal deformation, it is entirely possible that this conductance is responsible, at least in part, for the contraction and membrane depolarization associated with the myogenic response. Cl_{vol} channels have been recently identified in rabbit portal vein myocytes [115]. However, the question of whether or not Cl_{vol} activation is physiologically relevant in the myogenic response still remains unresolved. We propose to clarify this situation by studying the possible role of Cl_{vol} channels in the myogenic response in intact mesenteric arterioles.

For a long time, Cl^- currents were regarded as "background" currents within the cell and were largely ignored. After decades of intensive study of K^+ channels at both the biophysical and molecular bases, the tables have turned and the once-ignored Cl^- channels have come to the forefront. We are now confronted with at least four Cl^- channel superfamilies with their associated subfamilies, of which at least two seem to be volume- or stretch-sensitive (ClC-2 and ClC-3). The study of vascular tone and how it is regulated must now be re-examined to include a potential contribution by Cl_{vol}. On this note, we find it

essential to examine the role of Cl_{vol} in the myogenic response, as well as in α_1–adrenoceptor-induced vasoconstriction.

I-5 General hypotheses to be tested

Based on the current state of knowledge on the importance of delayed rectifier K^+ channels in regulating the resting membrane potential, and of Cl^- channels in modulating agonist-induced vascular contraction, we propose to test the following hypotheses:

1. 4-Aminopyridine depolarizes rabbit coronary artery smooth muscle cells by shifting the steady-state activation relationship of delayed rectifier K^+ channels (K_{dr}) towards more positive potentials.

2. 4-Aminopyridine preferentially blocks K_{dr} when the channels are in the closed state, and channel opening favors unbinding of the molecule ("reverse use-dependence").

3. Phenylephrine is a potent α_1-adrenoceptor agonist. In the intact rabbit endothelium-denuded mesenteric arteriole, α_1-adrenergic induces a nifedipine-sensitive constriction which is in part caused by a membrane depolarization mediated by the activation of Ca^{2+}-dependent Cl^- channels (Cl_{Ca}).

4. The relative contribution of Cl_{Ca} to the α_1-adrenoceptor-induced vasoconstriction is influenced by the level of transmural pressure and the state of receptor occupancy.

5. Volume-sensitive Cl^- channels participate in the development of myogenic tone or reactivity in the absence and presence of an α_1-adrenoceptor agonist.

METHODOLOGY

New Zealand white rabbits (1.5 - 3.0 kg) were sacrificed by cervical dislocation or by pentobarbitone overdose. The thorax was opened by a midline incision, and the heart was excised rapidly from the thorax. Short sections of the small intestine were excised with the attached microcirculatory bed to provide mesenteric arterioles. All tissues were placed in an oxygenated (95% O_2, 5% CO_2) low Ca^{2+} Krebs Henseleit solution (in mM: NaCl, 120; $NaHCO_3$, 25; KCl, 4.2; KH_2PO_4, 1.2; $MgCl_2$, 1.2; glucose, 11; taurine, 25; adenosine, 0.02; $CaCl_2$, 0.01) at room temperature (22-25°C) prior to use.

M-1 Voltage-clamp electrophysiology

A. Tissue and technique: advantages and pitfalls

In our investigation of the mechanism of action of 4-aminopyridine on K_{dr} channels, a freshly isolated coronary artery smooth muscle cell preparation was used for the following reasons. *i*) Notwithstanding the important of other vascular beds, the control of coronary artery blood flow is essential to the proper irrigation and functioning of cardiac muscle. *ii*) It enabled us to directly measure the currents produced by K_{dr} channels while controlling intracellular Ca^{2+} buffering, a task that would have been impossible to achieve in intact coronary arteries. *iii*) Cultured vascular smooth muscle cells de-differentiate over time after explantation, an effect which could compromise our interpretation of the effect of 4-AP in the intact tissue. *iv*) We can control the intracellular and extracellular media bathing the cell, thereby control cellular processes which might otherwise be 'contaminating' factors. On the other hand, there are some negative aspects of using isolated myocytes. *i*) The enzymes used to disperse the myocytes may damage the channel proteins underlying K_{dr} in a way that may

modulate the interaction of 4-AP with the channel(s). *ii*) Cells within a syncytium may behave differently than isolated cells, therefore the isolated cell approach may seem less 'physiological'.

B. Tissue preparation

The left anterior descending and the circumflex coronary arteries were carefully removed from the ventricular muscle and pinned onto a Sylgard®-coated petri dish. All adhering ventricular myocardium and connective tissue were carefully dissected from the arteries under binocular examination. Both vessels were then placed in individual tubes for enzymatic dispersion. The enzyme solution contained (per ml of 10 μM Ca^{2+} dissecting solution) 0.6 mg of collagenase type 1A (320 units/mg); 0.2 mg of trypsin inhibitor; 50 μl of protease type XXVII (1 mg/ml stock.). The arteries were left overnight in the enzyme solution at 4°C for a maximum of 16 hours. After digestion, the arteries were retrieved and rinsed several times with fresh 10 μM Ca^{2+} solution, placed in an oxygenated bovine serum albumin solution (1 mg/ml of 10 μM Ca^{2+} solution), and incubated at 35°C for 2 minutes.

Single smooth muscle cells were mechanically dispersed by triturating the tissues in 10 μM Ca^{2+} solution. All tissues and supernatant containing single cells were cold-stored in a 10 μM Ca^{2+} Krebs-Henseleit solution at 4°C following dispersal and were used within 8 hours of dissociation.

C. Experimental procedure and electrophysiological techniques

Patch-clamp experiments were carried out only on cells that remained in a relaxed state following the initial superfusion with the normal Hepes-bicarbonate solution used in the experiments. All experiments were performed at room temperature (21-23°C) using either of two inverted microscopes (Nikon model TMS, or Diaphot model TMD). The plexiglass

recording chamber (volume ~ 1 ml) mounted on a moveable stage was thoroughly cleaned with 95% ethanol before use. Prior to each experiment, a sample of the supernatant containing single cells was deposited in the experimental chamber and the cells were allowed to settle for approximately 30 minutes.

Borosilicate micropipettes used to patch onto the cells were pulled on a two-stage vertical puller (model PP-83, Narashige Scientific Instruments Laboratories) and heat-polished using a micro-forge (model MF-83, Narashige Scientific Instruments Laboratories). Pipette resistance ranged from 4 to 6 MΩ when the pipette was filled with internal solution.

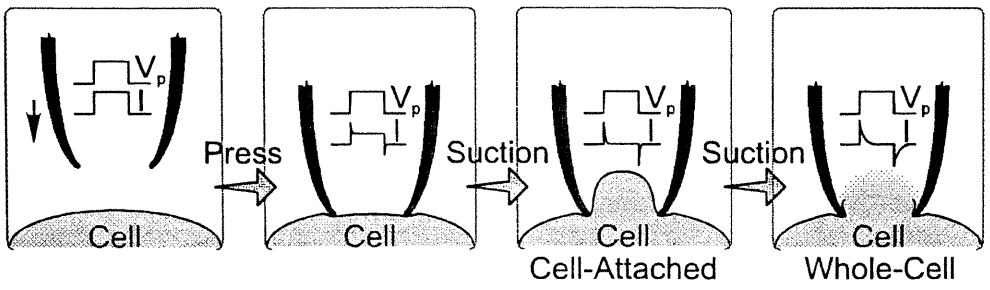

Fig. 7 Patch clamp technique: how to obtain a whole-cell configuration [119]

The pipette tip was approached to a single arterial smooth muscle cell using a motorized micromanipulator (models DC3001R MS-314, Fine Science Tools Inc.). A membrane-pipette gigaohm seal (2 to 10 GΩ) was established by applying gentle pressure to the cell, followed by negative pressure via a syringe attached to the micropipette holder (cell-attached configuration, Fig. 7)

The signal recorded from the micropipette was transmitted to the headstage (50 MΩ feedback resistor) of a patch clamp amplifier (model Axopatch-1D, Axon Instruments Inc.). Voltage-clamp protocols, data acquisition and analysis were performed by a computer (IBM

AT-486 compatible) using pCLAMP software (Version 5.5.1, Axon Instruments Inc.). All data were temporarily stored on the computer hard disk for later analysis.

D. Solutions

The standard bathing solution used to record $I_{K(V)}$ in whole-cell voltage-clamp experiments was the following (mM): 130 NaCl; 10 $NaHCO_3$; 4.2 KCl; 1.2 KH_2PO_4; 0.5 $MgCl_2$; 1.8 $CaCl_2$; 10 Hepes; 5.5 glucose. pH was adjusted to 7.35 with NaOH. 4-Aminopyridine was added in powder form to the standard external solution and pH readjusted to 7.35 before proceeding. Nifedipine (1μM, from a 10 mM stock in dimethyl sulfoxide (DMSO)) was added to suppress Ca_L channels. The standard pipette solution had the following composition (mM): 110 K-gluconate; 30 KCl; 0.5 $MgCl_2$; 5 Hepes; 10 NaCl; 1 ATP-Mg (pH 7.2 with KOH). EGTA (5 mM) was added to the solution to buffer intracellular Ca^{2+}; ATP and EGTA were included in the internal (pipette) solution to inhibit K_{ATP} and K_{Ca} channels, respectively.

The standard whole-cell configuration of the patch clamp technique was used to voltage clamp single coronary artery smooth muscle cells [125]. From the cell-attached configuration, intracellular access was achieved by applying suction {Fig. *7*}. Series resistance compensation was performed in all experiments.

E. Statistical analyses

Data are expressed as means ± S.E.M. with *n* referring to the number of coronary cells. A paired Students' *t* test was employed to assess statistical significance of the differences between experimental conditions. *P* values less than 0.05 were considered to be statistically significant.

F. Computer modeling

Theoretical simulations of the 4-AP-induced block of delayed rectifier K^+ current were performed on a 486SL IBM PS/Note portable computer (25 MHz) using the AXON ENGINEER software (Aeon Software, Madison, WI, USA). Ordinary differential equations were simultaneously solved by the Gear numerical integration method using 10 millisecond incremental time steps. All simulations in the absence or presence of 4-AP were initiated in the steady state.

M-2 Halpern pressure myography

Video (diameter), pressure, and membrane potential signals were recorded simultaneously on a conventional video tape (A. R. Vetter Co.) and on a 486-IBM-PC using Axotape or Axoscope software (Axon Instruments Inc.) at a sampling rate of 25 or 33.3 Hz. All analysis was performed using the Axotape or Axoscope (Axon Instruments Inc.), Quattro Pro for Windows (Corel Corporation), Origin (Microcal Software Inc.), and Statistica (StatSoft, Inc.) softwares.

A. Choice of the isobaric mesenteric arteriole preparation

For a more physiological (i.e. seeing how a syncytium of cells reacts to stimulation) than biophysical study, the use of multicellular preparations is warranted. There are two more common techniques used to study intact vessels. The traditional "isometric" wire myograph technique involves passing two steel wires through the lumen of a ring segment of the vessel to measure the amount of tension generated during stimulation. However, a relatively large artificial resting tension must be imposed on the vessel when using a wire myograph. This need for a significant pre-load tension can be alleviated by using a pressure-perfusion system

which allows for the study of resistance arterioles under more physiological conditions without requiring a significant and measurable pre-load tension. We chose the cannulated-artery system since it is generally considered to be a better experimental model than the wire myograph for at least three reasons [86, 92]. *i*) Cannulated arterioles maintain their physiological cylindrical shape. *ii*) Cannulated arterioles can develop myogenic tone upon increased transmural pressure. *iii*) Cannulated arteries show increased sensitivity to agonists (*i.e.* to angiotensin II, NE).

We relied on multiple criteria to choose mesenteric arterioles for this study. 1) The vessel calibre is an important determining factor. When the goal is to study the control of blood flow, resistance arterioles would be chosen for their increased myogenic reactivity to pressure changes. 2) Along the same lines, the nature of the tissue is also of importance: e.g. renal and cerebral arterioles will be more reactive to pressure alterations than will the mesenteric and iliac arteries. On the other hand, mesenteric arterioles typically will be better candidates to study the α_1–AR-induced vasoconstriction associated with norepinephrine (NE) release from nerve terminals because of their high degree of sympathetic innervation [112]. For the reasons outlined above, we believe that the use of a cannulated artery system was ideal for studying the physiological role of Cl^- channels in both α_1–AR stimulation and the myogenic response.

B. Tissue preparation

Rabbit mesenteric arterioles 1 – 2 mm in length (average lumen diameter ~ 70 μm) were carefully dissected from the vascular bed, mounted on borosilicate cannulae in a perfusion chamber, and attached using silk suture threads according to the technique put forth by Halpern [123] {Fig. *8*, panel *i*}. In all experiments, the endothelium was removed by

passage of an air embolism through the vessel {Fig. *8*, panel *ii*) to eliminate any contribution of endothelium-derived factors to agonist-induced and myogenic responses, and to ensure that effects of niflumic acid and DIDS were solely on vascular smooth muscle channels, and not due to inhibition of endothelial Cl_{Ca} and Cl_{vol} channels by these compounds [211, 212]. Removal of the endothelium was assessed by the failure of acetylcholine (1 μM) to relax vessels preconstricted with 1 μM phenylephrine [47, 98] {Fig. *8*, panel *iii* (bottom)}. Although, myogenic reactivity of these vessels was not assessed prior to endothelium removal, the phenomenon remained following air perfusion, suggesting that the embolism did not damage the arterioles. Viable arterioles contracted to boli of 1 M KCl and/or 10 mM phenylephrine (concentrations of stocks) following endothelium removal. Myogenic responses were not always observed in our mesenteric preparations. To study the effects of chloride channel inhibitors on the myogenic responses, only arterioles demonstrating such behaviour in control conditions (in the absence of TEA) were selected for experimentation.

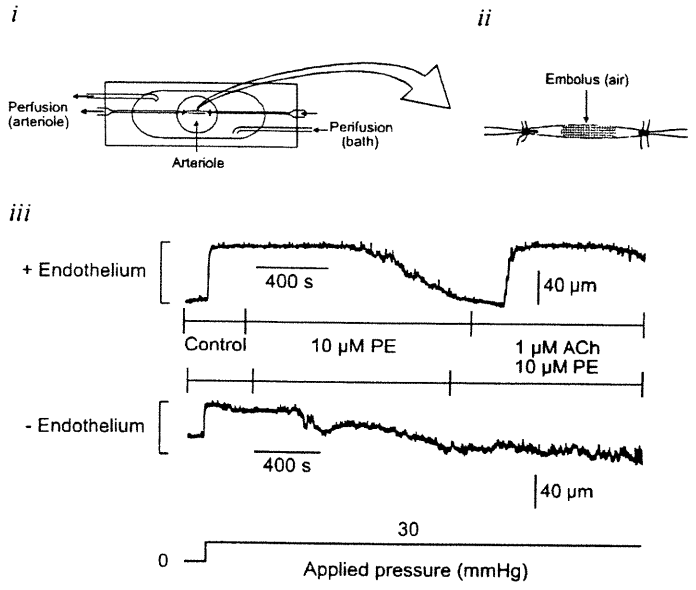

Fig. 8 Cannulation of mesenteric arterioles (i) and removal of endothelium (ii, iii)

Traces in panel *iii* are from two different arterioles (~90 μm diameter).

Suitable arterioles were then allowed to equilibrate at 40 mm Hg for 1 hour before initiating experimental protocols. The arterioles were constantly superfused with heated

(36 ± 0.5°C) and aerated (95% O_2 – 5% CO_2) physiological saline solution (PSS) (in mM): 120 NaCl, 25 $NaHCO_3$, 4.2 KCl, 0.6 KH_2PO_4, 1.2 $MgCl_2$, 11 glucose, 1.8 $CaCl_2$.

C. Pressure application and diameter measurement

Once the arterioles were mounted on cannulae, pressure transducers were attached to the proximal and distal ends of the bath, with the proximal transducer (P1) connecting to the proximal end of the arteriole {Fig. *9*}. The distal transducer (P2) was equipped with a three-

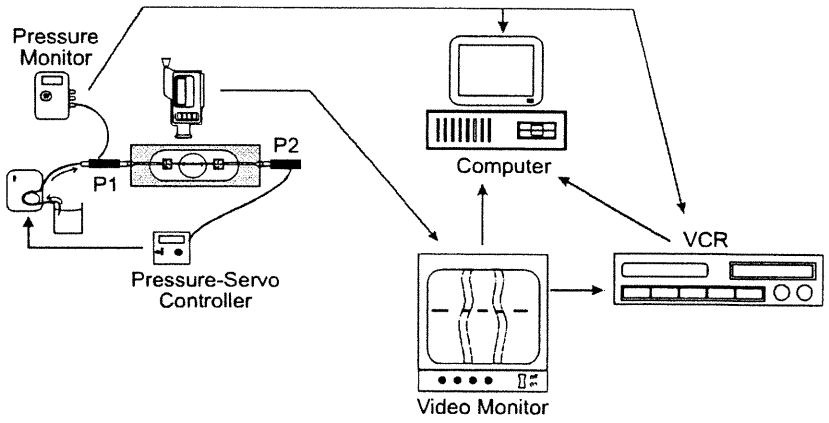

Fig. 9 Pressure myography: equipment, data acquisition and storage, and diameter measurement

way stopcock so as to "close off" the artery when applying pressure. The proximal transducer was connected to a pressure-servo and flow control unit (model PS/200/Q/Z, Living Systems Instrumentation, Inc.) and a digital pressure monitor (model PM-4, Living Systems Instrumentation, Inc.). With the distal stopcock closed, intravascular pressure was applied by flowing PSS into the artery. In the occasion of a pressure leak, the pressure-servo controller would activate the pump and push more solution into the arteriole. Any such "leaky" arteries were discarded. During an experiment, transmural pressure was applied and maintained for a minimum of 2 minutes. Pressures reported throughout the study were registered from the proximal transducer.

With the bath mounted on an inverted microscope (Nikon, model TMS), an image was projected onto a video monitor via a microscope-mounted CCD camera (KP-113, Hitachi) at a final magnification of 10X. Lumen diameter of the vessel was monitored continuously by a video dimension analyzer (model V94, Living Systems Instrumentation Inc., Burlington, VT). Steady state (*i.e.* at the end of the pressure step) lumen diameter is reported throughout.

D. Microelectrode studies

The mesenteric arterioles were cleaned and mounted as in the diameter monitoring experiments, checked for viability and pressure leaks, and allowed to equilibrate for one hour at 40 mm Hg pressure and 36 ± 0.5°C while being continuously superfused with physiological saline solution.

Glass capillary tubes (O.D. 1.2 mm, I.D.0.65 mm) with a microfilament were pulled using a Brown-Flaming micropipette puller (model P-87, Sutter Instrument Company) to produce high-resistance microelectrodes with 80-120 MΩ tip resistances. The electrodes were filled with 3 M KCl solution and connected to a Cyto 721 electrometer (World Precision Instruments) via a gold-plated miniature active probe. The microelectrode was approached to the arteriole using a motorized micromanipulator (models DC-3001R and MS-314, Fine Science Tools Inc.).

A successful impalement of the arteriole was viewed as a sudden drop in potential from baseline level, a stable recording for a minimum of 1 minute, and a sharp return to within 5 mV of the initial baseline level following extraction of the electrode from the tissue {Fig. *10*}. Between three and ten good impalements were performed on each arteriole for each experimental condition.

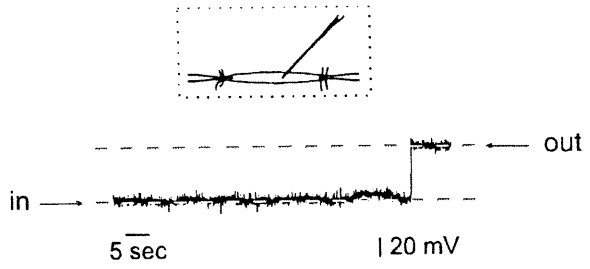

Fig. 10 Membrane potential recording in control conditions

Note the stable recording and the sharp return to baseline. The initial drop in potential upon impalement is not shown. *Inset:* cartoon of impaled artery.

E. Drugs and Solutions

The control (PSS, 130 mM Cl^-) solution was the same as the dissecting solution described previously. A Ca^{2+}-free solution was similar except that $CaCl_2$ was omitted, and 100μM EGTA was added to the medium. The high K^+ (45 mM) solution was obtained by equimolar replacement of NaCl by KCl in the control solution. Test solutions were prepared by adding drugs to the desired concentrations into the control solution. Phenylephrine was prepared as a 10 mM stock in H_2O. Niflumic acid and nifedipine stock solutions were prepared in DMSO at concentrations of 100 mM and 10 mM, respectively; the final concentration of DMSO never exceeded 0.1%. TEA and 4,4'-diisothiocyanatostilbene-2,2'-disulfonic acid (DIDS) were added in powder form to the desired concentration. All drugs were obtained from Sigma Chemical Co. (St. Louis, MO). Niflumic acid did not significantly alter the pH of the solution, monitored over a 45 minute period. Solutions were bubbled throughout with 5% CO_2, 95% O_2.

F. Statistical analyses

Data are expressed as means ± S.E.M. with *N* and *n* referring to the number of arterioles and impalements per cell, respectively. Statistical significance of steady-state

diameter and membrane potential measurements obtained under isobaric conditions was assessed using a standard one-way ANOVA with a Duncan's multiple range test and Tukey HSD for unequal N post-hoc tests, respectively. P values less than 0.05 were considered to be statistically significant and are marked by asterisks (*) or crosses (†‡).

RESULTS

R-1. Mechanism of inhibition of delayed rectifier K^+ current by 4-aminopyridine in rabbit coronary myocytes.

C. V. Remillard and N. Leblanc
Journal of Physiology (London) (1996) **491.2**: pp. 383-400.

R-2. Role of Ca^{2+}- and swelling-activated Cl^- channels in α_1–adrenoceptor-mediated tone in pressurized rabbit mesenteric arterioles.

C. V. Remillard, M.-A. Lupien, V. Crépeau and N. Leblanc
Cardiovascular Research (2000) **46.3**: pp. 557-568.

Journal of Physiology (1996), **491.2**, pp. 383-400

MECHANISM OF INHIBITION OF DELAYED RECTIFIER K^+ CURRENT BY 4-AMINOPYRIDINE IN RABBIT CORONARY MYOCYTES.

By C.V. Remillard and N. Leblanc

From the Département de Physiologie, Université de Montréal, and Centre de Recherche, Institut de Cardiologie de Montréal, Montréal, QC, Canada H1T 1C8

Running Title: 4-AP-induced block of $I_{K(V)}$ in coronary myocyte

Subject Headings: delayed rectifier, potassium current, aminopyridine

To whom all correspondence should be addressed:

Normand Leblanc, Ph.D.
Centre de Recherche
Institut de Cardiologie de Montréal
5000 est, rue Bélanger
Montréal (Québec)
CANADA H1T 1C8

Tel.: (514) 376-3330, ext. 3998
FAX: (514) 376-1355
E-mail: [redacted]

SUMMARY

1. The mechanisms involved in the 4-aminopyridine (4-AP)-induced block of delayed rectifier K^+ current ($I_{K(V)}$) in vascular smooth muscle cells were studied in cells enzymatically isolated from the rabbit coronary artery.
2. 4-AP inhibited slowly inactivating $I_{K(V)}$ in a dose-dependent manner (concentration producing half-maximal inhibition, $K_{½}$ = 1.37 mM), and shifted the steady-state activation and inactivation curves of $I_{K(V)}$ by +9 and +16 mV, respectively.
3. The time constant of activation was significantly increased by 4-AP at +20 mV; deactivation kinetics were unaffected upon repolarization to –40 mV. The fast ($\tau_f \approx 1$ s) and slow ($\tau_s \approx 5$ s) time constants of inactivation (0 and +20 mV), and its recovery kinetics ($\tau_r \approx 6$ s) at –60 mV were not significantly affected by 0.5 mM 4-AP. However, τ_f disappeared in the presence of 2 mM 4-AP while τ_s remained unaffected.
4. Use-dependent unblock of $I_{K(V)}$ was revealed at potentials ≥ -10 mV from analyses of the voltage-dependence of 4-AP-sensitive currents and the frequency dependent-changes ('reverse use-dependence') of $I_{K(V)}$ during the application of repetitive steps (-60 to +20 mV for 250 ms at a rate of 0.25 Hz) in control conditions, in the presence of 0.5 mM 4-AP, and after washout of the drug. These results suggested that 4-AP preferentially binds to the channel in the closed-state, and unbinding is promoted by transitions to the open state.
5. The channel was modelled as a simple three-state mathematical loop model incorporating single closed, open and inactivated states. The block by 4-AP was modelled as a state-dependent interaction with 4-AP primarily binding to the closed state. Computer

simulations support the hypothesis that 4-AP-induced block of the delayed rectifier K^+ (K_V) channel in the closed state is relieved during membrane depolarization.

6. Closed state binding of 4-AP to the K_V channel depolarizes vascular smooth muscle cells by shifting the activation curve of these channels to more positive potentials.

INTRODUCTION

A voltage-dependent delayed-rectifier K^+ (K_V) channel has been identified, and its properties studied, in various types of smooth muscle cells. Its importance in determining resting membrane potential (E_m) has been well-characterized in coronary artery (Leblanc, Wan & Leung, 1994), trachea (Boyle, Tomasic & Kotlikoff, 1992; Fleischmann, Washabau & Kotlikoff, 1993), portal vein (Miller, Morales, Leblanc & Cole, 1993), and pulmonary artery smooth muscle cells (Okabe, Kitamura & Kuriyama, 1987; Post, Hume, Archer & Weir, 1992; Smirnov, Robertson, Ward & Aaronson, 1994; Yuan, Tod, Rubin & Blaustein, 1994). These studies agree that the delayed rectifier K^+ current ($I_{K(V)}$) represents the dominant repolarizing conductance within the physiological range of membrane potentials (-50 to 0 mV) and is critical in determining E_m at low or normal intracellular Ca^{2+} levels ($[Ca^{2+}]_I$). The single-channel correlate of $I_{K(V)}$ exhibits a conductance in the range of 5-57 pS, is voltage-dependent, displays activation and inactivation kinetics, is blocked by intracellular Mg^{2+} or Ca^{2+} (Gelband & Hume, 1992), and is blocked by 4-aminopyridine (4-AP), while being relatively insensitive to tetraethylammonium chloride or charybdotoxin, which have been widely used to inhibit large conductance potassium channels (Beech & Bolton, 1989*b*; Volk, Matsuda & Shibata, 1991; Brayden & Nelson, 1992; Gelband & Hume, 1992; Volk & Shibata, 1993; Miller *et al.* 1993; Leblanc *et al.* 1994). Recently, the inhibition of $I_{K(V)}$ has been suggested to play a direct role in causing acute (Post *et al.* 1992; Yuan *et al.* 1994) as well as chronic (Smirnov *et al.* 1994) hypoxic pulmonary vasoconstriction.

The use of 4-aminopyridine as a specific blocker of $I_{K(V)}$ has been crucial in assessing its physiological function in smooth muscle. Although Ca^{2+}-activated K^+ channels were shown to be insensitive to 4-AP (Beech & Bolton, 1989*b*; Boyle *et al.* 1992; Gelband &

Hume, 1992; Miller *et al.* 1993; Leblanc *et al.* 1994), the compound has also been shown to block 'I_A-type' of transient outward K^+ current in smooth muscle cells (I_{to}) (Beech & Bolton, 1989*a*; Vogalis & Lang, 1994). However, I_{to} represented a relatively small fraction of total outward current in rabbit portal vein cells (Beech & Bolton, 1989*a*). In addition, the channel was reported to be largely inactivated at physiological membrane potentials recorded in vascular (Beech & Bolton, 1989*a*) and colonic (Vogalis & Lang, 1994) smooth muscle cells. Thus, under well-defined conditions, 4-AP appears to be a useful tool to investigate the role of K_V channel in vascular smooth muscle cells.

Despite extensive use of 4-AP to separate pharmacologically the different K^+ channels participating in total macroscopic current, few studies have elucidated the mechanisms involved in the inhibition of the K_V channel in smooth muscle cells. To date, a few suggested mechanisms have surfaced: (i) 4-AP decreases the open probability of the channel, with no effect on the amplitude of single channel unitary currents (Boyle *et al.*, 1992; Russell *et al.* 1994*b*); (ii) either ionized or non-ionized, 4-AP permeates the membrane to bind the channel from the inside (Okabe *et al.* 1987), (iii) 4-AP appears less potent at inhibiting $I_{K(V)}$ at more positive potentials, suggesting a reduced action on channels in the open state (Okabe *et al.* 1987; Volk *et al.* 1991; Gelband & Hume, 1992; Leblanc *et al.* 1994; Robertson & Nelson, 1994). We have previously reported that unblock of 4-AP from the K_V channel might be occurring in rabbit coronary myocytes; this is based on the analysis of a 4-AP-sensitive current evoked during ramp or step protocols (Leblanc *et al.* 1994). The major aim of this study was to investigate in further detail the mechanisms by which 4-AP blocks delayed rectifier K^+ currents in whole-cell voltage-clamped rabbit coronary myocytes.

Our data show that 4-AP preferentially binds to the K_V channel in the closed state and unbinds during membrane depolarization-induced channel activation. Closed state binding of 4-AP to K_V channels depolarizes vascular smooth muscle cells by shifting the activation curve of these channels to more positive potentials. This work has been presented in preliminary form (Remillard & Leblanc, 1995).

METHODS

Cell isolation procedure

This study was approved by the ethical and animal care committees of the Montreal Heart Institute (Montreal, Canada). Isolation of single coronary smooth muscle cells was performed using an enzymatic dispersion method. Briefly, albino rabbits (1.5-2.0 kg) of either sex were killed by cervical dislocation late in the day. The heart was quickly removed and placed in a cold and well-oxygenated (95% O_2-5% CO_2) 10 μM Ca^{2+} dissection solution containing (mM): NaCl, 120; $NaHCO_3$, 25; KCl, 4.2; KH_2PO_4, 1.2; $MgCl_2$, 1.2; glucose, 11; taurine, 25; adenosine, 0.02 (taurine and adenosine from Sigma Chemical Co., St-Louis, MO, USA); $CaCl_2$, 0.01. The left anterior descending and the circumflex coronary arteries were carefully removed from the ventricular muscle, and pinned onto a silicone elastomer-filled petri dish (Sylgard 184; Dow Corning Co., Midland, MI, USA). All adhering ventricular myocardium and connective tissue were carefully removed from the arteries under binocular examination. Both vessels were then placed in individual tubes for enzymatic dispersion. The composition of the enzyme solution was as follows (per ml of 10 μM Ca^{2+} dissecting solution): 0.6 mg of collagenase Type 1A (320 units mg^{-1}; Sigma Chemical Co.); 0.2 mg of trypsin inhibitor (Sigma Chemical Co.); 50 μl of protease Type XXVII (1 mg ml^{-1} stock; Sigma Chemical Co.). The arteries were left overnight in the enzyme solution at 4°C for a maximum of 16 h. After digestion, the arteries were retrieved and rinsed several times with fresh 10 μM Ca^{2+} solution, placed in a bovine serum albumin solution (1 mg ml^{-1} of 10 μM Ca^{2+} solution; Sigma Chemical Co.), and incubated at 35°C for 2 min. Single smooth muscle cells were mechanically dispersed by triturating the tissues in 10 μM Ca^{2+} solution. All

tissues and supernatant containing single cells were cold-stored at 4°C until use. Data were acquired within 4 to 8 h of cell isolation.

Experimental procedure and electrophysiological techniques

All experiments were performed at room temperature (21-23°C) using either of two inverted microscopes: Nikon Diaphot model TMD, or Nikon model TMS (Nikon Corp., Tokyo, Japan). The recording chamber (volume ≈ 1 ml) was mounted on a moveable stage, and cleaned thoroughly with 95% ethanol before use. Before each experiment, a sample of the supernatant containing single cells was deposited in the experimental chamber and the cells were allowed to settle for 30 min. Patch-clamp experiments were carried out only on cells which remained in a relaxed state following the initial superfusion with the normal Hepes-bicarbonate solution used in the experiments (see composition below).

The standard whole-cell configuration of the patch clamp technique was used to voltage-clamp single coronary artery smooth muscle cells (Hamill, Marty, Neher, Sakmann & Sigworth, 1981). Borosilicate patch micropipettes were pulled on a two-stage vertical puller (model PP-83; Narashige Scientific Instruments Laboratories, Tokyo, Japan) and heat-polished using a microforge (model MF-83; Narashige Scientific Instruments Laboratories). The micropipette diameter was 1-2 μm. Pipette resistance ranged from 4 to 6 MΩ when the pipette was filled with internal solution (see below for description).

The pipette tip was brought towards a single coronary artery smooth muscle cell using a motorized micromanipulator (Fine Science Tools Inc., North Vancouver, BC., Canada) driven by a control unit (model MS-314; Fine Science Tools Inc.). A membrane-pipette gigaohm seal (2 to 10 GΩ) was established by applying gentle pressure to the cell,

followed by negative pressure via a syringe attached to the micropipette holder. Intracellular access was then obtained by applying more suction. Series resistance compensation was performed in all experiments.

The signal recorded from the micropipette was transmitted to the headstage (50 MΩ feedback resistor) of a patch clamp amplifier (model Axopatch-1D, Axon Instruments Inc., Burlingame, CA, USA). Voltage-clamp protocols, data acquisition and analysis were performed by a computer (IBM AT-486 compatible) using the pCLAMP software (Version 5.5.1; Axon Instruments Inc.). All data were temporarily stored on the computer hard disk for later analysis. Current and voltage traces were displayed using a Hewlett Packard LaserJet printer (model Series III; Hewlett-Packard Co., Mountain View, CA, USA).

Solutions and drugs

The standard micropipette solution contained (mM): potassium-gluconate, 110; KCl, 30; $MgCl_2$, 0.5; Hepes, 5; NaCl, 10; ATP-Mg, 1 (pH adjusted to 7.2 with KOH). EGTA (5 mM) was added to the solution to buffer intracellular Ca^{2+}.

The standard external solution (normal) had the following composition (mM): NaCl, 130; $NaHCO_3$, 10; KCl, 4.2; KH_2PO_4, 1.2; $MgCl_2$, 0.5; $CaCl_2$, 1.8; Hepes, 10; glucose, 5.5; nifedipine (10 mM stock in DMSO; Sigma), 0.001 (pH adjusted to 7.35 with NaOH). 4-Aminopyridine (Sigma) was added in powder form at the desired final concentration to the normal external solution and pH readjusted to 7.35 before proceeding.

Statistical and computational analyses

The values in most graphs are expressed as means ± S.E.M. of N cells, unless the

results of a single experiment are represented. Where applicable, Students' paired *t* test was employed to assess statistical significance of the differences between control and test solutions. A probability of $P \leq 0.05$ was accepted as the level of significance.

Theoretical simulations of the 4-AP-induced block of delayed rectifier K_+ current were performed on a 486SL IBM PS/Note portable computer (25 MHz) using the AXON ENGINEER software (Axon Software, Madison, WI, USA). Ordinary differential equations were simultaneously solved by the Gear numerical integration method using 10 ms incremental time steps. All simulations in the absence or presence of 4-AP were initiated in the steady state. Results of the simulations were exported to ASCII files to be later processed by graphics softwares.

RESULTS

In these experiments, the activity of large conductance Ca^{2+}-activated K^+ (K_{Ca})and Cl^- (Cl_{Ca}) channels was minimized by using 5 mM EGTA in the pipette solution to buffer intracellular Ca^{2+} and, in some experiments, by superfusing the cells with 0.5 mM TEA (Figs. 2 and 3). Adenosine-triphosphate-sensitive K^+ (K_{ATP}) channels were suppressed by cell dialysis with 1 mM ATP. L-type Ca^{2+} channels were suppressed by 1 μM nifedipine.

4-AP inhibits $I_{K(V)}$ in a dose-dependent fashion

The first series of experiments was done to test the effectiveness of different 4-AP concentrations on $I_{K(V)}$ in our preparation. Figure 1*A* shows a sample experiment in which the effects of two concentrations of 4-AP were tested on $I_{K(V)}$ recorded in one myocyte. Membrane currents were elicited by 20 s steps to +20 mV from holding potential (V_h) of –60 mV at 60 s intervals. Figure 1*A a* shows selected traces in control (a) and after steady-state inhibition of $I_{K(V)}$ by 1 mM (b) and 10 mM (c) 4-AP. Figure 1*A b* displays the time course of changes in $I_{K(V)}$ during the application of 4-AP and during washout. The traces are labelled as in Fig. 1*A a*. $I_{K(V)}$ was measured by subtracting end from peak current during the step. 4-Aminopyridine inhibited $I_{K(V)}$ in a dose-dependent manner and the inhibition was almost completely reversible upon washout. Experiments such as the one described in Fig. 1*A* served to construct the dose-response relationship of inhibition of $I_{K(V)}$ by 4-AP as summarized in Fig. 1*B*. It was not possible to test all five concentrations of 4-AP (0.01, 0.1, 0.5, 1, 10 mM) in the same cell; we were able to test at most three concentrations in some cells. These results show that 4-AP inhibited coronary smooth muscle $I_{K(V)}$ with a concentration for half-maximal inhibition ($K_{1/2}$) of 1.37 mM.

4-AP affects steady-state activation and inactivation of $I_{K(V)}$

We first examined whether 4-AP affected $I_{K(V)}$ by shifting the steady-state activation curve. A standard double-pulse protocol was used to estimate the voltage dependence of $I_{K(V)}$ by tail current analysis in the presence and absence of 2 mM 4-AP. The top families of traces shown in Fig. 2*A* were evoked in response to 250 ms steps from –40 to +20 mV from a V_h of -60 mV, as depicted by the protocol shown at the bottom. Tail currents recorded upon repolarization to –40 mV for each voltage step are reproduced below the traces. In control conditions, tail currents became apparent at potentials -30 mV and increased to reach a maximum near +20 mV. In the presence of 2 mM 4-AP, tail currents were undetectable below –10 mV and increased for step potentials more positive than –20 mV, though it was apparent that their amplitude had still not reached a plateau near +20, as observed in the absence of drug.

Figure 2*B* depicts the effects of 2 mM 4-AP on the steady-state activation curve of $I_{K(V)}$. These curves were constructed using protocols similar to that shown in Fig. 2*A*. Two hundred and fifty millisecond steps were applied in 10 mV increments ranging from either –50 or –40 mV, depending on the magnitude of time-dependent current in individual cells. The initial step which activated $I_{K(V)}$ was followed by a constant 200 ms step to either –40 or –50 mV to record tail current. Steady-state activation curves were generated by plotting normalized tail current amplitude as a function of step potential for each condition. The graph shows that 2 mM 4-AP produced a significant positive shift of the steady-state activation curve of $I_{K(V)}$. Half-maximal activation was shifted by +9 mV in the presence of 4-AP; the voltage-dependence was also steepened in the presence of the blocker.

We then verified whether 4-AP influenced the relative availability of $I_{K(V)}$. A standard double-pulse protocol was used to examine the effects of 4-AP on the steady-state inactivation. Figure 2*C* shows a representative experiment in which we have tested the effects of 2 mM 4-AP. The protocol used was similar to that reported by our group (Leblanc *et al.* 1994). Ten second preconditioning steps ranging from –90 to +20 mV were applied in 10 mV increments from holding potential of –60 mV. Each preconditioning pulse was followed by a constant 250 ms test pulse to +20 mV to record $I_{K(V)}$. Two families of current traces obtained in control conditions (left) and after steady-state block by 2 mM 4-AP (right) are shown at the top of this panel. $I_{K(V)}$ recorded during the second step for selected preconditioning steps (labelled) are reproduced below for comparison. It can be appreciated that, while $I_{K(V)}$ was completely inactivated at potentials ≥ -10 mV in control condition, a significant fraction of $I_{K(V)}$ remained available at potentials more positive than +10 mV after application of 4-AP.

Figure 2*D* displays the summarized data showing means ± S.E.M. of relative state of availability in control (●) and in the presence of 2 mM 4-AP (○). The solid and dotted lines are least-square Boltzmann fits to the mean values illustrated. 4-Aminopyridine produced a +16 mV shift of half-maximal inactivation while having little, if any, effect on the slope of the relationship. The results reported in Fig. 2 suggest that 4-AP has a profound influence on the voltage-dependent mechanisms of gating of the K_V channel in the steady-state.

Effects of 4-AP on kinetics

Since 4-AP appears to interfere with the mechanisms of gating of the K_V channel, it is likely to have some effect on kinetics. Figure 2*A* clearly shows that the onset of activation of

the current elicited by short depolarizations was lengthened in the presence of 4-AP. Figure 3 shows the results of analyses of activation and deactivation kinetics. Figure 3*A* displays original current traces obtained in control conditions (larger current) and after steady-state block by 2 mM 4-AP. These currents were evoked by 250 ms steps to +20 mV from a V_h of –60 mV; the membrane was then repolarized for 200 ms to –40 mV to record tail current. The duration of the step to +20 mV was chosen to minimize time-dependent inactivation, although some inactivation was evident in control conditions. For both control and 4-AP, channel activation and deactivation at +20 mV and –40 mV, respectively, were reasonably well fitted by monoexponential functions (lines superimposed on the traces with their respective time constants as indicated). In this cell, 4-AP induced a 2.7-fold increase in the time constant of activation at +20 mV; in contrast, deactivation of $I_{K(V)}$ in the presence of 4-AP was similar to that measured in control conditions, with a small tendency for τ to be smaller with 4-AP.

Figure 3*B* presents a summary of similar data obtained in seven cells. Although the time constant of activation was enhanced by 3.9-fold on average, the time constant of deactivation was not statistically different in 4-AP-treated *versus* control cells, although a small difference was apparent which was just at the limit of significance ($P = 0.076$).

The effects of 4-AP on the kinetics of inactivation and recovery from inactivation were also examined and the results reported in Fig. 4. Figure 4*A* shows typical current traces obtained in control conditions (■) and in the presence of 4-AP (●) at two different step potentials (10 s in duration; V_h = -60 mV). Superimposed on each trace are double-exponential (control) and monoexponential (4-AP) fits to the data. The results of such an analysis are reported in Fig. 4*B*. The fast component of inactivation observed in control (τ_f;

□) was no longer detectable in the presence of 2 mM 4-AP at either potential. In contrast, the slow time constant of inactivation (τ_s; ■ and ▨) was not significantly affected by 4-AP. With 0.5 mM 4-AP (right set of bars), both τ_f and τ_s were apparent at +20 mV and were not significantly modified.

Figure 4*C* shows a representative experiment in which we have tested the effects of 0.5 mM 4-AP on the recovery from inactivation of $I_{K(V)}$. A double-pulse protocol was employed, which consisted of an initial 20 s pulse to +20 mV from a V_h of 60 mV (protocol shown at bottom) to inactivate $I_{K(V)}$. Reactivation of $I_{K(V)}$ was monitored upon the delayed application of a second step to +20 mV, 2 s in duration, from –60 mV. Only the membrane currents obtained after 0.5 s (first 3 pulses) and 2 s (last 9 pulses) incremental delays are shown for sake of clarity. It is evident from this experiment that the recovery from inactivation of $I_{K(V)}$ was similar in the presence and absence of 4-AP.

Figure 4*D* shows a plot of the percentage recovery from inactivation of $I_{K(V)}$ as a function of time. Each data point is a mean ± S.E.M. of relative current (P2/P1 × 100) recorded at variable delays at –60 mV in control conditions (■) and after 0.5 mM 4-AP (○). The continuous and dashed lines are least-square exponential fits to the mean data points. As reported by others, reactivation kinetics of $I_{K(V)}$ are extremely slow in vascular smooth muscle cells; for example, in the absence and presence of 4-AP, peak current had only partially recovered (87.3 ± 2.4 % and 91.6 ± 2.1 %, respectively) after an 18 s delay between control and test pulse. 4-Aminopyridine did not affect the time course of recovery from inactivation of $I_{K(V)}$ significantly.

Block is reversed during step depolarizations

The results of Fig. 2 suggested that the efficacy of 4-AP-induced block of $I_{K(V)}$ declined with membrane depolarization. Voltage-dependent unblock was also evident from examination of the recordings of Fig. 4*A*; the relative amount of block of $I_{K(V)}$ by 4-AP was greater at 0 mV than at +20 mV. Moreover, analysis of 4-AP-sensitive currents elicited during slow voltage ramps or long step protocols (5 s) also provided evidence consistent with the hypothesis of time-dependent unblock of 4-AP ('reverse use-dependence') at positive potentials (Leblanc *et al.* 1994). We explored this possibility further by analysing the effects of 2 mM 4-AP on $I_{K(V)}$ evoked by short (250 ms) depolarizing steps from a V_h of –70 mV (Fig. 5*A*, protocol at bottom). $I_{K(V)}$ was evoked using short steps in order to minimize time-dependent inactivation. Left and right families of traces in Fig. 5*A a* were obtained in control conditions and after block by 2 mM 4-AP, respectively. Figure 5*A b* shows the current-voltage relationship of the current measured at the end of the pulse for the families of current traces displayed in Fig. 5*A a*. As previously shown in Fig. 2, 4-AP inhibited $I_{K(V)}$ at all voltages. Figure 5*B a* shows the difference currents obtained by digital subtraction of the two families of currents. Our data show that, in the range of –40 to –20 mV, 4-AP-sensitive currents activated in a time-dependent manner but exhibited little, if any inactivation. However, at potentials positive to –20 mV, 4-AP-sensitive currents activated quickly but also displayed inactivation. While peak current continued to increase as a function of voltage, late current eventually exhibited signs of saturation. Figure 5*B b* shows the current-voltage relationship of the difference currents illustrated in Fig. 5*B a* measured at the peak and at the end of the depolarizing step. The 4-AP-sensitive peak current increased from –30 to +60 mV and displayed slight inward rectification at potentials more positive than +20 mV. In contrast,

the late current increased similarly between –30 and –10 mV but completely saturated at potentials ≥ 0 mV. One possibility that explains the transient nature of 4-AP-sensitive currents is that the decaying phase may reflect time-dependent unblock produced by transition to the open state. If unblock is purely state-dependent, then the kinetics of unblock should be steeply voltage-dependent within the activation voltage range. Figure 5*C* reports the voltage-dependence of the time constant of the decaying phase of 4-AP-sensitive currents analysed by least-square monoexponential fitting routines. The data points were fitted by a single exponential function, parameters of which are given in the figure legend. The data demonstrate a steep relationship between 0 and +20 mV, with little voltage-dependence beyond that range. These data, together with those reported in Fig. 2, are consistent with the idea that the interaction of 4-AP with K_V channels is state-dependent.

One possibility that explains these data is that the drug has greater affinity for binding the channel in the closed state. The apparent shifts of the steady-state activation and inactivation curves (Fig. 2), and slowing of the activation phase (Fig. 3), would also be consistent with this proposal. We therefore examined the effects of 4-AP on $I_{K(V)}$ evoked during trains of step depolarizations at a frequency of 0.25 Hz. Figure 6*A a* shows selected traces obtained in control conditions (top), in the presence of 0.5 mM 4-AP (middle) and after washout of 4-AP (bottom). Each train consisted of sixteen steps (250 ms) to +20 mV from a V_h of-60 mV (protocol shown at bottom). Control traces were obtained after ~ 5 min of intracellular dialysis following whole-cell access. Traces in the presence of 0.5 mM 4-AP and after washout were obtained after 10 min incubation or washout of drug while the membrane potential was kept constant at –60 mV. In control conditions, the amplitude of the time-dependent current decreased slightly with the number of pulses (Fig. 6*A a* top, traces 1

and 12 are shown) following a monoexponential time course (Fig. 6*A b*, ■); this was probably produced by cumulative inactivation of $I_{K(V)}$ due to slow recovery kinetics (Fig. 4). In the presence of 4-AP, current amplitude changed little with the number of stimulations. There was no evidence of use-dependent block by the drug. In fact, the decline of current amplitude followed a linear time course, the rate of which was slower than in controls (Fig. 6*A b*, ●). During the first pulse of the train after washout, the current had only recovered by 24%. Resumption of stimulation quickly restored $I_{K(V)}$ to its pre-drug control level (Fig. 6*A a* bottom, traces 1 and 13 are shown; Fig. 6*A b*, ▲).

Figure 6*B* and *C* shows the summarized data obtained in five myocytes for absolute current measurements (*B*) and relative currents (*C*) in control conditions (■), in 0.5 mM 4-AP (●) and after washout of the inhibitor (▲). Figure 6*C* confirms the suggestion of unblocking of 4-AP during the application of series of depolarizing steps. Normalized outward currents were significantly larger after the first pulse in the presence of 4-AP *versus* control. In a separate set of experiments, normalized 4-AP currents (0.1 mM) were not significantly different from control currents when the frequency of stimulation was reduced from 0.25 to 0.1 Hz ($N = 3$; data not shown). These results further reinforce the idea that 4-AP preferentially blocks K_V channel in the closed state. Moreover, the washout experiments suggest that unbinding of the blocker is promoted by channel opening and that 4-AP remains trapped in a large fraction of the channels.

Mathematical model of 4-AP-induced inhibition of K_{dr}

A simple formalism was used to reproduce mathematically the behaviour of macroscopic delayed rectifier K^+ current in rabbit coronary myocytes. Despite the fact that

activation follows a sigmoidal time course in this preparation, this based on our own observations (data not shown), and the fact that whole-cell and ensembles of single channels $I_{K(V)}$ were best fitted with the activation variable raised to the second power (n^2; Volk *et al.* 1991; Volk & Shibata, 1993), our main purpose was to construct a simplified model of the channel which would satisfactorily explain the interaction of 4-AP with the channel. For similar reasons, although the inactivation was best fitted by the sum of two exponential functions (Fig. 2*A* and *B*), fitting the inactivation with a single exponential relation revealed only a slight deviation near peak current, which represented less than 5% of total current in all cells studied, suggesting that the slow component of inactivation represents the dominant transition from open to inactivated state. Consistent with this proposal was the fact that only the slow component of inactivation was reported by Volk & Shibata (1993) from the analysis of ensemble averages of single delayed rectifier K^+ channels recorded in the same preparation. The channel itself was therefore modelled as a simple three-state loop model incorporating single closed (C), open (O) and inactivated (I) states, as illustrated below. The kinetic model also shows that 4-AP was postulated to bind to the closed state, leading to a single non-conducting blocked state (B), where α_x and β_x represent, respectively, the

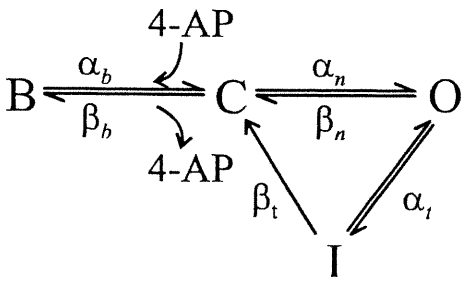

forward and backward rate constants of the various transitions. The rate constants involved in channel activation were obtained by determining the time constants of activation and deactivation of $I_{K(V)}$ at different potentials elicited by step protocols similar to those

described in Figs. 2*A* and 3. Figure 7*A a* shows a plot of the voltage dependence of the time constants of activation (■) and deactivation (□). Both processes could be well fitted by single exponential functions. The bell-shaped voltage-dependence of activation kinetics is similar to that reported by Volk *et al.* (1991) in the same preparation except that their values were about 3-fold larger than ours. Figure 7*A b* displays the voltage dependence of the rate constants, which were calculated according to the equations given in the inset, where n_∞ is the level of steady-state activation (Fig. 2*B*) and τ the time constant (Fig. 7*A a*). The lines passing through the data points are Boltzmann and single exponential fits, which express the voltage dependence of both rate constants for incorporation into the model (Table 1).

A similar approach was used to derive the rate constants involved in the inactivation of $I_{K(V)}$. The graph in Fig. 7*B a* reports the voltage dependence of the time constant of inactivation (■), which was estimated from currents elicited during long step protocols similar to that described in Fig. 2*C*. A single point (□) is shown for the recovery from inactivation which was taken from the experiments described in Fig. 4*D*. The time constants of Fig. 7*B a* were used to obtain the rate constants at different potentials. Figure 7*B b* shows a graph displaying the voltage dependence of the forward (α_t) and backward (β_t) rate constants involved in the slow inactivation process; these parameters were calculated according to the equations given in Fig. 7*B b* where t_∞ is the level of steady-state inactivation (Fig. 2*D*) and the time constant (Fig. 7*B a*). The mathematical functions expressing the voltage dependence of both rate constants are included in Table 1.

The block by 4-AP was modeled as a state-dependent interaction, with 4-AP primarily binding to the closed state. The voltage-dependence of the rate constants of association (α_b) and dissociation (β_b) of 4-AP were derived from analysis of the voltage

dependence of the time constant (τ) of the decaying phase of the 4-AP-sensitive currents and based on the following equation:

$$\tau = 1/\{(\alpha_b [4\text{-AP}]) + \beta_b\}$$

Binding of 4-AP was assumed to follow first-order rate reaction, with association being directly proportional to the concentration of 4-AP. Unbinding was assumed to be independent of the concentration of 4-AP (Castle & Slawsky, 1992). The amplitude of the sigmoidal voltage-dependence of the binding and unbinding rate constants (data not shown) was adjusted to account for the experimentally observed changes in whole-cell current kinetics and voltage dependence of steady-state activation and inactivation. The functions expressing these relationships (Table 1) also comprised a constant term to account for binding and unbinding of 4-AP at negative voltages (~ < -50 mV). These constants were obtained from analysis of the activation kinetics of $I_{K(V)}$ during trains of step depolarizations (Fig. 6; see also Fig. 9) and the amount of current recovery following washout (Fig. 6). The simple kinetic model presented above was resolved by the following system of first-order differential equations:

$$dC/dt = \beta_b B + \beta_n O + \beta_t I - C\,(\alpha_b + \alpha_n),$$

$$dB/dt = \alpha_b C\,[4\text{-AP}] - \beta_b B,$$

$$dO/dt = \alpha_n C + \beta_t I - O\,(\beta_n + \alpha_t),$$

$$dI/dt = \alpha_t O + \beta_t I,$$

$$0 = 1 - (B + C + I),$$

where α_X, β_X are the rate constants as defined above, and B, C, O, and I, represent the fraction of channels in the blocked, closed, open and inactivated states, respectively. The last equation ensures conservation of the total number of channels.

Figure 8*A* illustrates the results of simulations carried out to examine the effects of 2 mM 4-AP on $I_{K(V)}$ elicited by 250 ms steps to 0 or +20 mV from a V_h of –60 mV; tail currents were evoked by repolarizing the membrane to –40 mV. In the absence of drug, the model reproduced well the steady-state voltage dependence, kinetics and frequency-dependent changes of whole-cell $I_{K(V)}$ recorded in our preparation. As similarly observed in our experiments, the model was able to mimic the 4-AP-induced slowing of activation with little effect on deactivation kinetics, except for a small cross-over after ~ 6 s during long step depolarizing pulses (not shown). The model accounted well for the relative amount of block seen with this and other (Fig. 8*B*) concentrations of 4-AP, as well as the relatively greater degree of inhibition of $I_{K(V)}$ at more negative potentials (Figs 2*A*, 4*A* and 5*A a*), a result consistent with the observed positive shift of the activation curve (Fig. 2*B*).

Figure 8*B* illustrates the results of computer simulations designed to verify whether the model could account for the frequency-dependent effects of 4-AP in response to a train of stimulations. The protocol was identical to that of Fig. 6. The top and bottom graphs display simulated currents in control and after steady-state block by 0.5 mM 4-AP. The model reproduced both the exponential decline of peak current seen in control conditions, which is related to slow recovery kinetics of $I_{K(V)}$, and the fact peak current remained relatively unchanged during the train of pulses (Fig. 6).

One reason for selecting a binding rate constant of 500 $M^{-1}sec^{-1}$ at –60 mV (see Table 1) came from the observation that the time constant of activation of $I_{K(V)}$ increased

during the onset of the train after exposing the cell to 4-AP for 10 min while holding the membrane at –60 mV. Figure 9*A* shows a histogram of the estimated time constant (τ_{on}) of activation at +20 mV of the first (P1) and second (P2) pulse of the train; the data were collected from the same series of experiments described in Fig. 6. As expected, there were no significant changes in τ_{on} for currents elicited during P1 and P2 in control conditions. In contrast, activation was significantly faster during P2 than P1 in the presence of 4-AP, but did not appreciably change during subsequent pulses (data not shown).

The computer model corroborated these observations. The top and middle graphs in Fig. 9*B* show simulated currents in control conditions and in the presence of 0.5 mM 4-AP during P1 and P2. Control currents displayed nearly identical activation phases; in contrast, the current elicited by P2 displayed a faster onset than that triggered by P1 with 4-AP, consistent with the data presented in Fig. 9*A*. The bottom graph reports the time-dependent changes in the fraction of blocked channels during the 4-AP simulation (middle graph). At the start of the simulation, nearly all channels would be blocked by 4-AP. During P1, the fraction of blocked channels would rapidly decline due to state-dependent unbinding of 4-AP. Following repolarization to –40 (200 ms) and then to –60 mV (3.55 s), 4-AP would slowly reassociate to channels in the closed state. However, before the onset of P2, ~ 50 % of channels would still be in the closed state and readily available for opening. A consequence of this would be acceleration of the activation phase of the whole-cell current.

DISCUSSION

Our data show that block of the delayed rectifier K^+ current in rabbit coronary myocytes by 4-aminopyridine is state-dependent, with 4-AP primarily inhibiting the channels in the closed state. This conclusion is based on the following observations: (i) under steady-state blocking condition, 4-AP slowed activation kinetics but had little influence on the time course of deactivation; (ii) block developed fully in the absence of stimulations while holding the cells at negative holding potentials; (iii) inhibition of $I_{K(V)}$ by 4-AP was not promoted by repetitive depolarizations after resting block was complete; in contrast, opening of the channels evoked by depolarization slightly relieved the 4-AP-induced block of $I_{K(V)}$, a process ascribed as 'reverse use-dependence'. Our experiments also suggested that 4-AP is more tightly bound to the channel at negative voltages (closed or resting state block), and the block may be quickly relieved by opening of the channels at positive potentials.

Potency of block by 4-AP in rabbit coronary myocytes

Estimation of half-maximal inhibition of $I_{K(V)}$ by 4-AP revealed that the compound inhibits these channels with relatively low affinity. The $K_{½}$ value reported here (1.37 mM) is at the top end of the range of values obtained in other smooth muscle cells. $K_{½}$ values of 0.3 and 0.723 mM have been estimated in rabbit pulmonary artery (Okabe *et al*, 1987) and canine renal artery (Gelband & Hume, 1992) cells, respectively. In our experiments, application of 4-AP resulted in 81% block of $I_{K(V)}$, which is very similar to that reported by Volk *et al*. (1991), who documented 74% block at +10 mV with the same concentration of 4-AP. This supports the notion that the reported efficacy of inhibition of $I_{K(V)}$ by 4-AP in our

preparation is not the result of differences in experimental conditions or cell dispersion technique but truly reflects the interaction of 4-AP with K_V channels in this species.

However, one must be careful in interpreting the $K_{½}$ value in terms of kinetics of binding of 4-AP to the channel. Although it does reflect the concentration of 4-AP producing half-maximal inhibition of peak current, it cannot be used to estimate the rate constants of association and dissociation (where $K_{½} = k_{off} / k_{on}$) because: (i) the block is highly voltage-dependent, with declining potency as the membrane is depolarized; (ii) around peak, some channels are still unblocking, so that the potency of block is estimated under non steady-state conditions; in this context, if K_V channels were not inactivating, the concentration of 4-AP producing half-maximal inhibition would probably be higher than the value reported in this study.

Nature of the 4-AP-sensitive current

Proper current isolation was essential for analysing the mechanism of block induced by 4-AP. Our data support the idea that $I_{K(V)}$ recorded in our experiments largely reflects the behaviour of delayed rectifier K^+ channels with little contamination by other time-dependent ionic currents: This is based on the following observations. (i) L-type Ca^{2+} channels were inhibited by an effective dose of nifedipine (Leblanc *et al.* 1994). (ii) The activity of K_{Ca} and Cl_{Ca} channels was minimized by buffering intracellular Ca^{2+} with EGTA; in addition, in most experiments, the superfusate also contained 0.5 mM TEA to inhibit K_{Ca} (Leblanc *et al.* 1994). (iii) ATP (1 mM) was included in the pipette solution to minimize the activity of K_{ATP} channels; it is unlikely that these channels would have interfered with our measurements since they are time-independent (Clapp & Gurney, 1992). (iv) Besides the sigmoidal onset

during depolarizing steps, both activation and deactivation phases of $I_{K(V)}$ could be well fitted by single exponential functions at all voltages examined, which is inconsistent with the existence of a distinct K^+ channel unless its kinetics are identical to those of $I_{K(V)}$. It is unlikely that these currents would correspond to the voltage-dependent fast transient outward current (I_{fo} or I_{to}; 'I_A-like') reported in rabbit portal vein (Beech and Bolton, 1989*a*) and colonic (Vogalis & Lang, 1994) smooth muscle cells. These currents activate and inactivate at more negative potentials and display faster inactivation kinetics. Distinct components of time- and voltage-dependent delayed rectifier K^+ channels have been identified in dog colonic myocytes (Carl, 1995). Although the pharmacological profile of these components was clearly different from that of $I_{K(V)}$ in coronary myocytes (use- and voltage-dependence of block by 4-AP), we cannot rule out the possibility that several populations of K_V channels also exist in our preparation, even though a single component of delayed rectifier K^+ channels has been documented at the whole-cell (Volk *et al.* 1991; Leblanc *et al.* 1994) and single channel (Volk & Shibata, 1993) levels in the same preparation, and which shared many characteristics with those reported for tracheal (Boyle *et al.* 1992; Fleischmann *et al.* 1993), portal vein (Hume & Leblanc, 1989; Beech & Bolton, 1989*a*, *b*; Miller *et al.* 1993), renal (Gelband & Hume, 1992), cerebral (Brayden & Nelson, 1992; Robertson & Nelson, 1994), and pulmonary arterial (Okabe *et al.* 1987; Clapp & Gurney, 1992; Smirnov *et al.* 1994; Yuan *et al.* 1994) smooth muscle cells. The different sensitivity of the fast inactivation component to 0.5 and 2 mM 4-AP could be an indication that $I_{K(V)}$ reflects the activity of at least two components. However, even if this is the case, it would not compromise our major conclusions because the fast inactivation component represented less than 10% of total current (based on extrapolation of exponential fits to time zero) at potentials more positive

than 0 mV, and was not apparent at potentials below that level. Moreover, although τ_f was unaffected by 0.5 mM 4-AP, the estimated amplitude of the fast component decreased and paralleled the changes of the slow component.

State-dependent inhibition of $I_{K(V)}$

Previous studies suggested that the 4-AP-induced block of delayed rectifier K^+ channels is voltage dependent with diminished efficacy of the compound at depolarized membrane potentials (Okabe *et al.* 1987; Volk *et al.* 1991; Leblanc *et al.* 1994). Our data and computer simulations support the view that 4-AP preferentially interacts with rabbit coronary smooth muscle K_V channels when they are in the closed state, while membrane depolarization relieves the inhibition through a state-dependent mechanism. The following observations were consistent with this proposal: (i) 4-AP delayed the onset of activation of $I_{K(V)}$; deactivation and inactivation kinetics were little affected; (ii) 4-AP shifted the steady-state activation curve toward positive potentials and steepened the relationship; (iii) block developed fully while the channels were kept in the closed state with the use of negative holding potentials, and was partially alleviated by a train of depolarizing pulses, a phenomenon commonly referred to as 'reverse use-dependence'; (iv) a simple four-state mathematical model involving voltage-dependent kinetics of interaction of 4-AP with the closed state reproduced both the features of the control whole-cell $I_{K(V)}$ and its inhibition by the blocker. The behaviour of $I_{K(V)}$ in the presence of 4-AP was similar to that reported for the delayed rectifier K^+ current in squid axon (Yeh, Oxford, Wu & Narahashi, 1976; Kirsch, Yeh & Oxford, 1986), and for the rapidly inactivating transient outward K^+ current (I_{to}) in ventricular myocytes (Šimurda, Šimurdová & Christé, 1989; Castle & Slawsky, 1992;

Campbell, Qu, Rasmusson & Strauss, 1993; Jahnel, Klemm & Nawrath, 1994), and melanotrophs cells (Kehl, 1990). In squid axon (Kirsch *et al.* 1986) and ventricular myocytes (Castle & Slawsky, 1992; Campbell *et al.* 1993), the concentration and voltage dependence of block by 4-AP was explained by assuming that the sequential closed states through which the channel passes during activation would exhibit successfully lower affinity toward 4-AP, thus leading to time-dependent unblocking.

As reported by the above studies, our data and theoretical simulations were more consistent with a state-dependent mechanism than with a purely voltage-dependent interaction whereby 4-AP binding would depend on the transmembrane electric field. In addition to the observed positive displacements of the steady-state activation and inactivation curves, analysis of the voltage dependence of the time constant of the decaying phase of 4-AP-sensitive currents demonstrated a steep relationship within the activation range of $I_{K(V)}$, with little dependency at potentials more positive than +10 mV. Computer simulations based on this model were able to reproduce the data reasonably well. To account for the changes in kinetics, voltage dependence and frequency-dependent changes of $I_{K(V)}$ during a train of pulses, both the binding and unbinding rate constants had to be increased in a sigmoidal fashion as a function of voltage (see Table 1); however, the ratio of the unbinding over the binding rate constants increased by ~ 15-fold with 2 mM 4-AP from –60 mV to +20 mV. Unblocking of K_V channels at positive potentials would result from both the increased ratio of unbinding over binding rates, and the fact that the channels that did unblock would be subsequently available for either a transition to the open state, or for reassociation with 4-AP as driven by the law of mass action.

The features of 4-AP-induced inhibition of rabbit coronary $I_{K(V)}$ appear inconsistent with a mechanism which would require channel opening for 4-AP to reach its binding site. Open state block by 4-AP has been reported for voltage-gated K^+ channels in lymphocytes (Choquet & Korn, 1992), dorsal root ganglia neurons (Ogata & Tatebayashi, 1993), and expressed non or slowly inactivating K^+ channel clones from the *Drosophila Shaker* ($K_V1.1$: Stephens, Garratt, Robertson & Owen, 1994; $K_V1.2$: Russell *et al.* 1994*b*; $K_V1.4$: Yao & Tseng, 1994), *Shab* ($K_V2.1$) and *shaw* ($K_V3.1$) subfamilies (Kirsch & Drewe, 1993) which required channel opening for onset of block, and displayed use-dependent inhibition. Although we did not observe acceleration of current decay during the first and second pulse of a train protocol as typically reported for K^+ channels exhibiting open state block, we cannot rule out the possibility that 4-AP may interact with channels open at negative holding potentials due to a small but significant open probability. However, such a mechanism would be difficult to reconcile with the observed slowing of activation of $I_{K(V)}$ and its response during a train of depolarizing stimuli, unless channels that bind to 4-AP in the open state (open-bound state which would be non-conducting) could undergo a conformational change to a closed-bound state which would tightly retain or trap the molecule. The trapping phenomenon has been reported for certain K^+ channels that exhibited typical open state block by 4-AP (Choquet & Korn, 1992; Castle, Fadous, Logothetis, & Wang, 1994). In our experiments, the trapping of 4-AP by K_V channels in the closed state, and its rapid release by membrane depolarization, could be well reproduced by our computer model, which assumed an extremely slow dissociation constant of 4-AP at negative potentials (0.001 s^{-1}), and rapid unblocking due to state-dependent unbinding. The exact mechanism will require further investigation at the single channel level.

At a concentration of 0.5 mM, 4-AP produced little, if any, effect on inactivation kinetics and recovery from inactivation, supporting the view that it probably did not interfere *per se* with the inactivation gating mechanisms. Although we do not have an explanation for the disappearance of the fast time constant of inactivation with 2 mM 4-AP, one possibility may be that, since the fast component of inactivation represents a small fraction of total current, a higher concentration of 4-AP could result in a lower probability of finding channels undergoing a transition to rapid inactivation. This effect would be accentuated by a 4-AP-induced concentration-dependent shift of the steady-state activation relationship of $I_{K(V)}$. Another argument would be that, as discussed above, it is also possible that the fast and slow components represent two distinct populations of K_V (Carl, 1995) displaying different sensitivities to 4-AP. Another explanation may be that, at higher concentration, 4-AP may be competing for a common binding site with an endogenous β-subunit particle involved in rapid inactivation of $I_{K(V)}$, as recently demonstrated for selected members of the K_V1 subfamily of voltage-gated K^+ channels (Rettig, Heinemann, Wunder, Lorra, Parcej, Dolly, & Pongs, 1994). Nevertheless, our results are consistent with previous studies on various potassium channels, which concluded that 4-AP mainly interacts with the channels with their inactivation gate open, regardless of whether it involves a closed (Šimurda *et al.* 1989; Kehl, 1990; Castle & Slawsky, 1992; Campbell *et al.* 1993) or open state interaction (Yao and Tseng, 1994; Russell *et al.* 1994*b*), or both (Thompson, 1982). Moreover, the potency of block by 4-AP was promoted by deletion through site-directed mutagenesis of a peptide segment responsible for the fast inactivation gate of the $K_V1.4$ clone, suggesting that 4-AP binding and inactivation are mutually exclusive. Consistent with the latter was the observation that, in coronary smooth muscle cells, 2 mM 4-AP induced a +16 mV shift of the

steady-state inactivation curve of $I_{K(V)}$, a finding similar to that reported by others (Thompson, 1982; Kehl, 1990; Ogata & Tatebayashi, 1993). Our computer model, which is based on a closed state interaction, predicted a concentration-dependent shift of the availability curve, as observed by Castle & Slawsky (1992) for I_{to} in rat ventricular myocytes; half-maximal steady-state inactivation was shifted from a control value of –32 mV by +9, +13 and +14 mV with 0.5, 2 and 10 mM 4-AP, respectively. Interaction of 4-AP with the inactivation gate has however been proposed for inactivating K^+ currents in lymphocytes (Choquet & Korn, 1992).

Physiological significance of our findings

Our data support the notion that coronary myocytes delayed rectifier K^+ channels of coronary myocytes represent a family of channels that is distinct from the $K_V1.2$ recently cloned from colonic smooth muscle and expressed in *Xenopus* oocytes, which exhibited strict open state block by 4-AP (Russell *et al.* 1994*b*) with a $K_{½}$ of 74.4 μM (Hart *et al.* 1993). The above considerations are consistent with the recent demonstration that $K_V1.2$ is almost exclusively expressed in gastrointestinal smooth muscles (Overturf *et al.* 1994). A K^+ channel homologous to the $K_V1.5$ subtype was recently cloned from colonic circular smooth muscle and shown to be uniformly expressed in vascular, visceral and uterine smooth muscles (Overturf *et al.* 1994). The properties of this channel somewhat differed from that reported here with a $K_{½}$ of 211 μM. Our group also recently reported that rabbit coronary $I_{K(V)}$ is sensitive to charybdotoxin at concentrations of 50 and 100 nM (Leblanc *et al.* 1994) whereas visceral smooth muscle $K_V1.5$ is insensitive to this toxin at concentrations up to 300 nM (Russell, Overturf & Horowitz, 1994*a*). On the other hand, we cannot rule out the

possibility that $I_{K(V)}$ results from the assembly of a heterotetrameric structure involving varied proportions of monomers of different K^+ channel subtypes (Russell *et al.* 1994*b*).

In conclusion, our data suggest that 4-aminopyridine inhibits delayed rectifier K^+ channels in rabbit coronary myocytes by preferentially interacting with the channels in the closed state. Inhibition is alleviated by membrane depolarization due to a state-dependent unblocking process that is concurrent to the activation gating mechanism. 4-Aminopyridine depolarizes smooth muscle cells (Okabe *et al.* 1987; Gelband & Hume, 1992; Post *et al.* 1992; Miller *et al.* 1994; Fleischmann *et al.* 1993; Leblanc *et al.* 1994; Smirnov *et al.* 1994; Robertson & Nelson, 1994; Yuan *et al.* 1994) by inducing a positive displacement of the steady-state activation curve of $I_{K(V)}$. Rapid unbinding of 4-AP during depolarization warrants to be cautious in assessing the absolute and relative contributions of delayed rectifier K^+ channels in determining the resting membrane potential and total macroscopic currents at potentials more positive than –20 mV.

REFERENCES

Beech, D. J. & Bolton, T. B. (1989a). A voltage-dependent outward current with fast kinetics in single smooth muscle cells isolated from rabbit portal vein. Journal of Physiology (London) 412, 397-414.

BEECH, D. J. & BOLTON, T. B. (1989*b*). Two components of potassium current activated by depolarization of single smooth muscle cells from the rabbit portal vein. *Journal of Physiology (London)* **418**, 293-309.

BOYLE, J. P., TOMASIC, M. & KOTLIKOFF, M. I. (1992). Delayed rectifier potassium channels in canine and porcine airway smooth muscle cells. *Journal of Physiology* **447**, 329-350.

BRAYDEN, J. E. & NELSON, M. T. (1992). Regulation of arterial tone by activation of calcium-dependent potassium channels. *Science* **256**, 532-535.

CAMPBELL, D. L., QU, Y., RASMUSSON, R. L. & STRAUSS, H. C. (1993). The calcium-independent transient outward potassium current in isolated ferret right ventricular myocytes. *Journal of General Physiology* **101**, 603-626.

CARL, A. (1995). Multiple components of delayed rectifier K^+ current in canine colonic smooth muscle. *Journal of Physiology* **484.2**, 339-353.

CASTLE, N. A, FADOUS, S., LOGOTHETIS, D. E. & WANG, G. K. (1994). Aminopyridine block of $K_V1.1$ potassium channels expressed in mammalian cells and *Xenopus* oocytes. *Molecular Pharmacology* **45**, 1242-1252.

CASTLE, N. A. & SLAWSKY, M. T. (1992). Characterization of 4-aminopyridine block of the transient outward K^+ current in adult rat ventricular myocytes. *Journal of Pharmacology and Experimental Therapeutics* **264**, 1450-1459.

CHOQUET, D. & KORN, H. (1992). Mechanism of 4-aminopyridine action on voltage-gated potassium channels in lymphocytes. *Journal of General Physiology* **99**, 217-240.

CLAPP, L. H. & GURNEY, A. M. (1992). ATP-sensitive K^+ channels regulate resting potential of pulmonary arterial smooth muscle cells. *American Journal of Physiology* **262** (*Heart and Circulatory Physiology*, **31**), H916-H920.

FLEISCHMANN, B. K., WASHABAU, R. J. & KOTLIKOFF, M. I. (1993). Control of resting membrane potential by delayed rectifier potassium currents in ferret airway smooth muscle cells. *Journal of Physiology* **469**, 625-638.

GELBAND, C. H. & HUME, J. R. (1992). Ionic currents in single smooth muscle cells of the canine renal artery. *Circulation Research* **71**, 745-758.

HAMILL, O. P., MARTY, A., NEHER, E., SAKMANN, B., & SIGWORTH, J. (1981). Improved patch-clamp techniques for high-resolution current recording from cells and cell-free membrane patches. *Pflügers Archives* **391**, 85-100.

HART, P. J., OVERTURF, K. E., RUSSELL, S. N., CARL, A., HUME, J. R., SANDERS, K. M. & HOROWITZ, B. (1993). Cloning and expression of a $K_V1.2$ class delayed rectifier K^+ channel from canine colonic smooth muscle. *Proceedings from the National Academy of Sciences USA* **90**, 9659-9663.

HUME, J. R. & LEBLANC, N. (1989). Macroscopic K^+ currents in single smooth muscle cells of the rabbit portal vein. *Journal of Physiology* **413**, 49-73.

JAHNEL, U., KLEMM, P. & NAWRATH, H. (1994). Different mechanisms of the inhibition of the transient outward current in rat ventricular myocytes. *Naunyn-Schmiedeberg's Archives of Pharmacology* **349**, 87-94.

KEHL, S. J. (1990). 4-Aminopyridine causes a voltage-dependent block of the transient outward K^+ current in rat melanotrophs. *Journal of Physiology* **431**, 515-528.

KIRSCH, G. E. & DREWE, J. A. (1993). Gating-dependent mechanism of 4-aminopyridine block in two related potassium channels. *Journal of General Physiology* **102**, 797-816.

KIRSCH, G. E., YEH, J. Z. & OXFORD, G. S. (1986). Modulation of aminopyridine block of potassium currents in squid axon. *Biophysical Journal* **50**, 637-644.

LEBLANC, N., WAN, X. & LEUNG, P. M. (1994). Physiological role of Ca^{2+}-activated and voltage-dependent K^+ currents in rabbit coronary myocytes. *American Journal of Physiology* **266** (*Cell Physiology* **35**), C1523-C1537.

MILLER, A. L., MORALES, E., LEBLANC, N. R., & COLE, W. C. (1993). Metabolic inhibition enhances Ca^{2+}-activated K^+ current in smooth muscle cells of rabbit portal vein. *American Journal of Physiology* **265** (*Heart and Circulation Physiology* **34**), H2184-H2195.

OGATA, N. & TATEBAYASHI, H. (1993). Differential inhibition of a transient K^+ current by chlorpromazine and 4-aminopyridine in neurones of the rat dorsal root ganglia. *British Journal of Pharmacology* **109**, 1239-1246.

OKABE, K., KITAMURA, K. & KURIYAMA, H. (1987). Features of 4-aminopyridine sensitive outward current observed in single smooth muscle cells from the rabbit pulmonary artery. *Pflügers Archives* **409**, 561-568.

OVERTURF, K. E., RUSSELL, S. N., CARL, A., VOGALIS, F., HART, P. J., HUME, J. R., SANDERS, K. M. & HOROWITZ, B. (1994). Cloning and characterization of a $K_V1.5$ delayed rectifier K^+ channel from vascular and visceral smooth muscles. *American Journal of Physiology* **262** (*Cell Physiology* **36**), C1231-C1238.

POST, J. M., HUME, J. R., ARCHER, S. L. & WEIR, E. K. (1992). Direct role for potassium channel inhibition in hypoxic pulmonary vasoconstriction. *American Journal of Physiology* **262** (*Cell Physiology* **31**), C882-C890.

REMILLARD, C. V. & LEBLANC, N. (1995). Voltage- and state-dependent block of delayed rectifier K^+ current by 4-aminopyridine in rabbit coronary smooth muscle cells. *Biophysical Journal* **68.2**, A38.

RETTIG, J., HEINEMANN, S. H., WUNDER, F., LORRA, C., PARCEJ, D. N., DOLLY, J. O. & PONGS, O. (1994). Inactivation properties of voltage-gated K^+ channels altered by presence of beta-subunit. *Nature* **369**, 289-294.

ROBERTSON, B. E. & NELSON, M. T. (1994). Aminopyridine inhibition and voltage dependence of K^+ currents in smooth muscle cells from cerebral arteries. *American Journal of Physiology* **267** (*Cell Physiology* **36**), C1589-C1597.

RUSSELL, S. N., OVERTURF, K. E. & HOROWITZ, B. (1994a). Heterotetramer formation and charybdotoxin sensitivity of two K^+ channels cloned from smooth muscle. *American Journal of Physiology* **267** (*Cell Physiology* **36**), C1729-C1733.

RUSSELL, S. N., PUBLICOVER, N. G., HART, P. J., CARL, A., HUME, J. R., SANDERS, K. M. & HOROWITZ, B. (1994b). Block by 4-aminopyridine of a $K_V1.2$ delayed rectifier K^+ current expressed in *Xenopus* oocytes. *Journal of Physiology* **481.3**, 571-584.

ŠIMURDA, J., ŠIMURDOVÁ, M. & CHRISTÉ, G. (1989). Use-dependent effects of 4-aminopyridine on transient outward currents in dog ventricular muscle. *Pflügers Archives* **415**, 244-246.

SMIRNOV, S. V., ROBERTSON, T. P., WARD, J. P. T. & AARONSON, P. I. (1994). Chronic hypoxia is associated with reduced delayed rectifier K^+ current in rat pulmonary artery muscle cells. *American Journal of Physiology* **266** (*Heart and Circulation Physiology* **35**), H365-H370.

STEPHENS, G. J., GARRATT, J. C., ROBERTSON, B. & OWEN, D. G. (1994). On the mechanism of 4-aminopyridine action on the cloned mouse brain potassium channel $mK_V1.1$. *Journal of Physiology* **477.2**, 187-196.

THOMPSON, S. (1982). Aminopyridine block of transient potassium current. *Journal of General Physiology* **80**, 1-18.

VOGALIS, F. & LANG, R. J. (1994). Identification of single transiently opening ("A-type") K channels in rabbit coronary artery smooth muscle cells. *Pflügers Archives* **429**, 160-164.

VOLK, K. A., MATSUDA, J. J. & SHIBATA, E. F. (1991). A voltage-dependent potassium current in rabbit coronary artery smooth muscle cells. *Journal of Physiology (London)* **439**, 751-768.

VOLK, K. A. & SHIBATA, E. F. (1993). Single delayed rectifier potassium channels from rabbit coronary artery myocytes. *American Journal of Physiology* ***264*** *(Heart and Circulation Physiology* **33**), H1146-H1153.

YAO, J. A. & TSENG, G. N. (1994). Modulation of 4-AP block of a mammalian A-type K channel clone by channel gating and membrane voltage. *Biophysical Journal* **67**, 130-142.

YEH, J. Z., OXFORD, G. S., WU, C. H. & NARAHASHI, T. (1976). Dynamics of aminopyridine block of potassium channels in squid axon membrane. *Journal of General Physiology* **68**, 519-535.

YUAN, X. J., TOD, M. L., RUBIN, L. J. & BLAUSTEIN, M. P. (1994). Deoxyglucose and reduced glutathione mimic effects of hypoxia on K^+ and Ca^{2+} conductances in pulmonary artery cells. *American Journal of Physiology* **267** (*Lung Cellular and Molecular Physiology* **11**), L52-L63.

ACKNOWLEDGEMENTS

We are grateful to Marie-Andrée Lupien for isolating single smooth muscle cells. This work was supported by an operating grant from the Medical Research Council (MRC) of Canada. C. V. R. is a pre-doctoral fellow of the Heart and Stroke Foundation of Canada (HSFC). N. L. is a MRC Scholar of Canada.

Table 1. Parameters used to compute the mathematical model of the delayed rectifier K^+ current and its inhibition by 4-AP

Activation

$$\alpha_n (V) = 0.117 / \{1 + \exp [(-0.1 (V + 11.9)]\} \quad (ms^{-1})$$

$$\beta_n (V) = 0.251 \exp [-0.035 (V + 99)] \quad (ms^{-1})$$

Inactivation

$$\alpha_\tau (V) = 0.387 / \{1 + \exp [-0.103 (V + 21)]\} \quad (sec^{-1})$$

$$\beta_\tau (V) = 0.011 \exp [-0.0454 (V + 51)] \quad (sec^{-1})$$

4-AP binding and unbinding

$$\alpha_b (V) = \{(60 / [91.25 + (185.1 \exp (-0.182 V))] + 0.0005)\} [4\text{-AP}] \quad (mM^{-1} ms^{-1})$$

$$\beta_b (V) = \{0.02 / [1 + (2.03 \exp (-0.182 V))]\} + 0.000001 \quad (ms^{-1})$$

Conductance and selectivity

$G_{K_V} = 0.2$ mS cm^{-2} at 22°C

$E_K = -83$ mV

V, voltage; $\alpha_x (V)$ and $\beta_x (V)$ are the functions expressing the voltage dependence (in mV) of the rate constants between the different states as described in the text; [4-AP], concentration of 4-aminopyridine; G_{K_V}, approximate maximum conductance of K_V (based on total cell capacitance and whole-cell current measurements taken from Leblanc *et al.* 1994); E_K, Nernst equilibrium potential for K^+, which was calculated based on the following equation: $E_K = RT/zF \log [K^+]_o/[K^+]_I$, where $[K^+]_o$ and $[K^+]_I$ were set to 5.4 and 140 mM, respectively.

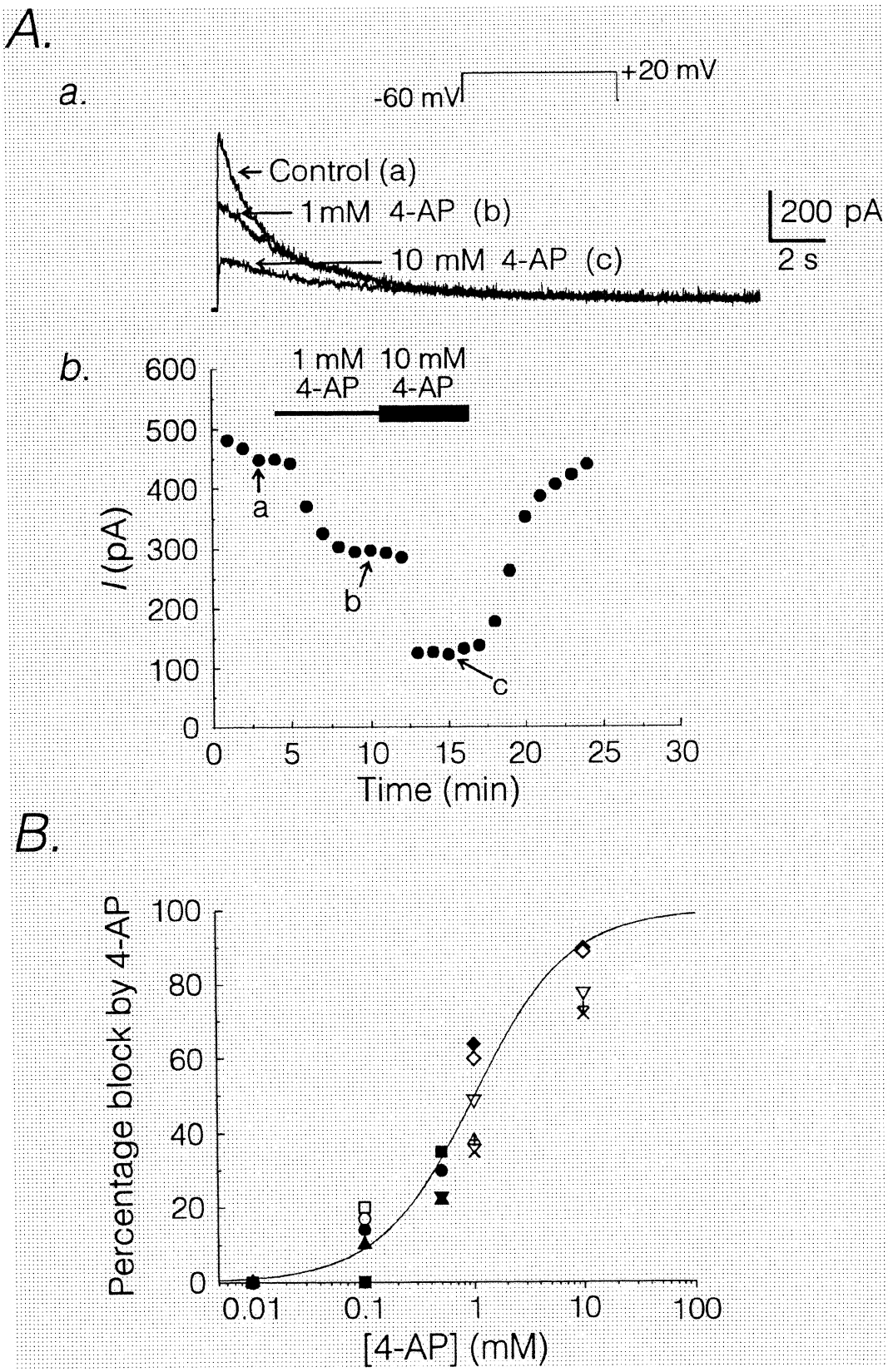
A.
a.
-60 mV
+20 mV
Control (a)
1 mM 4-AP (b)
10 mM 4-AP (c)
200 pA
2 s
b.
1 mM 4-AP
10 mM 4-AP
I (pA)
600
500
400
300
200
100
0
a
b
c
0
5
10
15
20
25
30
Time (min)
B.
Percentage block by 4-AP
100
80
60
40
20
0
0.01
0.1
1
10
100
[4-AP] (mM)

Figure 1. Concentration-dependent inhibition of $I_{K(V)}$ by 4-AP

A, sample experiment showing the effects of 1 and 10 mM 4-AP on $I_{K(V)}$. Pulse protocol is shown at the top and is described in the text. *A a*, selected traces are shown for control (a), 1 mM 4-AP (b), and 10 mM 4-AP (c) conditions. *A b* shows a plot of the time course of changes of $I_{K(V)}$ during the application (bars above data points) and washout of 4-AP. Current magnitude was measured by subtracting the current level at the end of the pulse from peak current. Data points labelled a, b and c correspond to measurements carried out on traces displayed in panel *A-a*. *B*, dose-response curve of 4-AP on $I_{K(V)}$. Data are results from 12 cells, each cell being represented by a different symbol. A minimum of 5 cells is shown for each concentration. The points were fit by a power logistic function described by the following equation: $Y = (I_{min} - I_{max}) / \{[1 + ([4\text{-AP}]/K_{½})^p] + I_{min}\}$ where I_{min} and I_{max} represent normalized minimal and maximal currents, and p and $K_{½}$ represent, respectively, the slope factor and concentration of 4-AP producing half-maximal inhibition of $I_{K(V)}$. In our experiments, p and $K_{½}$ were 0.705 and 1.37 mM, respectively.

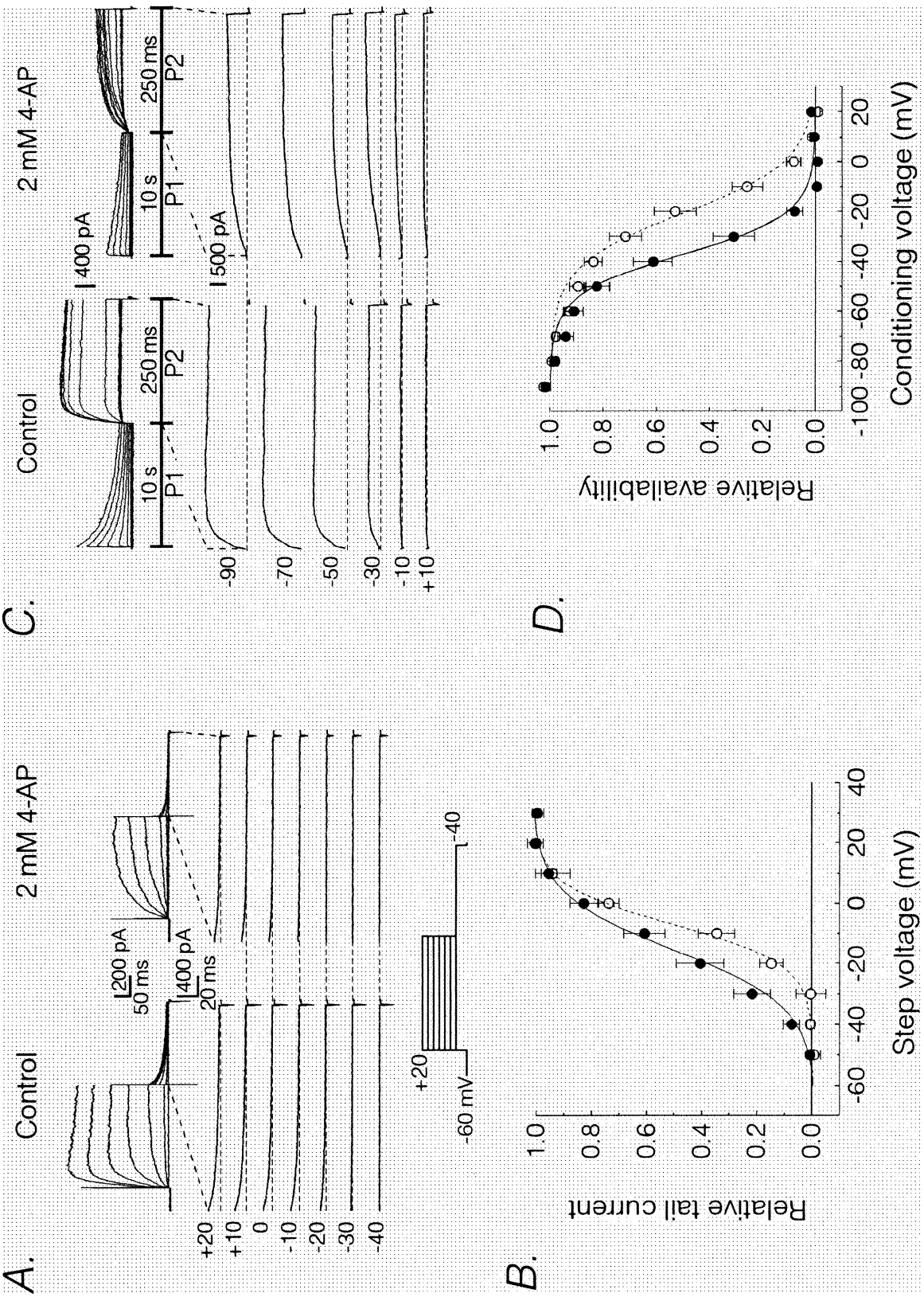
A.
Control
2 mM 4-AP
200 pA
50 ms
400 pA
20 ms
+20
+10
0
-10
-20
-30
-40
+20
-60 mV
-40
B.
Relative tail current
1.0
0.8
0.6
0.4
0.2
0.0
-60 -40 -20 0 20 40
Step voltage (mV)
C.
Control
2 mM 4-AP
400 pA
10 s
P1
250 ms
P2
500 pA
-90
-70
-50
-30
-10
+10
D.
Relative availability
1.0
0.8
0.6
0.4
0.2
0.0
-100 -80 -60 -40 -20 0 20
Conditioning voltage (mV)

Figure 2. 4-AP produces a positive shift of the steady-state activation and inactivation curves of $I_{K(V)}$

A, cells were subjected to a standard double pulse protocol as shown at the bottom of *A*. Traces at top left were elicited by pulsing from –40 to +20 mV in 10 mV increments from a V_h of –60 mV in control conditions. Tail currents evoked upon repolarization to –40 mV are shown at bottom left. Note that tail currents were apparent at –30 mV and reached a maximum level at +20 mV in control conditions (N.B. scales for top and bottom traces are different). Traces at top right show the effects of 2 mM 4-AP on currents evoked by an identical protocol. Representative tail currents are shown at bottom right. Tail currents became apparent only at –10 mV and saturated at potentials > +20 mV. *B*, effects of 4-AP on the steady-state activation curve of $I_{K(V)}$. Protocols used to generate the curves were similar to that described in *A*. Relative states of activation at each voltage and their fits are shown for control conditions (●, continuous line) and in the presence of 2 mM 4-AP (○, dashed line). Values are mean normalized tail currents ± S.E.M. of 10 and 6 cells in control conditions and 4-AP, respectively. Points were fitted using the following form of the Boltzmann equation: $Y = \{1 + \exp[(V_{½} - V)/k]\}^{-1}$ where $V_{½}$ represents half-maximal activation potential and k is the slope factor. $V_{½}$: -16 and –7 mV in control and 4-AP, respectively; k was 9.4 and 6.7 mV in control and 4-AP, respectively. *C*, current traces were generated using a double-pulse protocol as described in the text. Traces were digitized using a two-clock acquisition protocol. The first 10 s (preconditioning pulses or P1) and last 250 ms (test pulse or P2) were acquired at respective sampling rates of 100 Hz and 4 kHz. Traces obtained in control conditions (top left) and after steady-state block by 2 mM 4-AP (top right) are shown. Reproductions of current traces obtained during the second pulse for selected preconditioning

steps are shown below for controls (bottom left) and 4-AP (bottom right). *D*, steady-state inactivation curves were constructed from control (●, continuous line) and 2 mM 4-AP (○, dashed line) measurements. Each data point is a mean ± S.E.M. of I/I_{max} during P2 of 11 and 8 cells in control conditions and 4-AP, respectively. The curves were described by the following form of the Boltzmann equation: $Y = [1 + \exp [(V - V_{½})/k]\}^{-1}$. $V_{½}$: -37 and –21 mV in control conditions and 4-AP respectively; k was 8.0 and 10.4 mV in controls and 4-AP, respectively.

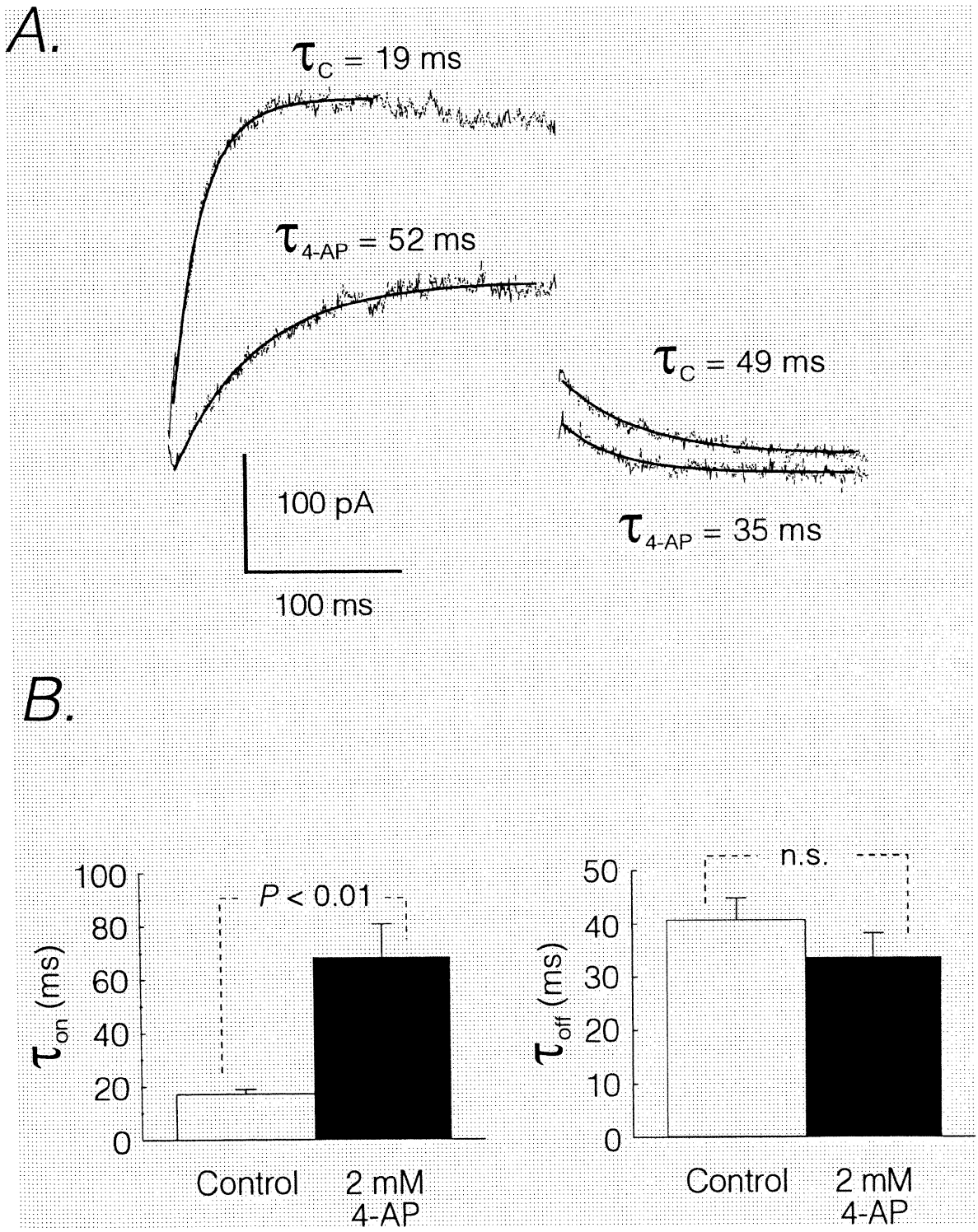
A.
τC = 19 ms
τ4-AP = 52 ms
τC = 49 ms
τ4-AP = 35 ms
100 pA
100 ms
B.
τon (ms)
100
80
60
40
20
0
P < 0.01
Control
2 mM 4-AP
τoff (ms)
50
40
30
20
10
0
n.s.
Control
2 mM 4-AP

Figure 3. Effects of 4-AP on the kinetics of activation and deactivation of $I_{K(V)}$

A, representative current traces evoked by 250 ms steps to +20 mV from a V_h of –60 mV in control conditions and after steady-state block by 2 mM 4-AP. The lines passing through the traces are monoexponential least-square fits to the data for activation of $I_{K(V)}$ at +20 mV and current deactivation at –40 mV; the resulting time constants obtained for the control (τ_c) and 4-AP ($\tau_{4\text{-AP}}$) are illustrated. *B*, histograms summarizing the data obtained in 7 cells submitted to an identical voltage clamp protocol to that described in *A*, in which activation (left histogram) and deactivation (right histogram) kinetics were analysed. For τ_{off}, $P = 0.076$. n.s., not significant.

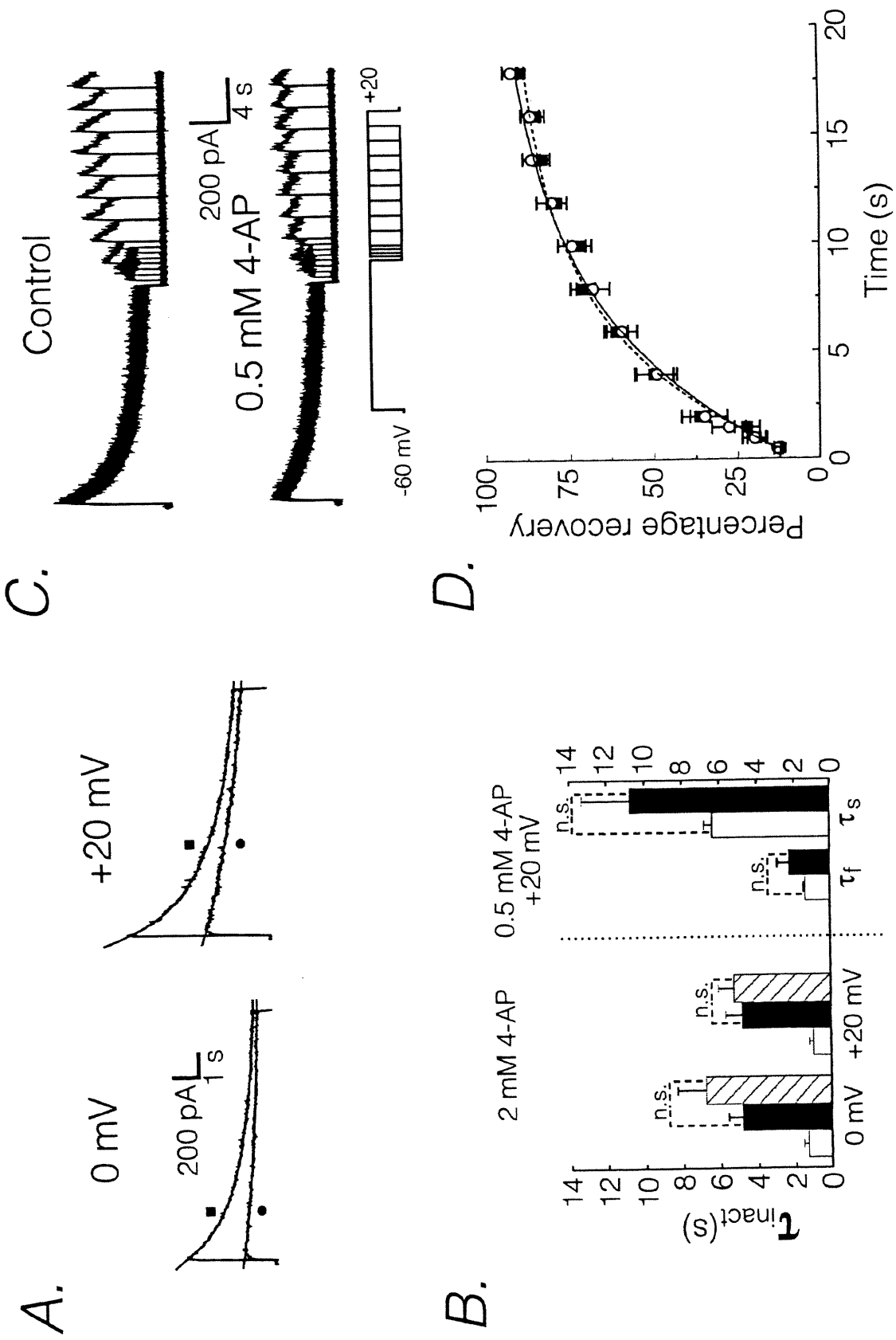
A.
0 mV
200 pA
1 s
+20 mV
B.
2 mM 4-AP
0.5 mM 4-AP
+20 mV
n.s.
0 mV
+20 mV
τinact(s)
τs
τf
C.
Control
0.5 mM 4-AP
200 pA
4 s
-60 mV
+20
D.
Percentage recovery
Time (s)

Figure 4. Effects of 4-AP on the kinetics of inactivation of $I_{K(V)}$

A, example of analysis of the effects of 4-AP on the kinetics of inactivation of $I_{K(V)}$ elicited by 10 s steps to either 0 (left traces) or +20 mV (right traces) from a V_h of –60 mV. The thin lines superimposed on the current traces are least-square double- and monoexponential fits for control (■) and 4-AP (●), respectively, at both voltages. *B*, histogram summarizing the inactivation kinetic data resulting from the analysis of the effects of 2 mM (left sets of bars; $N = 7$) and 0.5 mM (right sets of bars; $N = 4$) 4-AP. For 2 mM 4-AP: estimated means ± S.E.M. fast (τ_f) and slow (τ_s) time constants of inactivation of $I_{K(V)}$ in control (□ and ■, respectively) are reported for measurements performed at 0 mV (left set of bars) and +20 mV (right set of bars). Only slow time constants could be estimated in the presence of 2 mM 4-AP (▨), values which were not significantly different from the slow time constant calculated for the control traces; 0 mV: $P = 0.28$; +20 mV: $P = 0.61$. At 0 mV, $\tau_f = 1.2$ s and $\tau_s = 4.6$ s in controls, and $\tau_s = 6.1$ s. At +20 mV, $\tau_f = 0.8$ s and $\tau_s = 4.2$ s in controls, and $\tau_s = 7.1$ s in 4-AP. For 0.5 mM 4-AP: fast and slow time constants of inactivation were estimated in control (□) and in the presence of 0.5 mM 4-AP (■) at +20 mV; τ_f and τ_s were not significantly affected by 4-AP: $P = 0.25$, τ_f; $P = 0.19$, τ_s. n.s., not significant. *C*, a standard double-pulse protocol (shown at bottom) was used to estimate the recovery kinetics of $I_{K(V)}$ in the absence and presence of drug. Original recordings from a single cell in control (top) and after steady-state block by 0.5 mM 4-AP (bottom). An initial constant 20 s pulse (P1) to +20 mV served to inactivate $I_{K(V)}$. This was followed by a second pulse (P2) to +20 mV (2 s in duration), which was imposed at incremental delays from a V_h of –60 mV; interval between trains of pulses was 45 s. Reactivation of $I_{K(V)}$ was assessed by measuring the amplitude of $I_{K(V)}$ during P2 relative to that elicited by P1, and plotting the data as a function of time delay. *D*,

plot of relative state of recovery from inactivation (%) as a function of time delay between P1 and P2 (see *C*). Each data point is a mean ± S.E.M. of relative current {(P2/P1) × 100} (N = 4). Points were fitted by a monoexponential function of the following form: $Y = \{Y_{max} [1 - \exp(-t/\tau_r)]\}$, where t represents the time delay between the end of P1 and the onset of P2, and τ_r is the time constant of recovery from inactivation. The derived time constants were 5.7 and 6.8 s for controls (■, dashed line) and 0.5 mM 4-AP (○, continuous line), respectively. Mean values at each delay interval were not statistically different.

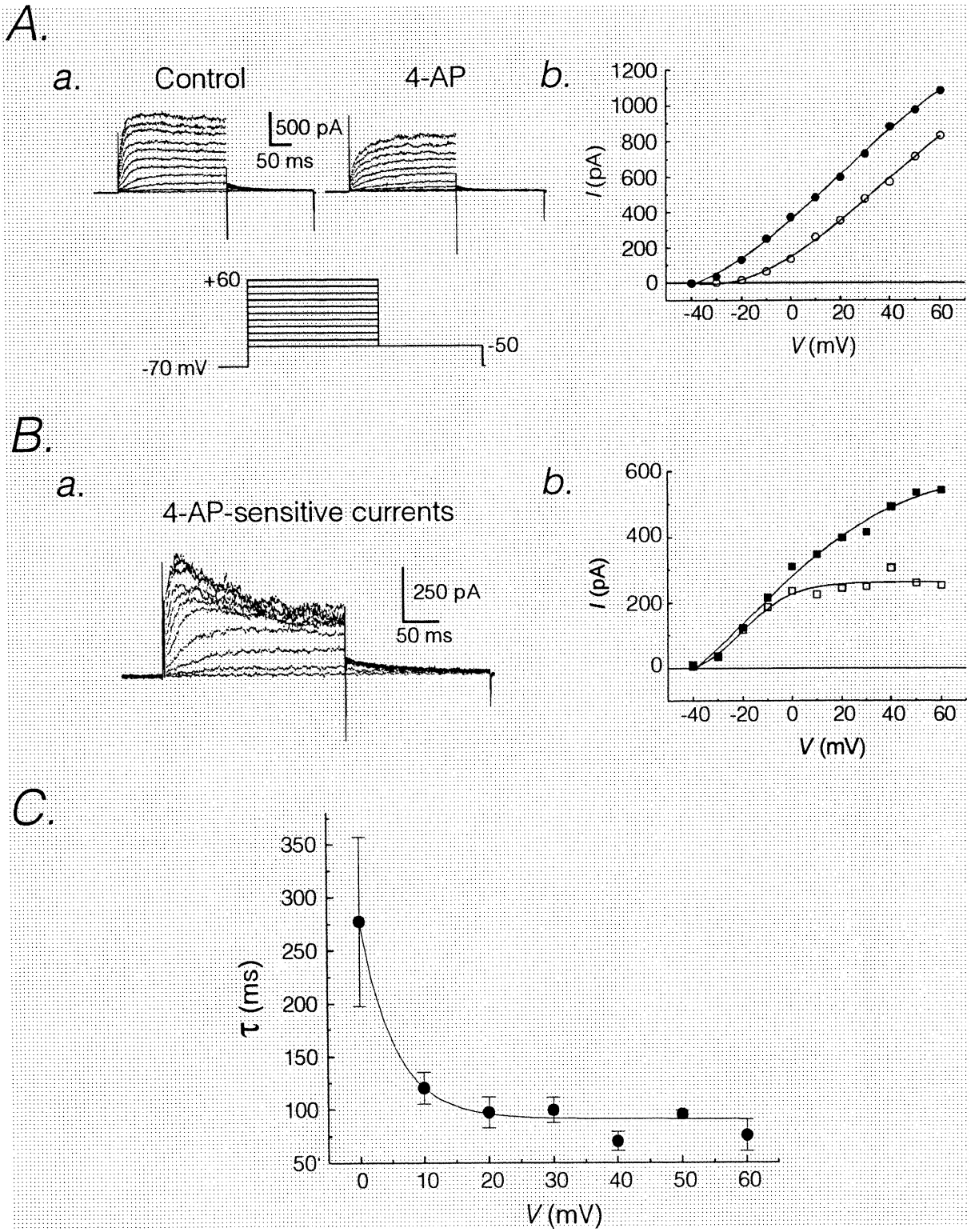
A.
a.
Control
4-AP
500 pA
50 ms
+60
-70 mV
-50
b.
1200
1000
800
600
400
200
0
I (pA)
-40 -20 0 20 40 60
V (mV)
B.
a.
4-AP-sensitive currents
250 pA
50 ms
b.
600
400
200
0
I (pA)
-40 -20 0 20 40 60
V (mV)
C.
350
300
250
200
150
100
50
τ (ms)
0 10 20 30 40 50 60
V (mV)

Figure 5. Evidence for unblock of 4-AP during short step depolarizations

A, from a V_h of –70 mV, 250 ms depolarizing steps were applied in 10 mV increments according to the protocol shown at the bottom in order to evoke activation of $I_{K(V)}$ with little time-dependent inactivation of the current. *A a*, traces in control conditions (left) and in 2 mM 4-AP (right). *A b* shows *I-V* relationships of the current measured at the end of the pulse (late current) for the control (●) and 4-AP (○) current families displayed in *A a*. *B a* shows 4-AP-sensitive currents obtained by digital subtraction of the families of currents illustrated in *A a*. Comparable results were obtained in 8 other myocytes. *B b*, *I-V* relationships of peak (■) and late (□) difference currents depicted in *B a*. *C*, voltage dependence of the time constant ( ) of the decaying phase of 4-AP-sensitive currents at potentials more positive than –10 mV. Each data point is a mean ± S.E.M. (N = 3 – 9). The line passing through the data points is a weighted least-squares monoexponential fit with the following parameters: τ = {185.1 exp (-V/5.49)} + 91.3.

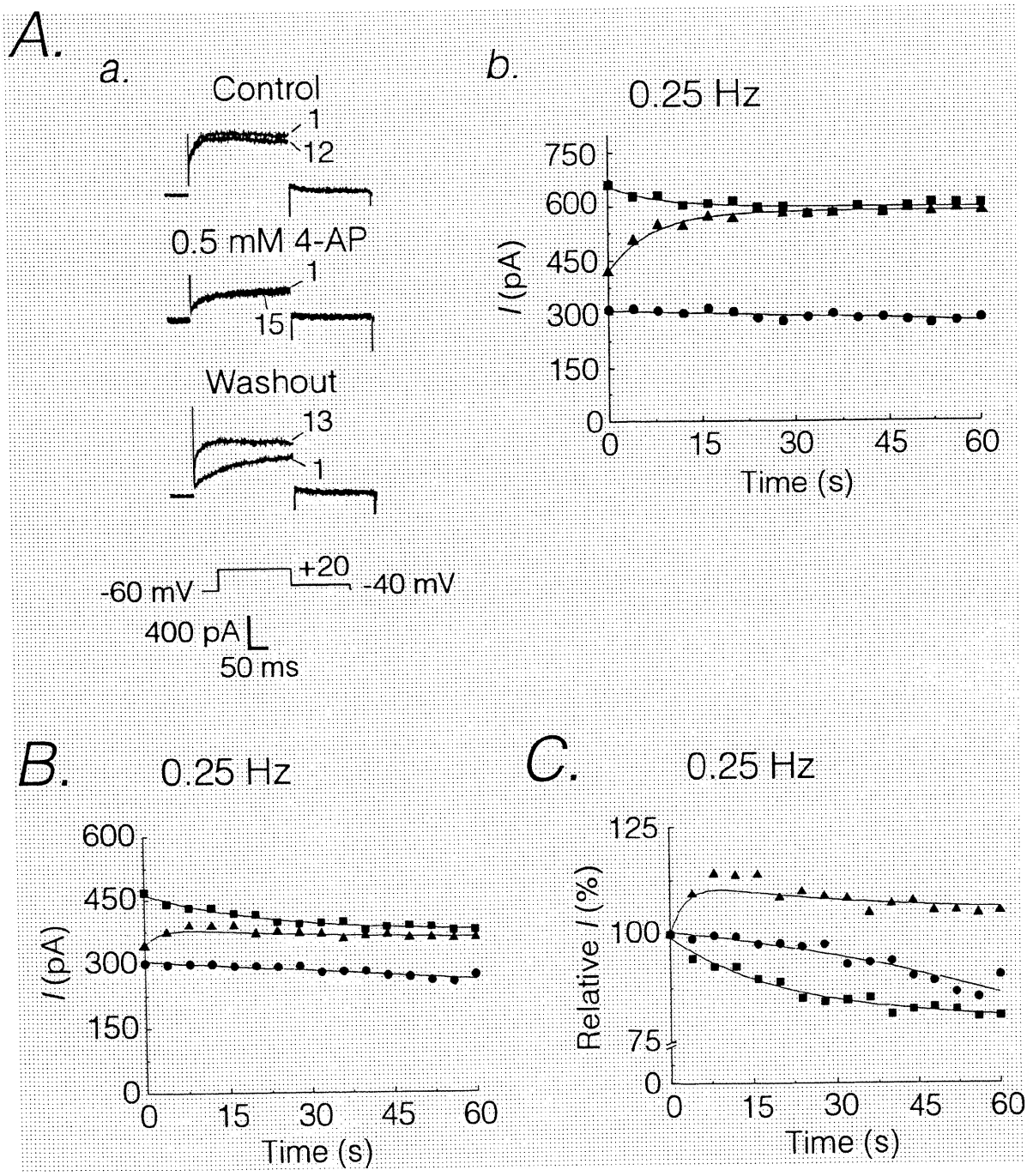
A.
a.
Control
1
12
0.5 mM 4-AP
1
15
Washout
13
1
-60 mV
+20
-40 mV
400 pA
50 ms
b.
0.25 Hz
750
600
450
300
150
0
I (pA)
0
15
30
45
60
Time (s)
B.
0.25 Hz
600
450
300
150
0
I (pA)
0
15
30
45
60
Time (s)
C.
0.25 Hz
125
100
75
0
Relative I (%)
0
15
30
45
60
Time (s)

Figure 6. Effects of repetitive depolarizations on 4-AP-induced block of $I_{K(V)}$

A, response of $I_{K(V)}$ to trains of short (250 ms) depolarizing pulses applied at 4 s intervals (protocol shown at bottom). Shown are sample traces in control conditions (*A a*, top), following 10 min exposure to 4-AP (*A a*, middle) and after washout of the drug (*A a*, bottom), during which membrane potential was kept constant at –60 mV. Numbers next to the traces represent pulse number in the train for each condition; note that pulse 1 represents time zero. *A b* displays a plot of the time course of changes of $I_{K(V)}$ current measured at the end of the pulse in control conditions (■), with 0.5 mM 4-AP (●), and washout (▲) for the cell shown in *A a*. *B* and *C*, summarized data (N = 5) obtained for absolute current measurements (*B*) and relative currents (*C*). For *B*, S.E.M. ranged from ±108 to ±142 pA in controls, ±89 to ±112 pA in 4-AP, and ±101 to ±119 pA following washout. For *C*, S.E.M. ranged from ±28% to ±31% in controls, ±34% to ±39% in 4-AP, and ±28% to ±33% following washout. Symbols are identical to those in *A b*.

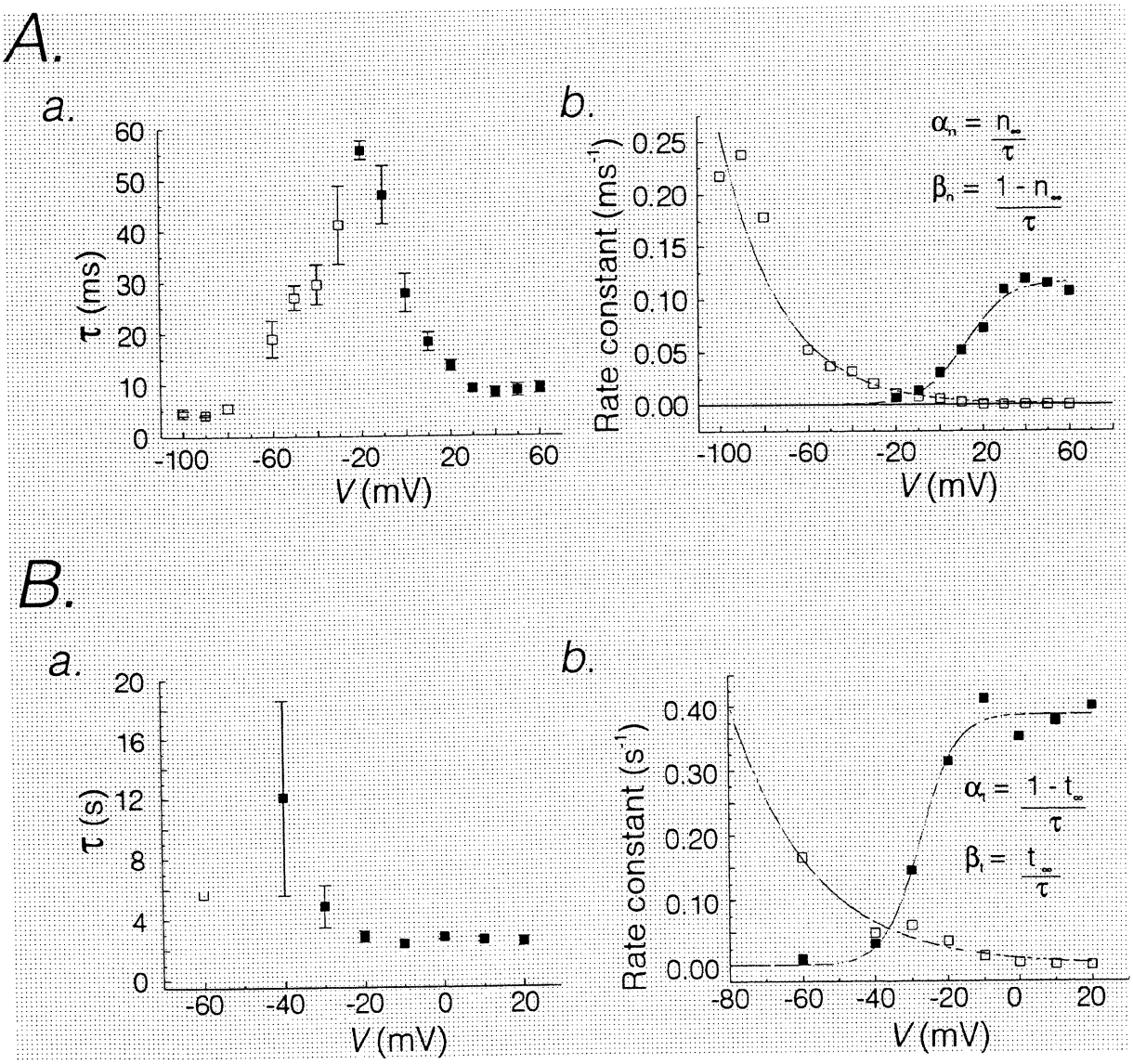
A.
a.
τ (ms)
V (mV)
b.
Rate constant (ms⁻¹)
$\alpha_n = \frac{n_\infty}{\tau}$
$\beta_n = \frac{1 - n_\infty}{\tau}$
V (mV)
B.
a.
τ (s)
V (mV)
b.
Rate constant (s⁻¹)
$\alpha_t = \frac{1 - t_\infty}{\tau}$
$\beta_t = \frac{t_\infty}{\tau}$
V (mV)

Figure 7. Extraction of rate constants from estimated time constants of activation, deactivation, inactivation, and recovery from inactivation, for construction of a computer model of $I_{K(V)}$

A a, voltage dependence of the time constants of activation (τ_{act}, ■) and deactivation (τ_{deact}, □). For activation, time constants were obtained from least-squares monoexponential fitting of time-dependent currents elicited in response to 250 ms steps from a V_h of-60 mV (see Fig. 2*A*). Deactivation time constants were obtained from a similar analysis of tail current kinetics; from a V_h of –60 mV, a constant 250 ms step to +20 mV (0.1 Hz) served to activate $I_{K(V)}$, followed by a second step from –100 to –30 mV (applied in 10 mV increments) to evoke tail current. Each data point is a mean ± S.E.M. of 3 – 7 measurements. *A b*, voltage dependence of the forward (α_n, ■) and backward (β_n, □) rate constants, which were calculated according to the equations displayed on the graph (see text for explanations), where τ and n_∞ represent, respectively, the time constants of activation or deactivation (*A a*) and relative state of activation (see Fig. 2*B*). The lines passing through the points are least-squares Boltzmann (α_n) and monoexponential (β_n) fits, parameters of which are given in Table 1. *B a*, voltage dependence of the time constants of inactivation (τ_{inact}, ■) and recovery from inactivation (τ_{recov}, □); these time constants were estimated from monoexponential fitting of currents evoked by protocols identical to those displayed in Figs. 2*C* and 4*C* and *D*. For τ_{inact}, each data point is a mean ± S.E.M. derived from 4 – 6 cells. For $_r$, the single data point at –60 mV originated from the experiments described in Fig. 4*C* and *D*. *B b*, voltage dependence of the forward (α_t, ■) and backward (β_t, □) rate constants which were calculated according to the equations displayed on the graph (see text for explanations) where τ and τ_∞ represent, respectively, the time constants of inactivation or recovery from inactivation (*B a*)

and relative availability of $I_{K(V)}$ (see Fig. 2*D*). As for the activation gate, the lines passing through the points are least-squares Boltzmann (α_t) and monoexponential (β_t) fits, parameters of which are given in Table 1.

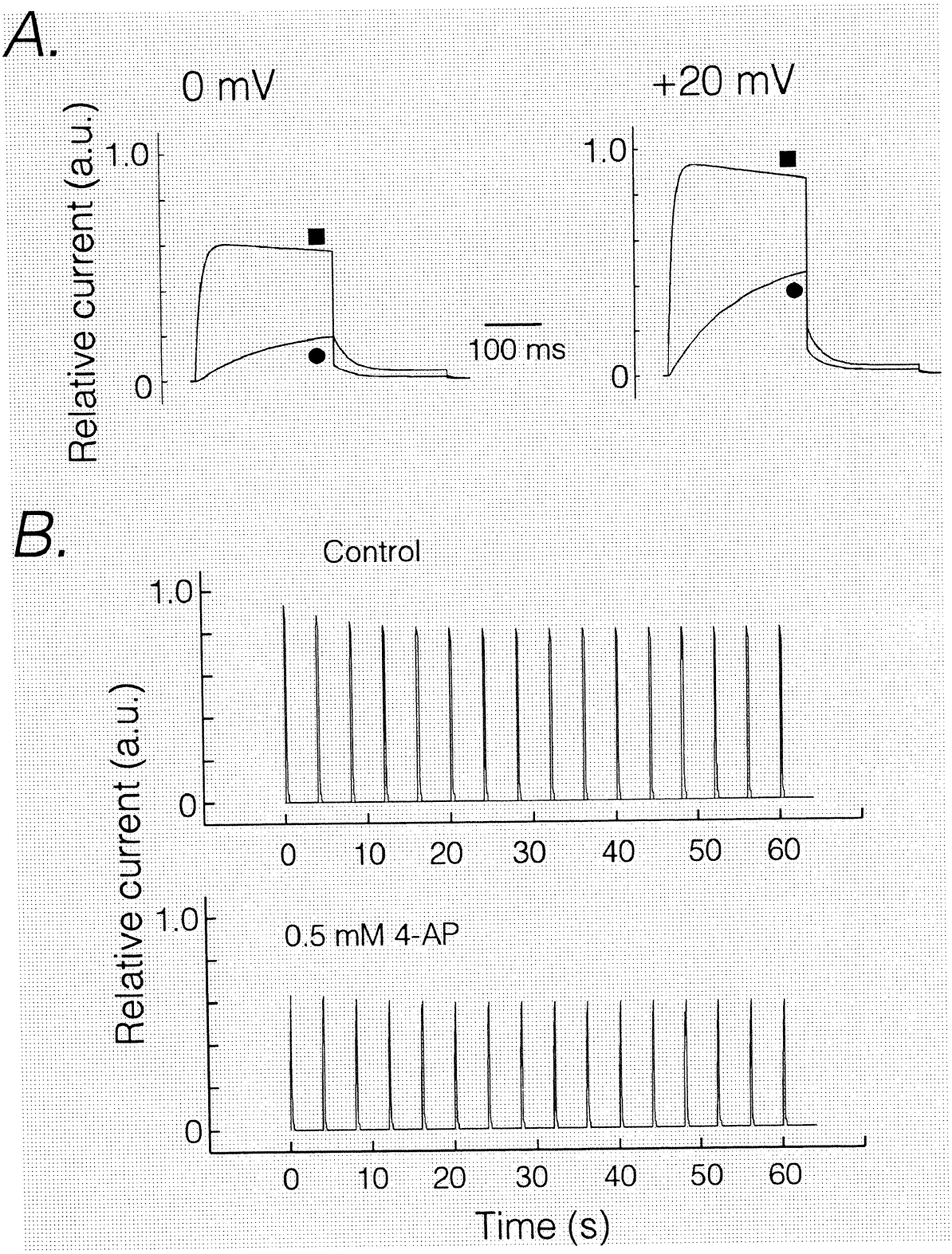
A.
0 mV
+20 mV
Relative current (a.u.)
1.0
0
100 ms
B.
Control
0.5 mM 4-AP
0
10
20
30
40
50
60
Time (s)

Figure 8. Computer simulations of whole-cell $I_{K(V)}$ and its inhibition by 4-AP

A, plotted on a relative scale (a.u., arbitrary units) are shown computer-generated control currents (■), and currents obtained following steady-state block by 2 mM 4-AP (●), at two different step potentials (250 ms in duration) as indicated. V_h = -60 mV; outward tail currents were elicited by repolarizing the membrane to –40 mV for 200 ms. *B*, reproduction by the computer model described in the text of the frequency dependence of $I_{K(V)}$ under control condition (top graph) and after steady-state block by 0.5 mM 4-AP (bottom graph). The voltage-clamp protocol (250 ms steps to +20 mV (0.25 Hz), V_h = -60 mV) is identical to that used in actual experiments (Fig. 6).

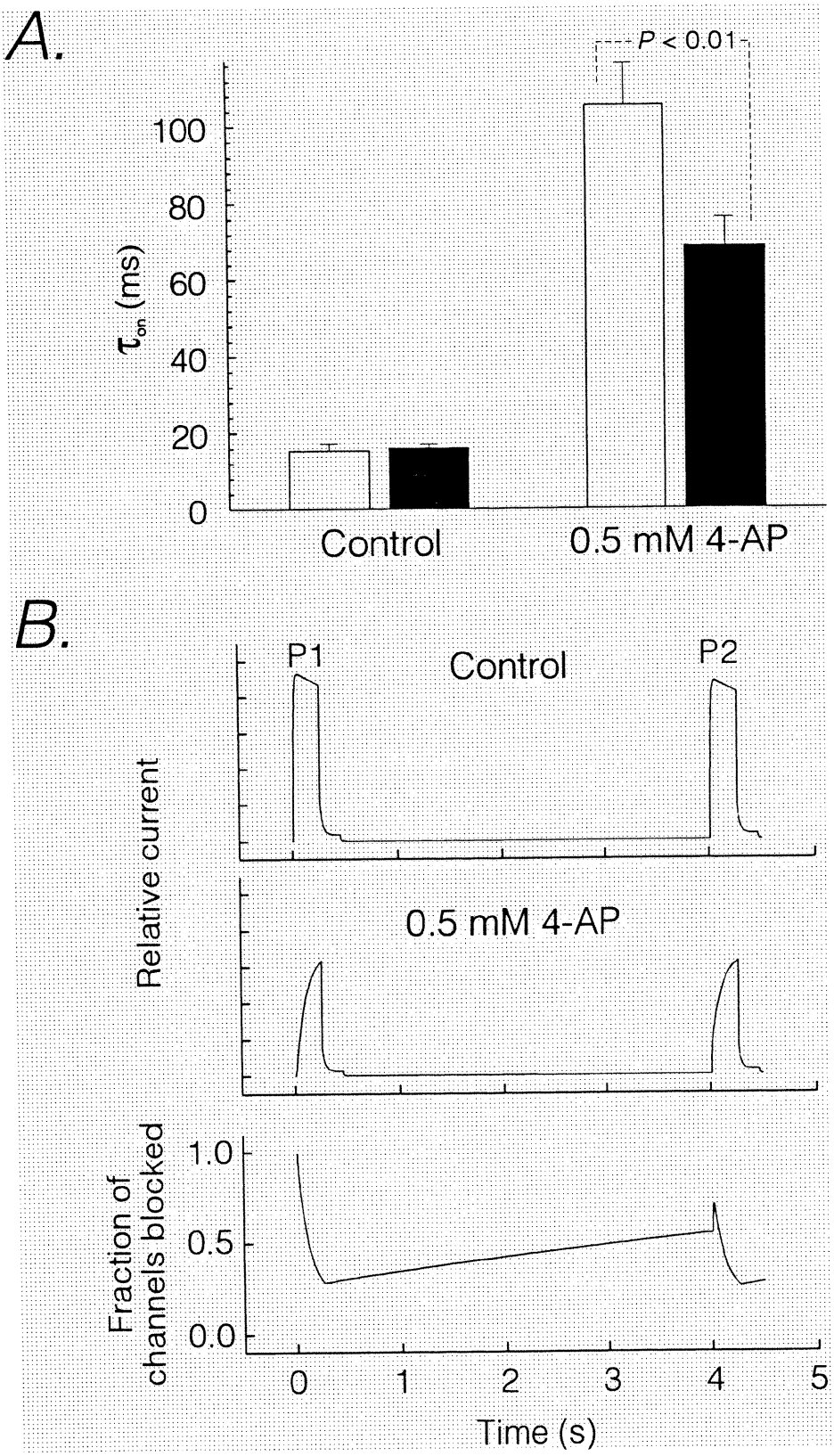
A.
P < 0.01
100
80
60
40
20
0
τ_{on} (ms)
Control
0.5 mM 4-AP
B.
P1
Control
P2
Relative current
0.5 mM 4-AP
Fraction of channels blocked
1.0
0.5
0.0
0
1
2
3
4
5
Time (s)

Figure 9. Evidence for unblocking of 4-AP during a train of depolarizing pulses provided by analysis of activation kinetics

A, time constants of activation (τ_{on}) of the first (P1, □) and second (P2, ■) pulses of a train of depolarizing steps to +20 mV from a V_h of –60 mV (0.25 Hz) in control conditions (left set of bars) and after steady-state inhibition by 0.5 mM 4-AP (right set of bars). These data were derived from the same experiments described in Fig. 6. Each bar is a mean ± S.E.M. ($N = 4$). *B*, on a relative scale are displayed computer-generated whole-cell currents in control conditions (top graph) and in the presence of 0.5 mM 4-AP (middle graph) in response to an identical voltage-clamp protocol to that of Fig. 6, which was designed to examine the frequency dependence of $I_{K(V)}$ in the absence and presence of drug. The bottom graph displays a plot of the time course of changes of the fraction of blocked channels following initiation of stimulation.

Cardiovascular Research (2000), **46.3**, *pp.* 557-568

ROLE OF Ca^{2+}- AND SWELLING-ACTIVATED Cl^- CHANNELS IN α_1–ADRENOCEPTOR-MEDIATED TONE IN PRESSURIZED RABBIT MESENTERIC ARTERIOLES.

Carmelle V. Remillard, Marie-Andrée Lupien, Valérie Crépeau, and N. Leblanc

Department of Physiology, University of Montréal, and

Research Centre, Montréal Heart Institute

Running Title: Role of $I_{Cl(Ca)}$ and $I_{Cl(swell)}$ in α_1–adrenoceptor-mediated tone

Discipline: Experimental. **Object of study:** Vasculature. **Level:** Multicellular. **Field of study:** Circulatory physiology. **Keywords:** Arteries; Cl^- channel; Mechanotransduction; Smooth Muscle; Vasoconstriction/Dilation

Word count: 7398

Corresponding author:

Normand Leblanc, Ph.D.
Associate Professor of Physiology
Research Centre
Montréal Heart Institute
5000 east, Bélanger St.
Montréal (Québec)
CANADA H1T 1C8

Tel.: (514) 376-3330, ext. 3998
FAX: (514) 376-1355
E-mail: [redacted]

ABSTRACT

C.V. Remillard, M.-A. Lupien, V. Crépeau, and N. Leblanc. Possible role of Ca^{2+}- and swelling-activated Cl^- channels in α_1–adrenoceptor-mediated tone in pressurized rabbit mesenteric arterioles. Ca^{2+}-activated ($I_{Cl(Ca)}$) and swelling-induced ($I_{Cl(swell)}$) Cl^- channels, respectively, have been postulated to participate in the membrane depolarization and contraction mediated by activation of α_1–adrenoceptors and vascular wall distension during pressurization. Their respective function in generating active force in pressurized arterioles during α_1–adrenoceptor stimulation remains unsettled. **Objectives:** Experimental protocols were designed to: (1) assess the relative contribution of $I_{Cl(Ca)}$ to the pressure-dependence of lumen diameter of mesenteric arterioles at different states of activation of the α_1–adrenoceptor, and (2) investigate the potential role of $I_{Cl(swell)}$ in spontaneous and agonist-mediated myogenic reactivity. **Methods:** Segments of endothelium-denuded rabbit mesenteric arterioles with a lumen diameter of ~ 70 μm were cannulated at both ends and studied under isobaric conditions at 36°C. Steady-state lumen diameter at each pressure step investigated (0 to 100 mm Hg, 20 mm Hg increments) was measured by a video-microscopy edge-detection technique. **Results:** Under control conditions, 23% of the arterioles developed nifedipine-sensitive spontaneous myogenic tone. In the presence of 1 mM tetraethylammonium chloride (TEA) to inhibit Ca^{2+}-dependent K^+ channels, the α_1–agonist phenylephrine (PE) contracted the vessels in a concentration-dependent manner (0.1 - 10 μM) and potentiated myogenic reactivity. The contraction mediated by 1 μM PE/TEA was abolished by 1 μM nifedipine, indicating that Ca^{2+} entry through voltage-gated Ca^{2+} channels was a necessary step in the cascade leading to contraction. Niflumic acid (NfA, 100 μM), a relatively selective inhibitor of $I_{Cl(Ca)}$, had no effect on myogenic tone but

reversed the PE-induced contraction, varying with the concentration of PE and transmural pressure. For PE concentrations between 0.1 and 1 μM, but not for 10 μM PE, the relaxing efficacy of NfA decreased as applied pressure was raised from 0 to 100 mm Hg. At all pressure steps, the NfA-induced relaxation was inversely related to the concentration of PE. DIDS (200 μM), another Cl^- channel blocker, inhibited spontaneous myogenic tone, and partially suppressed a component of contraction at elevated transmural pressures in arterioles incubated in 1 μM PE/1 mM TEA/100 μM NfA. **Conclusions:** Our data indicate that under low to moderate stimulation of the α_1–adrenoceptor signaling pathway, $I_{Cl(Ca)}$ channels play an important role in the sustained contraction produced. Their declining contribution to contraction with increasing transmural pressure may be explained, at least in part, by a progressive enhancement of stretch-induced ionic conductances, possibly volume-sensitive Cl^- channels.

1. INTRODUCTION

Noradrenaline (NA), a putative neurotransmitter released in blood vessel varicosities, induces a vasoconstriction that is usually accompanied in most vascular beds by a sustained membrane depolarization [1]. Among several postulated ionic mechanisms, it has been hypothesized that activation of a Ca^{2+}-activated Cl^- current ($I_{Cl(Ca)}$) by NA and other neurotransmitters and hormones plays a prime role in the associated depolarization observed in many vascular networks [2]. Consistent with single cell studies from which a putative physiological role was originally proposed, niflumic acid (NfA), a relatively specific blocker of $I_{Cl(Ca)}$ channels [2], and other fenamate compounds, partially or fully reversed the contraction mediated by activation of a_1–adrenoceptors [3-7]. These investigations have led support to the idea that activation of $I_{Cl(Ca)}$ plays a critical function in the sustained depolarization and contraction mediated by contractile agonists.

Many resistance arteries contract in response to stretch or an increase in transmural pressure. This endothelium-independent state of contraction, so-called myogenic tone or response, is thought to play a prime role in the autoregulation of blood flow in several vascular beds [8]. Besides a few exceptions (for a review, consult Davis and Hill [8]), myogenic tone generally occurs as a consequence of membrane depolarization [9] that leads to graded enhanced Ca^{2+} entry and modest elevations of intracellular Ca^{2+} concentration of 100 - 200 nM from a resting level of ~ 100 nM [10,11]. Several ionic mechanisms may participate actively in the depolarization and activation of myogenic tone. These include: (1) stretch-activated non-selective cation channels that are permeable to Ca^{2+} [12], (2) direct modulation of voltage-dependent Ca^{2+} channels by stretch [13], and (3) block of charybdotoxin- or TEA-sensitive Ca^{2+}-dependent K^+ channels [14]. Recently, Nelson *et al.*

[15] proposed that in cerebral arteries, myogenic tone may be the consequence of the activation of Cl^- channels that are distinct from $I_{Cl(Ca)}$ since: (1) niflumic acid was ineffective at reversing the depolarization and contraction evoked by increased transmural pressures, (2) DIDS and IAA-94, two commonly used chloride channel inhibitors, were shown to hyperpolarize cerebral arterioles and contribute to the myogenic contraction, and (3) lowering the extracellular Cl^- concentration potentiated the myogenic response. A Cl^- channel belonging to the ClC-3 subfamily of voltage-gated Cl^- channels was recently cloned from mammalian heart [16] and expressed in canine vascular smooth muscle cells [17]. This channel is regulated by changes in cell volume, is inhibited by DIDS, and is postulated to participate in the depolarization associated with the development of myogenic tone [17-19].

We hypothesized that the relative contribution of $I_{Cl(Ca)}$ in vasoactive tone induced by a constricting agonist changes when transmural pressure is altered in a manner consistent with a variable participation of these channels to overall membrane conductance. This hypothesis was tested by using niflumic acid as a pharmacological tool to assess the contribution of Ca^{2+}-dependent Cl^- channels to changes in active diameter of pressurized rabbit mesenteric arterioles stimulated with the α_1–adrenergic agonist phenylephrine. Two specific aims were sought: (1) to determine the effects of NfA on the pressure-diameter relationships obtained at different levels of activation of the α_1–adrenergic receptor; (2) to investigate the potential role of volume-sensitive Cl^- channels in spontaneous and agonist-mediated myogenic reactivity. Our results suggest that the contribution of $I_{Cl(Ca)}$ to membrane depolarization declines when transmural pressure is increased and this may be due, at least in part, to an enhanced contribution of volume-sensitive Cl^- channels recruited in response to

the increase in wall stress. Preliminary data have been published previously in abstract form [20].

2. METHODS

2.1 Tissue preparation

This study conforms with the *Guide to the Care and Use of Experimental Animals* published by the *Canadian Council on Animal Care,* and was approved by the *Animal Care Ethics Committee* of the Montréal Heart Institute. New Zealand white rabbits were sacrificed by cervical dislocation. Mesenteric arterioles 2 - 3 mm in length (mean lumen diameter 71 ± 2 μm, n = 106) were carefully dissected from the vascular bed, mounted on borosilicate cannulae in a perfusion chamber, and attached using silk suture threads. Criteria for viability of the arterioles included contraction to a bolus of 1 M KCl and/or 10 mM PE, and no pressure leaks between the proximal and distal ends of the vessel. In all experiments, the endothelium was removed by passage of a large air bubble through the vessel lumen; effective removal was assessed by the failure of acetylcholine (1 μM) to relax vessels pre-contracted with phenylephrine (1 μM). Suitable arterioles were then allowed to equilibrate at 40 mm Hg for 30-60 min at 36 ± 0.5°C before initiating experimental protocols.

2.2 Diameter measurements

An image of the arteriole was projected onto a video monitor via a microscope-mounted CCD camera (KP-113, Hitachi) at a final magnification of 10X. Lumen diameter of the vessel was monitored continuously by edge-detection (Living Systems Instrumentation Inc., Burlington, VT). Transmural pressures ranging from 0 to 100 mm Hg were applied for a minimum of 2 minutes at 20 mm Hg increments, maintained by a pressure-servo control

system, and monitored with a PM-4 pressure monitor (Living Systems Instrumentation Inc., Burlington, VT). Pressure transducers were attached at both the proximal and distal ends of the artery. Pressures reported throughout the study were registered from the proximal transducer.

Video (diameter) and pressure were recorded simultaneously on a conventional video tape (A. R. Vetter Co., Rebersburg, PA) and on a 486-IBM-PC using Axotape (version 2.0) or Axoscope software (version 7, Axon Instruments Inc., Foster City, CA) at a sampling rate of 25 or 33.3 Hz. Final analysis was performed using either Axotape or Axoscope, and Origin (version 4.1, Microcal Software Inc., Northampton, MA) softwares.

2.3 Solutions

The dissecting solution contained (mM): 120 NaCl, 25 $NaHCO_3$, 4.2 KCl, 0.6 KH_2PO_4, 1.2 $MgCl_2$, 11 glucose, 1.8 $CaCl_2$. The normal bathing (Control) solution was identical to the dissecting solution. Passive diameter changes to pressure were obtained by exposing the arteriole to a Ca^{2+}-free solution of similar composition, except for the omission of $CaCl_2$ and addition of 100 μM EGTA. The high K^+ (45 mM) solution was obtained by equiosmolar replacement of NaCl by KCl in the control solution. Test solutions were prepared by adding agents to the final concentrations into the control solution. Phenylephrine was prepared as a 10 mM stock in H_2O. Niflumic acid and nifedipine stock solutions were prepared in dimethyl sulfoxide (DMSO) at concentrations of 100 mM and 10 mM, respectively; the final concentration of DMSO never exceeded 0.1%. Tetraethylammonium chloride and DIDS were added in powder form to the final desired concentration. All drugs

were obtained from Sigma Chemical Co. (St. Louis, MO). Niflumic acid did not significantly alter the pH of the solution, monitored over a 45 minute period. Solutions were bubbled throughout with 5% CO_2, 95% O_2.

2.4 Equations used and statistical analysis

The concentration of phenylephrine, in the presence of TEA, resulting in 50% of maximal contraction (EC_{50}) was derived from a least-squares fit of mean data (including statistical errors as weighing factors) on a semi-logarithmic plot to a Logistic function for imposed transmural pressure steps in the range of 0 to 80 mm Hg. The maximal active force produced at each pressure step was estimated by subtracting the lumen diameter obtained with a saturating concentration of PE (10 μM) from that of the fully dilated vessel measured in Ca^{2+}-free medium. The relative contraction elicited by a given PE concentration and pressure (% Contraction $_{(P\text{-}x)}$) was estimated using the following equation:

$$\%\ Contraction_{(P=x)} = \{[Diam_{(PE=x)} - Diam_{(PE\text{-}10)}] / [Diam_{(0Ca)} - Diam_{(PE\text{-}10)}]\} \times 100 \quad [1]$$

where $Diam_{(PE=x)}$ and $Diam_{(PE\text{-}10)}$ are diameters measured at a given PE concentration and 10 μM PE, respectively, and $Diam_{(0Ca)}$ corresponds to the diameter obtained 0 Ca^{2+} - 100 μM EGTA.

Percent relaxation at a given pressure step (% Relaxation $_{(P=x)}$) due to niflumic acid was calculated using equation [2]:

$$\%\ Relaxation_{(P=x)} = \{[Diam_{(NfA)} - Diam_{([PE]/TEA)}] / [Diam_{(Ctrl)} - Diam_{(PE/TEA)}]\} \times 100 \quad [2]$$

where $Diam_{(NfA)}$, $Diam_{([PE]/TEA)}$, and $Diam_{(Ctrl)}$ are the diameters at the applied pressure in the presence of 100 μM NFA/PE/TEA, [*x*] PE/1 mM TEA and control solutions, respectively.

Data are expressed as means ± S.E.M. with *n* referring to the number of arterioles. Using the software Statistica for Windows 99 (version 5.5), statistical significance between individual means of steady-state lumen diameter (measured at the end of the pressure step) was assessed using a paired Students *t*-test when two groups were compared, or one-way ANOVA test with a Duncan's post-hoc multiple range test for repeated measure when more than two groups were analyzed. $P < 0.05$ was considered to be statistically significant.

3. RESULTS

3.1 Passive properties of rabbit mesenteric vessels

When pressurized to 40 mm Hg during equilibration, 23% (24/106) of the arterioles developed spontaneous myogenic tone, sometimes accompanied by slow cycles of constriction that usually disappeared after 30 min of pressurization. Figure 1A reports the passive characteristics of 30 of these vessels. Exposure to Ca^{2+}-free medium slightly but significantly dilated the arterioles at all pressures above 0 mm Hg. The relatively poor reactivity of these vessels in the absence of a contractile agent is consistent with other studies performed on the mesenteric vasculature [21,22].

3.2 The α_1–adrenoceptor-induced contraction is nifedipine-sensitive

Many chloride channel inhibitors, including members of the fenamate family such as niflumic acid, also stimulate large conductance Ca^{2+}-dependent K^+ (K_{Ca}) channels in vascular smooth muscle [23]. We first evaluated the effects of tetraethylammonium chloride (TEA) at a concentration (1 mM) that would be considered as relatively selective and potent for blocking K_{Ca} in vascular myocytes [24]. TEA significantly reduced lumen diameter relative to control at pressures between 20 and 60 mm Hg (Fig. 1B). These results suggest that K_{Ca} inhibition enhanced myogenic reactivity in our preparations.

We next tested the effects of TEA on pressure-diameter relationships in the presence of 0.1 or 1 μM phenylephrine (PE), a selective α_1–agonist. At 0.1 μM, PE had no effect on lumen diameter in the absence of pressure, but induced contraction with increasing pressure. Whereas TEA further contracted the arterioles in the presence of 0.1 μM PE (Fig. 1C), it failed to potentiate the contraction caused by 1 μM PE (Fig. 1D). These results suggest that

K_{Ca} may partly regulate the resting membrane potential and tone at low levels of α_1–adrenoceptor stimulation; however, this K^+ channel does not appear to play an important role at higher levels of receptor stimulation. In the presence of TEA, the EC_{50} for the PE-induced contraction was 352 (n = 45), 177 (n = 75) and 75 (n = 38) at 0, 40 and 80 mm Hg, respectively. These observations are consistent with the reported facilitation of myogenic reactivity following α_1–adrenoceptor stimulation [25].

Figure 1E shows that the contraction elicited by 1 μM PE in the presence of 1 mM TEA was totally reversed at all pressure steps by 1 μM nifedipine, a specific L-type Ca^{2+} channel blocker [26]. Our results are compatible with those obtained by others in rat small mesenteric arteries [21] and suggest that Ca^{2+} entry through voltage-dependent Ca^{2+} channels is mainly responsible for the sustained contraction induced by PE.

3.3 Role of Ca^{2+}-dependent Cl^- channels in α_1-adrenoceptor-induced tone

Figure 2 shows the results of two typical experiments in which we tested the effects of the $I_{Cl(Ca)}$ blocker niflumic acid (NfA) on vascular reactivity mediated by an intermediate (0.5 μM) and a saturating concentration (10 μM) of PE, in the presence of TEA. NfA produced differential pressure-dependent effects that varied with the concentration of PE. For the experiment using 0.5 μM PE (panel A), the arteriole passively dilated in the absence of drug (Control) in response to incremental pressure steps. Exposure to 0.5 μM PE/ 1 mM TEA contracted the arteriole from 84 to 18 μm in the absence of pressure and promoted myogenic reactivity when pressure was applied, consistent with studies in skeletal muscle arterioles [25]. In the continued presence of PE/TEA, 100 μM NfA dilated the arteriole in a pressure-dependent manner, but did not decrease myogenic reactivity. The graph displayed at the

lower right of Figure 2A summarizes the diameter-pressure relationships derived from this experiment. In the presence of NfA, the arteriole strongly autoregulated, displaying a fully relaxed state at 0 mm Hg, and a nearly fully contracted state at 80 and 100 mm Hg, relative to that measured in the absence of NfA. In the experiment using 10 μM PE (Fig. 2B) myogenic reactivity was apparent for pressure steps above 40 mm Hg in control conditions. Incubation of the arteriole with 10 μM PE/1 mM TEA led to a potent contraction at all pressures. Exposure to 100 μM NfA partially reversed the constriction induced by PE/TEA (lower right graph). Figure 3A shows pooled data in which we tested four concentrations of PE (0.1, 0.5, 1 and 10 μM) in separate series of experiments. At all PE concentrations except 10 μM, NfA was more effective at increasing lumen diameter at low transmural pressures. Its efficacy generally declined as pressure increased; this behavior was most striking with 0.5 μM, where no significant effect of NfA was apparent at 80 and 100 mm Hg. These differential effects of NfA are reflected better in panels A thru D of Figure 4 where the percentage of relaxation produced by NfA is plotted as a function of pressure for each concentration of PE studied. Separate series of experiments showed that the contraction remaining following exposure to NfA (in the presence of 1 μM PE/1 mM TEA) could be abolished by 1 μM nifedipine (n = 6; data not shown). Panel E also shows that NfA was progressively less potent at vasodilating the arterioles as the concentration of PE was increased for three selected pressure levels. In the absence of TEA (n = 5; data not shown), NfA completely reversed the contraction induced by PE, resulting in a "nifedipine-like" response (see Fig. 1E). These results are consistent with the idea that NfA stimulated K_{Ca}, an action that would hyperpolarize the resting membrane potential of the smooth muscle cells to an extent that activation of $I_{Ca(L)}$ by PE and/or $I_{Cl(Ca)}$ is prevented.

3.4 Effects of niflumic acid and DIDS on myogenic and α_1–adrenoceptor-mediated tone

The inverse-pressure dependent response to NfA with concentrations of PE in the range of 0.1 to 1 μM (Fig. 4) may be explained by the declining contribution of $I_{Cl(Ca)}$ as swelling-induced Cl^- channels ($I_{Cl(swell)}$) and/or other depolarizing ionic conductances are recruited by pressure-induced stretching of the myocytes. As reported by others in rat small mesenteric arteries [21], nifedipine (1 μM) abolished myogenic tone (n = 3; data not shown), consistent with a prerequisite function of $I_{Ca(L)}$ channels in the activation of this process. Since 4,4'-diisothiocyanatostilbene-2,2'-disulfonic acid (DIDS), a compound known to inhibit $I_{C(swell)}$ in vascular myocytes [17,19], has been recently shown to inhibit myogenic tone and hyperpolarize cerebral resistance arteries [15], we therefore tested the effects NfA and DIDS on mesenteric arteries that exhibited spontaneous myogenic tone. In these experiments, 1 mM TEA was also included to counteract the NfA-induced stimulation of K_{Ca}. Whereas NfA produced no effect on pressure-induced tone (Fig. 5A), 200 μM DIDS significantly alleviated the constriction apparent at pressures above 20 mm Hg (Fig. 5B), an observation consistent with that made by Nelson *et al.* [15] in cerebral vessels. Separate experiments revealed that NfA or DIDS did not affect the contraction induced by 45 mM KCl (with TEA) at 0 or 40 mm Hg (n = 6 for both), suggesting that these compounds likely exert little, if any, effect on $I_{Ca(L)}$ channels.

The effects of NfA and DIDS in the same preparation after pre-contraction with 1 μM PE/1 mM TEA were then investigated. Figure 6A reveals that combined PE/TEA contracted the arterioles at all pressures to a similar extent to experiments described in Figures 1 and 3.

Relative to the passive diameter of these vessels obtained after incubation in Ca^{2+}-free medium, 100 μM NfA relaxed the pre-contracted arterioles at all pressures, but with a more prominent effect at lower pressures. A subsequent exposure to 200 μM DIDS in the presence of PE/TEA/NfA caused a vasorelaxation at all pressures but with greater efficacy for pressures > 20 mm Hg. Figure 6B reports the relative relaxation (expressed as percent relaxation) produced by NfA, with and without DIDS. In the absence of DIDS, the percent relaxation mediated by NfA was still pressure-dependent, exhibiting a progressive decline as pressure increased. Although the preparations significantly dilated at 0 mm Hg in response to DIDS, this compound's major effect was to eliminate the pressure-dependence of relaxation in the range of 20 to 100 mm Hg. The vasodilation mediated by DIDS was not due to receptor desensitization since the constriction caused by 1 μM PE/1 mM TEA was maintained for over 90 min in separate experiments (n = 3).

4. DISCUSSION

4.1 Major findings

The major goal of this study was to investigate the role of Ca^{2+}-dependent Cl^- channels to α_1–adrenoceptor-mediated tone in pressurized rabbit mesenteric resistance-sized arteries. To our knowledge, our study is the first to demonstrate that niflumic acid (100 μM), a relatively selective blocker of $I_{Cl(Ca)}$ in vascular smooth muscle [2], reversed the contraction produced by the α_1–agonist phenylephrine (PE) in a manner that depended both on the concentration of the agonist and transmural pressure. For PE concentrations between 0.1 and 1 μM, the potency of NfA at causing relaxation decreased as applied pressure was raised from 0 to 100 mm Hg. In contrast, the relaxation exerted by NfA was relatively independent of pressure when the arterioles were exposed to 10 μM PE, a concentration that elicited maximal contraction in our preparation. The NfA-induced relaxation was inversely related to the concentration of PE. While NfA did not influence spontaneous myogenic tone, DIDS (200 μM), another Cl^- channel blocker, inhibited myogenic tone in the absence of PE, and partially suppressed a component of contraction at elevated transmural pressures in arterioles incubated in the presence of 1 μM PE/1 mM TEA /100 μM NfA. Our data indicate that at low to moderate stimulation of the α_1–adrenergic receptor signaling pathway, $I_{Cl(Ca)}$ channels play an important role in the sustained depolarization and contraction induced by these receptors. Their declining relative contribution to membrane potential and tone as transmural pressure or PE concentration is elevated may be explained by a progressive enhancement of stretch-induced ionic conductances, possibly volume-sensitive Cl^- channels as recently proposed by one group [17], or by other ionic or contractile mechanisms that are downstream of the α_1–adrenoceptor signaling pathway.

4.2 α_1–Adrenoceptor-induced contraction and role of Ca^{2+} channels

It is well known that noradrenaline (NA), an endogenous neurotransmitter released from nerve terminals of most blood vessels, induces vasoconstriction and membrane depolarization by predominantly interacting with α_1–adrenergic receptors. Phenylephrine, a full α_1–agonist, was used to assess the possible contribution of $I_{Cl(Ca)}$ on the diameter-pressure relationships induced by variable levels of stimulation of this pathway. We cannot rule out the possibility that shifts in the sensitivity to $[Ca^{2+}]_i$ may play a role in the response to various concentrations of PE [1,27,28]. However, inhibition by a dihydropyridine of PE-induced tone (Fig. 1) clearly indicates that Ca^{2+} entry through L-type Ca^{2+} channels is a prerequisite for the sustained contraction induced by α_1–adrenoceptors, a finding consistent with observations made by Wesselman *et al.* [21] in rat mesenteric small arteries. Similar to another study in rat small arteries [29], the complete suppression of tone by nifedipine also argues against a direct contribution from Ca^{2+} entry through non-selective cation channels.

4.3 $I_{Cl(Ca)}$ channels participate in α_1–adrenoceptor-mediated tone

Phenylephrine may elicit tone by an indirect activation of voltage-dependent Ca^{2+} channels resulting from the triggering of one or several depolarizing conductances. Among several postulated mechanisms, a possible role for Ca^{2+}-dependent Cl^- channels in agonist-induced membrane depolarization has recently received support in many vascular beds [2]. Niflumic acid was chosen rather than other Cl^- channel blockers because it is considered the most potent and relatively selective inhibitor of $I_{Cl(Ca)}$ [2]. In single cell studies, 100 μM NfA has been reported to nearly completely block $I_{Cl(Ca)}$ [23], have no effect on Ca^{2+} channels [30,31], and cause ~ 50% block of swelling-induced Cl^- channels [19]. This concentration

was chosen to achieve near complete block of $I_{Cl(Ca)}$ [32] and took into account its reduced efficacy at blocking $I_{Cl(Ca)}$ in the physiological range of membrane potentials [33]. One setback of using NfA is that it also enhances the activity of K_{Ca} channels [23]. To alleviate the contribution of K_{Ca} channel activation to the NfA-induced relaxation, we relied on TEA to effectively block these channels, an approach also used by Yuan in pulmonary arteries [7]. In vascular smooth muscle, TEA causes a relatively high affinity block of K_{Ca} channels with a $K_i \approx 200$ μM. At 1 mM, TEA would result in over 95% block of K_{Ca} channel activity [24,34]. This agent is known to increase the sensitivity of NA-induced contraction [35]. Consistent with this, TEA produced modest effects on the diameter-pressure curve in the absence of agonist (Fig. 1B) and potentiated the myogenic response in the presence of 100 nM PE (Fig. 1C). We cannot rule out the possibility that NfA might have other non specific effects on tension, other ionic channels or signal transduction mechanisms associated with α_1–adrenergic receptors. Although additional experiments at the single cell level will be required to fully address these issues, our results suggest that the main action of NfA was probably to exert its vasorelaxing effect by inhibiting $I_{Cl(Ca)}$: (1) NfA-sensitive $I_{Cl(Ca)}$ channels have been clearly identified in mesenteric arterial smooth muscle cells and suggested to play a major role in the depolarization mediated by hormone receptors coupled to G_q and phospholipase C [36,37]; (2) the NfA-induced vasodilation is not consistent with a direct inhibitory action on L-type Ca^{2+} channels or contractile mechanisms since NfA had no effect on KCl-induced contractions; (3) the latter observation also lends support to the hypothesis that α_1–adrenoceptor-induced activation of $I_{Cl(Ca)}$ depolarizes the myocytes since 45 mM KCl would be expected to shift membrane potential (~ -26 mV [38]) near the predicted equilibrium potential for Cl^- in smooth muscle (~ -25 to -35 mV [39]); (4) NfA had no effect

on spontaneous myogenic tone which suggests that it did not influence stretch-activated non-selective cation channels or $I_{Cl(swell)}$, both speculated to participate in the depolarization and contraction associated with this process [8]; (5) the level of tone produced by 0.5 μM PE and 1 mM TEA was not significantly altered at 80 and 100 mm Hg; (6) the stimulation of K_{Ca} by norepinephrine is not influenced by NfA [33] suggesting that this agent does not interfere with the α_1–adrenoceptor signaling pathway.

Similar to our study, 10 μM NfA has been shown to block the increase in perfusion pressure to 1 nM NA by 34% in the isolated rat mesenteric vascular bed [6] and the contraction to 1 μM NA by 38% in isolated rat aorta [3]. In pulmonary arteries, 10 and 50 μM NfA decreased the PE (0.5 μM)/TEA (1 mM)-induced contraction by approximately 50% and 86%, respectively [7]. By comparison, we measured an average relaxation of 61%, 44%, 48%, and 38% by 100 μM NfA at 40 mm Hg with 0.1, 0.5, 1, and 10 μM PE (1 mM TEA present) in the bathing solution, respectively. However, with 1 μM PE/1 mM TEA/100 μM NfA in the bathing medium, 1 μM nifedipine was still able to fully dilate the arterioles from the partially relaxed state induced by NfA. This suggests that NfA did not alleviate the requirement of functional Ca^{2+} channels for the contraction to take place and points to the involvement of additional mechanisms of stimulation of $I_{Ca(L)}$, either by a direct α_1–adrenoceptor-mediated interaction with the channel [40], or indirectly by promoting depolarization via a distinct membrane conductance.

One distinctive feature of the effects of NfA in our investigation was its diminished vasorelaxing ability as transmural pressure increased for PE concentrations between 0.1 and 1 μM; relaxation was pressure-independent with 10 μM PE. There is little doubt that the participation of $I_{Cl(Ca)}$ in the contractile response to 0.1 μM PE was overestimated due to the

block of K_{Ca} by TEA. The pressure-dependent effects of TEA clearly followed a reverse pattern to that produced by NfA (compare Fig. 1C to Fig. 3A). In the absence of TEA, 0.1 μM PE had no effect on diameter at 0 mm Hg (Fig. 1C), whereas NfA abolished the contraction mediated by PE in the presence of 1 mM TEA at the same pressure (Figs. 3A and 4A). Although these data limit our interpretation about the true contribution of $I_{Cl(Ca)}$, they nonetheless indicate that the latter can play a relatively more important function in determining membrane potential and tone when K_{Ca} channels are inhibited. We cannot rule out that a similar phenomenon may have occurred with 0.5 μM PE but this was probably not the case with 1 μM PE. In that instance, TEA failed to potentiate the effects of the α_1–agonist (Fig. 1D), suggesting that K_{Ca} channels played a relatively minor role under these conditions. In two separate but consistent series of experiments, NfA reversed the contraction by 1 μM PE and 1 mM TEA to a greater extent at lower pressures.

Subsequent experiments were devised to explore the possibility that vessel distention in response to pressure steps recruits swelling-induced Cl^- channels as recently proposed [15,17]. Activation by distension of $I_{Cl(swell)}$, or any other depolarizing conductance [12], would tend to diminish the relative contribution of $I_{Cl(Ca)}$ to membrane potential and vascular tone. As similarly reported in cerebral arterioles [15], 200 μM DIDS/1 mM TEA potently inhibited but did not abolish myogenic tone at a concentration that would block $I_{Cl(swell)}$ by ≥ 80% at -50 mV [19], an effect not shared by NfA (Fig. 5). In rabbit portal vein myocytes, DIDS has been reported to also inhibit $I_{Cl(Ca)}$, albeit with less potency than NfA (IC_{50} > 200 μM [41]). However this likely had a minor impact in our experiments since DIDS was always added after NfA in the experiments with PE (Fig. 6). As previously observed, DIDS did not significantly affect KCl-induced contraction at 0 or 40 mm Hg indicating that its

dilatory action does not involve a direct inhibition of L-type Ca^{2+} channels. These results are consistent with the reported lack of effect of DIDS on KCl-induced contractions [4,15] and whole-cell Ca^{2+} current [30,31]. However, since a systematic study examining the possible effects of DIDS on stretch-activated non-selective cation channels is presently lacking, interpretation regarding the possible involvement of $I_{Cl(swell)}$ channels must be undertaken with caution.

In arterioles pre-contracted with 1 μM PE/1 mM TEA, the application of DIDS in the presence of NfA mainly inhibited the remaining contraction at pressures above 20 mm Hg (Fig. 6A) resulting in flattening of the percent relaxation-pressure relationship (Fig. 6B). The DIDS-induced removal of the pressure-dependence of relaxation exerted by NfA, combined with the fact that the latter had no influence myogenic tone (Fig. 5A), or the constriction elicited by 0.5 μM PE/1 mM TEA at 80 and 100 mm Hg (Fig. 3B), support the following hypotheses: (1) swelling-induced Cl^- channels (and/or or possibly a DIDS-sensitive stretch-activated non-selective cation channel) play an important role in the depolarization that triggers the myogenic response in mesenteric arterioles; (2) this $I_{Cl(swell)}$-induced depolarization persists during stimulation of α_1-adrenoceptors and accounts, at least in part, for the reduced participation of $I_{Cl(Ca)}$ to overall membrane conductance as transmural pressure increases.

Taken together, our data strengthen further the concept that activation of distinct types of chloride channels may represent a key determinant of the electromechanical properties of rabbit mesenteric arterioles submitted to physiological transmural pressures during sympathetic stimulation. However, other mechanisms likely participate in driving or modulating tone during stimulation of this pathway. Consistent with this was the observation

that the efficacy of NfA to induce relaxation decreased as the concentration of phenylephrine increased from 0.1 to 10 μM. Moreover, with 10 μM PE, the relative relaxation produced by NfA did not vary with pressure, measuring between 27% and 37% in the range of 0 to 100 mm Hg (Fig. 5D). Whether the lack of pressure-dependence and reduced contribution of $I_{Cl(Ca)}$ to α_1-adrenoceptor-induced contraction at moderate to saturating agonist concentrations (via stimulation of G_q, PLC and/or PKC) involves: (1) a shift in the sensitivity of the contractile apparatus to intracellular Ca^{2+} concentrations [1,27,28], (2) a direct stimulation [40] or stretch-induced modulation of Ca^{2+} channels [10,13], (3) inhibition of $I_{Cl(swell)}$ [42], (4) activation of non-selective cation channels [12,43], or (5) block of other K^+ channels [44,45], will necessitate further experiments.

ACKNOWLEDGMENTS

The authors wish to thank Drs. Iain Greenwood, Michel Lavallée and Éric Thorin for helpful comments and suggestions during the course of this study. This work was supported by the Heart and Stroke Foundation of Québec, the Medical Research Council of Canada, and funds from the FCAR and Montréal Heart Institute. CVR was a traineeship awardee of the Heart and Stroke Foundation of Canada. NL is a FRSQ senior.

REFERENCES

[1] Bülbring E, Tomita T. Catecholamine action on smooth muscle. *Pharmacol Rev* 1987; 39: 49-96.

[2] Large WA, Wang Q. Characteristics and physiological role of the Ca^{2+}-activated Cl^- conductance in smooth muscle. Am J Physiol 1996; 271: C435-C454.

[3] Criddle DN, deMoura RS, Greenwood IA, Large WA. Effect of niflumic acid on noradrenaline-induced contractions of the rat aorta. Br J Pharmacol 1996; 118: 1065-1071.

[4] Lamb FS, Barna TJ. Chloride ion currents contribute functionally to norepinephrine-induced vascular contraction. Am J Physiol 1998; 275: H151-H160.

[5] He Y, Tabrizchi R. Effects of niflumic acid on α_1-adrenoceptor-induced vasoconstriction in mesenteric artery in vitro and in vivo in two-kidney one-clip hypertensive rats. Eur J Pharmacol 1997; 328: 191-199.

[6] Criddle DN, deMoura RS, Greenwood IA, Large WA. Inhibitory action of niflumic acid on noradrenaline- and 5-hydroxytryptamine-induced pressor responses in the isolated mesenteric vascular bed of the rat. Br J Pharmacol 1997; 120: 813-818.

[7] Yuan XJ. Role of calcium-activated chloride current in regulating pulmonary vasomotor tone. Am J Physiol 1997; 272: L959-L968.

[8] Davis MJ, Hill MA. Signaling mechanisms underlying the vascular myogenic response. Physiol Rev 1999; 79: 387-423.

[9] Harder DR. Pressure-dependent membrane depolarization in cat middle cerebral artery. Circ Res 1984; 55: 197-202.

[10] McCarron JG, Crichton CA, Langton PD, MacKenzie A, Smith GL. Myogenic contraction by modulation of voltage-dependent calcium currents in isolated rat cerebral arteries. J Physiol (Lond) 1997; 498: 371-379.

[11] Knot HJ, Nelson MT. Regulation of arterial diameter and wall [Ca^{2+}] in cerebral arteries of rat by membrane potential and intravascular pressure. J Physiol (Lond) 1998; 508: 199-209.

[12] Davis MJ, Donovitz JA, Hood JD. Stretch-activated single-channel and whole cell currents in vascular smooth muscle cells. Am J Physiol 1992; 262: 1083-1088.

[13] Langton PD. Calcium channel currents recorded from isolated myocytes of rat basilar artery are stretch sensitive. J Physiol (Lond) 1993; 471: 1-11.

[14] Wesselman JPM, Schubert R, VanBavel E, Nilsson H, Mulvany MJ. K_{Ca}-channel blockade prevents sustained pressure-induced depolarization in rat mesenteric small arteries. Am J Physiol 1997; 272: H2241-H2249.

[15] Nelson MT, Conway MA, Knot HJ, Brayden JE. Chloride channel blockers inhibit myogenic tone in rat cerebral arteries. J Physiol (Lond) 1997; 502: 259-264.

[16] Duan D, Winter C, Cowley S, Hume JR, Horowitz B. Molecular identification of a volume-regulated chloride channel. Nature 1997; 390: 417-421.

[17] Yamazaki J, Duan D, Janiak R, Kuenzli K, Horowitz B, Hume JR. Functional and molecular expression of volume-regulated chloride channels in canine vascular smooth muscle cells. J Physiol (Lond) 1998; 507: 729-736.

[18] Nelson MT. Bayliss, myogenic tone and volume-regulated chloride channels in arterial smooth muscle. J Physiol (Lond) 1998; 507: 629-629.

[19] Greenwood IA, Large WA. Properties of a Cl^- current activated by cell swelling in rabbit portal vein vascular smooth muscle cells. Am J Physiol 1998; 275: H1524-H1532.

[20] Remillard CV, Leblanc N. $I_{Cl(Ca)}$ currents participate in α_1–adrenoceptor-induced membrane potential and vessel diameter changes in pressurized mesenteric arterioles. Biophys J 1998; 74: A99.

[21] Wesselman JPM, Vanbavel E, Pfaffendorf M, Spaan JAE. Voltage-operated calcium channels are essential for the myogenic responsiveness of cannulated rat mesenteric small arteries. J Vasc Res 1996; 33: 32-41.

[22] Karibe A, Watanabe J, Horiguchi S, Takeuchi M, Suzuki S, Funakoshi M, Katoh H, Keitoku M, Satoh S, Shirato K. Role of cytosolic Ca^{2+} and protein kinase C in developing myogenic contraction in isolated rat small arteries. Am J Physiol 1997; 272: H1165-H1172.

[23] Greenwood IA, Large WA. Comparison of the effects of fenamates on Ca-activated chloride and potassium currents in rabbit portal vein smooth muscle cells. Br J Pharmacol 1995; 116: 2939-2948.

[24] Nelson MT, Patlak JB, Worley JF, Standen NB. Calcium channels, potassium channels, and voltage dependence of arterial smooth muscle tone. Am J Physiol 1990; 259: C3-C18.

[25] Meininger GA, Faber JE. Adrenergic facilitation of myogenic response in skeletal muscle arterioles. Am J Physiol 1991; 260: H1424-H1432.

[26] McDonald TF, Pelzer S, Trautwein W, Pelzer DJ. Regulation and modulation of calcium channels in cardiac, skeletal, and smooth muscle cells. Physiol Rev 1994; 74: 365-507.

[27] van Breemen C, Saida K. Cellular mechanisms regulating $[Ca^{2+}]_i$ smooth muscle. Ann Rev Physiol 1989; 51: 315-329.

[28] Chen XL, Rembold CM. Phenylephrine contracts rat tail artery by one electromechanical and three pharmacomechanical mechanisms. Am J Physiol 1995; 268: H74-H81.

[29] Nilsson H, Jensen PE, Mulvany MJ. Noradrenaline-induced calcium inflow appears not mediated by receptor-operated calcium channels in rat mesenteric small arteries. Resistance Arteries 1994; 83-92.

[30] Pacaud P, Loirand G, Lavie JL, Mironneau C, Mironneau J. Calcium-activated chloride current in rat vascular smooth muscle cells in short-term primary culture. Pflugers Arch 1989; 413: 629-636.

[31] Lamb FS, Volk KA, Shibata EF. Calcium-activated chloride current in rabbit coronary artery myocytes. Circ Res 1994; 75: 742-750.

[32] Greenwood IA, Large WA. Analysis of the time course of calcium-activated chloride "tail" currents in rabbit portal vein smooth muscle cells. Pflugers Arch 1996; 432: 970-979.

[33] Hogg RC, Wang Q, Large WA. Action of niflumic acid on evoked and spontaneous calcium- activated chloride and potassium currents in smooth muscle cells from rabbit portal vein. Br J Pharmacol 1994; 112: 977-984.

[34] Nelson MT, Quayle JM. Physiological roles and properties of potassium channels in arterial smooth muscle. Am J Physiol 1995; 268: C799-C822.

[35] Haeusler G, Thorens S. Effects of tetraethylammonium chloride on contractile, membrane and cable properties of rabbit artery muscle. J Physiol (Lond) 1980; 303: 203-224.

[36] Klöckner U. Intracellular calcium ions activate a low-conductance chloride channel in smooth-muscle cells isolated from human mesenteric artery. Pflugers Arch 1993; 424: 231-237.

[37] Klöckner U, Isenberg G. Endothelin depolarizes myocytes from porcine coronary and human mesenteric arteries through a Ca-activated chloride current. Pflugers Arch 1991; 418: 168-175.

[38] Doughty JM, Miller AL, Langton PD. Non-specificity of chloride channel blockers in rat cerebral arteries: block of the L-type calcium channel. J Physiol (Lond) 1998; 507: 433-439.

[39] Aickin CC, Brading AF. Measurement of intracellular chloride in guinea-pig vas deferens by ion analysis, chloride efflux and micro-electrodes. J Physiol (Lond) 1982; 326: 139-154.

[40] Leprêtre N, Mironneau J, Morel JL. Both α_{1A}- and α_{2A}-adrenoreceptor subtypes stimulate voltage-operated L-type calcium channels in rat portal vein myocytes - Evidence for two distinct transduction pathways. J Biol Chem 1994; 269: 29546-29552.

[41] Hogg RC, Wang Q, Large WA. Effects of Cl channel blockers on Ca-activated chloride and potassium currents in smooth muscle cells from rabbit portal vein. Br J Pharmacol 1994; 111: 1333-1341.

[42] Duan D, Cowley S, Horowitz B, Hume JR. A serine residue in CIC-3 links phosphorylation-dephosphorylation to chloride channel regulation by cell volume. J Gen Physiol 1999; 113: 57-70.

[43] Takenaka T, Suzuki H, Okada H, Hayashi K, Kanno Y, Saruta T. Mechanosensitive cation channels mediate afferent arteriolar myogenic constriction in the isolated rat kidney. J Physiol (Lond) 1998; 511: 245-253.

[44] Clement-Chomienne O, Walsh MP, Cole WC. Angiotensin II activation of protein kinase C decreases delayed rectifier K^+ current in rabbit vascular myocytes. J Physiol (Lond) 1996; 495: 689-700.

[45] Bonev AD, Nelson MT. Vasoconstrictors inhibit ATP-sensitive K^+ channels in arterial smooth muscle through protein kinase C. J Gen Physiol 1996; 108: 315-323.

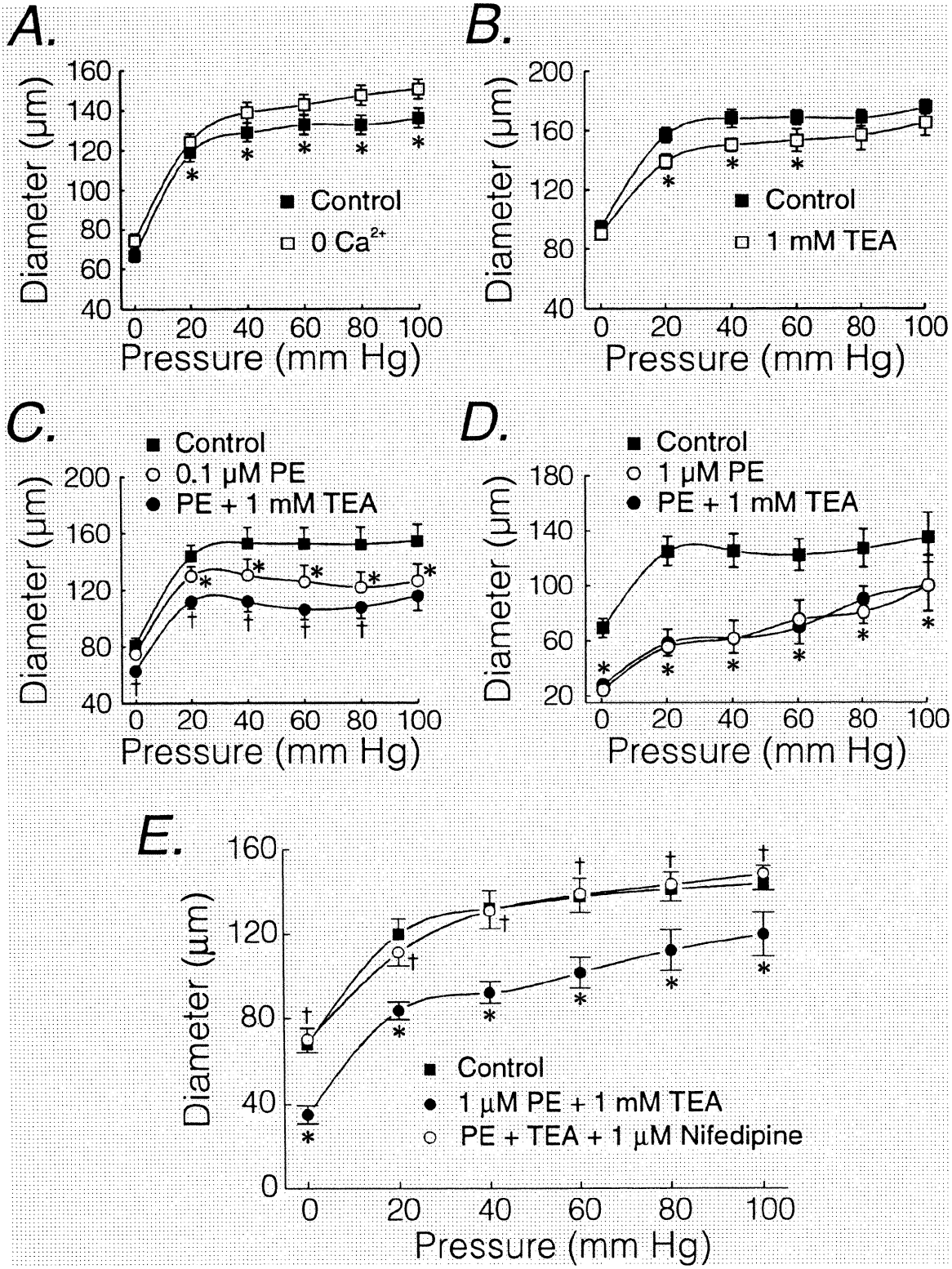
A.
Diameter (μm)
160
140
120
100
80
60
40
0 20 40 60 80 100
Pressure (mm Hg)
Control
0 Ca2+
B.
Diameter (μm)
200
160
120
80
40
0 20 40 60 80 100
Pressure (mm Hg)
Control
1 mM TEA
C.
Diameter (μm)
200
160
120
80
40
0 20 40 60 80 100
Pressure (mm Hg)
Control
0.1 μM PE
PE + 1 mM TEA
D.
Diameter (μm)
180
140
100
60
20
0 20 40 60 80 100
Pressure (mm Hg)
Control
1 μM PE
PE + 1 mM TEA
E.
Diameter (μm)
160
120
80
40
0
0 20 40 60 80 100
Pressure (mm Hg)
Control
1 μM PE + 1 mM TEA
PE + TEA + 1 μM Nifedipine

Fig. 1. Passive properties of pressurized vessels and contribution of TEA-sensitive K^+ channels. (A) Pressure steps were applied with 1.8 mM Ca^{2+} (Control, ■ or 0 Ca^{2+}/100 μM EGTA (□) in the bathing medium. A graph reporting the steady-state diameter ± S.E.M. (n = 30) *vs.* applied pressure is shown. **(B)** Arterioles were subjected to a similar pressure protocol with 1 mM TEA (n = 6) in the bathing solution to block K_{Ca} channels. Vessels contracted slightly to TEA (□) relative to Control (■). Panels **(C)** and **(D)** depict graphs showing the effects of 1 mM TEA (●) on the contraction elicited by 0.1 (n = 6) or 1 (n = 6) μM PE (○), respectively. As for panels **A** and **B**, the two graphs show mean steady-state diameter *vs.* pressure relationships. **(E)** Dihydropyridine inhibition of PE-induced tone. Mean diameter-pressure relationships from a total of 5 arterioles are displayed. The arterioles were subjected to pressure steps in Control (■), 1 μM PE/1 mM TEA (●) and 1 μM nifedipine/PE/TEA (○) conditions. For all panels: * significantly different from control ($P < 0.05$); panel **C**: † significantly different from 0.1 μM PE ($P < 0.05$); panel **E**: † significantly different from 1 μM PE + 1 mM TEA ($P < 0.05$).

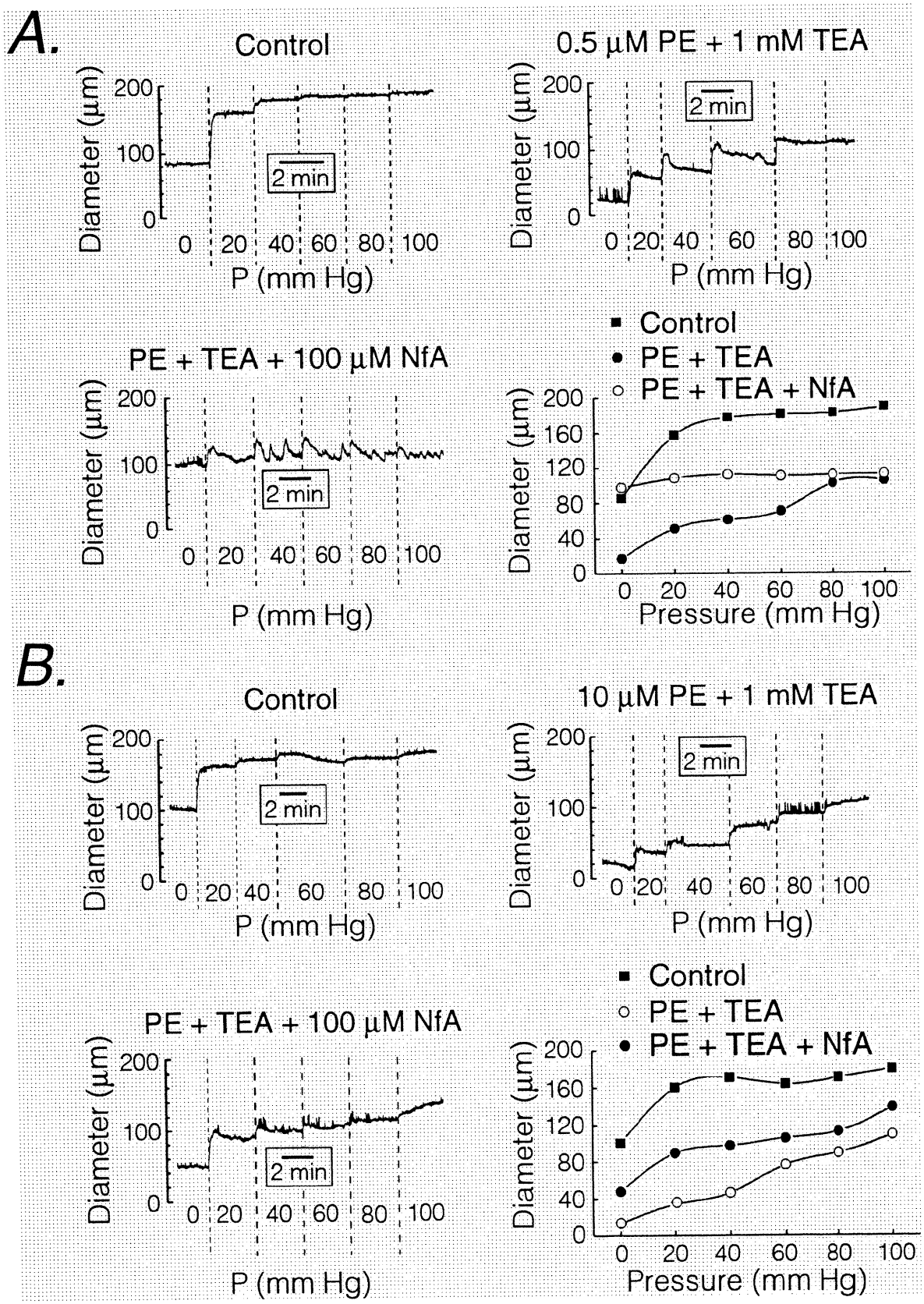
A.
Control
0.5 µM PE + 1 mM TEA
PE + TEA + 100 µM NfA
Diameter (µm)
200
100
0
2 min
0 20 40 60 80 100
P (mm Hg)
Control
PE + TEA
PE + TEA + NfA
160
120
80
40
Pressure (mm Hg)
B.
Control
10 µM PE + 1 mM TEA
PE + TEA + 100 µM NfA

Fig. 2. Representative traces showing relaxation by NfA of PE-induced vasoconstriction. Data from sample experiments with two PE concentrations are shown: 0.5 **(A)** and 10 **(B)** μM. In panel **A**, PE /1 mM TEA (top right trace) contracted the arteries at all pressures (P) and promoted myogenic reactivity. NfA (100 μM) reversed the contraction induced by PE/TEA at pressures between 0 and 60 mm Hg, and between 0 and 100 mm Hg for 0.5 and 10 μM PE, respectively (bottom left panels). At the lower right hand side of each panel is shown a graph illustrating the diameter-pressure relationships derived from each particular experiment.

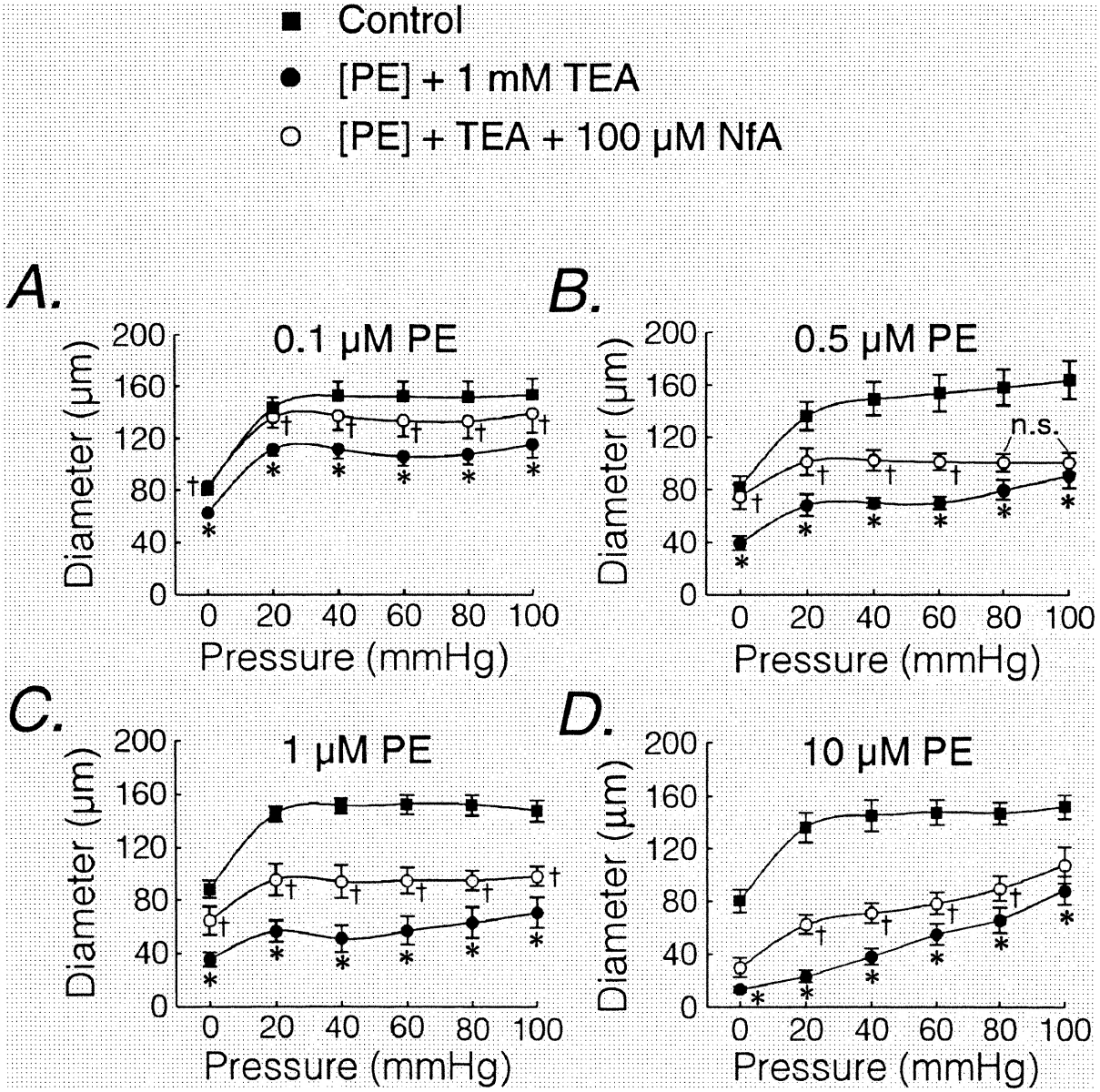
Control
[PE] + 1 mM TEA
[PE] + TEA + 100 µM NfA
A.
0.1 µM PE
B.
0.5 µM PE
n.s.
C.
1 µM PE
D.
10 µM PE
Diameter (µm)
Pressure (mmHg)
0
40
80
120
160
200
0
20
40
60
80
100

Fig. 3. Effects of NfA on the pressure-dependence of contraction induced by four different concentrations of PE. Pressure-dependence of mean lumen diameter measured in Control (■), [PE]/1 mM TEA (●), and 100 μM NFA/PE/TEA (○) conditions. The four graphs summarize results obtained in four separate series of experiments in which a single PE concentration was tested. Panels **A**, **B**, **C** and **D** show data obtained using 0.1 (n = 6), 0.5 (n = 6), 1 (n = 6), and 10 (n = 5) μM PE, respectively. Steady-state diameters are plotted as a function of applied transmural pressure. * Significantly different from control ($P < 0.05$); † notifies a significant vasorelaxation by NfA from the level of tone measured in the presence of a given PE concentration and 1 mM TEA ($P < 0.05$); n.s.: not significant.

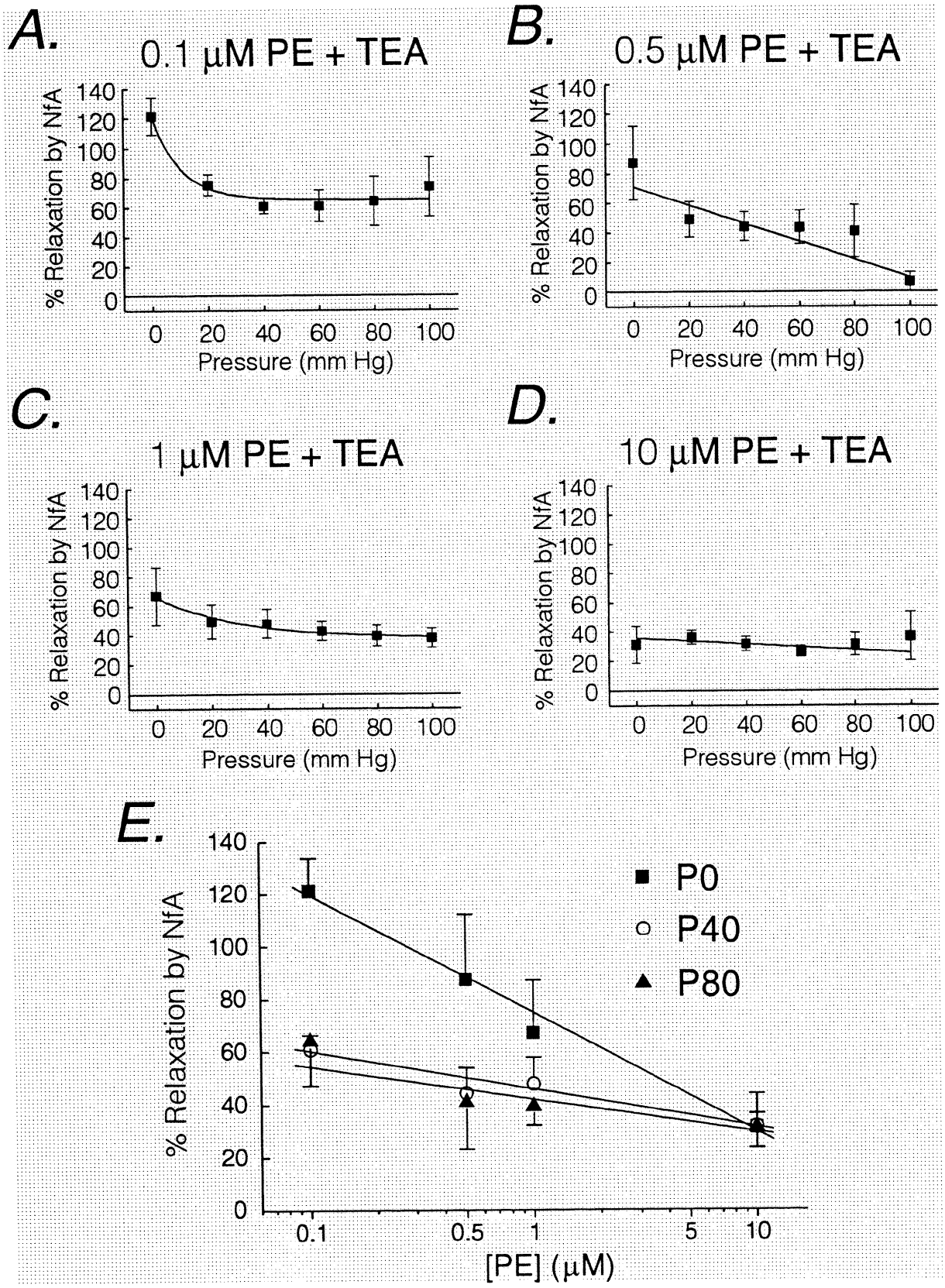
A.
0.1 μM PE + TEA
% Relaxation by NfA
Pressure (mm Hg)
B.
0.5 μM PE + TEA
% Relaxation by NfA
Pressure (mm Hg)
C.
1 μM PE + TEA
% Relaxation by NfA
Pressure (mm Hg)
D.
10 μM PE + TEA
% Relaxation by NfA
Pressure (mm Hg)
E.
% Relaxation by NfA
P0
P40
P80
[PE] (μM)

Fig. 4. Relaxation by NfA is pressure- and [PE]-dependent. The relative relaxation produced by 100 μM NfA (expressed as mean % relaxation relative to the control level) was calculated from the steady-state diameters measured in individual vessels for the series of experiments described in Fig. 3 and plotted as a function of transmural pressure for the four experimental PE concentrations tested in the presence of 1 mM TEA: 0.1 μM **(A)**, 0.5 μM **(B)**, 1 μM **(C)**, and 10 μM **(D)**. Percent relaxation was calculated using equation [2] (see *Methods*). **(E)** Graph reporting mean % relaxation by NfA as a function of PE concentration on a logarithmic scale for three selected pressure steps (P: 0, 40 and 80 mm Hg) as indicated. For panels **A** and **C**, the solid lines are least-squares mono-exponential fits to the mean data points with the error bars as weighing factors. For panels **B**, **D** and **E**, the solid lines are linear regressions to the data points. Except for panel **D**, all regressions yielded slopes which were significantly different from 0 ($P < 0.01$).

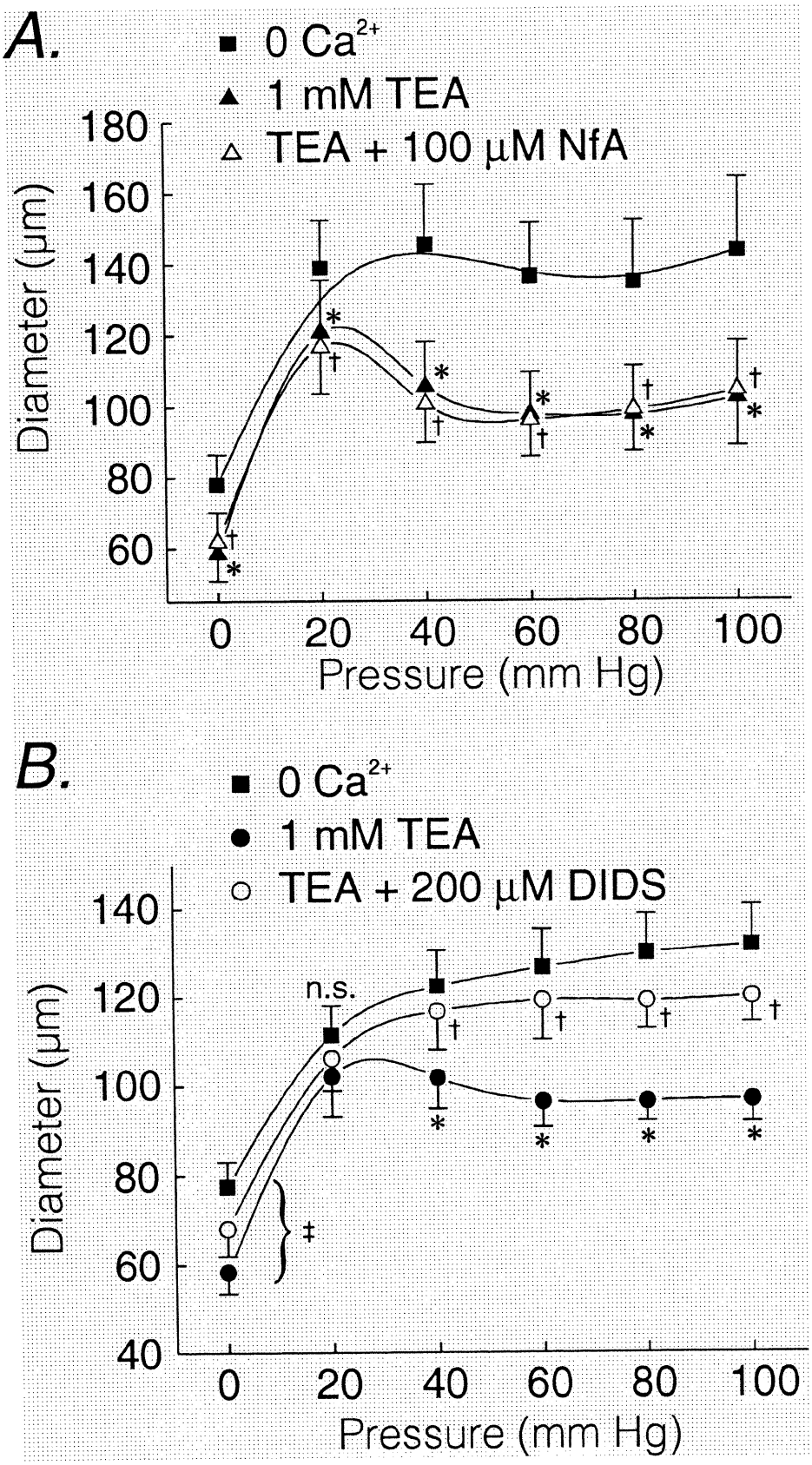
A.
0 Ca2+
1 mM TEA
TEA + 100 µM NfA
Diameter (µm)
180
160
140
120
100
80
60
0
20
40
60
80
100
Pressure (mm Hg)
B.
0 Ca2+
1 mM TEA
TEA + 200 µM DIDS
Diameter (µm)
140
120
100
80
60
40
n.s.
‡
0
20
40
60
80
100
Pressure (mm Hg)

Fig. 5. Effects of niflumic acid and DIDS on the myogenic response of arterioles incubated with TEA. Only arterioles exhibiting myogenic reactivity in control conditions were selected for these experiments. **(A)** Mean data from 6 experiments in which the arterioles were incubated in the presence of 1 mM TEA (▲) and TEA + 100 μM NfA (△). **(B)** Summarized data from 6 arterioles exposed to TEA (●) and TEA + 200 μM DIDS (○). For panels **A** and **B**, data obtained in Ca^{2+}-free medium (0 Ca^{2+}; ■) are included for comparison to the effects of NfA or DIDS. The results obtained in control conditions were omitted from these graphs for clarity's sake. For both panels, * indicates a significant difference from the 0 Ca^{2+} level ($P < 0.05$); in panel **A**: † notifies a significant difference between TEA + NFA and 0 Ca^{2+} ($P < 0.05$); in panel **B**: † significantly different from the level obtained in 1 mM TEA ($P < 0.05$); ‡ all three points were significantly different from each other ($P < 0.05$); n.s.: not significant.

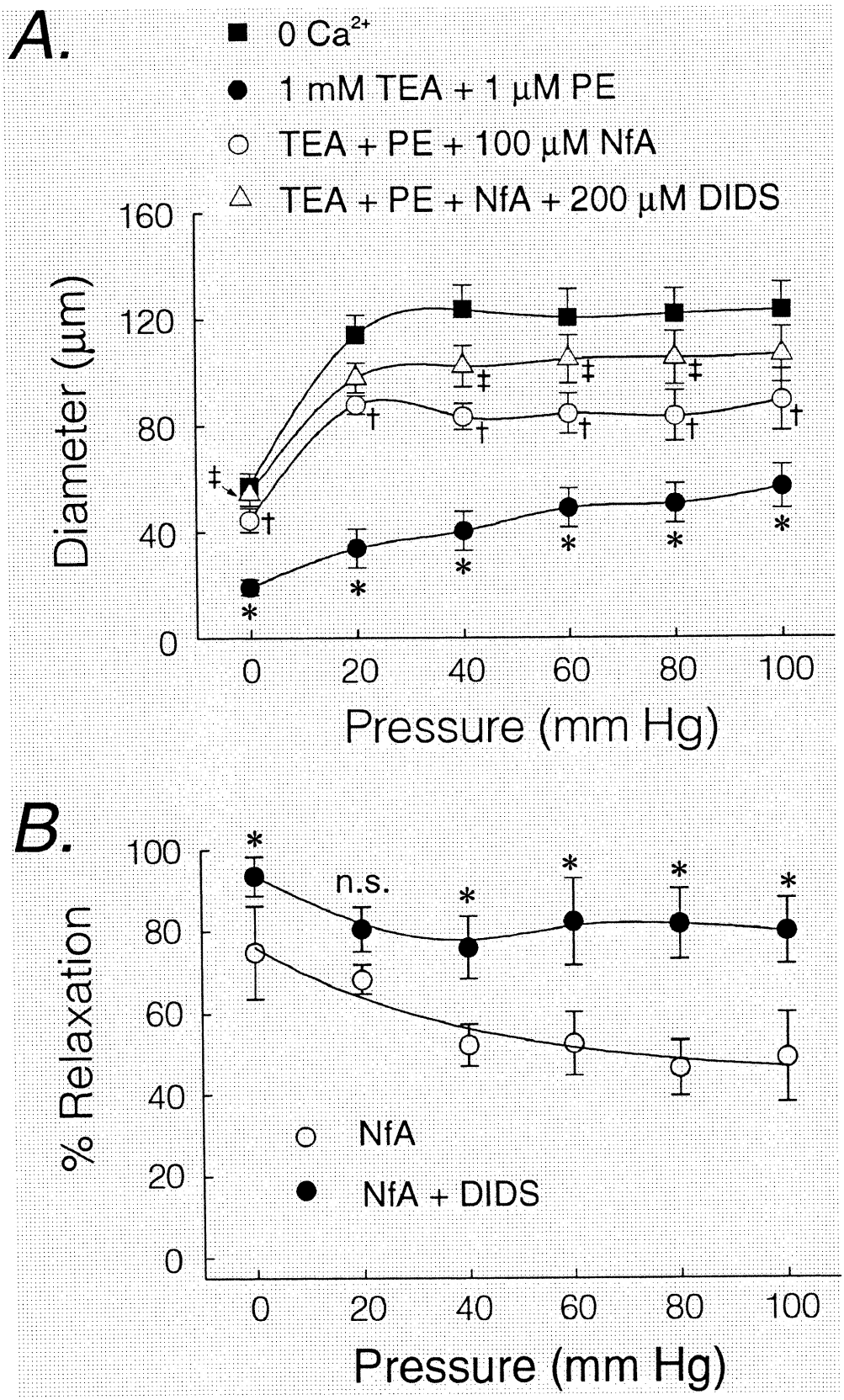
A.
0 Ca2+
1 mM TEA + 1 µM PE
TEA + PE + 100 µM NfA
TEA + PE + NfA + 200 µM DIDS
Diameter (µm)
160
120
80
40
0
0
20
40
60
80
100
Pressure (mm Hg)
B.
% Relaxation
100
80
60
40
20
0
n.s.
NfA
NfA + DIDS
0
20
40
60
80
100
Pressure (mm Hg)

Fig. 6. Effects of NfA and DIDS on the contraction induced by PE. (A) Vessels pressurized between 0 and 100 mm Hg were perfused with media containing 100 μM EGTA (■), 1 μM PE/1 mM TEA (●), 100 μM NfA/PE/TEA (○), or 200 μM DIDS/NfA/PE/TEA (△) (n = 6). * Significantly different from the 0 Ca^{2+} level ($P < 0.05$); † significantly different from the level obtained in 1 mM TEA + 1 μM PE ($P < 0.05$); ‡ significantly different from the level reached in the presence of TEA + PE + 100 μM NfA. **(B)** The relative relaxation induced by NfA (○) and NfA/DIDS (●) (calculated from panel **A**) are plotted against pressure. * Significantly different from the level of relaxation exerted by NfA alone ($P < 0.05$); n.s.: not significant.

DISCUSSION

D-1 Summary of findings

Modulation of K^+ and Cl^- channel activity is essential in controlling changes in membrane potential, myogenic activity, and lumen diameter at rest and following α_1–adrenoreceptor stimulation. More precisely, this study has shown that, in conduit rabbit coronary arteries, 4-aminopyridine inhibits K_{dr} channels while the channel is in a closed state, and that this inhibition is relieved upon channel transition to the open state during depolarization. Furthermore, inhibition of K_{dr} by 4-AP causes membrane depolarization likely by shifting the steady-state activation curve toward more positive potentials. From a second study, there is functional evidence that Cl^- channels (Cl_{Ca} and DIDS-sensitive) participate in PE-enhanced vascular tone in intact rabbit mesenteric arterioles. The relaxation by niflumic acid (NfA), an inhibitor of Cl_{Ca}, is dependent on both applied transmural pressure and the level of receptor stimulation, *i.e.* PE concentration. The relaxation by NfA decreases with increasing pressure when PE concentration ranges between 0.5 and 1 μM, but is independent of pressure with 10μM PE in the bathing medium, varying little over the entire pressure range. Pressure-dependence of relaxation is not evident in the presence of DIDS. The apparent reduced efficacy of NfA at higher pressures may reflect enhanced activity of a DIDS-sensitive Cl^- channel, and/or possibly a DIDS-sensitive cation channel, due to membrane stretch, thereby partially masking the contraction by Cl_{Ca} at these pressures. Cl_{Ca} activation by α_1–AR stimulation results in a significant membrane depolarization. Finally, the DIDS-sensitive Cl^- current, but not Cl_{Ca}, is involved in the myogenic response observed in normal saline solutions.

D-2 The interaction between 4-aminopyridine and K_{dr} channels

Our data has identified the most probable mechanism by which 4-AP causes inhibition of voltage-dependent K_{dr} channels. Initial studies had indicated that 4-AP was more effective at more negative membrane potentials, implying that inhibition occurred while the channel was in the closed or rested state. In rabbit coronary artery myocytes, 4-AP preferentially binds K_{dr} channels in the closed state to cause inhibition, and remains trapped in the closed channel until the membrane is depolarized. This is based on the observation that *i*) the activation of K_{dr} was slower in the presence of 4-AP, *ii*) blockade exhibited "reverse use-dependence" based on the partial and time-dependent relief of inhibition by repetitive depolarizing pulses, and *iii*) block is achieved while the channels are kept in a closed state (holding potential maintained at –60 mV during 4-AP wash-in). Computer simulations using time constants derived from our data support our conclusion of closed-state and reverse use-dependent inhibition of K_{dr} channels by 4-AP.

A. Comparison of studies on the interaction of 4-AP with voltage-dependent K^+ channels

K_{dr} channels have been extensively studied because of their primary role in regulating membrane potential. 4-Aminopyridine has been a major contributing factor in the advancement of our current understanding of the biophysical properties and functional roles of K_{dr} and other K^+ channel classes. The actions of 4-AP on K_{dr}, I_{to} / I_A and K_{ATP} currents are summarized in *Table 5* and discussed further below.

Despite its seemingly non-specific effects, the range of activity of 4-AP on the outward currents is relatively small when measured at depolarized potentials (typically > 0 mV). The $K_{½}$ value of 4-AP measured at +20 mV (1.37 mM) is generally higher than that reported in the literature at similar membrane potentials [103, 110, 221], but matches that

measured in isolated other coronary artery myocytes [110, 296]. This value is not likely to be inflated because of non-specific effects on either K_{Ca} or K_{ATP} channels since these were minimized by the inclusion of EGTA and ATP in the pipette solution. Furthermore, the percentage of inhibition reported here is very similar to that reported by others in isolated coronary artery myocytes [110, 296]. However, caution is warranted when interpreting $K_{½}$ values for 4-AP blockade of K_{dr} channels because of the voltage-dependent nature of the channel and because of its inhibition by 4-AP.

Voltage modulates not only the activity of K_{dr}, but also the binding and release of 4-AP. The reverse use-dependence of 4-AP, *i.e.* 4-AP dissociation from the channel upon membrane depolarization is in agreement with other reports for both K_{dr} [43, 45, 51, 103, 186, 221, 246, 248, 321], and I_{to} / I_A [42, 145, 158, 218, 261, 280] channels. Some studies have also shown a use-dependent inhibition by 4-AP, *i.e.* increased inhibition with depolarization for K_{ATP} [69], as well as for other K_{dr} [162] and I_{to} / I_A [319] channels.

Property	***Us*** [242]	***Literature***
$K_{½}$	1.37 mM	0.089 to 3.1 mM [15, 44, 45, 51, 103, 109, 221, 270]
Channel binding state	Closed-state	Closed-state [42, 44, 45, 145, 158, 163, 221, 246, 296] Open-state [51, 69, 162, 218, 248, 261, 270, 319] Open- and inactivated state [280] None [43]
Relief of inhibition with depolarization	YES	YES [42, 45, 51, 83, 145, 158, 186, 218, 221, 248, 261, 280, 321] NO [69, 162, 163, 319]
Binding site	Not investigated	Cytoplasmic [51, 69, 162, 221, 270, 319] Intra- and extra- cellular [280, 321]
Interaction with inactivation gating mechanisms	Not likely	YES [51] NO [42, 45, 158, 248, 261, 280, 319]

Table 5: Known interactions of 4-AP with K^+ channels

4-AP actions on K_{dr}, I_{to} / I_A and K_{ATP} in various tissues, including smooth muscle. $K_{½}$, concentration for half-maximal inhibition of current.

Our data suggest that the binding and release of 4-AP are voltage-dependent, and that they correlate with the channel being in the closed or open states, respectively. This is quite clear if one interpolates from the observations classified in *Table 5*. For example, Šimurda *et al.* [261] have reported open-state-inhibition of I_{to} currents by 4-AP in dog ventricular myocytes. However they also stated that, even though inhibition is greatest early in the depolarizing step (consistent with an open-state interaction), prolonged depolarizations (> 50 – 100 ms) promoted unbinding of 4-AP. Other reports of open-state inhibition clearly showed use-dependent [69, 162, 319] or reverse use-dependent [51, 218, 248] mechanisms. In contrast, reports showing closed-state binding typically demonstrated reverse use-dependence, whether the channels are K_{dr} or I_{to} / I_A types [42, 44, 45, 145, 158, 221, 246, 296]. Our experimental observations and computer simulations concur with the latter statement.

The nature of the interaction of 4-AP with the open, closed, or inactivated (resting) states remains elusive, especially in vascular smooth muscle. At this time, data strongly suggest a closed-state interaction with K_{dr} from rabbit pulmonary [221], coronary [296], and cerebral [246] arterial myocytes. There are no reports of open-state binding of 4-AP to K_{dr} channels in VSM. However, tissue type is not likely to be the only determinant of the nature of the interaction of 4-AP with K_{dr} channels since cloning techniques have suggested that 4-AP interacts differently with the various $K_V\alpha$ that comprise K_{dr} channels in vascular smooth muscle cells. It has been assumed that K_{dr} channels in our preparation are made of a single $K_V\alpha$ component, as has been suggested from whole-cell [186, 296] and single channel [297] experiments in rabbit coronary artery. The kinetics and voltage-dependence we observed also resembled those observed for K_{dr} in other preparations [33, 103, 246, 325]. However, based on the differential effects of two concentrations of 4-AP on the fast inactivation kinetics, it is

possible that the K_{dr} channel in our preparation is composed of two or more $K_V\alpha$ components. It is also quite possible that, in fact, several populations of K_V channels make up K_{dr} channels in other myocytes, thereby reflecting the different sensitivity to 4-AP and activity of 4-AP on those proteins. This is based on the variety of combinations of known α and β subunits that may occur to form the heterotetrameric K_{dr} channels.

The interaction of 4-AP with the closed state could also suggest the modulation of gating mechanisms, particularly the inactivation and recovery from inactivation. This is unlikely in our preparation since we did not observe any appreciable effect on inactivation or reactivation kinetics. This has also been observed for both I_{to} / I_A and K_{dr} channels [42, 45, 158, 248, 261, 280, 319]. The use of molecular tools has resolved that 4-AP inhibition and K_{dr} channel inactivation are mutually exclusive [248, 319].

One important feature of drug binding is the location of the binding site, whether it is intracellular, extracellular, or within the channel pore. Indeed, parenthetically, this is possibly one of the only aspects of 4-AP binding that is generally agreed upon by the supporters of any type of interaction of 4-AP with either K_{dr} or I_{to} / I_A channels. The consensus is that 4-AP has an intracellular binding site that must be reached for inhibition to occur. 4-AP is a weak base (pKa = 9.17); thus, at physiological pH (7.2 – 7.3) approximately 99% of the drug is in the charged form [221]. Studies involving variations of extracellular pH [51, 221] have indicated that non-ionized 4-AP crosses the membrane and binds to a cytoplasmic site on or near K_{dr} channels to cause inhibition. Use of a membrane-impermeant form of 4-AP, 4-aminopyridine methiodide, has further supported the cytoplasmic 4-AP binding site theory [162, 270]. There are also indications that 4-AP inhibits K_{ATP} from an intracellular site in skeletal muscle [69], suggesting a common binding site for 4-AP among different K^+

channel proteins. The diversity of 4-AP's actions on different K^+ channels makes it a useful model for exploring drug-K^+ channel interactions and their molecular mechanisms.

B. A mathematical simulation supports our contention of closed-state interaction

A strength of our study was the use of mathematical simulations to generate a schematic model of the interaction of 4-AP with the K_{dr} channel in rabbit coronary artery myocytes. Using rate constants derived from the data and based on a closed-state interaction (as clearly indicated by our results with depolarizing trains), our model reasonably reproduced K_{dr} currents in the absence and presence of 4-AP {Fig. *4-AP-8A*}, their frequency-dependence {Fig. *4-AP-8B*}, activation time constants {Fig. *4-AP-9A*}, and effects during depolarization trains {Fig. *4-AP-9B*}. Our computer model also predicted a concentration-dependent shift of the availability curve (steady-state inactivation) by 4-AP, confirming the findings shown in Fig. *4-AP-2D*. In conclusion, we have provided the first complete model of the mechanism of interaction of 4-AP with voltage-dependent delayed rectifier K^+ channels in vascular smooth muscle. As a consequence, we have brought together the putative hypotheses proposed for 4-AP's mechanism of action and provided some supporting evidence for observations in VSM and non-VSM cell types.

C. Speculation as to the α subunit composition of coronary artery K_{dr} channels

As was suggested above, it is quite possible that the K_{dr} channel we have studied in coronary myocytes is not a homotetramer of subunits. Although we cannot elucidate the subunit composition of our channels, we can speculate based on current knowledge of how the different α-subunits are modulated by 4-AP and based on the similarity of the native currents shown here to those generated by the clones.

As was discussed earlier, 4-AP preferentially binds K_{dr} channels in the closed state in coronary cells. $K_V\alpha1.1$, $K_V\alpha1.2$, $K_V\alpha1.4$, $K_V\alpha2.1$, and $K_V\alpha3.1$ channels are blocked in the open-state by 4-AP [162, 248, 270, 319], therefore these subunits are likely not incorporated into the channels reported here. We can further eliminate the $K_V\alpha1.2$ as a candidate for the following reasons: 1) measured $K_{½}$ values for 4-AP are typically lower for $K_V\alpha1.2$ channels, 74 – 211 μM [128, 224] than what is shown here (1.37 mM); 2) $K_V\alpha1.2$ channels are insensitive to charybdotoxin, even at higher concentrations [247], which is contrary to what our lab has shown for this macroscopic current [186]; 3) although it can be detected in vascular smooth muscle, $K_V\alpha1.2$ is more prominent in gastrointestinal and visceral tissues [224]. In addition to the open-state block by 4-AP, $K_V\alpha1.4$ channels may also be excluded because they generate rapidly inactivating currents [319, 328] quite unlike ours. From the original list of seven possible α components of VSM K_{dr} channels, we are left with only three choices: $K_V\alpha1.5$, $K_V\alpha1.6$, and $K_V\alpha4.3$. While all three are expressed in vascular smooth muscle cells [328], $K_V\alpha1.5$ subunits are a likely component of native K_{dr} channels in vascular smooth muscle [55]. The latter study derived a cDNA clone encoding $K_V\alpha1.5$ from rabbit portal vein and expressed it in mammalian cells. Their expression system had some similarities (kinetics and voltage-dependence of activation, inactivation recovery kinetics, single channel conductance) with native portal vein K_{dr} currents [55]. However, there are differences in the kinetics and voltage-sensitivity of inactivation between the native and 'cloned' currents, suggesting that the channels likely are not comprised solely of $K_V\alpha1.5$ subunits. Therefore, the channels' structure may involve heteromultimers of $K_V\alpha$ with or without $K_V\beta$ subunits. Furthermore, the biophysical properties of our coronary K_{dr} currents are similar to those from native and cloned portal vein K_{dr} channels. This further supports our

conclusion that the coronary K_{dr} channel is comprised of more than one pore-forming α-subunit, including $K_V\alpha 1.5$.

There is a problem with comparing data from cloned channels with those of native channels: the expression system (usually *Xenopus* oocytes or mammalian cell lines) is not the same as the native cell. This may be the result of different modulation of the channel (phosphorylation or glycosylation) within the expression cell. This is shown quite clearly in the study by Clément-Chomienne *et al.* [55] where the same cloned rabbit portal vein $K_V1.5$ gene presents very different activation, inactivation, and deactivation kinetics when expressed in murine connective tissue L cells compared to expression in human HEK293 cells. In their system, the two reconstitutions of the same channel were also different from native K_{dr} channels: L cell-expressed currents differ in inactivation kinetics from native $I_{K(V)}$, and HEK293 cell-expressed currents differ in activation, inactivation, and deactivation from their native counterparts. Therefore, if the so-called 'control' current from identical channels is different when reconstituted into two cell types, it is safe to assume that the interaction with 4-AP will also differ significantly. As a result, extrapolating from observations of cloned channels in expression systems must be done carefully as the recombinant channels do not behave alike or like the native currents.

D-3 Chloride channels and vascular tone

The ultimate goal of this section of our study was to investigate the possible role of Ca^{2+}-activated Cl^- channels in the contraction and depolarization induced by α_1–AR stimulation by phenylephrine in pressurized mesenteric arterioles. Later, the topic was expanded to include the potential role of DIDS-sensitive (possibly volume-sensitive) Cl^-

currents under similar conditions. Many background experiments were performed to establish the basis for our experimental protocols, only a few of which have been mentioned in the manuscript submitted for publication. From our work, we have determined the following. *i*) The PE-induced vasoconstriction is completely inhibited by Ca_L blockade. *ii*) While having no effect on KCl-induced contraction or myogenic tone, NfA, a relatively selective blocker of Cl_{Ca}, partially relieves the contraction induced by PE in a concentration- and pressure-dependent manner at different PE concentrations (0.1 – 10 μM and 0.5 – 1 μM, respectively). *iii*) Cl_{Ca} channels appear to be mainly responsible for the PE-induced depolarization. Application of NfA completely reversed the depolarization induced by PE at 40 mm Hg, thereby implicating Cl_{Ca} currents in the α_1-AR depolarization. *iv*) With 1 μM PE and 1 mM TEA, DIDS (a putative Cl^- channel blocker) abolished the pressure-dependent relaxation mediated by NfA. *v*) DIDS inhibited the development of myogenic tone but had little, if any, effect on KCl-induced constriction.

A. Specificity of NfA and DIDS relative to Cl_{Ca} and Cl_{vol}

One concern of this study was the cross-activity of the Cl^- channel inhibitors. Both niflumic acid and DIDS have been used extensively to characterize both Cl_{Ca} and Cl_{vol} channels in smooth muscle, neurons, endothelial cells, and cardiomyocytes. Both NfA and DIDS have been shown to exert non-specific effects on other ionic conductances {*Table 3*}. They can also inhibit Cl_{Ca} and Cl_{vol} depending on the concentrations used {*Table 6*}.

Without distinguishing between effects on evoked or spontaneously activated Cl_{Ca}, the effective inhibitory concentration range of niflumic acid is between ~7 and 100 μM in VSM [60, 61, 115, 121, 138, 139, 161, 177, 179, 185, 227, 244, 303, 323], respiratory (bronchi and trachea) [146-148] and urethral [58] smooth muscles, endothelial cells [211], cardiac tissue [57,

333], *Xenopus* oocytes [313], and neurons [64, 184]. In smooth muscle, niflumic acid inhibits Cl_{Ca} evoked by NE, caffeine, angiotensin II, or 5-HT. The *caveat* associated with interpreting the $K_{½}$ values is the voltage-dependence of niflumic acid, *i.e.* NfA is up to four times more effective at depolarized membrane potentials (+50 mV) [114, 138, 211]. Unlike for Cl_{Ca}, inhibition of Cl_{vol} currents by NfA is not as widely reported, but does occur at higher concentrations, *i.e.* in the range of 50 to 600 μM [115, 184, 211, 252].

	Niflumic acid	DIDS
Voltage-dependence of block?	Yes (more effective at positive E_m)	Yes (more effective at positive E_m)
Cl_{Ca} inhibition		
STIC	10 – 100 μM (VSM; neurons; smooth muscle, endothelium, cardiac muscle)	100 μM – 1 mM (VSM, smooth muscle, endothelium; cardiac muscle)
Agonist-induced	7 – 100 μM (VSM, smooth muscle)	250 μM – 1 mM (VSM)
Cl_{vol} inhibition	50 – 600 μM (VSM, neurons, endothelium)	20 – 100 μM (VSM, endothelium)

Table 6: Comparative effects of NfA and DIDS

Approximate $K_{½}$ values reported from the literature are given for NfA and DIDS. "STIC", spontaneous transient inward currents activated by spontaneous bursts of Ca^{2+} from intracellular stores. "Agonist-induced" Cl_{Ca} triggered by NE or caffeine. "E_m" refers to the membrane potential.

We used 100 μM NfA to block Cl_{Ca} in our study. As can be ascertained, this is at the higher end of the effective range for NfA on Cl_{Ca} activity, and in the lower range for Cl_{vol} inhibition. Nonetheless, there have been other studies where this concentration of NfA was used to study Cl_{Ca} channel in VSM cells. At this concentration, there are conflicting reports that NfA may [114, 138, 223] or may not [147, 148, 161, 244] activate K_{Ca} currents. Regardless of whether NfA could affect K_{Ca} currents in our preparation, measurements were done with TEA (1 or 5 mM) in the bathing medium to inhibit K_{Ca} channels and to remove them from suspicion {Fig. *Cl-1B*}. This proved to be a sound decision since experiments performed without TEA (with PE and NfA present) distinctly showed a TEA-sensitive component

activated by PE and/or NfA. In addition to effects on K_{Ca} channels, there are reports that NfA and other Cl^- channel inhibitors may exert some effect on Ca_L channels [78, 207]. Our data do not support this: NfA does not inhibit contractions induced by KCl, hence due to Ca_L activation [60, 61, 131, 147, 161, 323], even at concentrations as high as 100 μM [161, 177].

Like NfA, the inhibition by DIDS is also voltage-dependent, becoming more effective with membrane depolarization [115, 317]. This compound can inhibit Cl_{vol} currents at micromolar concentrations (20 – 100 μM) in VSM and endothelial cells [29, 115, 207, 211]. Blockade of Cl_{Ca} by DIDS occurs at much higher concentrations, ranging between 100 μM and 1 mM for STICs or unevoked Cl_{Ca} [57, 111, 130, 139, 179, 211, 227] and 250 μM and 1 mM for agonist-evoked Cl_{Ca} [10, 17, 121, 139, 177]. The concentration of DIDS we have used (200 μM) is likely low enough so as to have little effect on PE-stimulated Cl_{Ca} channels although this was not systematically tested. This concurs with our observations and those of another study showing that DIDS does not influence Ca_L activity [17]. Consistent with this idea was the observation that while NfA had no effect on the myogenic response in the absence of agonist, DIDS significantly alleviated this process {Fig. *Cl-6*}.

Based on these arguments, we are confident that our choice of concentration for NfA and DIDS was sound, and, with the support of the appropriate control experiments, allow us to speculate that the possible contaminating effects (K_{Ca} enhancement) and the known cross-over effects between the two chloride channel inhibitors likely were minimal.

B. The α_1–adrenergic vasoconstriction

The mesenteric vascular bed, is richly innervated by sympathetic postganglionic vasoconstrictor fibers [112], with NE being the major neurotransmitter released. Both the vasoconstriction and the membrane depolarization associated with sympathetic NE release

have been studied extensively for years, but the mechanisms by which the cells depolarize and contract have not been completely elucidated. Similar to conclusions from other studies [48, 213, 289], we provide supporting evidence that Ca_L channels likely are involved in the sustained contraction: our experiments clearly showed that PE-activated nifedipine-sensitive channels cause vasoconstriction {Fig. *Cl-1E*}. Preliminary data have also described a nifedipine-sensitive component of the contraction that is not dependent on Cl_{Ca} activity, suggesting that PE may activate Ca_L channels by a non-Cl_{Ca}-dependent mechanism [188, 191, 210].

Breakthrough work by Pacaud *et al.* in 1989 [228] first showed that Cl_{Ca} channel activation is an important modulator of NE-induced tone. In their experiments, blockade of Cl_{Ca} channels with 9-AC produced relaxation to the same degree as that produced by Ca_L inhibition by isradipine, suggesting that Cl_{Ca} inhibition necessarily precluded the activation of Ca_L during NE exposure [225]. Since then, experimentation with other Cl^- channel inhibitors has identified niflumic acid as the most potent Cl_{Ca} inhibitor in various vascular smooth muscle types [183]. Despite its poor specificity, this compound has been used almost exclusively in recent years to characterize Cl_{Ca} currents in isolated vascular myocytes.

In multicellular vascular preparations, inhibition of NE-induced Cl_{Ca} currents by NfA typically results in partial relaxation of the tissue. For example, NfA (10 μM) has been shown to block the contraction induced by 1 nM and 1 μM NE by 34% and 38%, respectively in rat aorta and mesenteric bed [60, 61]. In the rat portal vein, application of 30 and 100 μM NfA has resulted in 25% and ~80%, respectively, inhibition of the maintained contraction due to 10 μM NE [161]. The contraction induced by 100 μM NE was reduced to 42% of control by 10 μM NfA in rat pulmonary artery myocytes [303]. Of more

relevance to us, 10 and 50 μM NfA decreased the contraction induced by PE (1 μM) / TEA (1 mM) by 50 % and 86%, respectively, in rat pulmonary artery rings [323]. In comparison to the latter study, we measured an average relaxation of 61%, 44%, 48%, and 38% by 100 μM NfA at 40 mm Hg with 0.1, 0.5, 1 and 10 μM PE / 1 mM TEA, respectively, in rabbit mesenteric arterioles. The relaxation is thus not only partial, but also dependent on the relative amount of contraction by PE {Fig. *Cl-4E*}. A plausible explanation for these results is that incremental concentrations of PE progressively induced more depolarization. In fact, we have observed a negative shift in the maximal contraction induced by PE/TEA, *i.e.* the maximum contraction due to PE occurs at lower transmural pressures with increasing PE concentration. Similarly, EC_{50} values for PE/TEA decreased from 350 ± 58 nM to 75 ± 19 nM with transmural pressures increasing from 20 to 80 mm Hg. Finally, we have established that the effect of NfA is pressure-dependent {Figs. *Cl-2* to *Cl-4*} with intermediate (0.5 and 1 μM, $R = 0.936$ and 0.915, respectively; $P < 0.05$) but not with 0.1 and 10 μM PE doses ($R = 0.621$ and 0.612, respectively) for pressures ranging from 0 to 100 mm Hg. Higher PE concentrations likely activate some non-Cl_{Ca}-related mechanisms that contribute to the active tone, thus rendering NfA less effective. PE at high concentrations has also been known to *i*) increase intracellular Ca^{2+} concentrations, and heightened Ca^{2+}-sensitivity of force during the sustained contraction [48], *ii*) activate CaL channels directly [188] or by stretch [182, 196], *iii*) activate non-selective cation channels [70, 277], as well as *iv*) block K_{dr} [56, 200] and/or K_{ATP} [30] channels. We propose that the combined depolarization due to pressurization (membrane stretch) and PE stimulation (activation of depolarizing currents) may be driving membrane potential closer to the reversal potential for

chloride, making NfA less effective at modulating membrane potential changes at higher transmural pressures (80 – 100 mm Hg), thus explaining the pressure-dependent relaxation.

The pressure-dependence of the percent relaxation by NfA data {Fig. *Cl-4*} allows for the argument that the pressure-dependence is not evident if the point at 0 mm Hg is removed. The same data, when re-plotted with the points at 0 mm Hg and re-fitted with linear regressions (not shown), show that, indeed, the relaxation is pressure-dependent for 0.5 and 1 μM PE (R = 0.930 and 0.981, respectively; $P < 0.05$), but not for 0.1 and 10 μM PE ($R = 0.426$ and 0.659, respectively). Since excluding the points at 0 mm Hg significantly changed the slopes of these regressions, it is apparent that a large part of the relaxation induced by NfA occurs at low intravascular pressures ranging between 0 and 20 mm Hg.

In 2 – 3 kg rabbits (same size as our subjects), mean arterial pressure (MAP) is approximately 70 mm Hg [27]. Pressure in the superior mesenteric artery is 10 – 15 mm Hg lower, so ~60 mm Hg [27], and there is a further 10 – 15 mm Hg drop in pressure at the first arterial arcade (inner diameter ~170 μm). Finally, another ~10 mm Hg decrease is measured in second-order arterioles (inner diameter ~40 μm) [27]. As stated previously, the arterioles we used had a mean diameter of 71 μm. Thus, the usual physiological pressure in these vessels rests between 30 and 50 mm Hg (~60% of MAP). Therefore, the 20 – 100 mm Hg range of pressures we used is physiologically relevant.

In non-physiological (*i.e.* pathological) situations, pressures < 20 mm Hg may be of great importance as well. For example, lipopolysaccharide-induced septic shock causes hypotension due to unregulated NO production and guanylate cyclase activation, as well as decreased mesenteric blood flow [49, 157]. In rabbits with a resting MAP of ~90 mm Hg, septic shock causes a ~30 mm Hg drop in arterial pressure. In our conditions, septic shock

should produce a pressure of at least 20 - 35 mm Hg in our second-order arterioles. Similarly, diabetic rats have a MAP of 97 mm Hg, which translates to approximately 85 mm Hg pressure in 390 μm arterioles (thus lower still in smaller arterioles) [61].

Perhaps the most dramatic effects on mesenteric circulation are observed during hypovolemic or hemorrhagic shock. The ensuing cascade of events (the "fight-or-flight response") due to this phenomenon is characterized by a redistribution of the diminished cardiac output away from the mesenteric organs to the brain, heart, skeletal muscle, and kidney [24, 74]. A recent study in swine [282] showed that hemorrhagic shock with 50% of blood volume lost caused, as expected, a decrease in MAP (from 115 to 61 mm Hg) and an increase in total peripheral resistance (TPR; 63% increase). The increased TPR was associated with a disproportionate and marked decrease in total mesenteric blood flow (26% of baseline), compared to the only 41% decrease in non-mesenteric blood flow. The decreased MAP and total mesenteric blood flow due to massive hemorrhaging will thereby reflect a decrease in mesenteric arteriole pressure as well. Therefore, all the above arguments support the inclusion of low (≤ 20 mm Hg) intravascular pressures in our analysis, if more for relevance in the pathological vs. physiological states. Further, there is yet another level of even smaller diameter arterioles that will experience yet smaller transmural pressures. This also imparts some importance to the enhanced effect of NfA at lower intravascular pressures that we observed, irrespective of the level of α_1–adrenergic stimulation.

C. Effects of NfA and DIDS on myogenic and α_1-adrenoceptor-induced tone

The pressure-dependence at intermediate PE concentrations may also be explained by the distension-induced recruitment of stretch- or swelling-induced Cl^- channels (Cl_{vol}) that have been shown in other VSM cells [207, 317]. Activation of this or any other depolarizing

conductance might thus diminish the relative contribution of Cl_{Ca} to changes in membrane potential and arterial tone. In rabbit mesenteric arterioles, we have demonstrated that external Ca^{2+} is essential for developing tone {Fig. *Cl-1A*}, and that Ca^{2+} influx via nifedipine-sensitive Ca_L channels is an important component of the myogenic response we observed. Evidence put forth by Nelson *et al.* [207] and the recent identification of a ClC-3 channel in human [178] and canine [317] VSM support the postulate that DIDS-sensitive Cl^- channels could also underlie, at least in part, the myogenic response. In experiments performed on arteries that exhibited spontaneous myogenic tone, we showed that NfA (100 μM, with 1 mM TEA present) had no effect on pressure-induced tone {Fig. *Cl-5A*}. However, DIDS (200 μM, with 1 mM TEA present) diminished the myogenic response at pressures > 40 mm Hg {Fig. *Cl-5B*}. This is in agreement with recent observations in rat cerebral arteries [207], that also provided some electrophysiological evidence for the role of Cl^- channels in the myogenic response. Arterioles pressurized to 80 mm Hg depolarized to approximately –39 mV, well within the Ca_L window current range. Application of DIDS (1 mM) produced a significant hyperpolarization of 14 mV, thereby driving membrane potential our of the window current range for Ca_L. It is thus likely that Cl^- channels are also regulated by cell membrane stretch. Coupled with the depolarization observed with DIDS [206] and the lack of effect of both DIDS and NfA on KCl-induced contractions, our observation that a DIDS-sensitive Cl^- conductance modulates the myogenic response would support the notion that a Cl^- conductance is activated, leading to membrane depolarization, enhanced Ca^{2+} influx through Ca_L channels, and the development of tone.

Our pharmacological data also indicate that α_1–adrenergic stimulation enhanced a DIDS-sensitive conductance in our preparation. However, identification of this current as

Cl_{vol} would require electrophysiological studies on the isolated mesenteric myocytes. This work will be the focus of future study. Nonetheless, we have shown that part of the NfA-resistant contraction produced by PE is inhibited by 200 μM DIDS {Fig. *Cl-6A*}. Comparing the relaxation by NfA in the presence and in the absence of DIDS further illustrates the contribution of Cl^- channels to the PE-induced vasoconstriction. NfA alone and NfA / DIDS had maximal effects when nominal pressure was applied (67 ± 5% vs. 94 ± 5% for NfA and NfA / DIDS, respectively) {Fig. *Cl-6B*}. At 40 mm Hg, NfA alone relaxed these vessels by 52 ± 5%, while NfA / DIDS relaxed them by 76 ± 8%. The pressure-dependent relaxation of 1 μM PE / TEA-preconstriction by NfA was no longer apparent when DIDS was present, ranging between 94 and 80% relaxation in the entire pressure range The most striking difference in the relative relaxation is noticed at pressures ≥ 60 mm Hg where DIDS / NfA produced between 29 and 35% more relaxation that NfA alone. We have hypothesized that increasing the pressure within the arteriole causes membrane stretching, which may activate Cl_{vol} further as pressure increases. As a result, DIDS would appear to be a more effective vasorelaxant as transmural pressure increases. Assuming that the efficacy of NfA does not change with DIDS present, it is possible that the relative contribution of Cl_{Ca} to the overall conductance decreases as a result of activation of Cl_{vol} (or possibly of a DIDS-sensitive stretch-activated non-selective cation channel) by membrane stretch. Thus, the "enhancement" of the NfA-induced relaxation due to DIDS may represent the contribution of Cl_{Ca} activity to the α_1–AR-induced vasoconstriction when Cl_{vol} channels are blocked. This theory is difficult to prove under our experimental conditions since Cl^- channel inhibitors have promiscuous effects, and will require further investigation at the single-cell level.

D. α_1–Adrenergic stimulation and membrane potential

Since chloride ions are relatively concentrated inside the smooth muscle cell, the activation of a chloride conductance (resulting in Cl^- efflux) represents a potentially important depolarizing mechanism in response to cell stimulation. Indeed, a Cl^--based depolarization has been observed in response to NE [9, 39, 225, 228, 286], angiotensin II [121], endothelin [111, 167, 287], vasopressin [287], neurokinin A [130], histamine [108], and 5-HT [323]. Because of the Ca^{2+}-dependence and the reversal potential of this Cl^- conductance, it has been speculated that Cl_{Ca} underlies this agonist-induced depolarization in smooth muscle, although this has been disputed by some [213]. Nonetheless, the possibility remains that another chloride conductance may also contribute to the membrane depolarization accompanying the vasoconstriction. Based on these findings, the relaxation of PE / TEA-preconstricted arterioles by NfA we observed (data not shown) would be consistent with membrane hyperpolarization following inhibition of Cl_{Ca} channels. Such a mechanism has been reported for 5-HT-induced membrane depolarization in rat pulmonary arteries [323].

Although we cannot exclude the involvement of other channels, we propose that Cl_{Ca} channel activation is responsible for the membrane depolarization associated with α_1–AR stimulation. A recent study by Mistry & Garland [200] showed that a minor effect of phenylephrine is to reduce outward K^+ (likely K_{dr}) currents in rabbit mesenteric arteries, thereby causing membrane depolarization. In our study, the similarity of the depolarizations induced by 1 μM PE with 1 and 5 mM TEA in the bath does not implicate a change in K^+ conductance. Moreover, 5 mM TEA may also be expected to inhibit K_{dr} currents in VSM, therefore NfA would have to enhance K_{dr} currents in order to cause the measured

hyperpolarization, an effect that has so far not been reported.

Similar experiments to those presented here will need to be performed in the absence of TEA to verify the extent of the depolarization due to Cl_{Ca} in the presence of PE when K_{Ca} channels are active. Nonetheless, the changes we measured in membrane potential support earlier speculation that Cl_{Ca} are involved in the α_1-AR-induced contraction via membrane depolarization. More experiments will have to be performed to ascertain the role of the DIDS-sensitive conductance in the α_1–AR-induced depolarization. It will also be interesting to see if the hyperpolarization by NfA decreases with increasing transmural pressure, and if DIDS can diminish this effect as we have proposed from the isobaric experiments. Finally, since the sodium-calcium exchanger can also produce a small inward current upon mobilization of intracellular Ca^{2+} by NE, it will be interesting to determine its contribution, if any, to polarity and, more importantly, to vascular tone.

E. Future directions

Our observations have provided some interesting hypotheses regarding the ionic bases of α_1–adrenoreceptor-induced vasoconstriction and depolarization. Our data suggest that one or more Cl^- conductances play a role in both phenomena. From this point, it will become increasingly important to dissociate between the actions of the NfA- and DIDS-sensitive conductances in both the α_1–AR-induced vasoconstriction and depolarization.

It is clear that Cl_{Ca} plays a substantial role in the depolarization induced by PE. Similar experiments need to be performed with DIDS instead of NfA to determine the extent to which the DIDS-sensitive channel is involved in this process. It will also be interesting to see if the latter's activation during the myogenic response in physiological saline solution produces the membrane depolarization commonly associated with the myogenic response.

With respect to the PE-induced vasoconstriction, since there is evidence that a Cl^- channel putatively involved in the myogenic response may be sensitive to swelling (Cl_{vol}), it may be prudent to replace DIDS with tamoxifen, a much more potent inhibitor of Cl_{vol} channels. This compound does not seem to have any potential cross-over effects on Cl_{Ca}. Furthermore, the masking effect that we have proposed for a DIDS-sensitive current will require further study at the unicellular level. It will be interesting to see if lowering extracellular Cl^- diminishes DIDS-sensitive current in the presence of PE, especially since classical techniques used to evoke macroscopic Cl_{vol} currents include exposure to hypo-osmotic media.

It has proven difficult to record Cl_{Ca} activity in isolated mesenteric myocytes, possibly due to difficulty in the isolation procedure. Nonetheless, we hope to eventually be able to characterize Cl_{Ca} channels in these arterioles. We also hope, whether by electrophysiological or by molecular techniques, to distinguish between the activity of different Cl^- conductances during α_1–AR stimulation, in a different preparation that clearly shows Cl_{Ca} activity, such as rabbit portal vein, and coronary or pulmonary artery.

Finally, the modulation of both Cl_{Ca} and Cl_{vol} by PKC is a high priority study that must be undertaken because little is known about the properties and role of Cl_{vol} channels in vascular smooth muscle. The molecular identification of VSM Cl_{vol} as the PKC-sensitive ClC-3 clone will also require some attention. This will have to be established more clearly before we can determine how PKC activity modulates α_1–AR-induced tone.

OVERALL PHYSIOLOGICAL RELEVANCE

Understanding how ion channels control vasomotor activity via graded membrane potential changes is important for understanding excitation-contraction coupling in smooth muscle. In the case of chloride, calcium, sodium, and potassium ions, a small change in conductance may mean the difference between being normotensive or hypertensive, suffering from coronary artery disease or not. It all depends on the intricate ion ballet that occurs in the sarcolemmae of the cells.

We have provided a basis for the further development of pharmacological tools for pathologies such as hypertension, that involve abnormal activity of ion channels. With the combined efforts of molecular biology and biophysics, we can target areas on the channel protein that modulate its activity. In the case of hypertension, we can focus on disabling the inhibitory sites on the K^+ channel proteins so that the channels become constitutively active, thereby relieving pressure. On the other hand, we can also target ion channels responsible for the vasoconstriction and inhibit their activity in order to reduce total peripheral resistance. This becomes even more important in the heart and brain, where even a mild vasoconstriction can, in some situations, lead to ischemia and severe dysfunction. Increased blood pressure also puts a strain on the rest of the organism since it translates into increased peripheral resistance, thereby affecting other organs such as the kidney and liver.

While our work with 4-AP does not bear direct clinical importance, it is potentially relevant to cardiac ischemic damage, where an early improvement in coronary perfusion may help reduce the area of ischemic damage post-infarct, or may help reduce angina. Understanding how a potent inhibitor like 4-AP interacts with the channel protein may allow

us to identify the malfunctioning channel subunits more readily, thereby facilitating the development of tools to target very specific defects in channel function.

Our understanding of the importance of Cl^- channels is still in its infancy. This thesis helps to elucidate some of the roles and responsibilities of these channels. From our research, for example, we can predict a significant involvement of these channels in hypotension and hemorrhage, and identify Cl^- channels as a novel target for further study and for therapeutic evolution. Furthermore, understanding the behaviour of Cl^- channels in response to norepinephrine stimulation in the splanchnic circulation provides a clue as to how total peripheral resistance may be better controlled in a hypertensive situation. Locally released neurotransmitters (such as NE), circulating hormones, and vasoactive peptides (AVP, angiotensin II, endothelin-1), all potential causes of hypertension, act via Cl^- channels to cause vasoconstriction. Since we know this, we can now diversify the pharmacological approaches and target Cl^- channels in order to relieve vasoconstrictions due to the increased perfusion pressure associated with hypertension.

CONCLUSIONS

1) Mechanism of 4-AP block of K_{dr}

- 4-AP blocks K_{dr} channels in the closed-state (state-dependent).
- 4-AP inhibition is reverse use-dependent, *i.e.* block is relieved when channels are opened by depolarization.
- 4-AP binding depolarizes the cell by shifting the activation of K_{dr} to more positive potentials.

2) Cl^- channels and α_1-adrenergic tone

- Niflumic acid and DIDS do not affect KCl-induced contractions attributed to the activation of Ca_L currents.
- Phenylephrine-induced vasoconstriction is inhibited by blockers of Ca_L and Cl^- channels.
- NfA-induced relaxation is pressure-dependent at intermediate (0.5 – 1 μM) phenylephrine concentrations.
- Activation of a DIDS-sensitive conductance by stretch and phenylephrine may partially "mask" part of the vasoconstriction due to Cl_{Ca} activation.
- Activation of a DIDS-sensitive conductance by membrane stretch accounts for part of the myogenic response and reactivity observed in both physiological and stimulated (α_1–AR) conditions, respectively; Cl_{Ca} channels do not appear to be involved in the myogenic response.
- Cl_{Ca} activation is an important contributor to the α_1–adrenergic depolarization.

SOURCES DOCUMENTAIRES

1. Agnel, M., Vermat, T., and Culouscou, J. -M. Identification of three novel members of the calcium-dependent chloride channel (CaCC) family predominantly expressed in the digestive tract and trachea. *FEBS Lett.*, **455**: 295-301, 1999.
2. Ahlquist, R.P. A study of the adrenotropic receptors. *Am. J. Physiol.*, **153**: 586-600, 1948.
3. Ahn, D. S., and Hume, J. R. pH regulation of voltage-dependent K^+ channels in canine pulmonary arterial smooth muscle cells. *Pflügers Arch.*, **433**: 758-765, 1997.
4. Aickin, C. C., and Brading, A. F. Measurement of intracellular chloride in guinea-pig vas deferens by ion analysis, ^{36}chloride efflux and micro-electrodes. *J. Physiol. (Lond.)*, **326**: 139-154, 1982.
5. Aiello, E. A., Malcolm. A. T., Walsh, M. P., and Cole, W. C. Beta-adrenoceptor activation and PKA regulate delayed rectifier K^+ channels of vascular smooth muscle cells. *Am. J. Physiol. Heart Circ. Physiol.*, **275**: H448-H459, 1998.
6. Aiello, E. A., Walsh, M. P., and Cole, W. C. Phosphorylation by protein kinase A enhances delayed rectifier K^+ current in rabbit vascular smooth muscle cells. *Am. J. Physiol. Heart Circ. Physiol.*, **268**: H926-H934, 1995.
7. Akbarali, H. I., and Giles, W. R. Ca^{2+} and Ca^{2+}-activated Cl^- currents in rabbit oesophageal smooth muscle. *J. Physiol. (Lond.)*, **460**: 117-133, 1993.
8. Amédée, T., Benham, C. D., Bolton, T. B., Byrne, N. G., and Large, W. A. Potassium, chloride and non-selective cation conductances opened by noradrenaline in rabbit ear artery cells. *J. Physiol. (Lond.)*, **423**: 551-568, 1990.

9. Amédée, T., and Large, W. A. Microelectrode study on the ionic mechanisms which contribute to the noradrenaline-induced depolarization in isolated cells of the rabbit portal vein. *Br. J. Pharmacol.*, **97**: 1331-1337, 1989.

10. Amédée, T., Large, W. A., and Wang, Q. Characteristics of chloride currents activated by noradrenaline in rabbit ear artery cells. *J.Physiol. (Lond.)*, **428**: 501-516, 1990.

11. Archer, S. L. Diversity of phenotypes and function of vascular smooth muscle cells. *J. Lab. Clin. Med.*, **127**: 524-529, 1996.

12. Archer, S. L., Huang, J. M. C., Reeve, H. L., Hampl, V., Tolarova, S., Michelakis, E., and Weir, E. K. Differential distribution of electrophysiologically distinct myocytes in conduit and resistance arteries determines their response to nitric oxide and hypoxia. *Circ. Res.*, **78**: 431-442, 1996.

13. Archer, S. L., Souil, E., Dinh-Xuan, A. T., Schremmer, B., Mercier, J. C., El Yaagoubi, A., Nguyen-Huu, L., Reeve, H. L., and Hampl, V. Molecular identification of the role of voltage-gated K^+ channels Kv1.5 and Kv2.1 in hypoxic pulmonary vasoconstriction and control of resting membrane potential in rat pulmonary artery myocytes. *J. Clin. Invest.*, **101**: 2319-2330, 1998.

14. Asano, M., Kuwako, M., Nomura, Y., Suzuki, Y., Shibuya, M., Sugita, K., and Ito, K. Possible mechanism of the potent vasoconstrictor responses to ryanodine in dog cerebral arteries. *Eur. J. Pharmacol.*, **311**: 53-60, 1996.

15. Baker, M., Howe, J. R., and Ritchie, J. M. Two types of 4-aminopyridine-sensitive potassium current in rabbit Schwann cells. *J. Physiol. (Lond.)*, **464**: 321-342, 1993.

16. Baron, A., Frieden, M., and Beny, J. L. Epoxyeicosatrienoic acids activate a high-conductance, Ca^{2+}-dependent K^+ channel on pig coronary artery endothelial cells. *J. Physiol. (Lond.)*, **504**: 537-543, 1998.

17. Baron, A., Pacaud, P., Loirand, G., Mironneau, C., and Mironneau, J. Pharmacological block of Ca^{2+}-activated Cl^- current in rat vascular smooth muscle cells in short-term primary culture. *Pflügers Arch.*, **419**: 553-558, 1991.

18. Bayliss, W. M. On the local reactions of the arterial wall to changes of internal pressure. *J. Physiol. (Lond.)*, **28**: 220-231, 1902.

19. Beech, D. J. Actions of neurotransmitters and other messengers on Ca^{2+} channels and K^+ channels in smooth muscle cells. *Pharmacol. Ther.*, **73**; 91-119, 1997.

20. Beech, D. J., and Bolton, T. B. Properties of the cromakalim-induced potassium conductance in smooth muscle cells isolated from the rabbit portal vein. *Br. J. Pharmacol.*, **98**: 851-864, 1989.

21. Beech, D. J., and Bolton, T. B. Two components of potassium current activated by depolarization of single smooth muscle cells from the rabbit portal vein. *J. Physiol. (Lond.)*, **418**: 293-309, 1989.

22. Beech, D. J., and Bolton, T. B. A voltage-dependent outward current with fast kinetics in single smooth muscle cells isolated from rabbit portal vein. *J. Physiol. (Lond.)*, **412**: 397-414, 1989.

23. Berger, M. G., Vandier, C., Bonnet, P., Jackson, W. F., and Rusch, N. J. Intracellular acidosis differentially regulates K_V channels in coronary and pulmonary vascular smooth muscle. *Am. J. Physiol. Heart Circ. Physiol.*, **275**: H1351-1359, 1997.

24. Berne, R. M., and Levy, M. N. Chapter 33: The Peripheral Circulation and its Control, in Physiology The C.V. Mosby Company, St. Louis, MI: 508-524, 1988.

25. Beuckelmann, D. J., Näbauer, M., and Erdmann, E. Alterations of K^+ currents in isolated human ventricular myocytes from patients with terminal heart failure. *Circ. Res.*, **73**: 379-385, 1993.

26. Bialecki, R. A., and Stinsonfisher, C. K_{Ca} channel antagonists reduce NO donor-mediated relaxation of vascular and tracheal smooth muscle. *Am. J. Physiol. Lung Cell. Mol. Physiol.*, **268**: L152-L159, 1995.

27. Bohlen, H. G. Determinants of resting and passive intestinal vascular pressures in rat and rabbit. *Am. J. Physiol. Gastrointest. Liver Physiol.*, **253**: G587-G595, 1987.

28. Bolotina, V. M., Najibi, S., Palacino, J. J., Pagano, P. J., and Cohen, R. A. Nitric oxide directly activates calcium-dependent potassium channels in vascular smooth muscle. *Nature*, **368**: 850-853, 1994.

29. Bond, T. D., Ambikapathy, S., Mohammad, S., and Valverde, M. A. Osmosensitive Cl^- currents and their relevance to regulatory volume decrease in human intestinal T_{84} cells: outwardly vs. inwardly rectifying currents. *J. Physiol. (Lond.)*, **511**: 45-54, 1998.

30. Bonev, A. D., and Nelson, M. T. Vasoconstrictors inhibit ATP-sensitive K^+ channels in arterial smooth muscle through protein kinase C. *J. Gen. Physiol.*, **108**: 315-323, 1996.

31. Bonnet, P., Vandier, C., Cheliakine, C., and Garnier, D. Hypoxia activates a potassium current in isolated smooth muscle cells from large pulmonary arteries of the rabbit. *Exper. Physiol.*, **79**; 597-600, 1994.

32. Bowles, D. K., Hu, Q., Laughlin, M. H., and Sturek, M. Heterogeneity of L-type calcium current density in coronary smooth muscle. *Am. J. Physiol. Heart Circ. Physiol.*, **273**: H2083-2089, 1997.

33. Boyle, J. P., Tomasic, M., and Kotlikoff, M. I. Delayed rectifier potassium channels in canine and porcine airway smooth muscle cells. *J. Physiol. (Lond.)*, **447**: 329-350, 1992.

34. Brandt, S., and Jentsch, T. J. ClC-6 and ClC-7 are two novel broadly expressed members of the ClC chloride channel family. *FEBS Lett.*, **377**: 15-20, 1995.

35. Brayden, J. E., and Nelson, M. T. Regulation of arterial tone by activation of calcium-dependent potassium channels. *Science*, **256**: 532-535, 1992.

36. Bülbring, E., and Tomita, T. Catecholamine action on smooth muscle. *Pharmacol. Rev.*, **39**: 49-96, 1987.

37. Buyse, G., Trouet, D., Voets, T., Missiaen, L., Droogmans, G., Nilius, B., and Eggermont, J. Evidence for the intracellular location of chloride channel (ClC)-type proteins: co-localization of ClC-6a and ClC-6c with the sarco/endoplasmic-reticulum Ca^{2+} pump SERCA2b. *Biochem. J.*, **330**: 1015-1021, 1998.

38. Bylund, D. B., Eikenberg, D. C., Hieble, J. P., Langer, S. Z., Lefkowitz, R. J., Minneman, K. P., Molinoff, P. B., Ruffolo, R. R. Jr., and Trendelenburg, U. IV. International union of pharmacology nomenclature of adrenoceptors. *Pharmacol. Rev.*, **46**: 121-136, 1994.

39. Byrne, N. G., and Large, W. A. Action of noradrenaline on single smooth muscle cells freshly dispersed from the rat anococcygeus muscle. *J. Physiol. (Lond.)*, **389**: 513-525, 1987.

40. Byrne, N. G., and Large, W. A. Membrane ionic mechanisms activated by noradrenaline in cells isolated from the rabbit portal vein. *J. Physiol. (Lond.)*, **404**: 557-573, 1988.

41. Cabell, F., Weiss, D. S., and Price, J. M. Inhibition of adenosine-induced coronary vasodilation by block of large-conductance Ca^{2+}-activated K^+ channels. *Am. J. Physiol. Heart Circ. Physiol.*, **267**: H1455-H1460, 1994.

42. Campbell, D. L., Qu, Y. H., Rasmusson, R. L., and Strauss, H. C. The calcium-independent transient outward potassium current in isolated ferret right ventricular myocytes. Two closed state reverse use-dependent block by 4-aminopyridine. *J. Gen. Physiol.*, **101**: 603-626, 1993.

43. Carl, A. Multiple components of delayed rectifier K^+ current in canine colonic smooth muscle. *J. Physiol. (Lond.)*, **484**: 339-353, 1995.

44. Castle, N. A., Fadous, S., Logothetis, D. E., and Wang, G. K. Aminopyridine block of $K_V1.1$ potassium channels expressed in mammalian cells and *Xenopus* oocytes. *J. Pharmacol. Exp. Ther.*, **45**: 1242-1252, 1994.

45. Castle, N. A., and Slawsky, M. T. Characterization of 4-aminopyridine block of the transient outward K^+ current in adult rat ventricular myocytes. *J. Pharmacol. Exp. Ther.*, **264**: 1450-1459, 1993.

46. Chen, C., and Wagoner, P. K. Endothelin induces a nonselective cation current in vascular smooth muscle cells. *Circ. Res.*, **69**: 447-454, 1991.

47. Chen, G., and Cheung, D. W. Effect of K^+-channel blockers on ACh-induced hyperpolarization and relaxation in mesenteric arteries. *Am. J. Physiol. Heart Circ. Physiol.*, **272**: H2306-H2312, 1997.

48. Chen, X. L., and Rembold, C. M. Phenylephrine contracts rat tail artery by one electromechanical and three pharmacomechanical mechanisms. *Am. J. Physiol. Heart Circ. Physiol.*, **268**: H74-H81, 1995.

49. Cheng, X, and Pang, C. C. Pressor and vasoconstrictor effects of methylene blue in endotoxaemic rats. *Naunyn Schmiedeberg's Arch. Pharmacol.*, **357**: 648-653, 1998.

50. Chik, C. L., Li, B., Ogiwara, T., Ho, A. K., and Karpinski, E. PACAP modulates L-type Ca^{2+} channel currents in vascular smooth muscle cells: involvement of PKC and PKA. *FASEB J.*, **10**: 1310-1317, 1996.

51. Choquet, D., and Korn, H. Mechanism of 4-aminopyridine action on voltage-gated potassium channels in lymphocytes. *J. Gen. Physiol.*, **99**: 217-240, 1992.

52. Clancy, J. P., McCann, J. D., Li, M., and Welsh, M. J. Calcium-dependent regulation of airway epithelial chloride channels. *Am. J. Physiol. Lung Cell. Mol. Physiol.*, **258**: L25-L32, 1990.

53. Clapp, L. H., Gurney, A. M., Standen, N. B., and Langton, P. D. Properties of the ATP-sensitive K^+ current activated by levcromakalim in isolated pulmonary arterial myocytes. *J. Membr. Biol.*, **140**: 205-213, 1994.

54. Clapp, L. H., Turner, J. L., and Kozlowski, R. Z. Ca^{2+}-activated Cl^- currents in pulmonary arterial myocytes. *Am. J. Physiol. Heart Circ. Physiol.*, **270**: H1577-H1584, 1996.

55. Clément-Chomienne, O., Ishii, K., Walsh, M. P., and Cole, W. C. Identification, cloning and expression of rabbit vascular smooth muscle $K_V1.5$ and comparison with native delayed rectifier K^+ current. *J. Physiol. (Lond.)*, **515**: 653-667. 1999.

56. Clément-Chomienne, O., Walsh, M. P., and Cole, W. C. Angiotensin II activation of protein kinase C decreases delayed rectifier K^+ current in rabbit vascular myocytes. *J. Physiol. (Lond.)*, **495**: 689-700, 1996.

57. Collier, M. L., Levesque, P. C., Kenyon, J. L., and Hume, J. R. Unitary Cl^- channels activated by cytoplasmic Ca^{2+} in canine ventricular myocytes. *Circ. Res.*, **78**: 936-944, 1996.

58. Cotton, K. D., Hollywood, M. A., McHale, N. G., and Thornbury, K. D. Ca^{2+} current and Ca^{2+}-activated chloride current in isolated smooth muscle cells of the sheep urethra. *J. Physiol. (Lond.)*, **505**: 121-131, 1997.

59. Cousin, J. L., and Motais, R. Inhibition of anion permeability by amphiphilic compounds in human red cell: evidence for an interaction of niflumic acid with the band 3 protein. *J. Membr. Biol.*, **46**: 125-153, 1979.

60. Criddle, D. N., Soares de Moura, R., Greenwood, I. A., and Large, W. A. Effect of niflumic acid on noradrenaline-induced contractions of the rat aorta. *Br. J. Pharmacol.*, **118**: 1065-1071, 1996.

61. Criddle, D. N., Soares de Moura, R., Greenwood, I. A., and Large, W. A. Inhibitory action of niflumic acid on noradrenaline- and 5-hydroxytryptamine- induced pressor responses in the isolated mesenteric vascular bed of the rat. *Br. J. Pharmacol.*, **120**: 813-818, 1997.

62. Crijns, F. R. L., Wolffenbuttel, B. H. R., De Mey, J. G. R., and Struijker Boudier, H. A. J. Mechanical properties of mesenteric arteries in diabetic rats: consequences of outward remodeling. *Am. J. Physiol. Heart Circ. Physiol.*, **276**: H1672-H1677, 1999.

63. Cunningham, S. A., Awayda, M. S., Bubien, J. K., Ismailov, I. I., Arrate, M. P., Berdiev, B. K., Benos, D. J., and Fuller, C. M. Cloning of an epithelial chloride channel from bovine trachea. *J. Biol. Chem.*, **270**: 31016-31026, 1995.

64. Currie, K. P. M., Wootton, J. F., and Scott, R. H. Activation of Ca^{2+}-dependent Cl^- currents in cultured rat sensory neurones by flash photolysis of DM-nitrophen. *J. Physiol. (Lond.)*, **482**: 291-307, 1995.

65. D'Angelo, G., and Osol, G. Regional variation in resistance artery diameter responses to α-adrenergic stimulation during pregnancy. *Am. J. Physiol.Heart Circ. Physiol.*, **264**: H78-H85, 1993.

66. Daniel, E. E., Shi, A. G., Wang, Z. L., Guan, Y. Y., Hoo, K., Cragoe, E. J., and Kwan, C. Y. Alpha-adrenoceptors in vascular smooth muscle: all is not well. *Blood Vessels*, **28**: 104-114, 1991.

67. Dart, C., and Standen, N. B. Activation of ATP-dependent K^+ channels by hypoxia in smooth muscle cells isolated from the pig coronary artery. *J. Physiol. (Lond.)*, **483**: 2939, 1995.

68. Davie, C. S., Kubo, M., and Standen, N. B. Potassium channel activation and relaxation by nicorandil in rat small mesenteric arteries. *Br. J. Pharmacol.*, **125**: 1715-1725, 1998.

69. Davies, N. W., Pettit, A. I., Agarwal, R., and Standen, N. B. The flickery block of ATP-dependent potassium channels of skeletal muscle by internal 4-aminopyridine. *Pflügers Arch.*, **419**: 25-31, 1991.

70. Davis, M. J., Donovitz, J. A., and Hood, J. D. Stretch-activated single-channel and whole cell currents in vascular smooth muscle cells. *Am. J. Physiol. Cell Physiol.*, **262**: C1083-C1088, 1992.

71. Davis, M. J.,and Hill, M.A. Signaling mechanisms underlying the vascular myogenic response. *Physiol. Rev.*, **79**: 387-423, 1999.

72. Davis, M. J., Meininger, G. A., and Zawieja, D. C. Stretch-induced increases in intracellular calcium of isolated vascular smooth muscle cells. *Am. J. Physiol. Heart Circ. Physiol.*, **263**: H1292-H1299, 1992.

73. Declerck, I., Himpens, B., Droogmans, G., and Casteels, R. The α_1-agonist phenylephrine inhibits voltage-gated Ca^{2+} -channels in vascular smooth muscle cells of rabbit ear artery. *Pflügers Arch.*, **417**: 117-119, 1990.

74. Despopoulos, A., and Silbernagl, S. (editors) Heart and Circulation, in Color Atlas of Physiology. Thieme Medical Publishers, Inc., New York, NY: 154-191, 1991.

75. Despopoulos, A., and Silbernagl, S. (editors) Nerve and Muscle, in Color Atlas of Physiology. Thieme Medical Publishers, Inc., New York, NY: 22-49, 1991.

76. Docherty, J. R. Subtypes of functional α_1- and α_2-adrenoceptors. *Eur. J. Pharmacol.*, **361**: 1-15, 1998.

77. Dong, H., Waldron, G. J., Galipeau, D., Cole, W. C., and Triggle, C. R. NO/PGI_2-independent vasorelaxation and the cytochrome P450 pathway in rabbit carotid artery. *Br. J. Pharmacol.*, **120**: 695-701, 1997.

78. Doughty, J. M., Miller, A. L., and Langton, P. D. Non-specificity of chloride channel blockers in rat cerebral arteries: block of the L-type calcium channel. *J. Physiol. (Lond.)*, **507**: 433-439, 1998.

79. Du. X. Y., and Sorota, S. Protein kinase C stimulates swelling-induced chloride current in canine atrial cells. *Pflügers Arch.*, **437**: 227-234, 1999.

80. Duan, D., Cowley, S., Horowitz, B., and Hume, J. R. A serine residue in ClC-3 links phosphorylation-dephosphorylation to chloride channel regulation by cell volume. *J. Gen. Physiol.*, **113**: 57-70, 1999.

81. Duan, D., Fermini, B., and Nattel, S. Potassium channel blocking properties of propafenone in rabbit atrial myocytes. *J. Pharmacol. Exp. Ther.*, **264**: 1113-1124, 1993.

82. Duan, D., Hume, J. R., and Nattel, S. Evidence that outwardly rectifying Cl^- channels underlie volume-regulated Cl^- currents in heart. *Circ. Res.*, **80**: 103-113, 1997.

83. Duan, D., Winter, C., Cowley, S., Hume, J. R., and Horowitz, B. Molecular identification of a volume-regulated chloride channel. *Nature*, **390**: 417-421, 1997.

84. Duchatelle-Gourdon, I., Hartzell, H. C., and Lagrutta, A. A. Modulation of the delayed rectifier potassium current in frog cardiomyocytes by β-adrenergic agonists and magnesium. *J. Physiol. (Lond.)*, **415**: 251-274, 1989.

85. Dumas, J. P., Goirand, F., Bardou, M., Dumas, M., Rochette, L., Advenier, C., and Giudicelli, J. F. Role of potassium channels and nitric oxide in the relaxant effects elicited by β-adrenoceptor agonists on hypoxic vasoconstriction in the isolated perfused lung of the rat. *Br. J. Pharmacol.*, **127**: 421-428, 1999.

86. Dunn, W. R., Wellman, G. C., and Bevan, J. A. Enhanced resistance artery sensitivity to agonists under isobaric compared with isometric conditions. *Am. J. Physiol. Heart Circ. Physiol.*, **266**: H147-H155, 1994.

87. England, S., and McFadzean, I. Inhibition of voltage-dependent Ca^{2+} current by α-adrenoceptor agonists in smooth muscle cells. *Eur. J. Pharmacol.*, **288**: 355-364, 1995.

88. Esneu, M., Gallo-Payet, N., and Payet, M. D. Mibefradil, a T-type calcium channel antagonist in Y1 cells. *Endocrine Res.*, **24**: 449-454, 1998.

89. Evans, A. M., Clapp, L. H., and Gurney, A. M. Augmentation by intracellular ATP of the delayed rectifier current independently of the glibenclamide-sensitive K-current in rabbit arterial myocytes. *Br. J. Pharmacol.*, **111**: 972-974, 1994.

90. Evans, A. M., Cobban, H. J., and Nixon, G. F. ET_A receptors are the primary mediators of myofilament calcium sensitization induced by ET-1 in rat pulmonary artery smooth muscle: a tyrosine kinase independent pathway. *Br. J. Pharmacol.*, **127**: 153-160, 1999.

91. Faber, J. E., and Meininger, G. A. Selective interaction of α-adrenoceptors with myogenic regulation of microvascular smooth muscle. *Am. J. Physiol. Heart Circ. Physiol.*, **259**: H1126-H1133, 1990.

92. Falloon, B. J., Stephens, N., Tulip, J. R., and Heagerty, A. M. Comparison of small artery sensitivity and morphology in pressurized and wire-mounted preparations. *Am. J. Physiol. Heart Circ. Physiol.*, **268**: H670-H678, 1995.

93. Feres, T., Borges, A. C., Silva, E. G., Paiva, A. C. M., and Paiva, T. B. Impaired function of $alpha_2$ adrenoceptors in smooth muscle of mesenteric arteries from spontaneously hypertensive rats. *Br. J. Pharmacol.*, **125**: 1144-1149, 1998.

94. Fleischmann, B. K., Washabau, R. J., and Kotlikoff, M. I. Control of resting membrane potential by delayed rectifier potassium currents in ferret airway smooth muscle cells. *J. Physiol. (Lond.)*, **469**: 625-638, 1993.

95. Franco-Obregón, A., and López-Barneo, J. Low PO_2 inhibits calcium channel activity in arterial smooth muscle cells. *Am. J. Physiol. Heart Circ. Physiol.*, **271**: H2290-H2299, 1996.

96. Franco-Obregón, A., Ureña, J., and López-Barneo, J. Oxygen-sensitive calcium channels in vascular smooth muscle and their possible role in hypoxic arterial relaxation. *Proc. Natl Acad. Sci. USA*, **92**: 4715-4719, 1995.

97. Furchgott, R.F. Role of endothelium in responses of vascular smooth muscle. *Circ. Res.*, **53**:557-573, 1983.

98. Furchgott, R. F., and Zawadzki, J. V. The obligatory role of endothelial cells in the relaxation of arterial smooth muscle by acetylcholine. *Nature*, **288**: 373-376, 1980.

99. Furukawa, T., Virag, L., Sawanobori, T., and Hiraoka, M. Stilbene disulfonates block ATP-sensitive K^+ channels in guinea pig ventricular myocytes. *J. Memb. Biol.*, **136**: 289-302, 1993.

100. Gandhi, R., Elble, R. C., Gruber, A. D., Schreur, K. D., Ji, H. L., Fuller, C. M., and Pauli, B. U. Molecular and functional characterization of a calcium-sensitive chloride channel from mouse lung. *J. Biol. Chem.*, **273**: 32096-32101, 1998.

101. Gebremedhin, D., Bonnet, P., Greene, A. S., England, S. K., Rusch, N. J., Lombard, J. H., and Harder, D. R. Hypoxia increases the activity of Ca^{2+}-sensitive K^+ channels in cat cerebral arterial muscle cell membranes. *Pflügers Arch.*, **428**; 621-630, 1989.

102. Gelband, C. H., and Gelband, H. Ca^{2+} release from intracellular stores is an initial step in hypoxic pulmonary vasoconstriction of rat pulmonary artery resistance vessels. *Circulation*, **96**: 3647-3654, 1997.

103. Gelband, C. H., and Hume, J. R. Ionic currents in single smooth muscle cells of the canine renal artery. *Circ. Res.*, **71**: 745-758, 1992.

104. Gelband, C. H., and Hume, J. R. $[Ca^{2+}]_i$ inhibition of K^+ channels in canine renal artery. Novel mechanism for agonist-induced membrane depolarization. *Circ. Res.*, **77**: 121-130, 1995.

105. Gelband, C. H., Ishikawa, T., Post, J. M., Keef, K. D., and Hume, J. R. Intracellular divalent cations block smooth muscle K^+ channels. *Circ. Res.*, **73**: 24-34, 1993.

106. Gelband, C. H., Warth, J. D., Mason, H. S., Zhu, M., Moore, J. M. Kenyon, J. L., Horowitz, B., and Sumners, C. Angiotensin II type 1 receptor-mediated inhibition of K^+ channel subunit $K_V2.2$ in brain stem and hypothalamic neurons. *Circ. Res.*, **84**: 352-359, 1999.

107. Gögelein, H., Dahlem, D., Englert, H. C., and Lang, H. J. Flufenamic acid, mefenamic acid and niflumic acid inhibit single nonselective cation channels in the rat exocrine pancreas. *FEBS Lett.*, **268**: 79-82, 1990.

108. Gokina, N.I., and Bevan, J. A. Role of intracellular Ca^{2+} in histamine-induced depolarization in rabbit middle cerebral artery. *Am. J. Physiol. Heart Circ. Physiol.*, **278**: H2105-H2114, 2000.

109. Gokina, N. I., Wellman, T. D., Bevan, R. D., Walters, C. L., Penar, P. L., and Bevan, J. A. Role of Ca^{2+}-activated K^+ channels in the regulation of membrane potential and tone of smooth muscle in human pial arteries. *Circ. Res.*, **79**: 881-886, 1996.

110. Gollasch, M., Ried, C., Bychkov, R., Luft, F. C., and Haller, H. K^+ currents in human coronary artery vascular smooth muscle cells. *Circ. Res.*, **78**: 676-688, 1996.

111. Gordienko, D. V., Clausen, C., and Goligorsky, M. S. Ionic currents and endothelin signaling in smooth muscle cells from rat renal resistance arteries. *Am. J. Physiol. Renal Physiol.*, **266**: F325-F341, 1994.

112. Granger, D. N., Richardson, P. D. J., Kvietys, P. R., and Mortillaro, N. A. Intestinal blood flow. *Gastroenterelogy*, **78**: 837863, 1980.0

113. Greenwood, I. A., Hogg, R. C., and Large, W. A. Effect of frusemide, ethacrynic acid and indanyloxyacetic acid on spontaneous Ca-activated currents in rabbit portal vein smooth muscle cells. *Br. J. Pharmacol.*, **115**: 733-738, 1995.

114. Greenwood, I. A., and Large, W. A. Comparison of the effects of fenamates on Ca-activated chloride and potassium currents in rabbit portal vein smooth muscle cells. *Br. J. Pharmacol.*, **116**: 2939-2948, 1995.

115. Greenwood, I. A., and Large, W. A. Properties of a Cl^- current activated by cell swelling in rabbit portal vein vascular smooth muscle cells. *Am. J. Physiol. Heart Circ. Physiol.*, **275**: H1524-H1532, 1998.

116. Gruber, A. D. and Pauli, B. U. Molecular cloning and biochemical characterization of a truncated, secreted member of the human family of Ca^{2+}-activated Cl^- channels. *Biochim. Biophys. Acta*, **1444**: 418-423, 1999.

117. Gruber, A. D., Schreur, K. D., Ji, H. L., Fuller, C. M., and Pauli, B. U. Molecular cloning and transmembrane structure of hCLCA2 from human lung, trachea, and mammary gland. *Am. J. Physiol. Cell Physiol.*, **276**: C1261-C1270, 1999.

118. Gu, H., Trajkovic, S., and LaBelle, E. F. Norepinephrine-induced phosphatidylcholine hydrolysis by phospholipases D and C in rat tail artery. *Am. J. Physiol. Cell Physiol.*, **262**: C1376-C1383, 1992.

119. Guia, A., Remillard, C. V., and Leblanc, N. Concepts for patch clamp recording of whole-cell and single-channel K^+ currents in cardiac and vascular myocytes, in Potassium Channels in Cardiovascular Biology. Archer, S. L. and Rusch, N. (editors), Kluwer Academic/Plenum Publishers, New York, NY, 2001.

120. Guia, A., Wan, X., Courtemanche, M., and Leblanc, N. Local Ca^{2+} entry through L-type Ca^{2+} channels activates Ca^{2+}-dependent K^+ channels in rabbit coronary myocytes. *Circulation*, **84**: 1032-1042, 1999.

121. Guilbert, C., Marthan, R., and Savineau, J. P. Oscillatory Cl^- current induced by angiotensin II in rat pulmonary arterial myocytes: Ca^{2+} dependence and physiological implication. *Cell Calcium*, **21**: 421-429, 1997.

122. Haeusler, G. Relationship between noradrenaline-induced depolarization and contraction in vascular smooth muscle. *Blood Vessels*, **15**: 46-54, 1978.

123. Halpern, W., and Kelley, M. In vitro methodology for resistance arteries. *Blood Vessels*, **28**: 245-251, 1991.

124. Hamada, H., Damron, D. S., Hong, S. J., Van Wagoner, D. R., and Murray, P. A. Phenylephrine-induced Ca^{2+} oscillations in canine pulmonary artery smooth muscle cells. *Circ. Res.*, **81**: 812-823, 1997.

125. Hamill, O. P., Marty, A., Neher, E., Sakmann, B., and Sigworth, F. J. Improved patch-clamp techniques for high-resolution current recording from cells and cell-free membrane patches. *Pflügers Arch.*, **391**: 85-100, 1981.

126. Harder, D. R. Pressure-dependent membrane depolarization in cat middle cerebral artery. *Circ. Res.*, **55**: 197-202, 1984.

127. Harder, D. R., Gilbert, R., and Lombard, J. H. Vascular muscle cell depolarization and activation in renal arteries on elevation of transmural pressure. *Am. J. Physiol. Renal Physiol.*, **253**: F778-F781, 1987.

128. Hart, P. J., Overturf, K. E., Russell, S. N., Carl, A., Hume, J. R., Sanders, K. M., and Horowitz, B. Cloning and expression of a $K_V1.2$ class delayed rectifier K^+ channel from canine colonic smooth muscle. *Proc. Natl Acad. Sci. USA*, **90**: 9659-9663, 1993.

129. Harvey, R. D. Effects of stilbenedisulfonic acid derivatives on the cAMP-regulated chloride currents in cardiac myocytes. *Pflügers Arch.*, **422**: 436-442, 1993.

130. Hazama, H., Nakajima, T., Hamada, E., Omata, M., and Kurachi, Y. Neurokinin A and Ca^{2+} current induce Ca^{2+}-activated Cl^- currents in guinea-pig tracheal myocytes. *J. Physiol. (Lond.)*, **492**: 377-393, 1996.

131. He, Y., and Tabrizchi, R. Effects of niflumic acid on α_1-adrenoceptor-induced vasoconstriction in mesenteric artery in vitro and in vivo in two-kidney one-clip hypertensive rats. *Eur. J. Pharmacol.*, **328**: 191-199, 1997.

132. Hecker, M., Mülsch, A., Bassenge, E., and Busse, R. Vasoconstriction and increased flow: two principal mechanisms of shear stress-dependent endothelial autacoid release. *Am. J. Physiol. Heart Circ. Physiol.*, **265**: H828-H833, 1993.

133. Heinemann, A., Horina, G., Stauber, R. E., Pertl, C., Holzer, P., and Peskar, B. A. Lack of effect of a selective vasopressin V_{1A} receptor antagonist SR 49,059, on potentiation by vasopressin of adrenoceptor-mediated pressor responses in the rat mesenteric arterial bed. *Br. J. Pharmacol.*, **125**: 1120-1127, 1998.

134. Helliwell, R. M., and Large, W. A. α_1-Adrenoceptor activation of a non-selective cation current in rabbit portal vein by 1,2-diacyl-*sn*-glycerol. *J. Physiol. (Lond.)*, **499**: 417-428, 1997.

135. Hille, B. (editor) Classical biophysics of the squid giant axon, in Ionic channels of excitable membranes. Pub. Sinauer Associates Inc., Sunderland, MA: 23-54, 1992.

136. Hirakawa, Y., Gericke, M., Cohen, R. A., and Bolotina, V. M. Ca^{2+}-dependent Cl^- channels in mouse and rabbit aortic smooth muscle cells: regulation by intracellular Ca^{2+} and NO. *Am. J. Physiol. Heart Circ. Physiol.*, **277**: H1732-H1744, 1999.

137. Hogg, R. C., Wang, Q., Helliwell, R. M., and Large, W. A. Properties of spontaneous inward currents in rabbit pulmonary artery smooth muscle cells. *Pflügers Arch.*, **425**: 233-240, 1993.

138. Hogg, R. C., Wang, Q., and Large, W. A. Action of niflumic acid on evoked and spontaneous calcium- activated chloride and potassium currents in smooth muscle cells from rabbit portal vein. *Br. J. Pharmacol.*, **112**: 977-984, 1994.

139. Hogg, R. C., Wang, Q., and Large, W. A. Effects of Cl channel blockers on Ca-activated chloride and potassium currents in smooth muscle cells from rabbit portal vein. *Br. J. Pharmacol.*, **111**: 1333-1341, 1994.

140. Holland, M., Langton, P. D., Standen, N. B., and Boyle, J. P. Effects of the BK_{Ca} channel activator, NS1619, on rat cerebral artery smooth muscle. *Br. J. Pharmacol.*, **117**: 119-129, 1996.

141. Ishikawa, T., Eckman, D. M., and Keef, K. D. Characterization of delayed rectifier K^+ currents in rabbit coronary artery cells near resting membrane potential. *Can. J. Physiol. Pharmacol.*, **75**: 1116-1122, 1997.

142. Ishikawa, T., Hume, J. R., and Keef, K. D. Modulation of K^+ and Ca^{2+} channels by histamine H_1-receptor stimulation in rabbit coronary artery cells. *J. Physiol. (Lond.)*, **468**: 379-400, 1993.

143. Iwamuro, Y., Miwa, S., Zhang, X. F., Minowa, T., Enoki, T., Okamoto, Y., Hasegawa, H., Furutani, H., Okazawa, M., Ishikawa, M., Hishimoto, N., and Masaki, T. Activation of three types of voltage-independent Ca^{2+} channel in A7r5 cells by endothelin-1 as revealed by a novel Ca^{2+} channel blocker LOE 908. *Br. J. Pharmacol.*, **126**: 1107-1114, 1999.

144. Jaggar, J. H., Mawe, G. M., and Nelson, M. T. Voltage-dependent K^+ currents in smooth muscle cells from mouse gallbladder. *Am. J. Physiol. Gastrointest. Liver Physiol.*, **274**: G687-G693, 1998.

145. Jahnel, U., Klemm, P., and Nawrath, H. Different mechanisms of the inhibition of the transient outward current in rat ventricular myocytes. *Naunyn Schmiedeberg's Arch. Pharmacol.*, **349**: 87-94, 1994.

146. Janssen, L. J. Acetylcholine and caffeine activate Cl^- and suppress K^+ conductances in human bronchial smooth muscle. *Am. J. Physiol. Lung Cell. Mol. Physiol.*, **270**: L772-L781, 1996.

147. Janssen, L. J., and Sims, S. M. Ca^{2+}-dependent Cl^- current in canine tracheal smooth muscle cells. *Am. J. Physiol. Cell Physiol.*, **269**: C163-C169, 1995.

148. Janssen, L. J., and Sims, S. M. Spontaneous transient inward currents and rhythmicity in canine and guinea-pig tracheal smooth muscle cells. *Pflügers Arch.*, **427**: 473-480, 1994.

149. Jensen, P. E., Hughes, A., Boonen, H. C. M., and Aalkjær, C. Force, membrane potential, and $[Ca^{2+}]_i$ during activation rat mesenteric small arteries with norepinephrine, potassium, aluminum fluoride, and phorbol ester. *Circ. Res.*, **73**: 314-324, 1993.

150. Jentsch, T. J., and Günther, W. Chloride channels: an emerging molecular picture. *BioEssays*, **19**: 117-126, 1997.

151. Jentsch, T. J., Günther, W., Püsch, M., and Schwappach, B. Properties of voltage-gated chloride channels of the ClC gene family. *J. Physiol. (Lond.)*, **482**: 19S-25S, 1995.

152. Jentsch, T. J., Steinmeyer, K., and Schwarz, G. Primary structure of *Torpedo marmorata* chloride channel isolated by expression cloning in *Xenopus* oocytes. *Nature*, **348**: 510-514, 1990.

153. Jiang, M. J., and Morgan, K. G. Intracellular calcium levels in phorbol ester-induced contractions of vascular muscle. *Am. J. Physiol. Heart Circ. Physiol.*, **253**: H1365-H1371, 1987.

154. Johnson, P. C. Autoregulation of blood flow. *Circ. Res.*, **59**: 483-495, 1986.

155. Kachintorn, U., Vongkovit, P., Vajanaphanich, M., Dinh, S., Barrett, K. E., and Dharmsathaphorn, K. Dual effects of a phorbol ester on calcium-dependent chloride secretion by T84 epithelial cells. *Am. J. Physiol. Cell Physiol.*, **262**: C15-C22, 1992.

156. Kawasaki, M., Uchida, S., Monkawa, T., Miyawaki, A., Mikoshiba, K., Marumo, F., and Sasaki, S. Cloning and expression of a protein kinase C-regulated chloride channel abundantly expressed in rat brain neuronal cells. *Neuron*, **12**: 597-604, 1994.

157. Keaney, J. F. Jr., Puyana, J. C., Francis, S., Loscalzo, J. F., Stamler, J. S., and Loscalzo, J. Methylene blue reverses endotoxin-induced hypotension. *Circ. Res.*, **74**: 1121-1125, 1994.

158. Kehl, S .J. 4-Aminopyridine causes a voltage-dependent block of the transient outward K^+ current in rat melanotrophs. *J. Physiol. (Lond.)*, **431**: 515-528, 1990.

159. Khan, S. A., Mathews, W. R., and Meisheri, K. D. Role of calcium-activated K^+ channels in vasodilation induced by nitroglycerine, acetylcholine and nitric oxide. *J. Pharmacol. Exp. Ther.*, **267**: 1327-1335, 1993.

160. Kieferle, S., Fong, P., Bens, M., Vandewalle, A., and Jentsch, T. J. Two highly homologous members of the ClC chloride channel family in both rat and human kidney. *Proc. Natl Acad. Sci. USA*, **91**: 6943-6947, 1994.

161. Kirkup, A. J., Edwards, G., Green, M. E., Miller, M., Walker, S. D., and Weston, A. H. Modulation of membrane currents and mechanical activity by niflumic acid in rat vascular smooth muscle. *Eur. J. Pharmacol.*, **317**: 165-174, 1996.

162. Kirsch, G. E., and Drewe, J. A. Gating-dependent mechanism of 4-aminopyridine block in two related potassium channels. *J. Gen. Physiol.*, **102**: 797-816, 1993.

163. Kirsch, G. E., Yeh, J. Z., and Oxford, G. S. Modulation of aminopyridine block of potassium currents in squid axon. *Biophys. J.*, **50**: 637-644, 1986.

164. Kirton, C. A., and Loutzenhiser, R. Alterations in basal protein kinase C activity modulate renal afferent arteriolar myogenic reactivity. *Am. J. Physiol. Heart Circ. Physiol.*, **275**: H467-H475, 1998.

165. Klöckner, U. Intracellular calcium ions activate a low-conductance chloride channel in smooth-muscle cells isolated from human mesenteric artery. *Pflügers Arch.*, **424**: 231-237, 1993.

166. Klöckner, U., and Isenberg, G. Calcium channel current of vascular smooth muscle cells: extracellular protons modulate gating and single channel conductance. *J. Gen. Physiol.*, **103**: 665-678, 1994.

167. Klöckner, U., and Isenberg, G. Endothelin depolarizes myocytes from porcine coronary and human mesenteric arteries through a Ca-activated chloride current. *Pflügers Arch.*, **418**: 168-175, 1991.

168. Klöckner, U., and Isenberg, G. Intracellular pH modulates the availability of vascular L-type Ca^{2+} channels. *J. Gen. Physiol.*, **103**: 647-663, 1994.

169. Knauf, P. A., and Mann, N. A. Use of niflumic acid to determine the nature of the asymmetry of the human erythrocyte anion exchange system. *J. Gen. Physiol.*, **83**: 703-725, 1984.

170. Knot, H. J., and Nelson, M. T. Regulation of membrane potential and diameter by voltatge-dependent K^+ channels in rabbit myogenic cerebral arteries. *Am. J. Physiol. Heart Circ. Physiol.*, **269**: H348-H355, 1995.

171. Kong, J. Q., Taylor, D. A., and Fleming, W. A. Functional distribution and role of α_1 adrenoceptor subtypes in the mesenteric vasculature of the rat. *J. Pharmacol. Exp. Ther.*, **268**: 1153-1159, 1994.

172. Korenaga, R., Ando, J., Tsuboi, H., Yang, W. D., Sakuma, I., Toyooka, T., and Kamiya, A. Laminar flow stimuates ATP- and shear stress-dependent nitric oxide production in cultured bovine endothelial cells. *Biochem. Biophys. Res. Comm.*, **198**: 213-219, 1994.

173. Kume, H., Hall, I. P., Washabau, R. J., Takagi, K., and Kotlikoff, M. I. β-Adrenergic agonists regulate K_{Ca} channels in airway smooth muscle by cAMP-dependent and -independent mechanisms. *J. Clin. Invest.*, **93**: 371-379, 1994.

174. Kuo, L., Davis, M. J., and Chilian, W. M. Endothelium-dependent, flow-induced dilation of isolated coronary arterioles. *Am. J. Physiol. Heart Circ. Physiol.*, **259**: H1063-H1070; 1990.

175. Lachnit, W. G., Tran, A. M., Clarke, D. E., and Ford, A. P. D. W. Pharmacological characterization of an α_{1A}-adrenoceptor mediating contractile responses to noradrenaline in isolated caudal artery of rat. *Br. J. Pharmacol.*, **120**: 819826, 1997.

176. Lam, E., Skarsgard, P., and Laher, I. Inhibition of myogenic tone by mibefradil in rat cerebral arteries. *Eur. J. Pharmacol.*, **358**: 165-168, 1998.

177. Lamb, F. S., and Barna, T. J. Chloride ion currents contribute functionally to norepinephrine-induced vascular contraction. *Am. J. Physiol. Heart Circ. Physiol.*, **275**: H151-H160, 1995.

178. Lamb, F. S., Clayton, G. H., Liu, B. X., Smith, R. L., Barna, T. J., and Schutte, B. C. Expression of CLCN voltage-gated chloride channel genes in human blood vessels. *J. Mol. Cel. Cardiol.*, **31**: 657-666, 1999.

179. Lamb, F. S., Volk, K. A., and Shibata, E. F. Calcium-activated chloride current in rabbit coronary artery myocytes. *Circ. Res.*, **75**: 742-750, 1994.

180. Lamontagne, D., Pohl, U., and Busse, R. Mechanical deformation of vessel wall and shear stress determine the basal release of endothelium-derived relaxing factor in the intact rabbit coronary vascular bed. *Circ. Res.*, **70**; 123-130, 1992.

181. Langer, S. Z., and Hicks, P. E. Alpha-adrenoceptor subtypes in blood vessels: physiology and pharmacology. *J. Cardiovasc. Pharmacol.*, **6**: S547-S558, 1984.

182. Langton, P. D. Calcium channel currents recorded from isolated myocytes of rat basilar artery are stretch sensitive. *J. Physiol. (Lond.)*, **471**: 111, 1993.

183. Large, W. A., and Wang, Q. Characteristics and physiological role of the Ca^{2+}-activated Cl^- conductance in smooth muscle. *Am. J. Physiol. Cell Physiol.*, **271**: C435-C454, 1996.

184. Leaney, J. L., Marsh, S. J., and Brown, D. A. A swelling-activated chloride current in rat sympathetic neurones. *J. Physiol. (Lond.)*, **501**: 555-564, 1997.

185. Leblanc, N., and Leung, P. M. Indirect stimulation of Ca^{2+}-activated Cl^- current by Na^+/Ca^{2+} exchange in rabbit portal vein smooth muscle. *Am. J. Physiol. Heart Circ. Physiol.*, **268**: H1906-H1917, 1995.

186. Leblanc, N., Wan, X. D., and Leung, P. M. Physiological role of Ca^{2+}-activated and voltage-dependent K^+ currents in rabbit coronary myocytes. *Am. J. Physiol. Cell Physiol.*, **266**: C1523-C1537, 1994.

187. Lelkes, P. I. New aspects of endothelial cell biology. *J. Cell. Biochem.*, **45**: 242-244, 1991.

188. Leprêtre, N., Mironneau, J., and Morel, J. L. Both α_{1A}- and α_{2A}-adrenoreceptor subtypes stimulate voltage-operated L-type calcium channels in rat portal vein myocytes. *J. Biol. Chem.*, **269**: 29546-29552, 1994.

189. Li, P. L., and Campbell, W. B. Epoxyeicosatrienoic acids activate K^+ channels in coronary smooth muscle through a guanine nucleotide binding protein. *Circ. Res.*, **80**: 877-884, 1997.

190. Li, P. L., Zou, A. P., and Campbell, W. B. Regulation of potassium channels in coronary artery smooth muscle by endothelium-derived vasodilators. *Hypertension*, **29**: 262-267, 1997.

191. Liu, J., Hill, M. A., and Meininger, G. A. Mechanisms of myogenic enhancement by norepinephrine. *Am. J. Physiol. Heart Circ. Physiol.*, **266**: H440-H446, 1994.

192. Llano, I., and Marty, A. Protein kinase C activators inhibit the inositol trisphosphate-mediated muscarinic current responses in rat lacrimal cells. *J. Physiol. (Lond.)*, **394**: 239-248, 1987.

193. Loirand, G., Faiderbe, S., Baron, A., Geffard, M., and Mironneau, J. Autoanti-phosphatidylinositide antibodies specifically inhibit noradrenaline effects on Ca^{2+} and Cl^- channels in rat portal vein myocytes. *J. Biol. Chem.*, **267**: 4312-4316, 1992.

194. Loirand, G., Pacaud, P., Mironneau, C., and Mironneau, J. GTP-binding proteins mediate noradrenaline affects on calcium and chloride currents in rat portal vein myocytes. *J. Physiol. (Lond.)*, **428**: 517-529, 1990.

195. Matsuda, J. J., Volk, K. A., and Shibata, E. F. Calcium currents in isolated rabbit coronary arterial smooth muscle myocytes. *J. Physiol. (Lond.)*, **427**: 657-680, 1990.

196. McCarron, J. G., Crichton, C. A., Langton, P. D., MacKenzie, A., and Smith, G. L. Myogenic contraction by modulation of voltage-dependent calcium currents in isolated rat cerebral arteries. *J. Physiol. (Lond.)*, **498**: 371-379, 1997.

197. Meyer, M. C., Cummings, K., and Osol, G. Estrogen replacement attenuates resistance artery adrenergic sensitivity via endothelial vasodilators. *Am. J. Physiol. Heart Circ. Physiol.*, **272**: H2264-H2270, 1997.

198. Miller, A. L., Morales, E., Leblanc, N. R., and Cole, W. C. Metabolic inhibition enhances Ca^{2+}-activated K^+ current in smooth muscle cells of rabbit portal vein. *Am. J. Physiol. (Lond.)*, **265**: H2184-H2195, 1993.

199. Mironneau, J., Arnaudeau, S., Macrez-Leprêtre, N., and Boittin, F. X. Ca^{2+} sparks and Ca^{2+} waves activate different Ca^{2+}-dependent ion channels in single myocytes from rat portal vein. *Cell Calcium*, **20**: 153-160, 1999.

200. Mistry, D. K., and Garland, C. J. The influence of phenylephrine on outward potassium currents in single smooth muscle cells from the rabbit mesenteric artery. *Gen. Pharmacol.*, **33**: 389-399, 1999.

201. Morales, E., Cole, W. C., Remillard, C. V., and Leblanc, N. Block of large conductance Ca^{2+}-activated K^+ channels in rabbit vascular myocytes by internal Mg^{2+} and Na^+. *J. Physiol. (Lond.)*, **495**: 701-716, 1996.

202. Morris, A. P., and Frizzell, R. A. Ca^{2+}-dependent Cl^- channels in undifferentiated human colonic cells (HT-29). II. Regulation and rundown. *Am. J. Physiol. Cell Physiol.*, **26**: C977-C985, 1993.

203. Mulvany, M. J., and Aalkjær, C. Structure and function of small arteries. *Physiol. Rev.*, **70**; 921-961, 1990.

204. Mulvany, M. J., Nilsson, H., and Flatman, J. A. Role of membrane potential in the response of rat small mesenteric arteries to exogenous noradrenaline stimulation. *J. Physiol. (Lond.)*, **332**: 363-373, 1982.

205. Murphy, M. E., and Brayden, J. E. Nitric oxide hyperpolarizes rabbit mesenteric arteries via ATP-sensitive potassium channels. *J. Physiol. (Lond.)*, **486**: 47-58, 1995.

206. Nelson, M. T., Cheng, H., Rubart, M., Santana, L. F., Bonev, A. D., Knot, H. J., and Lederer, W. J. Relaxation of arterial smooth muscle by calcium sparks. *Science*, **270**: 633-637, 1995.

207. Nelson, M. T., Conway, M. A., Knot, H. J., and Brayden, J. E. Chloride channel blockers inhibit myogenic tone in rat cerebral arteries. *J. Physiol. (Lond.)*, **502**: 259-264, 1997.

208. Nelson, M. T., Patlak, J. B., Worley, J. F., and Standen, N. B. Calcium channels, potassium channels, and voltage dependence of arterial smooth muscle tone. *Am. J. Physiol. Cell Physiol.*, **259**: C3-C18, 1990

209. Nelson, M. T., and Quayle, J. M. Physiological roles and properties of potassium channels in arterial smooth muscle. *Am. J. Physiol. Cell Physiol.*, **268**: C799-C822, 1995.

210. Nelson, M. T., Standen, N. B., Brayden, J. E., and Worley, J. F. III. Noradrenaline contracts arteries by activating voltage-dependent calcium channels. *Nature*, **336**: 382-385, 1988.

211. Nilius, B., Prenen, J., Szücs, G., Wei, L., Tanzi, F., Voets, T., and Droogmans, G. Calcium-activated chloride channels in bovine pulmonary artery endothelial cells. *J. Physiol. (Lond.)*, **498**: 381-396, 1997.

212. Nilius, B., Prenen, J., Voets, T., Eggermont, J., and Droogmans, G. Activation of volume-regulated chloride currents by reduction of intracellular ionic strength in bovine endothelial cells. *J. Physiol. (Lond.)*, **506**: 353-361, 1998.

213. Nilsson, H., Videbæk, L. M., Toma, C., and Mulvany, M. J. Role of intracellular calcium for noradrenaline-induced depolarization in rat mesenteric small arteries. *J. Vasc. Res.*, **35**: 36-44, 1998.

214. Nishimura, J., Khalil, R. A., and van Breemen, C. Agonist-induced vascular tone. *Hypertension*, **13**: 835-844, 1989.

215. Nishina, H., Ozaki, T., Hanson, M. A., and Poston, L. Mechanisms of noradrenaline-induced vasorelaxation in isolated femoral arteries of the neonatal rat. *Br. J. Pharmacol.*, **127**: 809-812, 1999.

216. Noble, D., and Tsien, R. W. Outward membrane currents activated in the plateau range of potentials in cardiac Purkinje fibres. *J. Physiol. (Lond.)*, **200**: 205-231, 1969.

217. O'Donnell, M. E., and Owen, N. E. Regulation of ion pumps and carriers in vascular smooth muscle. *Physiol. Rev.*, **74:** 683-721, 1994.

218. Ogata, N., and Tatebayashi, H. Differential inhibition of a transient K^+ current by chlorpromazine and 4-aminopyridine in neurones of the rat dorsal root ganglia. *Br. J. Pharmacol.*, **109**: 1239-1246, 1993.

219. Ohyanagi, M., Faber, J. E., and Nishigaki, K. Differential activation of α_1- and α_2-adrenoceptors on microvascular smooth muscle during sympathetic nerve stimulation. *Circ. Res.*, **68**: 232-244, 1991.

220. Oike, M., Schwarz, G., Sehrer, J., Jost, M., Gerke, V., Weber, K., Droogmans, G., and Nilius, B. Cytoskeletal modulation of the response to mechanical stimulation in human vascular endothelial cells. *Pflügers Arch.*, **428**: 569-76, 1994.

221. Okabe, K., Kitamura, K., and Kuriyama, H. Features of 4-aminopyridine sensitive outward current observed in single smooth muscle cells from the rabbit pulmonary artery. *Pflügers Arch.*, **409**: 561-568, 1987.

222. Osipenko, O. N., Evans, A. M., and Gurney, A. M. Regulation of the resting potential of rabbit pulmonary artery myocytes by a low threshold, O_2-sensing potassium current. *Br. J. Pharmacol.*, **120**: 1461-1470, 1997.

223. Ottolia, M., and Toro, L. Potentiation of large conductance K_{Ca} channels by niflumic, flufenamic, and mefenamic acids. *Biophys. J.*, **67**: 2272-2279, 1994.

224. Overturf, K. E., Russell, S. N., Carl, A., Vogalis, F., Hart, P. J., Hume, J. R., Sanders, K. M., and Horowitz, B. Cloning and characterization of a $K_V1.5$ delayed rectifier K^+ channel from vascular and visceral smooth muscles. *Am. J. Physiol. Cell Physiol.*, **262**: C1231-C1238, 1994.

225. Pacaud, P., Loirand, G., Baron, A., Mironneau, C., and Mironneau, J. Ca^{2+} channel activation and membrane depolarization mediated by Cl^- channels in response to noradrenaline in vascular myocytes. *Br. J. Pharmacol.*, **104**: 1000-1006, 1991.

226. Pacaud, P., Loirand, G., Grégoire, G., Mironneau, C., and Mironneau, J. Calcium-dependence of the calcium-activated chloride current in smooth muscle cells of rat portal vein. *Pflügers Arch.*, **421**: 125-130, 1992.

227. Pacaud, P., Loirand, G., Lavie, J., Mironneau, C., and Mironneau, J. Calcium-activated chloride current in rat vascular smooth muscle cells in short-term primary culture. *Pflügers Arch.*, **413**: 629-636, 1989.

228. Pacaud, P., Loirand, G., Mironneau, C., and Mironneau, J. Noradrenaline activates a calcium-activated chloride conductance and increases the voltage-dependent calcium current in cultures single cells of rat portal vein. *Br. J. Pharmacol.*, **97**: 139-146, 1989.

229. Park, M. K., Bae, Y. M., Lee, S. H., Ho, W. K., and Earm, Y. E. Modulation of voltage-dependent K^+ channel by redox potential in pulmonary and ear arterial smooth muscle cells of the rabbit. *Pflügers Arch.*, **434**: 764-771, 1997.

230. Parkinson, N. A. and Hughes, A. D. The mechanism of action of α_2-adrenoceptors in human isolated subcuteneous resistance arteries. *Br. J. Pharmacol.*, **115**: 1463-1468, 1995.

231. Perez, D. M., DeYoung, M. B., and Graham, R. M. Coupling of expressed α_{1B}- and α_{1D}-adrenergic receptor to multiple signaling pathways is both G protein and cell type specific. *Mol. Pharmacol.*, **44**: 784-795, 1993.

232. Pfründer, D., and Kreye, V. A. W. Tedisamil inhibits the delayed rectifier K^+ current in single smooth muscle cells of the guinea-pig portal vein. *Pflügers Arch.*, **421**: 22-25, 1992.

233. Pohl, U., Herlan, K., Huang, A., and Bassenge, E. EDRF-mediated shear-induced dilation opposes myogenic constriction in small rabbit arteries. *Am. J. Physiol. Heart Circ. Physiol.*, **261**: H2016-H2023, 1991.

234. Poronnik, P., Ward, M. C., and Cook, D. I. Intracellular Ca^{2+} release by flufenamic acid and other blockers of the non-selective cation channel. *FEBS Lett.*, **296**: 245-248, 1992.

235. Post, J. M., Gelband, C. H., and Hume, J. R. $[Ca^{2+}]_i$ inhibition of K^+ channels in canine pulmonary artery. Novel mechanism for hypoxia-induced membrane depolarization. *Circ. Res.*, **77**: 131-139, 1995.

236. Post, J. M., Hume, J. R., Archer, S. L., and Weir, E. K. Direct role for potassium channel inhibition in hypoxic pulmonary vasoconstriction. *Am. J. Physiol. Cell Physiol.*, **262**: C882-C890, 1992.

237. Quayle, J. M., Bonev, A. D., Brayden, J. E., and Nelson, M. T. Calcitonin-gene-related peptide activated ATP-sensitive K^+ currents in rabbit arterial smooth muscle via protein kinase A. *J. Physiol. (Lond.)*, **475**: 9-13, 1994.

238. Quayle, J. M., Dart, C., and Standen, N. B. The properties and distribution of inward rectifier potassium currents in pig coronary arterial smooth muscle. *J. Physiol. (Lond.)*, **494**: 715-720, 1996.

239. Quayle, J. M., and Standen, N. B. K_{ATP} channels in vascular smooth muscle. *Cardiovasc. Res.*, **28**: 797-804, 1994.

240. Quignard, J. F., Frapier, J. M., Harricane, M. C., Albat, B., Nargeot, J., and Richard, S. Voltage-gated calcium channel currents in human coronary myocytes - Regulation by cyclic GMP and nitric oxide. *J. Clin. Invest.*, **99**: 185-193, 1997.

241. Quilley, J., Fulton, D., and McGiff, J. C. Hyperpolarizing factors. *Biochem. Pharmacol.*, **54**; 1059-1070, 1997.

242. Remillard, C. V., and Leblanc, N. Mechanism of inhibition of delayed rectifier K^+ current by 4- aminopyridine in rabbit coronary myocytes. *J. Physiol. (Lond.)*, **491**: 383-400, 1996.

243. Rettig, J., Heinemann, S. H., Wunder, F., Lorra, C., Parcej, D. N., Dolly, J. O., and Pongs, O. Inactivation properties of voltage-gated K^+ channels altered by presence of β-subunit. *Nature*, **369**: 289-294, 1994.

244. Robertson, B. E. Inhibition of calcium-activated chloride channels by niflumic acid dilates rat cerebral arteries. *Acta Physiol. Scand.*, **163**: 417-418, 1998.

245. Robertson, B. E., Bonev, A. D., and Nelson, M. T. Inward rectifier K^+ currents in smooth muscle cells from rat coronary arteries: block by Mg^{2+}, Ca^{2+}, and Ba^{2+}. *Am. J. Physiol. Heart Circ. Physiol.*, **271**: H696-H705, 1996.

246. Robertson, B. E., and Nelson, M. T. Aminopyridine inhibition and voltage dependence of K^+ currents in smooth muscle cells from cerebral arteries. *Am. J. Physiol. Cell Physiol.*, **267**: C1589-C1597, 1994.

247. Russell, S. N., Overturf, K. E., and Horowitz, B. Heterotetramer formation and charybdotoxin sensitivity of two K^+ channels cloned from smooth muscle. *Am. J. Physiol. Cell Physiol.*, **267**: C1729-C1733, 1994.

248. Russell, S. N., Publicover, N. G., Hart, P. J., Carl, A., Hume, J. R., Sanders, K. M., and Horowitz, B. Block by 4-aminopyridine of a $K_V1.2$ delayed rectifier K^+ current expressed in *Xenopus* oocytes. *J. Physiol. (Lond.)*, **481**: 571-584, 1994.

249. Sakata, K., Ozaki, H., Kwon, S.-C., and Karaki, H. Effects of endothelin on the mechanical activity and cytosolic calcium levels of various types of smooth muscle. *Br. J. Pharmacol.*, **98**: 483-492, 1989.

250. Salter, K. J., and Kozlowski, R. Z. Endothelin receptor coupling to potassium and chloride channels in isolated rat pulmonary arterial myocytes. *J. Pharmacol. Exp. Ther.*, **279**: 1053-1062, 1996.

251. Salvail, D., Alioua, A., and Rousseau, E. Functional identification of a sarcolemmal chloride channel from bovine tracheal smooth muscle. *Am. J. Physiol. Cell Physiol.*, **271**: C1716-C1724, 1996.

252. Sánchez-Olea, R., Morales, M., Gárcia., O., and Pasantes-Morales, H. Cl channel blockers inhibit the volume-activated efflux of Cl and taurine in cultured neurons. *Am. J. Physiol. Cell Physiol.*, **270**: C1703-1708, 1996.

253. Sanguinetti, M. C., and Jurkiewicz, N. K. Two components of cardiac delayed rectifier K^+ current. Differential sensitivity to block by class III antiarrhythmic agents. *J. Gen. Physiol.*, **96**: 195-215, 1990.

254. Satoh, M., Enomoto, K., Niwano, H., Fujimura, H., Toyama, Y., Takayanagi, I., and Koike, K. Regional differences in α_1-adrenoceptor subtypes and mechanisms in rabbit arteries. *Eur. J. Pharmacol.*, **350**: 67-73, 1998.

255. Schlenker, T., and Fitz, J. G. Ca^{2+}-activated Cl^- channels in human biliary cell line: regulation by Ca^{2+}/calmodulin- dependent protein kinase. *Am. J. Physiol. Gastrointest. Liver Physiol.*, **271**: G304-G310, 1996.

256. Schumann, M. A., and Raffin, T. A. Activation of a voltage-dependent chloride current in human neutrophils by phorbol-12-myristate 13-acetate and formyl-methionyl-leucyl phenylalanine. The role of protein kinase C. *J. Biol. Chem.*, **269**: 2389-2398, 1994.

257. Scornik, F. S., and Toro, L. U46619, a thromboxane-A_2 agonist, inhibits K_{Ca} channel activity from pig coronary artery. *Am. J. Physiol. Cell Physiol.*, **262**: C708-C713, 1992.

258. Shimoda, L. A., Sylvester, J. T., and Sham, J. S. K. Inhibition of voltage-gated K^+ current in rat intrapulmonary arterial myocytes by endothelin-1. *Am. J. Physiol. Lung Cell. Mol. Physiol.*, **274**: L842-L853, 1998.

259. Shrier, A., and Clay, J. R. Repolarization currents in embryonic chick atrial heart cell aggregates. *Biophys. J.*, **50**: 861-874, 1986.

260. Sims, S. M., Clapp, L. H., Walsh, J. V. Jr., and Singer, J. J. Dual regulation of M current in gastric smooth muscle cells: β-adrenergic-muscarinic antagonism. *Pflügers Arch.*, **417**: 291-302, 1990.

261. Šimurda, J., Šimurdová, M., and Christé, G. Use-dependent effects of 4-aminopyridine on transient outward current in dog ventricular muscle. *Pflügers Arch.*, **415**: 244-246, 1989.

262. Smirnov, S. V., and Aaronson, P. I. Inhibition of vascular smooth muscle cell K^+ currents by tyrosine kinase inhibitors genistein and ST 638. *Circ. Res.*, **76**: 310-316, 1995.

263. Smirnov, S. V., and Aaronson, P. I. Modulatory effects of arachidonic acid on the delayed rectifier K^+ current in rat pulmonary arterial myocytes. Structural aspects and involvement of protein kinase C. *Circ. Res.*, **79**: 20-31, 1996.

264. Smirnov, S. V., Robertson, T. P., Ward, J. P. T., and Aaronson, P. I. Chronic hypoxia is associated with reduced delayed rectifier K^+ current in rat pulmonary artery muscle cells. *Am. J. Physiol. Heart Circ. Physiol.*, **266**: H365-H370, 1994.

265. Sobey, C. G., and Faraci, F. M. Inhibitory effect of 4-aminopyridine on responses of the basilar artery to nitric oxide. *Br. J. Pharmacol.*, **126**: 1437-1443, 1999.

266. Solc, C. K., and Wine, J. J. Swelling-induced and depolarization-induced Cl^- channels in normal and cystic fibrosis epithelial cells. *Am. J. Physiol. Cell Physiol.*, **261**: C658-C674, 1991.

267. Standen, N. B., Quayle, J. M., Davies, N. W., Brayden, J. E., Huang, Y., and Nelson, M. T. Hyperpolarizing vasodilators activate ATP-sensitive K^+ channels in arterial smooth muscle. *Science*, **245**: 177-180, 1989.

268. Steinmeyer, K., Ortland, C., and Jentsch, T. J. Primary structure and functional expression of a developmentally regulated skeletal muscle chloride channel. *Nature*, **354**: 301-304, 1991.

269. Steinmeyer, K., Schwappach, B., Bens, M., Vandewalle, A., and Jentsch, T. J. Cloning and functional expression of rat CLC-5, a chloride channel related to kidney disease. *J. Biol. Chem.*, **270**: 31172-31177, 1995.

270. Stephens, G. J., Garratt, J. C., Robertson, B., and Owen, D. G. On the mechanism of 4-aminopyridine action on the cloned mouse brain potassium channel $mK_V1.1$. *J. Physiol. (Lond.)*, **477**: 187-196, 1994.

271. Stoddard, J. S., Steinbach, J. H., and Simchowitz, L. Whole cell Cl^- currents in human neutrophils induced by cell swelling. *Am. J. Physiol. Cell Physiol.*, **265**: C156-C165, 1993.

272. Sturek, M., and Hermsmeyer, K. Calcium and sodium channels in spontaneously contracting vascular muscle cells. *Science*, **233**: 475-478, 1986.

273. Suzuki, E., Tsujimoti, G., Tamura, K., and Hashimoto, K. Two pharmacologically distinct α_1-adrenoceptor subtypes in the contraction of rabbit aorta: each subtype couples with a different Ca^{2+} signalling mechanism and plays a different physiological role. *Mol. Pharmacol.*, **38**: 725-736, 1990.

274. Szentiványi, M. Jr., Bérczi, V., Hüttl, T., Reneman, R. S., and Monos, E. Venous myogenic tone and its regulation through K^+ channels depends on chronic intravascular pressure. *Circ. Res.*, **81**: 988-995, 1997.

275. Takenaka, T., Epstein, M., Forster, H., Landry, D. W., Iijima, K., and Goligorsky, M. S. Attenuation of endothelin effects by a chloride channel inhibitor, indanyloxyacetic acid. *Am. J. Physiol. Renal Physiol.*, **262**: F799-F806, 1992.

276. Takenaka, T., Kanno, Y., Kitamura, Y., Hayashi, K., Suzuki, H., and Saruta, T. Role of chloride channels in afferent arteriolar constriction. *Kidney Int.*, **50**: 864-872, 1996.

277. Takenaka, T., Suzuki, H., Okada, H., Hayashi, K., Kanno, Y., and Saruta, T. Mechanosensitive cation channels mediate afferent arteriolar myogenic constriction in the isolated rat kidney. *J. Physiol. (Lond.)*, **511**: 245-253, 1998.

278. Thakker, R. V. The role of renal chloride channel mutations in kidney stone disease and nephrocalcinosis. *Cur. Opin. Nephrol. Hypertens.*, 7: 385-388, 1998.

279. Thiemann, A., Gründer, S., Pusch, M., and Jentsch, T. J. A chloride channel widely expressed in epithelial and non-epithelial cells. *Nature*, **356**: 57-60, 1992.

280. Thompson, S. Aminopyridine block of transient potassium current. *J. Gen. Physiol.*, **80**: 1-18, 1982.

281. Tohse, N., Nakaya, H., and Kanno, M. α_1-Adrenoceptor stimulation enhances the delayed rectifier K^+ current of guinea pig ventricular cells through the activation of protein kinase C. *Circ. Res.*, **71**: 1441-1446, 1992.

282. Toma, C., Greenwood, I. A., Helliwell, R. M., and Large, W. A. Activation of potassium currents by inhibitors of calcium-activated chloride conductance in rabbit portal vein smooth muscle cells. *Br. J. Pharmacol.*, **118**: 513-520, 1996.

283. Toung, T., Reilly, P. M., Fuh, K. C., Ferris, R., and Bulkley, G. B. Mesenteric vasoconstriction in response to hemorrhagic shock. *Shock*, **13**: 267-273, 2000.

284. Unger, T. Neurohormonal modulation in cardiovascular disease. *Am. Heart. J.*, **139**: 2-8, 2000.

285. Van Breemen, C., and Saida, K. Cellular mechanisms regulating $[Ca^{2+}]_i$ smooth muscle. *Ann. Rev. Physiol.*, **51**: 315-329, 1989.

286. Van Helden, D. F. An α-adrenoceptor-mediated chloride conductance in mesenteric veins of the guinea-pig. *J. Physiol. (Lond.)*, **401**: 489-501, 1988.

287. Van Renterghem, C., and Lazdunski, M. Endothelin and vasopressin activate low conductance chloride channels in aortic smooth muscle cells. *Pflügers Arch.*, **425**: 156-163, 1993.

288. Van Renterghem, C., and Lazdunski, M. Identification of the Ca^{2+} current activated by vasoconstrictors in vascular smooth muscle cells. *Pflügers Arch.*, **429**: 1-6, 1994.

289. VanBavel, E., Wesselman, J. P. M., and Spaan, J. A. E. Myogenic activation and calcium sensitivity of cannulated rat mesenteric small arteries. *Circ. Res.*, **82**: 210-220, 1998.

290. Vanhoutte, P. M. Endothelium, and control of vascular function: state of the art lecture. *Hypertension*, **13**; 658-667, 1989.

291. Varnum, M. D., Busch, A. E., Bond, C. T., Maylie, J., and Adelman, J. P. The minK channel underlies the cardiac potassium current I_{Ks} and mediates species-specific responses to protein kinase C. *Proc. Natl Acad. Sci. USA*, **90**: 11528-11532, 1993.

292. Veldkamp, M. W., Van Ginneken, A. C., and Bouman, L. N. Single delayed rectifier channels in the membrane of rabbit ventricular myocytes. *Circ. Res.*, **72**: 865-878, 1993.

293. Voets, T., Droogmans, G., and Nilius, B. Potent block of volume-activate chloride currents in endothelial cells by the uncharged form of quinine and quinidine. *Br. J. Pharmacol.*, **118**: 1869-1871, 1996.

294. Voets, T., Manolopoulos, V., Eggermont, J., Ellory, C., Droogmans, G., and Nilius, B. Regulation of a swelling-activated chloride current in bovine endothelium by protein tyrosine phosphorylation and G proteins. *J. Physiol. (Lond.)*, **506**: 341-352, 1998.

295. Vogalis, F., and Lang, R. J. Identification of single transiently opening ("A-type") K channels in guinea-pig colonic myocytes. *Pflügers Arch.*, **429**: 160-164, 1994.

296. Volk, K. A., Matsuda, J. J., and Shibata, E. F. A voltage-dependent potassium current in rabbit coronary artery smooth muscle cells. *J. Physiol. (Lond.)*, **439**: 751-768, 1991.

297. Volk, K. A., and Shibata, E. F. Single delayed rectifier potassium channels from rabbit coronary artery myocytes. *Am. J. Physiol. Heart Circ. Physiol.*, **264**: H1146-H1153, 1993.

298. Wade, G. R., Barbera, J., and Sims, S. M. Cholinergic inhibition of Ca^{2+} current in guinea-pig gastric and tracheal smooth muscle cells. *J. Physiol. (Lond.)*, **491**: 307-319, 1996.

299. Walsh, K. B., and Kass, R. S. Distinct voltage-dependent regulation of a heart delayed I_K by protein kinase-A and kinase-C. *Am. J. Physiol. Cell Physiol.*, **261**: C1081-C1090, 1991.

300. Walsh, K. B., and Wang, C. Effect of chloride channel blockers on the cardiac CFTR chloride and L-type calcium currents. *Cardiovasc. Res.*, **32**: 391-399, 1996.

301. Wang, J., Juhaszova, M., Rubin, L. J., and Yuan, X. J. Hypoxia inhibits gene expression of voltage-gated K^+ channel α subunits in pulmonary artery smooth muscle cells. *J. Clin. Invest.*, **100**: 2347-2353, 1997.

302. Wang, Q., and Large, W. A. Noradrenaline-evoked cation conductance recorded with the nystatin whole-cell method in rabbit portal vein cells. *J. Physiol. (Lond.)*, **435**: 21-39, 1991.

303. Wang, Q., Wang, Y. X., Yu, M., and Kotlikoff, M. I. Ca^{2+}-activated Cl^- currents are activated by metabolic inhibition in rat pulmonary artery smooth muscle cells. *Am. J. Physiol. Cell Physiol.*, **273**: C520-C530, 1997.

304. Wang, Y. X., and Kotlikoff, M. I. Inactivation of calcium-activated chloride channels in smooth muscle by calcium/calmodulin-dependent protein kinase. *Proc. Natl Acad. Sci. USA*, **94**: 14918-14923, 1997.

305. Warner, T. D., Mitchell, J. A., de Nucci, G., and Vane, J. R. Endothelin-1 and endothelin-3 release EDRF from isolated perfused arterial vessels of the rat and rabbit. *J. Cardiovasc. Pharmacol.*, **13**; S85-S88, 1989.

306. Watanabe, J., Horiguchi, S., Keitoku, M., Karibe, A., Takeuchi, M., Suzuki, S., Satoh, S., and Shirato, K. The role of extracellular cations in the development of myogenic contraction in isolated rat small arteries. *Jap. Circ. J.*, **60**: 239-246, 1996.

307. Weir, E. K., and Archer, S. L. The mechanism of acute hypoxic pulmonary vasoconstriction: the tale of two channels. *FASEB J.*, **9**; 183-189, 1995.

308. Wellman, G. C., and Bevan, J. A. Barium inhibits the endothelium-dependent component of flow but not acetylcholine-induced relaxation in isolated rabbit cerebral arteries. *J. Pharmacol. Exp. Ther.*, **274**: 47-53, 1995.

309. Wesselman, J. P. M., Schubert, R., VanBavel, E. D., Nilsson, H., and Mulvany, M. J. K_{Ca}-channel blockade prevents sustained pressure-induced depolarization in rat mesenteric small arteries. *Am. J. Physiol. Heart Circ. Physiol.*, **272**: H2241-H2249, 1997.

310. Wesselman, J. P. M., Van Bavel, E., Pfaffendorf, M., and Spaan, J. A. E. Voltage-operated calcium channels are essential for the myogenic responsiveness of cannulated rat mesenteric small arteries. *J. Vasc. Res.*, **33**: 32-41, 1996.

311. West, G. A., Leppla, D. C., and Simard, J. M. Effects of external pH on ionic currents in smooth muscle cells from the basilar artery of the guinea pig. *Circ. Res.*, **71**: 201-209, 1992.

312. White, C. R., Elton, T. S., Shoemaker, R. L., and Brock, T. A. Calcium-sensitive chloride conductance in vascular smooth muscle cells. *Soc. Exp. Biol. Med.*, **208**: 255-262, 1995.

313. White, M. M., and Aylwin, M. Niflumic and flufenamic acids are potent reversible blockers of Ca^{2+}-activated Cl^- channels in *Xenopus* oocytes. *Mol. Pharmacol.*, **37**: 720-724, 1990.

314. White, R. E., Darkow, D. J., and Falvo Lang, J. L. Estrogen relaxes coronary arteries by opening BK_{Ca} channels through a cGMP-dependent mechanism. *Circ. Res.*, 77: 933-942, 1995.

315. Xie, W., Kaetzel, M. A., Bruzik, K. S., Dedman, J. R., Shears, S. B., and Nelson, D .J. Inositol 3,4,5,6-tetrakisphosphate inhibits the calmodulin-dependent protein kinase II-activated chloride conductance in T84 colonic epithelial cells. *J. Biol. Chem.*, **271**: 14092-14094, 1996.

316. Xie, W., Solomons, K. R. H., Freeman, S., Kaetzel, M. A., Bruzik, K. S., Nelson, D. J., and Shears, S. B. Regulation of Ca^{2+}-dependent Cl^- conductance in a human colonic epithelial cell line (T_{84}): cross-talk between Ins(3,4,5,6)P_4 and protein phosphatases. *J. Physiol. (Lond.)*, **510**: 661-673, 1998.

317. Yamazaki, J., Duan, D., Janiak, R., Kuenzli, K., Horowitz, B., and Hume, J. R. Functional and molecular expression of volume-regulated chloride channels in canine vascular smooth muscle cells. *J. Physiol. (Lond.)*, **507**: 729-736, 1998.

318. Yamazaki, J., and Hume, J. R. Inhibitory effects of glibenclamide on cystic fibrosis transmembrane regulator, swelling-activated, and Ca^{2+}-activated Cl^- channels in mammalian cardiac myocytes. *Circ. Res.*, **81**: 101-109, 1997.

319. Yao, J. A., and Tseng, G. N. Modulation of 4-AP block of a mammalian a-type K channel clone by channel gating and membrane voltage. *Biophys. J.*, **67**: 130-142, 1994.

320. Yatani, A., Seidel, C. L., Allen, J., and Brown, A. M. Whole-cell and single-channel calcium currents of isolated smooth muscle cells from saphenous vein. *Circ. Res.*, **60**: 523-533, 1987.

321. Yeh, J. Z., Oxford, G. S., Wu, C. H., and Narahashi, T. Dynamics of aminopyridine block of potassium channels in squid axon membrane. *J. Gen. Physiol.*, **68**: 519-535, 1976.

322. Yoshida, M., Suzuki, A., and Itoh, T. Mechanisms of vasoconstriction induced by endothelin-1 in smooth muscle of rabbit mesenteric artery. *J. Physiol. (Lond.)*, **77**: 253-265, 1997.

323. Yuan, X. J. Role of calcium-activated chloride current in regulating pulmonary vascular tone. *Am. J. Physiol. Lung Cell. Mol. Physiol.*, **272**: L959-L968, 1997.

324. Yuan, X. J. Voltage-gated K^+ currents regulate resting membrane potential and $[Ca^{2+}]_i$ in pulmonary arterial myocytes. *Circ. Res.*, **77**: 370-378, 1995.

325. Yuan, X. J., Tod, M. L., Rubin, L. J., and Blaustein, M. P. Deoxyglucose and reduced glutathione mimic effects of hypoxia on K^+ and Ca^{2+} conductances in pulmonary artery cells. *Am. J. Physiol. Lung Cell. Mol. Physiol.*, **267**: L52-L63, 1994.

326. Yuan, X. J., Tod, M. L., Rubin, L. J., and Blaustein, M. P. NO hyperpolarizes pulmonary artery smooth muscle cells and decreases the intracellular Ca^{2+} concentration by activating voltage-gated K^+ channels. *Proc. Natl Acad. Sci. USA*, **93**: 10489-10494, 1996.

327. Yuan, X. J., Wang, J., Juhaszova, M., Gaine, S. P., and Rubin, L. J. Attenuated K^+ channel gene transcription in primary pulmonary hypertension. *Lancet*, **351**: 726-727, 1998.

328. Yuan, X. J., Wang, J., Juhaszova, M., Golovina, V. A., and Rubin, L. J. Molecular basis and function of voltage-gated K^+ channels in pulmonary arterial smooth muscle cells. *Am. J. Physiol. Lung Cell. Mol. Physiol.*, **274**: L621-L635, 1998.

329. Zhao, Y. J., Wang, J., Rubin, L. J., and Yuan, X. J. Inhibition of K_V and K_{Ca} channels antagonizes NO-induced relaxation in pulmonary artery. *Am. J. Physiol. Heart Circ. Physiol.*, **272**: H904-H912, 1997.

330. Zhou, S. S., Takai, A., Tominaga, M., and Okada, Y. Phosphatase-mediated enhancement of cardiac cAMP-activated Cl^- conductance by a Cl^- channel blocker, anthracene-9-carboxylate. *Circ. Res.*, **81**: 219-228, 1997.

331. Zhou, Z., and Lipsius, S. L. Delayed rectifier potassium current (I_K) in latent atrial pacemaker cells isolated from cat right atrium. *Pflügers Arch.*, **426**: 341-347, 1994.

332. ZhuGe, R., Sims, S. M., Tuft, R. A., Fogarty, K. E., and Walsh, J. V. Jr. Ca^{2+} sparks activate K^+ and Cl^- channels, resulting in spontaneous transient currents in guinea-pig tracheal myocytes. *J. Physiol. (Lond.)*, **513**: 711-718, 1998.

333. Zygmunt, A. C., and Gibbons, W. R. Calcium-activated chloride current in rabbit ventricular myocytes. *Circ. Res.*, **68**: 424-437, 1991.